CAT AND *BEN* GENE REGULATION: THE ROLE OF CATM AND BENM, TWO LYSR-TYPE TRANSCRIPTIONAL REGULATORS OF *ACINETOBACTER BAYLYI* STRAIN ADP1

by

MELISSA PATRICIA TUMEN-VELASQUEZ

(Under the Direction of Ellen L. Neidle)

ABSTRACT

BenM and CatM are LysR-type transcriptional regulators (LTTR) from *Acinetobacter baylyi* ADP1 that control a complex regulon involved in benzoate catabolism. Although previous studies demonstrate similarities in the structure and function of these paralogs, there are key differences that distinguish their regulatory roles. As described in this thesis, mutants were isolated and characterized that grow on benzoate without BenM. In the wild-type strain, benzoate consumption is prevented by the failure of CatM to activate high-level transcription of the *benABCDE* operon. At this locus, CatM typically activates low-level transcription in response to, *cis,cis*-muconate, a catabolite of benzoate. The goal of the current research was to alter CatM to make it function more like BenM. This approach was used to reveal the molecular basis of transcriptional control by these two regulators and, by extrapolation, other members of the important LTTR family.

Amino acid changes that enable CatM variants to substitute for the loss of BenM were identified in all regions of the protein: the N-terminal DNA-binding domain, the linker helix, and the C-terminal effector-binding domain. In no previous study had mutations been isolated that affect the DNA-binding domain or linker-helix region of these proteins. The novel CatM variants increased *ben*-gene expression via elevated transcriptional regulation in response to muconate.

However, these changes did not confer a distinct regulatory feature of BenM, the ability to respond to two effector compounds and activate transcription of the *benABCDE* operon synergistically. A different approach was successful in generating this feature. CatM variants that were engineered by rational design acquired the synergistic response to two effectors when changes were made in both the N- and C-terminal domains. Engineered regulatory variants were also examined for their transcriptional effects at two other promoter regions (*catA* and *catBCIJFD*). These studies show that the N-terminal domain is not solely responsible for promoter specificity. Similarly, the C-terminal domain does not solely control the response to effectors. Rather, there appears to be subtle interplay between the domains that can affect transcription. These studies expand our understanding of LTTRs and microbial aromatic metabolism. They also facilitate the development of new biotechnology applications.

INDEX WORDS: *Acinetobacter baylyi* strain ADP1, BenM, CatM, LysR-type transcriptional regulators, benzoate, *cis, cis*-muconate, synergistic response, β-ketoadipate pathway, aromatic compound degradation, transcriptional regulation, crystal structure, DNA-binding domain, Linker Helix, Effector binding domain, catechol 1, 2-dioxygenase, 4-hydroxybenzoate, LeuR, leucine biosynthesis, (2*S*)-2-isopropylmalate, *leuC*.

CAT AND *BEN* GENE REGULATION: THE ROLE OF CATM AND BENM, TWO LYSR-TYPE TRANSCRIPTIONAL REGULATORS OF *ACINETOBACTER BAYLYI* STRAIN ADP1

by

MELISSA PATRICIA TUMEN-VELASQUEZ

B.S., The University of Georgia, 2008

A Dissertation Submitted to the Graduate Faculty of The University of Georgia in Partial Fulfillment of the Requirements for the Degree

DOCTOR OF PHILOSOPHY

ATHENS, GEORGIA

2014

CAT AND *BEN* GENE REGULATION: THE ROLE OF CATM AND BENM, TWO LYSR-TYPE TRANSCRIPTIONAL REGULATORS OF *ACINETOBACTER BAYLYI* STRAIN ADP1

by

MELISSA PATRICIA TUMEN-VELASQUEZ

Major Professor:	Ellen L. Neidle Cory Momany
Committee:	Timothy Hoover Lawrence Shimkets Eric Stabb

Electronic Version Approved:

Julie Coffield
Interim Dean of the Graduate School
The University of Georgia
August 2014

DEDICATION

I dedicate this project to the most marvelous and free spirited person that has ever existed, my rock, hope, unconditional love, and brother, Edson Alberto Tumen - whose spiritual presence and great memories have helped me to keep on with this journey. I will forever miss you my beautiful “Papacito”

ACKNOWLEDGEMENTS

This project would have not been possible without the help and encouragement of a great group of people. Individuals whose kindness and intelligence continue to amaze me everyday. There are not sufficient words to explain my gratitude to those that have helped me tremendously with these studies. With great thanksgiving, I would like to acknowledge the following people:

- First and foremost, I would like to thank my amazing husband Eric, whose encouragement and thoughtful words have helped me to continue with all these projects. I thank his unconditional sympathetic ear that listened to all science-related nonsense I would say during great or not so good days.
- To my family, whose never-ending love and words of encouragement that have enabled me to realize my potential. Thank you mama and daddy for the immense sacrifice of leaving our beloved Peru in order to provide us with bigger and better opportunities. I will be forever grateful. To my brother, Mario, whose time, intelligence and heartwarming words are highly treasured and cherished.
- Ellen Neidle, for giving me the opportunity to grow as a scientist through her dedicated, enthusiastic and energetic mentoring. Thank you so much for your support and patience but most importantly for giving me the freedom to pursue various projects.
- Cory Momany, for providing insightful discussions about my research as well as offering great ideas for different experiments in this thesis. Thank you for your help and guidance.
- Anna Karls, for giving me the opportunity to find myself as a scientist through the UGA Summer Undergraduate Research Program. Thanks a million for believing in me and for your continuing guidance throughout these years. You are truly inspiring.

- Eric Stabb, for all your support and guidance as my former undergraduate research advisor and now member of my PhD committee. Thanks for giving me the opportunity to grow as a scientist in your lab, which influenced me tremendously to pursue a career in research.
- Larry Shimkets and Tim Hoover for your helpful scientific and career advice as my undergraduate professors and PhD committee members.
- Katherine Elliott, Sarah Craven-Seaton, and Laura Cuff for making the transition to the Neidle lab a welcoming and great one. Thanks girls for your enthusiasm, kindness and help with all my projects.
- Noreen Lyell for providing me with all the different skills to become a scientist. Your enthusiasm on science is contagious.
- Nicole Laniohan for being there for me at all times. I will forever treasure our science and non-science (cat related obviously!) conversations over tamales and platanos at Cali-n-titos. You are truly amazing!
- Stephanie Thurmond for enlightening and engaging discussions on many science and non-science related topics.
- Curtis Bacon, Cassandra Bartlett, Walker Whitley, Patrice Parkinson and Maliha Ishaq for working with me on the many different and exciting projects. You guys are spectacular and extremely hard-working. Thanks for bringing out the best in me.
- The Microbiology Staff for always being there to provide help with all my questions.
- Friends and relatives whose support and encouragement have truly helped throughout these years.
- My beautiful cats (Chiquito, Nenna, Cosito and Bonita) for your unconditional love and purrs…

TABLE OF CONTENTS

Page

LIST OF TABLES

Page

LIST OF FIGURES

Page

CHAPTER 1

INTRODUCTION AND LITERATURE REVIEW

Purpose of study

Harmful man-made pollutants, including polychlorinated biphenyls (PCBs) and other petroleum derivatives, have increased the already abundant natural occurrence of aromatic compounds in the environment (19). Studies of aromatic metabolic pathways are fundamental for designing bioremediation strategies against these aromatic pollutants (30). Benzoate is a naturally occurring aromatic compound and similar in structure to PCB that is readily metabolized by many soil microorganisms from diverse environmental niches (21, 22, 36). This dissertation focuses in the regulatory circuit that governs benzoate degradation in *Acinetobacter baylyi* strain ADP1. Genes implicated in benzoate metabolism are controlled by two LysR-type transcriptional regulators (LTTRs), BenM and CatM (15, 52). These paralogs are 59% similar in amino acid sequence and play overlapping regulatory roles for genes involved in benzoate degradation. Both regulators respond to *cis, cis*-muconate (hereafter referred to as muconate), a metabolite from the pathway, but only BenM responds to benzoate (27). In addition, BenM activates expression from the *benABCDE* operon synergistically in response to benzoate and muconate (9). CatM cannot activate genes necessary for growth on benzoate in the absence of BenM. Studies of an engineered synergistic response in CatM concomitant with CatM-mediated benzoate degradation described here have improved our understanding of LTTR-transcriptional activation.

An extensive literature review is provided in this section on topics pertinent to this work. Chapter 2 addresses studies of synergistic transcriptional activation of the *benABCDE* and *catBCIJFD* operons by CatM in the absence of BenM. Wild-type CatM cannot activate genes synergistically in response to benzoate and muconate because it lacks a benzoate response. Crystallography studies have shown that Arg160 and Tyr293 directly interact with the carboxyl group of benzoate in BenM. When these residues were changed to those of CatM (His160 and Phe293), the resultant BenM variant protein lost its ability to respond to benzoate. Through mutational studies described in this chapter, CatM was modified to acquire benzoate responsiveness. Interestingly, replacements of residues His160 and Phe293 in CatM with Arg160 and Tyr293 from BenM failed to recreate the benzoate response. Only the replacements of full-length BenM-DNA binding domain (BenM-DBD) in CatM along with the two amino acid changes permit CatM to respond to benzoate. This benzoate responsive CatM activates transcription synergistically at all promoters tested, which differs from BenM-dependent activation. Further mutagenesis studies with both BenM and CatM revealed a combined role of DNA-binding domain interactions and effector response that dictates promoter specificity with both LTTRs. In addition to engineered CatM variants, CatM-mediated benzoate degradation was further studied by isolating and characterizing seven independent CatM variants. In this chapter, four CatM variants are studied in detail to establish how modulation of different operons permits benzoate degradation without BenM.

Based on studies described in chapter 2, CatM-mediated regulation in benzoate degradation was explored further in light of three independent mutations. These *catM* alleles encoded amino acid replacements at the linker helix region, a protein region that

connects DNA and effector-binding domains. Chapter 3 focuses on studies in CatM-mediate regulation by these CatM variants to reveal the role of this region in transcriptional activation, which was previously underscored by dimerization properties. In addition, a model for CatM-mediated benzoate degradation is proposed by these linker helix variants, which reinforces the ability of these regulators to modulate transcriptional activation at different operons to permit benzoate degradation in the absence of BenM.

Chapter 3 showed the importance of regulation of the *catA* gene, which encodes the enzyme responsible for muconate generation (catechol 1,2-dioxygenase), the effector molecule needed for successful CatM-mediated regulation by linker helix CatM variants. BenM and CatM have equally important regulatory roles at this promoter. Chapter 4 focuses on addressing *catA* regulation and reveals similarities to *benABCDE* operon-control. BenM activates *catA* transcription synergistically in response to benzoate and muconate.

Acinetobacter baylyi strain ADP1 general characteristics and natural transformation

A. baylyi belongs the genus *Acinetobacter,* which is comprised of heterogeneous bacteria that are classified in the gamma subdivision of the Proteobacteria. Members of this genus are ubiquitous and can be found in water and soil environments. ADP1 is a Gram-negative, non-motile and strictly aerobic bacterium, which is commonly found in the soil (59). ADP1 thrives by growing on substrates found in the soil such as organic acids and aromatic compounds. A study published by Baumann *et al.* compared organisms from different taxa with a large number of physiological characters, which included nutritional properties, G+C content, absence of flagella and cell shape. The

investigation concluded that these organisms represented a single genus, and the genus was named *Acinetobacter* (4, 5). A variety of methods, including DNA-DNA hybridization, 16S ribosomal gene restriction analysis, and high resolution fingerprinting approaches have been used to evaluate the diversity of this genus at species and strain levels (26, 33, 45). Thus far, 32 genomic groups have been described (25). Due to the lack of a practical identification scheme, several species in the *Acinetobacter* genus have not been definitively classified.

A. baylyi ADP1 was first isolated as a mutant from the soil isolate BD4 (BD refers to butanediol) which was isolated from a medium with *meso* 2,3-butanediol as the sole carbon source in 1969 by Elliot Juni. This strain produced high levels of polysaccharide which hampered manipulation (37). A mutant from BD14, called BD413 was obtained by ultraviolet irradiation. Strain BD413 later called ADP1 was identified to belong to the *A. baylyi* species less than ten years ago by Vaneechoutte *et al* (59). Transformation studies have shown that ADP1 and *A. baylyi* strain 93A2, an *Acinetobacter* strain isolated using kynurenine as sole carbon source (Baumann, 1968), share comparable natural transformation frequencies (11, 59). Natural transformation is the feature that defines and differentiates *A. baylyi* species from the rest of *Acinetobacter* species (59).

The high efficiency for natural transformation by ADP1 is a powerful mechanism for studies of chromosomal rearrangements, DNA amplification events and evolution of metabolic traits (51, 55). This property allows physiological studies and genetic manipulation with relative ease, and it has provided insights into its nutritional versatility (3, 41). In ADP1, DNA uptake is divalent cation-dependent (Mg^{2+}, Ca^{2+}, and Mn^{2+}) and requires energy (50). In addition, ADP1 offers the advantage to induce competence

following fresh carbon addition and does not discriminate between homologous and heterologous DNA (37). Several events such as homologous recombination, homology-facilitated illegitimate recombination, and site-specific homology-independent illegitimate recombination allow the ADP1 chromosome to integrate DNA from any source (24, 51). DNA acquisition by the ADP1 chromosome depends on the stability of the incoming single stranded DNA, where ssDNA-binding proteins and the RecN protein might affect stabilization (38, 43).

Mutational studies leaded to the identification of sixteen genes involve in the natural transformation system of ADP1(2). These "competence" genes are distributed in seven distinct chromosomal loci and are not physically linked. Some of these genes encode proteins that resemble components of type II secretion systems and type IV pili, which are commonly found in transformation machineries (2, 12). Based on these similarities and extensive experimental studies, a hypothetical model for ssDNA translocation has been proposed (2). Based on this model, ComQ proteins form a ring structure in the outer membrane with a central channel that has a sufficiently large diameter to accommodate ssDNA (2). This channel might be a dynamic channel that opens by signals resulting from DNA binding to the ComC protein. DNA might be translocated via retractable short pseudopili formed by proteins ComP, ComE, ComF, and ComB which extends from the cytoplasmic membrane via the periplasm to the outer membrane. The structures are thought to extend in length by polymerization and initiate opening of the outer membrane channel that pulls down DNA through the channel by depolymerization (2). Lastly, DNA enters the cytoplasmic membrane through the ComA translocation channel (12). The uptake of DNA in ADP1 is energy dependent and may be

driven by a proton motion force or ATP hydrolysis. It is not clear whether this energy is required for active state of competence proteins or to drive DNA transport (50).

The high efficiency of transformation and homologous recombination make ADP1 a formidable model system for many of the experiments described in this dissertation. Construction of hybrid versions of *benM* and *catM* were introduced into the ADP1 chromosome with ease as well as mutations generated by Polymerase chain reaction (PCR). Large constructs including genes with the counterselectable marker *sacB* for feasible recombination are possible in ADP1. Also, regions of interest (genes and promoters) with potential mutations could be recovered by a gap repair method, which allows recovery of specific chromosomal segments in recombinant plasmids (49). Constructs for assessing gene expression *in vivo* were also possible with ADP1. This outstanding system greatly facilitated studies to improve understanding of CatM-mediated regulation and the regulatory scheme exhibited by BenM and CatM for expression of the *ben-cat* supraoperonic cluster.

Aromatic compound degradation by *A. baylyi*

Lignin, a complex molecule composed of phenylpropane units, is an abundant plant polymer and the most prevalent source of aromatic compounds in nature. Fungi, predominantly basidomycetes, and some bacteria slowly degrade lignin to generate a wide array of aromatic compounds (20, 39). These lignin-derived aromatics serve as sources of carbon and energy for soil microorganisms (19). Thus, soil microorganisms are essential for mineralization of the benzene ring and significant contributors to carbon turnover. Aromatics are highly stable compounds due the resonance energy of the ring

structure; hence, degradation is more limited than for non-aromatics compounds (8, 21, 30). Despite this chemical recalcitrance, microorganisms have developed different strategies to overcome the challenge. In O_2 tolerant conditions, oxygenases play a central role in aromatic ring activation by converting structurally diverse compounds into dihydroxylated compounds that are cleaved by substrate-specific dioxygenases (21, 22). Intermediates generated from these pathways are funneled to the *ortho*-cleavage or β-ketoadipate pathway for further degradation (35). Under O_2 -limited scenarios, aromatics may be attacked by monooxygenases to form non-aromatic epoxides, which are cleavage by hydrolysis. The intermediates of this metabolic route can be diverted to aerobic or anaerobic metabolic pathways based on O_2 availability. Substrates are metabolized as CoA thioesters throughout this pathway, which facilitates otherwise non-feasible reactions. In O_2 -free environments, aromaticity is disrupted by reduction followed by ATP-dependent or ATP-independent reactions for further reduction and ring cleavage (30).

Acinetobacter baylyi strain ADP1 has been shown to thrive on a wide assortment of aromatic compounds as growth substrates, thus contributing greatly to natural carbon circulation (3, 59). Regardless of the relatively small genome (3.6 Mb), ADP1 has extraordinary metabolic versatility with more than 600 genes dedicated to catabolic functions and about 300 genes involved in transport (59). These metabolic characteristics related to adaptation and versatility have permitted ADP1 to be a tool for biotechnical applications and biodegradation.

Benzoate is readily and preferably metabolized by ADP1 compared to other aromatic derivatives such as 4-hydroxybenzoate (31). Organic acids, such as succinate

and acetate suppress expression of genes required for benzoate degradation (29). In ADP1, regulatory mechanisms create a precise order in which carbon sources are consumed. This hierarchy in carbon preferences reveals distinct levels of regulation to ensure maximal energy conservation (6, 7, 31, 32, 60).

β-ketoadipate pathway in *Acinetobacter baylyi* strain ADP1

The β-ketoadipate pathway is considered a convergent route for aromatic compound degradation, which has been identified in a majority of soil microorganisms associated with plants and fungi (35). The β-ketoadipate pathway was discovered long ago and heavily studied in both *Acinetobacter* and *Pseudomonas putida* as reviewed in Hardwood *et al* (35). The different steps and enzymatic reactions identified demonstrated homology between these species concerning this pathway. This similarity indicates that the β-ketoadipate pathway from ADP1 and *Pseudomonas putida* are derived from a common ancestor (10, 46-48). However, this conservation is not solely observed in these two bacteria, studies on the different enzymes involved in the pathway and amino acid sequences reveal that this pathway is highly conserved among soil bacteria (35).

Degradation of aromatics is accomplished in via reactions that funnel many different starting compounds into the lower portion of the β-ketoadipate pathway (Figure 1.1). First, the aromatic compound is activated by undergoing a series of oxygen-dependent modification reactions that result in the formation of one of two dihydroxylated benzene ring intermediates. Based on the chemical structure of the substrate source, the aromatic compounds can be degraded to the hydroxylated catechol and/or protocatechuate (3,4-dyhydroxybenzoate) (35). The next steps in aromatic

Figure 1.1. The β-ketoadipate pathway in ADP1. (A) Aromatic compound degradation proceeds via two branches of the β-ketoadipate pathway (catechol and protocatechuate). Regulators that control gene expression in this pathway are indicated. The (-) represents regulation of the *vanAB* and *hcaCAB* operons by protocatechuate. Primary activators are shown. Many genes needed to convert compounds to catechol and then further degrade it are clustered on the chromosome in one catabolic island (34). Similarly, many genes involved in protocatechuate formation and further catabolic funneling are clustered in another chromosome island (56). **(B)** *ben* and *cat* genes are organized in an approximately 20 kbp chromosomal cluster. Expression of these genes is controlled by BenM and CatM at four major operator-promoter regions (numbered diamonds). The *benPK* and *benE* genes encode membrane proteins (14, 16). Two open reading frames located downstream of *catA*, ORF1 and ORF2, are not expressed during growth on benzoate and muconate (Tumen-Velasquez and Neidle, unpublished results).

A

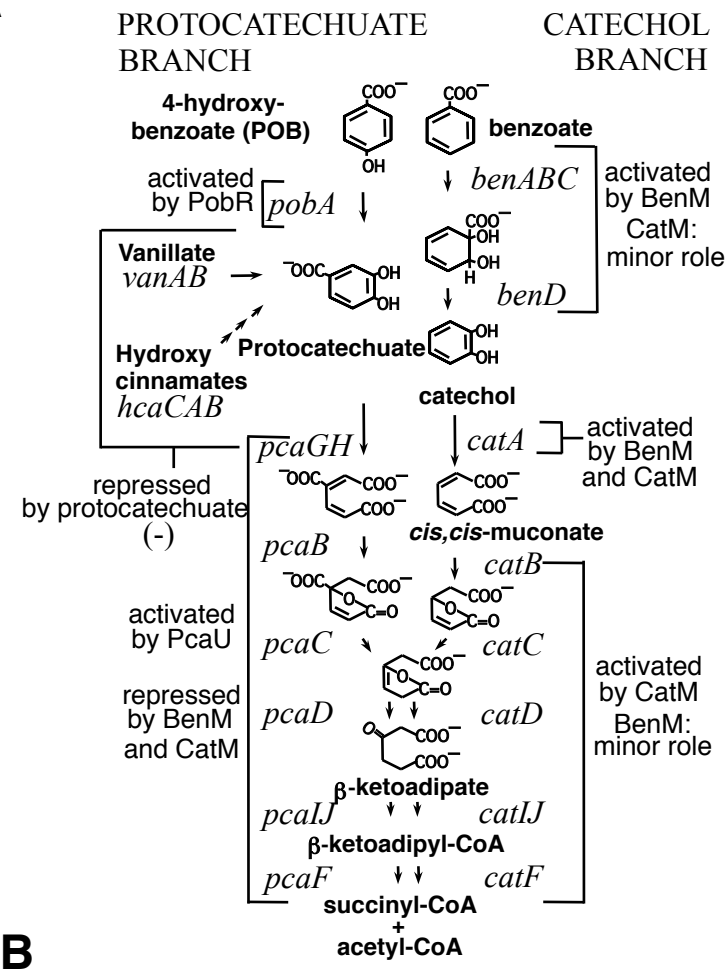
PROTOCATECHUATE BRANCH
CATECHOL BRANCH
4-hydroxy-benzoate (POB)
benzoate
activated by PobR
pobA
benABC
activated by BenM
CatM: minor role
Vanillate
vanAB
benD
Hydroxy cinnamates
hcaCAB
Protocatechuate
catechol
pcaGH
catA
activated by BenM and CatM
repressed by protocatechuate (-)
cis,cis-muconate
pcaB
catB
activated by PcaU
pcaC
catC
repressed by BenM and CatM
pcaD
catD
activated by CatM
BenM: minor role
β-ketoadipate
pcaIJ
catIJ
β-ketoadipyl-CoA
pcaF
catF
succinyl-CoA
+
acetyl-CoA

B

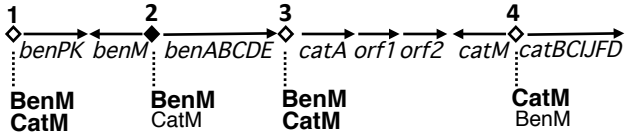
1
2
3
4
benPK
benM
benABCDE
catA orf1 orf2
catM
catBCIJFD
BenM CatM
BenM CatM
BenM CatM
CatM BenM

degradation include ring fission between the hydroxylated groups, the *ortho* or intradiol position, and further breakdown by enzymes involved in these pathways generating succinyl-CoA and acetyl-CoA. These products enter central metabolism via the tricarboxilic acid cycle. The catechol and protocatechuate routes have different enzymes for comparable pathways. This difference is due to the presence of the carboxyl group in protocatechuate that it is not present in catechol, which affects subsequent steps. Thus, ring cleavage for the catechol and protocatechuate pathways is catalyzed by catechol 1, 2-dioxygenase and protocatechuate 3, 4-dioxygenase, respectivately. As expected, both branches have different enzymes and intermediates for following steps, but the reactions become identical at the enol lactone step, when decarboxylation of protocatechuate takes place. Although the reactions are the same, two independently regulated isofunctional enzymes carry out the last three steps of the pathway reflecting different transcriptional regulation of the genes (23, 35). In *Pseudomonas putida* one enzyme carries out the final steps after enol lactone formation. In ADP1, two isofunctional sets of enzymes found in the catechol (*catIJF*) and protocatechuate (*pcaIJF*) branches carry out these last steps of degradation to tricarboxylic acid cycle intermediates (Figure 1.1) (10).

Regulation of benzoate metabolism in ADP1

In *A. baylyi,* BenM and CatM, two LysR-type transcriptional regulators (LTTRs) control benzoate degradation in a dual regulatory system. In this system, the levels of effector compounds that interact with BenM and CatM govern benzoate degradation (15, 52). The BenM and CatM regulatory system provides a unique model for identifying key interactions among effectors, proteins and DNA. The genes needed for benzoate

degradation (*ben-cat* genes) are clustered in the chromosome, where BenM and CatM control expression from multiple promoters (Figure 1.1B). Both regulators play equal regulatory roles at the *benPK* operon, where activation is muconate-dependent (14, 16). At the *benABCDE* operon, BenM is the major regulator and induces gene expression synergistically in response to the presence of benzoate and one of its metabolites, muconate (9, 15). Despite binding to the *benABCDE* promoter, CatM fails to activate sufficient *ben*-gene transcription to sustain benzoate growth in a strain lacking BenM (15, 27).

As proposed previously, BenM and CatM control regulation of the *catA* gene, whose expression is required for the conversion of catechol to muconate (15). Studies described in detail in chapter 4 revealed that BenM also activates this promoter synergistically in response to benzoate and muconate. On the other hand, CatM activates high levels of *catA* gene expression in response to muconate only. CatM is the major regulator of the *catBCIJFD* operon and activates gene expression in response to muconate only (52). The gene products of the latter *cat* genes are responsible for converting muconate to succinyl-CoA and acetyl-CoA. Chapter 2 reveals that BenM can also activate the *catBCIJFD* promoter but only in response to muconate. In a strain lacking CatM, this muconate-dependent activation of the *cat* genes allows very slow growth on benzoate (27). Intermediates such as muconate are toxic to the cell. Therefore, it is reasonable to assume that muconate generation mediated by CatA and degradation mediated by CatB are tightly regulated in this system and encoded from different promoters. BenM and CatM, similar to other LTTRs, regulate their own gene expression. This tight control of the

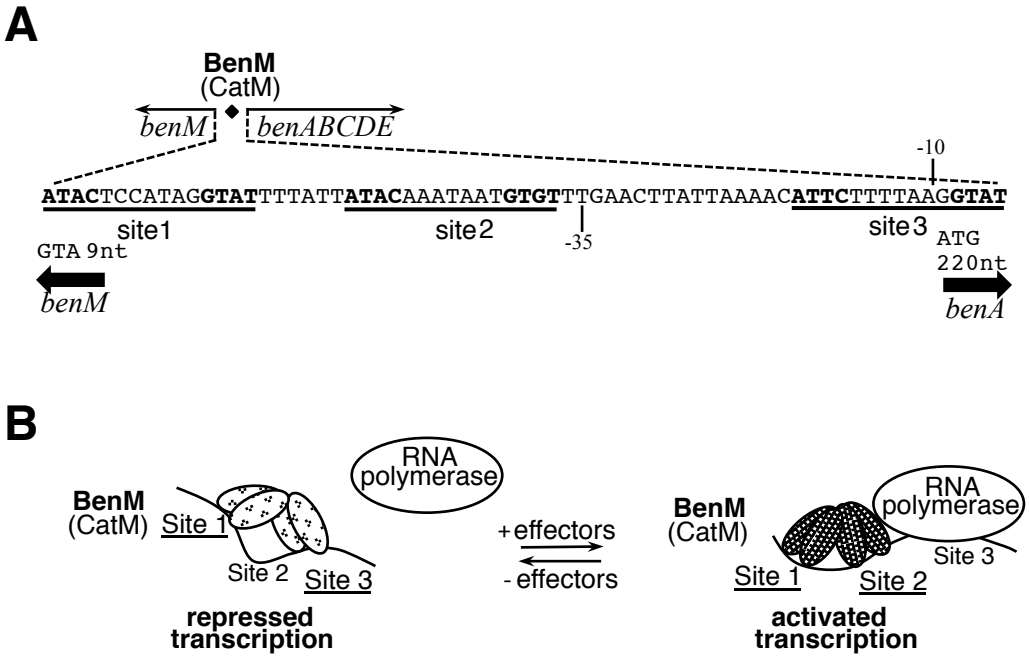

Figure 1.2. BenM and CatM regulon of ADP1. (A) Potential binding sites for BenM and CatM at the *benMA* intergenic region. Site 1 matches the consensus (underlined) LTTR-binding motif (T-N_{11}-A). Site 2 and Site 3 differ by one nucleotide from the consensus sequence, which reduces the dyad symmetry. Transcriptional start site (+1) for *benA* is not shown. Promoter elements (-10 and -35) are indicated for this promoter. In this locus, BenM controls transcription of its own expression as well as the divergent *benABCDE.* **(B)** Model of *benA* regulation. Both BenM and CatM bind Site 1 and Site 3 in the absence of effectors. In this conformation transcription is repressed. With effectors, BenM or CatM reposition to Site 1 and Site 2. However, in this conformation, BenM activates *benA* transcription (18).

pathway at the transcriptional level allows ADP1 to utilize benzoate as its sole carbon source.

BenM and CatM DNA binding characteristics

Studies on LTTR-DNA binding have shown that in the presence or absence of their cognate effectors LTTRs occupy different sites in the promoter regions of the genes under their regulation (40, 54). DNase I footprinting experiments have shown that the intergenic region between *benM-benA* holds multiple binding sites (Figure 1.2.A). As with other LTTRs, BenM and CatM function as tetramers, thus they bind a large region of promoter DNA.

In the absence of effectors, BenM and CatM repress *benA* expression (Figure 1.2.B). At this region, three DNA sequences recognized by BenM and CatM are found. These sequences contain a LTTR consensus binding site with a T-eleven nucleotides-A (T-N_{11}-A) where the T and A reside in a short segments with dyad symmetry that can vary in both base pair composition and length (40). BenM and CatM bind to sequences that display, ATAC-N_7-GTAT. In the absence of effectors, a BenM tetramer binds to sites 1 and 3 repressing *benA*. Site 3 overlaps directly with the -10 promoter region. Thus, when this site is protected, it may block RNA polymerase binding to this promoter sequence. With effectors, benzoate and muconate, the BenM tetramer repositions to site 1 and 2 (Figure 1.2.B) (15). In this conformation, BenM activates *benA* transcription, probably by contacting RNA polymerase. The presence of either or both effectors causes BenM to have a similar position on the DNA. However, the activation levels are different

because muconate alone promotes higher levels of *benA* transcription than benzoate alone. As explained above, both effectors cause a synergistic effect at this locus.

CatM-mediated regulation of benzoate degradation in ADP1

Although BenM and CatM are 59% similar in amino acid sequence, these proteins are not redundant. A BenM-mediated response alone is insufficient to activate the appropriate levels of gene expression for growth on benzoate as the carbon source. Similarly, CatM-dependent regulation is not enough to activate the genes responsible for benzoate degradation, despite the response of both LTTRs to muconate (15, 27). Interestingly, in a *benM* mutant background, growth on benzoate can be achieved by mutations in operator-promoter regions (*benA* and *catB*) and/or the *catM* gene that result in altered promoter specificity. A point mutation in the -35 region of the *benA* promoter enables a *benM*-disrupted strain to grow on benzoate. This single nucleotide change in *benA*-promoter located at site 1 makes this mutated sequence resemble that of *catB*-promoter site 1, where CatM has been shown to bind. Another point mutation in the *benA* promoter located at -9 relative to the transcription start site also permits CatM-mediated regulation. With either mutation, *ben*-gene activation is high with no effector and this activation increases in the presence of muconate. This activation without an effector most likely allows initial benzoate degradation until levels of muconate are sufficient to increase *ben* genes activation to enable benzoate degradation (27). These mutations not only affect the *ben* operon, but regulation at other promoters controlled by CatM (Tumen-Velasquez and Neidle, unpublished results).

Mutations in the *catM* gene have been identified which allow CatM-mediated activation of benzoate degradation in the absence of BenM. CatM[R156H] activates expression from *benA, catA,* and *catB* in the absence of muconate. However, expression from these promoters increases further with muconate. CatM[V158M], unlike wild-type CatM has been shown to increase *benA* expression in response to muconate. It has the opposite effect at the *catB* and *catA* promoters, which also differs from wild-type CatM-mediated activation (27). Studies on these variants suggest that levels of muconate control activation at these promoters and allow growth of benzoate as a sole carbon source. As described in detail in chapter 2 and 3, seven independent CatM variants have been isolated. Studies on these newly characterized CatM variants suggest distinct alterations of protein-promoter DNA interactions and protein oligomerization caused by single amino acid changes.

BenM and CatM structural features and studies

BenM and CatM protein structures have been extensively studied, and effector binding domain (EBD) structures of both regulators with and without their cognate effectors were the first structures of these regulators to be solved by X-ray crystallography (13, 28). Due to low solubilization properties, the initial protein structures of BenM and CatM lacked the first 80 N-terminal residues, which includes the DNA binding domains (DBD) and linker helix (LH). Similar to other LysR-type structures, the EBDs of BenM and CatM consist of two α/β domains (EBD I and EBD II) that use Rossmann folds divided by a hinge formed from the central regions of the antiparallel β-strands (Figure 1.3). EBD I contains amino acid residues from 87-161 and

268-300 (C-terminal helix), while EBD II confers residues 162 to 267. BenM-EBD and CatM-EBD structures are nearly identical and their subunits associate to form stable dimers (28).

BenM-EBD crystals soaked with muconate show binding of this effector to the pocket region between domains EBD I and EBD II (Figure 1.3). This region was described as the primary effector-binding site in BenM. This site is similar to the one occupied by muconate in the CatM-EBD crystal. Benzoate can also occupy this pocket in BenM-EBD, but not in CatM-EBD (28). Interestingly, benzoate was found to bind an additional binding site located inside the hydrophobic core of EBD I in the BenM-EBD (Figure 1.3). This site is described as the secondary binding site in BenM-EBD. Low and high concentrations of benzoate failed to bind to the CatM-EBD, which correlates to the inability of CatM to respond to benzoate as an effector. It was also discovered that CatM lacks key amino acids residues that directly interact with benzoate in the secondary binding site of BenM-EBD (17, 28). As described in more detail in chapter 2, changes of some of these residues in CatM-EBD do not recreate a benzoate response in CatM (57).

Muconate that is bound to the cleft between EBDI and EBD II in BenM and CatM permits transcriptional activation from the *ben* and *cat* genes. Muconate-mediated-EBD interactions in the primary binding site are highly conserved between BenM and CatM with only one amino acid difference at this site (Ser98 in CatM and Gly98 in BenM). EBD structures with and without muconate revealed that muconate-regulator interactions cause the two EBD domains to move towards each other (28). Water molecules bridge some of these interactions along with direct interactions between the carboxylate atoms

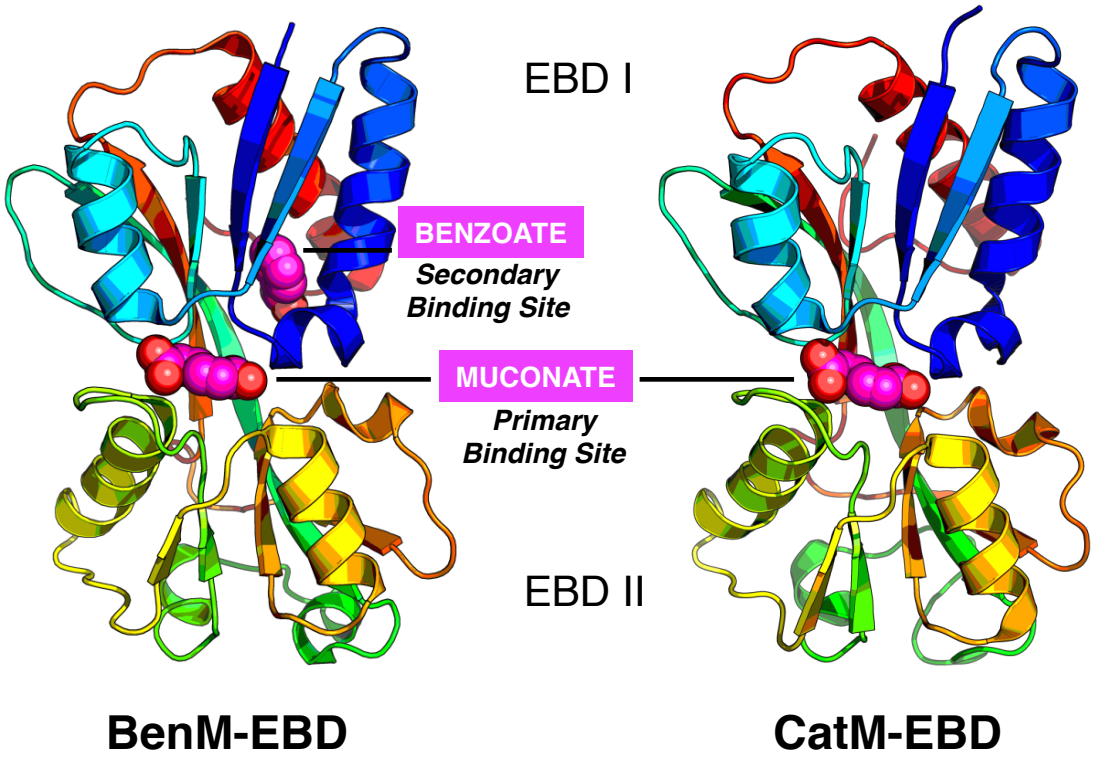

Figure 1.3. Ribbon representation of BenM-EBD and CatM-EBD subunits. Muconate is bound to the primary binding site present in both BenM and CatM, and benzoate is bound to the secondary binding site only in BenM. EBD I contains amino acid residues from 87-161 and 268-300 (C-terminal helix), while EBD II contains residues 162 to 267. BenM-EBD and CatM-EBD structures are nearly identical and their subunits associate to form stable homo-dimers (Figure adapted from Ezezika *et al.*, 2007 and Craven *et al.,* 2009).

of muconate and the residues in this pocket (Figure 1.4.A). The negatively charged carboxyl groups of bound muconate are stabilized by the positive dipole moments due to the orientation of the four helices located in this region. There are no positively charged residues in this region, thus these interactions are very significant. It is predicted that enhancement of the dipole moments of these helices by local mutations or ligand binding could lead to an increase in transcriptional activation. Even when interactions with residues at this region form, benzoate binds loosely to this site (28).

In the secondary binding site in BenM-EBD, the carboxyl group of benzoate forms a salt bridge with the side chain of Arg160 (Figure 1.4.B). The hydroxyl of Tyr293 and the main chain amide of Leu104 form hydrogen bonds with the carboxyl group of benzoate as well. Hydrophobic interactions are significant between the side chains of residues Leu100, Leu105, Ile108, Phe144, Leu159, Ile269 and Ile289 and the phenyl ring of benzoate. This hydrophobic pocket is also observed in CatM-EBD, but unlike BenM the residues that directly interact with benzoate such as Tyr293 and Arg160 are absent in CatM.

In CatM-EBD, His160 fails to interact directly with benzoate because it is too distant and Phe293 cannot form a hydrogen bond to benzoate as Tyr293 does in BenM (28). When these residues from CatM were changed in BenM, the resultant BenM variants failed to bind benzoate to the secondary binding site, and lost the benzoate response. In addition, these BenM variants were unable to grow on benzoate as a sole carbon source (17). Only benzoate, and not muconate, can bind to this site in BenM-EBD.

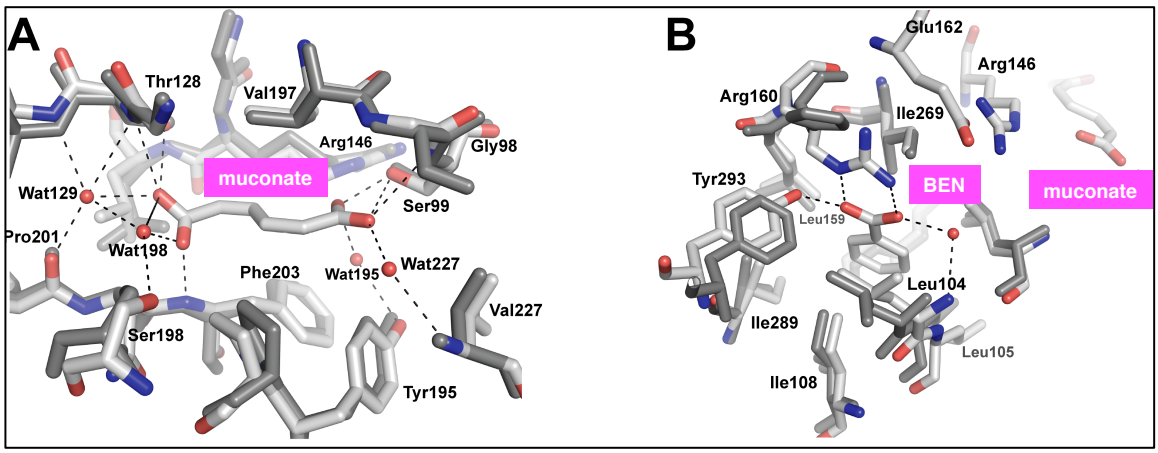

Figure 1. 4. Primary (A) and Secondary (B) effector-binding sites of BenM-EBD and CatM-EBD. The CatM-EBD was superimposed (dark grey) onto that of BenM (light grey with darker nitrogen and oxygen atoms). In **(A)**, muconate is shown bound in the primary sites of BenM. For clarity, only the water molecules coordinated to BenM are depicted. Water molecules (Wat) are numbered according to their nearest amino acid. Residues from the primary binding site are essentially the same in BenM and CatM except for Gly98, which corresponds to Ser98 in CatM. In **(B)**, a benzoate molecule can only bind in the secondary site of BenM-EBD. Residues that bind to the carboxylate group of benzoate (Try293 and Arg160) are not found in CatM where Phe293 and His160 are found instead (Figure adapted from Craven *et, al*. 2008) (18).

In one BenM-EBD subunit, muconate and benzoate are bound to the primary and secondary binding sites respectively. Benzoate bound to the secondary site is proposed to produce the synergistic response of BenM by accentuating the signal from muconate bound to the primary site. This synergistic activation of BenM most likely involves two mechanisms, the bulk displacement of the hydrophobic core around the benzoate-binding site and /or a change in the electrostatic environment (28). It is suggested that Glu162 is a key residue that links regulatory effects from primary and secondary binding sites. Neighboring interactions between Glu162 and Arg160 or Arg146 can change the electrostatic distribution within BenM. Upon benzoate binding to the secondary binding site, Arg160 forms a salt bridge with the carboxyl group of the benzoate, and Glu162 form a salt bridge with Arg146 (Figure 1.5). The neutralization of Arg146 enhances the negative charge of muconate and therefore the surrounding helices should draw towards muconate more strongly. These changes most likely stabilize conformational changes needed for transcriptional activation (28). Without benzoate, Glu162 forms a salt bridge with Arg160. Therefore, the positively charged Arg146 might weaken the electrostatic pull between the surrounding helices and muconate. These alterations could account for the conformational changes between the tetramer bound to one or both effectors.

Oligomerization of BenM

Full-length BenM crystallized as a dimer with each subunit displaying two conformations (compact and extended) to form an asymmetric unit (Figure 1.6.B). The EBD II/EBD II interface resembles previous BenM-EBD structures, which refers to residues located on the surface of helix 9, in α10, and in the loop region between β3 and

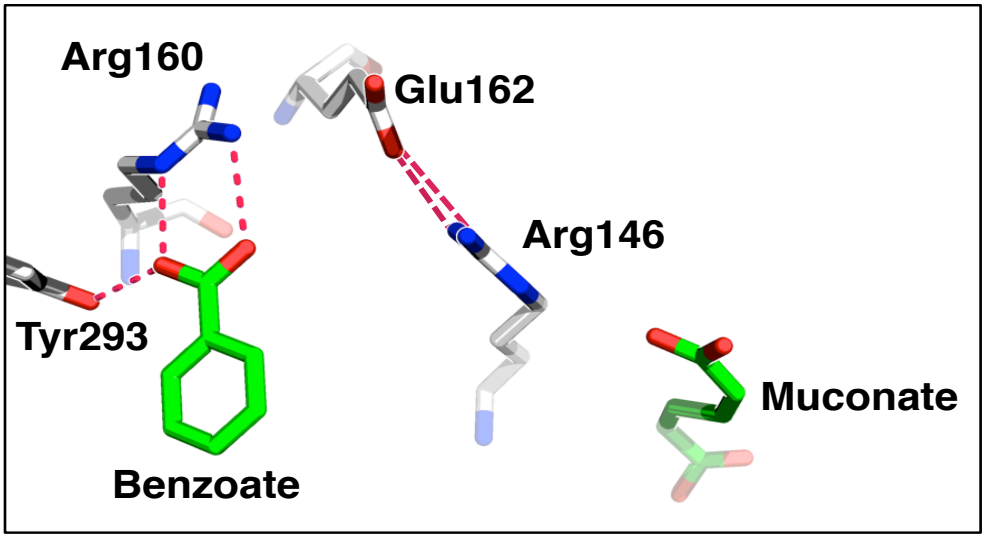

Figure 1. 5. Residues in a charge relay system proposed to underlie the synergistic response of BenM to benzoate and muconate. Synergistic transcriptional activation may rely on simultaneous occupation of the primary and secondary effector-binding sites by muconate and benzoate, respectively. In the absence of benzoate, Glu162 may interact with either Arg160 or Arg146. Upon benzoate binding, the interaction between Arg160 and benzoate permits Glu162 to associate solely with Arg146. It is proposed that the presence of benzoate diminishes the ability of the positively charged Arg146 to neutralize the negatively charged muconate. The net result of this shielding effect of Glu162 on Arg146 is to enhance the interactions of muconate at the primary binding site, which may increase conformational changes that draw the helices more closely toward muconate (Ezezika *et al.,* 2007a; Craven *et al.,* 2009) (18, 28).

β4. This interface has been described as the α10-α10 tetramer interface located between EBD dimers in a functional tetramer (Figure 1.6.A). The α10-α10 tetramer interface has been observed previously on EBD crystal structures solved under high pH conditions (53). Seven residues including Lys148, Ser150, Asn185, Asn209, Ser212, Asp213, and Asp262 contribute hydrogen bond interactions between the EBD II subunits. This interface is most likely influenced by effector binding due to the proximity of the effector binding sites to the interface. A variant, CatM[R156H], with an amino acid substitution in this region was shown to alter molecular interactions associated with this region (17). This substitution in CatM allows CatM-mediated activation of the *ben* genes without BenM. As described in chapter 2, two variants with changes located in this α10-α10 tetramer interface, CatM[ΔD264] and CatM[K148Q], activate high muconate-inducible levels of *benA* expression without BenM. These amino acids are directly involved in molecular interactions within the α10-α10 tetramer interface. Thus, mutations in this interface are likely to promote changes in transcriptional activation. A detailed analysis of the latter CatM variants in chapter 2 supports the regulatory importance of interface interactions.

Another interface between EBD subunits observed in all known LTTR structures is also present in full-length BenM (Figure 1.6.A). This interface, termed α6/β2-α11dimer interface involves interactions between these regions and helix12. The α6/β2-α11dimer interface is organized by subunits arranged in an antiparallel fashion. Previous BenM variants (BenM[R225H] and BenM[E226K]) identified in spontaneously isolated mutants were found to activate high levels of *benA* transcription without effectors. These residues

Figure 1.6 Interlocking BenM molecules via common LysR-type interfaces (A) and extended and compact forms of CbnR (B). A BenM dimer in one asymmetric unit interacts with another BenM dimer through the α6/β2-α11 dimer interfaces of the EBDs. This interface is found in all known LTTR crystal structures. Two helices of the asymmetric unit interact with one another at the α10-α10 tetramer interface (Figure adapted from Ruangprasert *et al.*, 2010) (53). **(B)** Similar to CbnR subunits, BenM subunits fold into an extended form and compact form. (Figure adapted from Muraoka *et al*., 2003) (44, 53)

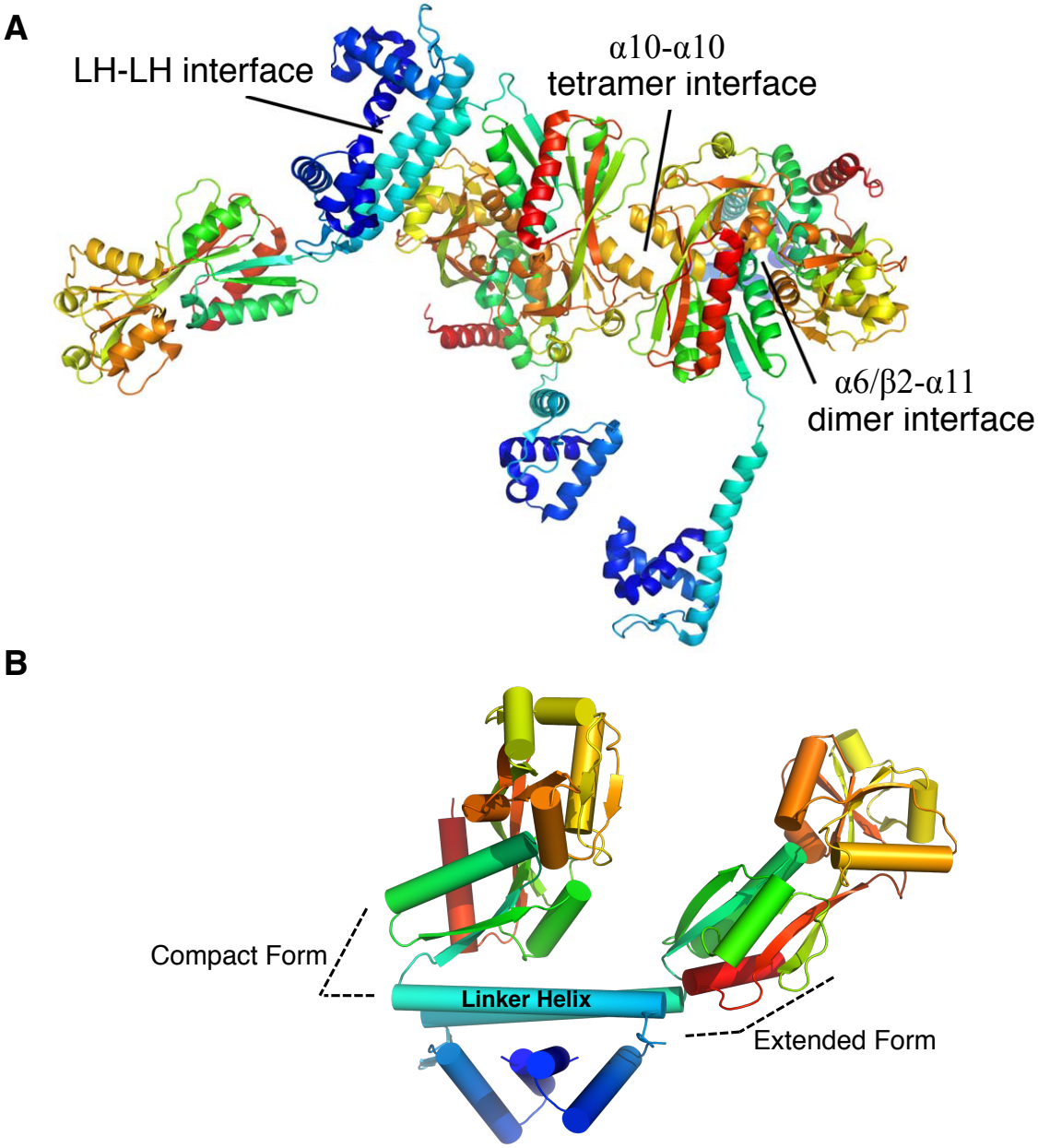
A
LH-LH interface
α10-α10
tetramer interface
α6/β2-α11
dimer interface
B
Compact Form
Linker Helix
Extended Form

are located at the center of the α6/β2-α11dimer interface and are conserved between BenM and CatM. In chapter 2, a CatM variant (CatM[G232S]) was able to activate higher than normal *benA* transcription in the absence of BenM. Gly232, an amino acid conserved in CatM and BenM is located in α11 and contributes through hydrophobic interactions with neighboring side-chains to the dimer interface. Thus, amino acid changes in this region in both BenM and CatM most likely affect the dimer interface environment and results in proteins with altered transcriptional activation properties (17, 57).

As described in Ruangprasert *et al.*, BenM forms a tetramer by an oligomerization arrangement termed Scheme I (42, 53). This scheme is assigned to LTTRs that oligomerized via the α10-α10 tetramer interface and additional DBD interactions. Regulators identified to form a tetramer via this scheme include CbnR, BenM, and DntR. Scheme II describes oligomerization without using the α10-α10 tetramer interface, but using the α6/β2-α11dimer interface and DBD/LH interactions. ArgP, AphB, CrgA and TsaR adopt this organization for assembly. Lastly, Scheme III refers to an arrangement different to those of Scheme I and II. Only a putative LTTR from *Pseudomonas putida*, 3FZV is reported to assemble with this scheme (53). While tetramer formation via the α10-α10 tetramer interface or the α6/β2-α11dimer interface appears to vary in all LTTR full-length structures, the interface formed through the linker helixes of two subunit structures (LH-LH interface) is well-conserved in all tetramers. This interface describes dimerization of LHs from two asymmetric subunits through an antiparallel arrangement (Figure 1.7.B). Therefore, the LH-LH interface may be the main contributor to oligomer assembly in LTTRs. Studies on CatM-mediated benzoate degradation described

extensively in chapters 2 and 3 resulted from CatM variants with amino acid replacements found in all interfaces described above, which are essential for protein oligomerization. Consequently, residues located at these regions are key for tetramer formation and changes at these residues in CatM results in altered transcriptional activation.

BenM and CatM DBD characteristics and structural studies

LysR-type regulators use highly conserved interactions between amino acids and nucleic acid bases of their cognate promoter and many less conserved interactions. These proteins-DNA interactions contribute to DNA recognition and promoter specificity. Structural studies of the BenM-DNA recognition domain (DBD-LH) alone and with complexes of two subunits bound to Site 1 of promoter regions (*benA* and *catB*) revealed important residues, sequence-specific recognition and key protein-DNA interactions (1).

BenM and CatM are nearly identical in this domain (84% amino acid sequence identity) and only differ in 9 amino acids in their DBDs. As described in this dissertation, electrophoretic mobility shift assays have shown that both regulators can bind to *benA, catA,* and *catB*, despite mediating transcriptional activation differently at these promoters. Alignment of operator-promoter regions of *benA* and *catB,* shows that site 1 of both promoters have the perfect ATAC-N_7-GTAT palindrome that most likely anchors BenM or CatM to the promoter. This DNA sequence is essential for BenM binding to the *benA* promoter and is probably essential for CatM-*catB* binding as well. Site 2 and Site 3 differ from the consensus of Site 1 and these two sites are also different between both promoters.

As described in chapter 2, the replacement of CatM-DBD with that of BenM resulted in a variant CatM protein capable of binding with relative high affinity to *benA* and *catB*. Subsequently, two BenM amino acid replacements at positions 18 and 38 in CatM also resulted in variant regulators with altered promoter specificity, which supports the importance of these specific residues for protein-DNA interactions. Interestingly, these DBD studies revealed the involvement of this domain in the benzoate-mediated response. CatM can acquire a benzoate response only when the DBD is replaced with that of BenM along with amino acid replacements at positions 293 and 160. With these changes, CatM can synergistically activate *benA* in response to muconate and benzoate. However, the most important property exhibit by these studies is the requirement of the BenM-DBD for the synergistic response at the *catB* promoter, a promoter recognized by CatM. These DBD studies provide a framework to elucidate regulatory roles of distinct domains in CatM and BenM as well as the interconnection to transmit signals upon DNA and effector binding. Collectively, this dissertation clarifies the essential connections between regulatory domains of BenM and CatM with promoter DNA needed for effective transcriptional activation. These interactions are crucial for proper benzoate degradation in *Acinetobacter baylyi* strain ADP1.

LTTR studies in ADP1: From the bench to the classroom!

Previous studies conducted in the Neidle lab have strengthened the role of ADP1 as an ideal organism for functional and structural studies of LysR-type regulators (15, 17, 27, 52). As described in Craven *et al.* 2008*,* there are 44 predicted LTTRs in *A. baylyi* with proposed functions involved in varied cellular processes (18). BenM and CatM have

been extensively studied functionally and structurally in *A. baylyi* and are the focal point of most studies described throughout this dissertation. These studies have provided insights about transcriptional regulation and aromatic compound catabolism. With the LTTR repertoire provided by *A. baylyi,* similar studies used in BenM and CatM characterization can be used to begin assessing functions of other LysR homologs in ADP1.

Taking advantage of the natural competency and genetic malleability of *A. baylyi*, a laboratory course (MIBO 4600L, designed by Dr. Anna Karls, Dr. Ellen Neidle and Dr. Katherine Elliott) was designed to implement comprehensive LTTR studies where students performed distinct experimental tasks to determine and characterize functions of several LTTR homologs. With the help of MIBO 4600L students from spring 2012, spring 2013 and students from the Neidle and Momany Labs, eight new LTTRs have been characterized. Studies of five of these proteins serve as the foundation for subsequent projects for graduate students in the Neidle lab. A concise overview of some of these studies is provided below.

ACIAD2597 (ACIAD corresponds to the unique identification of putative genes in the ADP1 genome described in Barbe *et al.,* 2004) was renamed CysB based on its function of cysteine synthesis and sulfur/sulfonate metabolism. Deletion or disruption of the *cysB* gene resulted in cysteine auxotrophy. Based on preliminary studies, this CysB regulator might exhibit a different regulation than a previously studied CysB, a homolog regulator from *Escherichia coli* (Stephanie Thurmond, unpublished data). A full-length structure has been solved for this LTTR, which reveals an unusual oligomerization where DBDs might require conformational rearrangement in order to interact with promoter

DNA (Melesse Nune and Cory Momany, unpublished data). ACIAD0746, predicted to encode a FinR homolog, has been identified to be an essential gene in ADP1. However, further bioinformatics analysis revealed that FinR has homology with CysL, a regulator from *Bacillus subtilis* involve in regulation of sulfite/sulfide metabolism. Gel shift assays shown that FinR binds a region upstream *cysI,* whose product encodes a sulfite reductase. Therefore, FinR along with CysR are regulators with roles in cysteine synthesis. Further studies are conducted to clarify details on cysteine regulation in *A. baylyi* mediated by FinR and CysR (Stephanie Thurmond, unpublished data). A crystal structure for full-length FinR has been solved as well (Melesse Nune and Cory Momany, unpublished data).

ACIAD1543 and ACIAD1537 (renamed TclR and TcuR respectively) are paralogs involved in tricarballylate degradation in ADP1. Tricarballylate degradation has been extensively studied in *Salmonella enterica serovar Typhimurium* str. LT2, where TcuR is the only regulator of the *tcu* genes needed for tricarballylate consumption. In ADP1, deletion of *tcuR* and not *tclR* abolished growth on tricarballylate as sole source of carbon and energy. Thus, TcuR might be the main regulator for the *tcu* genes with tricarballylate as its cognate effector. Starting from a *tcuR* disruption strain (strain unable to growth on tricarballylate), spontaneous tcu+ mutants have been isolated and characterized (Nicole Laniohan, unpublished data). Interestingly, single point mutations have been identified in the *tclR* gene that encoded amino acid replacements at the EBD portion of the protein. Thus, these TclR variants can compensate for the absence of TcuR and carry out tricarballylate degradation. Further studies are conducted to determine the

TclR-mediated regulation exhibit by these TclR variants (Nicole Laniohan, unpublished data).

Lastly, bioinformatic analysis on ACIAD0461 (renamed LeuR) predicted a function involved in regulation of leucine biosynthesis. As described in detail in appendix A, LeuR acts as a repressor for genes engaged in this pathway, which differs from LeuO, the leucine activator found in *Escherichia coli* and *Salmonella enterica* (58). Given the importance of LysR-type transcriptional regulators, LTTR studies on ADP1 describe here are expanding our understanding of diversity in microbial metabolism and ease the elaboration of biotechnology applications.

References

1. **Alanazi AM, Neidle EL, Momany C.** 2013. The DNA-binding domain of BenM reveals the structural basis for the recognition of a T-N11-A sequence motif by LysR-type transcriptional regulators. Acta. Crystallogr. D. **69:**1995-2007.
2. **Averhoff B, Graf I.** 2008. The Natural Transformation System of *Acinetobacter baylyi* ADP1: A Unique DNA Transport Machinery. In Acinetobacter Molecular Biology. Gerischer, U. (ed.). Norfolk: Caiester Academic Press, pp. 119-139. .
3. **Barbe V, Vallenet D, Fonknechten N, Kreimeyer A, Oztas S, Labarre L, Cruveiller S, Robert C, Duprat S, Wincker P, Ornston LN, Weissenbach J, Marliere P, Cohen GN, Medigue C.** 2004. Unique features revealed by the genome sequence of *Acinetobacter* sp. ADP1, a versatile and naturally transformation competent bacterium. Nucleic. Acids. Res. **32:**5766-5779.
4. **Baumann P.** 1968. Isolation of *Acinetobacter* from soil and water. J. Bacteriol. **96:**39-42.
5. **Baumann P, Doudoroff M, Stanier RY.** 1968. A study of the *Moraxella* group. II. Oxidative-negative species (genus *Acinetobacter*). J. Bacteriol. **95:**1520-1541.
6. **Bleichrodt FS, Fischer R, Gerischer UC.** 2010. The beta-ketoadipate pathway of *Acinetobacter baylyi* undergoes carbon catabolite repression, cross-regulation and vertical regulation, and is affected by Crc. Microbiology. **156:**1313-1322.
7. **Brzostowicz PC, Reams AB, Clark TJ, Neidle EL.** 2003. Transcriptional cross-regulation of the catechol and protocatechuate branches of the beta-ketoadipate pathway contributes to carbon source-dependent expression of the *Acinetobacter sp.* strain ADP1 *pobA* gene. Appl. Environ. Microbiol. **69:**1598-1606.

8. **Bugg TD, Ahmad M, Hardiman EM, Singh R.** 2011. The emerging role for bacteria in lignin degradation and bio-product formation. Curr. Opin. Biotechnol. **22:**394-400.

9. **Bundy BM, Collier LS, Hoover TR, Neidle EL.** 2002. Synergistic transcriptional activation by one regulatory protein in response to two metabolites. Proc. Natl. Acad. Sci. U. S. A. **99:**7693-7698.

10. **Canovas JL, Stanier RY.** 1967b. Regulation of the enzymes of the beta-ketoadipate pathway in *Moraxella calcoacetica*. 1. General aspects. Eur. J. Biochem. **1:**289-300.

11. **Carr EL, Kampfer P, Patel BK, Gurtler V, Seviour RJ.** 2003. Seven novel species of *Acinetobacter* isolated from activated sludge. Int. J. Syst. Evol. Microbiol. **53:**953-963.

12. **Chen I, Dubnau D.** 2003. DNA transport during transformation. Front. Biosci. **8:**s544-556.

13. **Clark T, Haddad S, Neidle E, Momany C.** 2004. Crystallization of the effector-binding domains of BenM and CatM, LysR-type transcriptional regulators from *Acinetobacter* sp. ADP1. Acta. Crystallogr. D. **60:**105-108.

14. **Clark TJ, Momany C, Neidle EL.** 2002. The *benPK* operon, proposed to play a role in transport, is part of a regulon for benzoate catabolism in *Acinetobacter* sp. strain ADP1. Microbiology. **148:**1213-1223.

15. **Collier LS, Gaines GL, 3rd, Neidle EL.** 1998. Regulation of benzoate degradation in *Acinetobacter* sp. strain ADP1 by BenM, a LysR-type transcriptional activator. J. Bacteriol. **180:**2493-2501.

16. **Collier LS, Nichols NN, Neidle EL.** 1997. *benK* encodes a hydrophobic permease-like protein involved in benzoate degradation by *Acinetobacter* sp. strain ADP1. J. Bacteriol. **179:**5943-5946.

17. **Craven SH, Ezezika OC, Haddad S, Hall RA, Momany C, Neidle EL.** 2009. Inducer responses of BenM, a LysR-type transcriptional regulator from *Acinetobacter baylyi* ADP1. Mol. Microbiol. **72:**881-894.

18. **Craven SH, Ezezika OC, Momany C, Neidle EL.** 2008. LysR Homologs in *Acinetobacter* : Insights into a Diverse Family of Transcriptional Regulators. In *Acinetobacter Molecular Biology*. Gerischer, U. (ed.). Norfolk: Caiester Academic Press, pp. 163-202.

19. **Dagley S.** 1987. Lessons from biodegradation. Annu. Rev. Microbiol. **41:**1-23.

20. **Dagley S.** 1978b. Microbial catabolism, the carbon cycle and environmental pollution. Naturwissenschaften. **65:**85-95.

21. **Dagley S, Chapman PJ, Gibson DT, Wood JM.** 1964. Degradation of the benzene nucleus by bacteria. Nature. **202:**775-778.

22. **Dagley S, Fewster ME, Happold FC.** 1953. The bacterial oxidation of aromatic compounds. J. Gen. Microbiol. **8:**1-7.

23. **Dagley S, Gibson DT.** 1965. The Bacterial degradation of catechol. Biochem. J. **95:**466-474.

24. **de Vries J, Wackernagel W.** 2002. Integration of foreign DNA during natural transformation of *Acinetobacter* sp. by homology-facilitated illegitimate recombination. Proc. Natl. Acad. Sci. U. S. A. **99:**2094-2099.

25. **Dijkshoorn L, Nemec A.** 2008. The diversity of the genus *Acinetobacter*. In Acinetobacter Molecular Biology. Gerischer, U. (ed.). Norfolk: Caiester Academic Press, pp. 1-34.

26. **Dijkshoorn L, Van Harsselaar B, Tjernberg I, Bouvet PJ, Vaneechoutte M.** 1998. Evaluation of amplified ribosomal DNA restriction analysis for identification of *Acinetobacter* genomic species. Syst. Appl. Microbiol. **21:**33-39.

27. **Ezezika OC, Collier-Hyams LS, Dale HA, Burk AC, Neidle EL.** 2006. CatM regulation of the *benABCDE* operon: functional divergence of two LysR-type paralogs in *Acinetobacter baylyi* ADP1. Appl. Environ. Microbiol. **72:**1749-1758.

28. **Ezezika OC, Haddad S, Clark TJ, Neidle EL, Momany C.** 2007. Distinct effector-binding sites enable synergistic transcriptional activation by BenM, a LysR-type regulator. J. Mol. Biol. **367:**616-629.

29. **Fischer R, Bleichrodt FS, Gerischer UC.** 2008. Aromatic degradative pathways in *Acinetobacter baylyi* underlie carbon catabolite repression. Microbiology. **154:**3095-3103.

30. **Fuchs G, Boll M, Heider J.** 2011. Microbial degradation of aromatic compounds - from one strategy to four. Nat. Rev. Microbiol. **9:**803-816.

31. **Gaines GL, 3rd, Smith L, Neidle EL.** 1996. Novel nuclear magnetic resonance spectroscopy methods demonstrate preferential carbon source utilization by *Acinetobacter calcoaceticus*. J. Bacteriol. **178:**6833-6841.

32. **Gerischer U.** 2002. Specific and global regulation of genes associated with the degradation of aromatic compounds in bacteria. J. Mol. Microbiol. Biotechnol. **4:**111-121.

33. **Gerner-Smidt P, Tjernberg I, Ursing J.** 1991. Reliability of phenotypic tests for identification of *Acinetobacter* species. J. Clin. Microbiol. **29:**277-282.

34. **Gralton EM, Campbell AL, Neidle EL.** 1997. Directed introduction of DNA cleavage sites to produce a high-resolution genetic and physical map of the *Acinetobacter* sp. strain ADP1 (BD413UE) chromosome. Microbiology. **143 (Pt 4):**1345-1357.

35. **Harwood CS, Parales RE.** 1996. The beta-ketoadipate pathway and the biology of self-identity. Annu. Rev. Microbiol. **50:**553-590.

36. **Ismail W.** 2008. Benzoyl-coenzyme A thioesterase of *Azoarcus evansii*: properties and function. Arch. Microbiol. **190:**451-460.

37. **Juni E, Janik A.** 1969. Transformation of *Acinetobacter calcoaceticus* (Bacterium anitratum). J. Bacteriol. **98:**281-288.

38. **Kidane D, Graumann PL.** 2005. Intracellular protein and DNA dynamics in competent *Bacillus subtilis* cells. Cell. **122:**73-84.

39. **Lehmler HJ, Robertson LW.** 2001. Synthesis of polychlorinated biphenyls (PCBs) using the Suzuki-coupling. Chemosphere. **45:**137-143.

40. **Maddocks SE, Oyston PC.** 2008. Structure and function of the LysR-type transcriptional regulator (LTTR) family proteins. Microbiology. **154:**3609-3623.

41. **Metzgar D, Bacher JM, Pezo V, Reader J, Doring V, Schimmel P, Marliere P, de Crecy-Lagard V.** 2004. *Acinetobacter* sp. ADP1: an ideal model organism for genetic analysis and genome engineering. Nucleic. Acids. Res. **32:**5780-5790.

42. **Momany C, Neidle EL.** 2012. Defying stereotypes: the elusive search for a universal model of LysR-type regulation. Mol. Microbiol. **83:**453-456.

43. **Morrison DA, Mannarelli B.** 1979. Transformation in *Pneumococcus*: nuclease resistance of deoxyribonucleic acid in the eclipse complex. J. Bacteriol. **140:**655-665.

44. **Muraoka S, Okumura R, Ogawa N, Nonaka T, Miyashita K, Senda T.** 2003. Crystal structure of a full-length LysR-type transcriptional regulator, CbnR: unusual combination of two subunit forms and molecular bases for causing and changing DNA bend. J. Mol. Biol. **328:**555-566.

45. **Nemec A, De Baere T, Tjernberg I, Vaneechoutte M, van der Reijden TJ, Dijkshoorn L.** 2001. *Acinetobacter ursingii* sp. nov. and *Acinetobacter schindleri* sp. nov., isolated from human clinical specimens. Inter. J. Syst. Evol. Microbiol. **51:**1891-1899.

46. **Ornston LN.** 1966b. The conversion of catechol and protocatechuate to beta-ketoadipate by *Pseudomonas putida*. II. Enzymes of the protocatechuate pathway. J. Biol. Chem. **241:**3787-3794.

47. **Ornston LN.** 1966a. The conversion of catechol and protocatechuate to beta-ketoadipate by *Pseudomonas putida*. IV. Regulation. J. Biol. Chem. **241:**3800-3810.

48. **Ornston LN, Stanier RY.** 1966d. The conversion of catechol and protocatechuate to beta-ketoadipate by *Pseudomonas putida*. J. Biol. Chem. **241:**3776-3786.

49. **Palmen R, Hellingwerf KJ.** 1997. Uptake and processing of DNA by *Acinetobacter calcoaceticus*. Gene. **192:**179-190.

50. **Palmen R, Vosman B, Buijsman P, Breek CK, Hellingwerf KJ.** 1993. Physiological characterization of natural transformation in *Acinetobacter calcoaceticus*. J. Gen. Microbiol. **139:**295-305.

51. **Reams AB, Neidle EL.** 2003. Genome plasticity in *Acinetobacter*: new degradative capabilities acquired by the spontaneous amplification of large chromosomal segments. Mol. Microbiol. **47:**1291-1304.

52. **Romero-Arroyo CE, Schell MA, Gaines GL, 3rd, Neidle EL.** 1995. *catM* encodes a LysR-type transcriptional activator regulating catechol degradation in *Acinetobacter calcoaceticus*. J. Bacteriol. **177:**5891-5898.

53. **Ruangprasert A, Craven SH, Neidle EL, Momany C.** 2010. Full-length structures of BenM and two variants reveal different oligomerization schemes for LysR-type transcriptional regulators. J. Mol. Biol. **404:**568-586.

54. **Schell MA.** 1993. Molecular biology of the LysR family of transcriptional regulators. Annu. Rev. Microbiol. **47:**597-626.

55. **Seaton SC, Elliott KT, Cuff LE, Laniohan NS, Patel PR, Neidle EL.** 2012. Genome-wide selection for increased copy number in *Acinetobacter baylyi* ADP1: locus and context-dependent variation in gene amplification. Mol. Microbiol. **83:**520-535.

56. **Segura A, Bunz PV, D'Argenio DA, Ornston LN.** 1999. Genetic analysis of a chromosomal region containing *vanA* and *vanB*, genes required for conversion of either ferulate or vanillate to protocatechuate in *Acinetobacter*. J. Bacteriol. **181:**3494-3504.

57. **Tumen-Velasquez MP, Bacon C, Laniohan NS, Neidle EL, Momany C.** 2014a. Engineering CatM, a LysR-type Transcriptional Regulator, to respond synergictically to two different effectors (manuscript in preparation).

58. **Tumen-Velasquez MP, Elliott KT, Bartlett C, Nune M, Karls A, Momany C, Neidle EL.** 2014c. A new LysR-type Transcriptional Regulator, LeuR, controls Leucine Biosynthesis in *Acinetobacter baylyi* strain ADP1. (manuscript in preparation).

59. **Vaneechoutte M, Young DM, Ornston LN, De Baere T, Nemec A, Van Der Reijden T, Carr E, Tjernberg I, Dijkshoorn L.** 2006. Naturally transformable *Acinetobacter* sp. strain ADP1 belongs to the newly described species *Acinetobacter baylyi*. Appl. Environ. Microbiol. **72:**932-936.

60. **Zimmermann T, Sorg T, Siehler SY, Gerischer U.** 2009. Role of *Acinetobacter baylyi* Crc in catabolite repression of enzymes for aromatic compound catabolism. J. Bacteriol. **191:**2834-2842.

CHAPTER 2

ENGINEERING CATM, A LYSR-TYPE TRANSCRIPTIONAL REGULATOR, TO RESPOND SYNERGISTICALLY TO TWO DIFFERENT EFFECTORS*

* Melissa P. Tumen-Velasquez, Nicole Laniohan, Curtis Bacon, Cory Momany and Ellen L. Neidle to be submitted to the *Journal of Bacteriology.*

Abstract

LysR-type regulators form the largest family of prokaryotic transcriptional regulators. Despite their widespread importance, structural and functional data remain poorly integrated for these proteins. Here we focus on two well-studied members of this family from a soil bacterium, *Acinetobacter baylyi* ADP1. Although these paralogs, BenM and CatM, have similar structures and functions, there are significant differences in how they regulate genes for aromatic compound degradation. BenM, unlike CatM, responds synergistically to benzoate and one of its metabolites, *cis,cis*-muconate, to activate high levels of *benABCDE* expression. In contrast, CatM responds solely to *cis,cis*-muconate and activates low-level transcription of this operon. The relative importance of each regulator is reversed for *catBCIJFD,* an operon where CatM is the primary activator and BenM effects low-level expression. Two amino acids in the effector-binding domain of BenM are critical for binding benzoate, R160 and Y293. As reported here, replacement of these residues with those in CatM, H160 and F293, failed to generate a benzoate-responsive CatM. However, an engineered variant responded to benzoate when both amino acid replacements were introduced along with the DNA-binding domain of BenM. This CatM variant responded to benzoate at the *benA* and *catB* promoters. It also responded synergistically to both effectors. Surprisingly, benzoate-dependent *catB* expression required the CatM variant to have the DNA-binding domain of BenM. Only nine amino acids differ between the DNA-binding domains of the two proteins. These studies help define the interconnected roles of different protein domains and extend understanding of LysR-type proteins beyond simple models of modular functionality.

Introduction

Two LysR-type transcriptional regulators (LTTRs) control the degradation of benzoate by the soil bacterium *Acinetobacter baylyi* ADP1 (6, 9, 20). While these paralogs, BenM and CatM, have similar structures and overlapping functions, they co-regulate several promoter regions in different ways (Fig. 2.1). BenM controls the initial steps in benzoate consumption by activating transcription of the *benABCDE* operon in response to benzoate and one of its metabolites, *cis,cis*-muconate (5, 6). In contrast, CatM responds solely to muconate and activates only low-level expression of the *benABCDE* operon (20). The goal of the current study was to improve our understanding of effector-mediated transcription by isolating and characterizing a benzoate-responsive CatM variant.

The sequences of BenM and CatM are 84% identical in their N-terminal DNA-binding domains (22) (Fig. 2.2). Thus, it is not surprising that both regulators bind to the same regions of the *benA* promoter (Fig. 2.3A.B). A regulatory homotetramer binds to Site 1, which is recognized by winged helix-turn-helix motifs (wHTH) in two subunits, and additionally to either Site 2 or Site 3, which is recognized by the other two subunits. In the absence of effectors, binding to Site 3 represses transcription initiation. However, conformational changes in response to the appropriate effector(s) can reposition the tetramer to activate transcription via interactions with Site 2 (Fig. 2.3.B) (4, 5, 10).

Even though BenM and CatM display similar protein-DNA localization, CatM is unable to activate sufficiently high *ben*-gene transcription to allow growth on benzoate as the sole carbon source in the absence of BenM (5). Previous studies identified several spontaneous mutations that individually increase the ability of CatM to activate *benA*

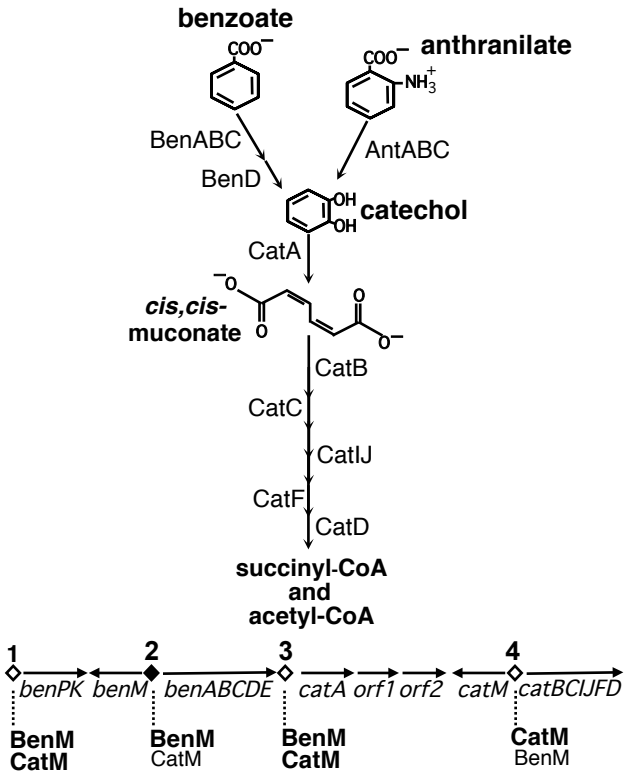

FIGURE 2.1. Benzoate degradation in ADP1. Enzymes encoded by the *ben* and *cat* genes convert aromatic compounds to intermediates of the tricarboxylic acid cycle (top). These genes are clustered on the chromosome (bottom) such that expression is controlled by BenM and CatM at four operator-promoter regions (numbered diamonds). In regions 1 and 3, both regulators play major regulatory roles. In regions 2 and 4, one regulator plays a major role (indicated by bold text), and one regulator plays a minor role. This study focuses on region 2 (filled diamond) where CatM normally activates low-level expression from the *benA* promoter in response to muconate. Regulation at region 4 is also studied in this section. The *benPK* and *benE* genes encode membrane proteins. BenM and CatM are not needed to activate expression of the distally located *antABC* genes.

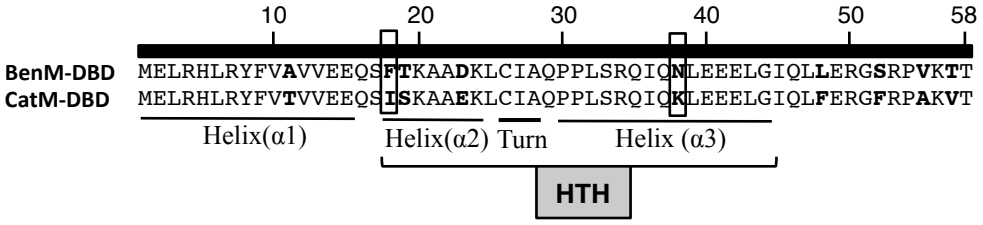

Figure 2.2. **Similarity in amino acid sequence between BenM and CatM DBDs.** DBDs for BenM and CatM differ at nine amino acids (bold). The DNA binding motif [HTH] is indicated by Helix (α2)-Turn-Helix (α3). The turn is described to have a critical role in activating transcription via direct contact with RNA polymerase (Lochowska *et. al* 2001) (14). Boxed amino acids at positions 18 and 38 were investigated in these studies. Glutamine at position 29 is highly conserved in LTTRs.

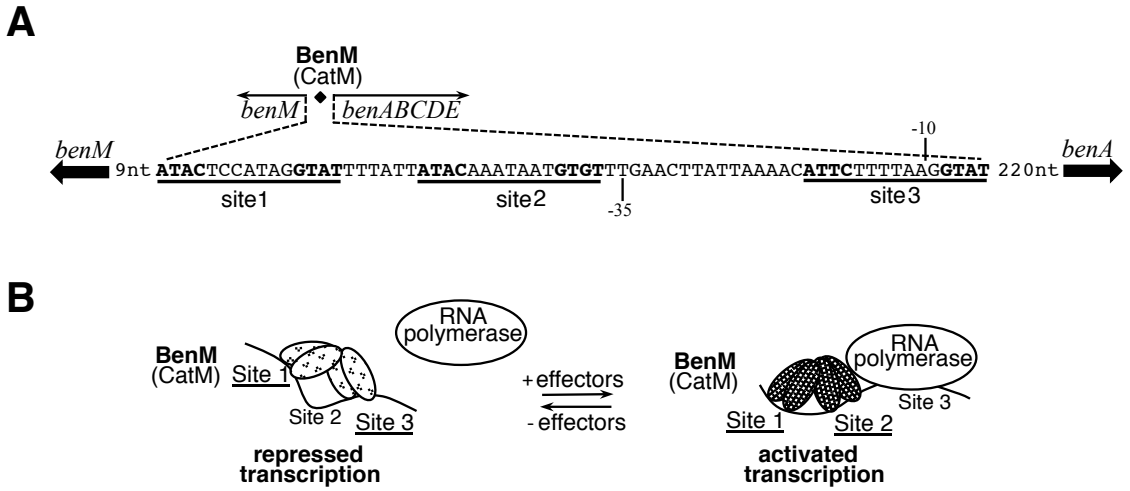

FIGURE 2.3. Regulatory model for P_{benA}. BenM is the primary transcriptional regulator of the *benABCDE* operon. CatM plays a minor role at this region (A) Binding sites for BenM and CatM at the *benMA* intergenic region. Site 1 matches the consensus (underlined) LTTR-binding motif (T-N_{11}-A). Site 2 and Site 3 differ by one nucleotide from the consensus sequences which reduces the dyad symmetry. Promoter regions (-10 and -35) are indicated for *benA.* In this locus, BenM controls transcription of its own expression as well as the divergent *benABCDE.* (B) Model of *benA* regulation. Both BenM and CatM bind Site 1 and Site 3 in the absence of effectors. In this conformation transcription is repressed. With inducers, BenM or CatM reposition to Site 1 and Site 2. However, in this conformation, BenM activates *benA* transcription (5, 10).

transcription (10). Mutations that improve CatM-dependent *benA* expression either augment transcription in response to muconate or allow activation without an exogenous effector. None of the characterized mutations enable CatM to respond to benzoate (7, 10).

Structural studies of the effector-binding domains suggest that benzoate binds in a hydrophobic pocket of BenM but not in the corresponding region of CatM (8, 11). This benzoate-binding site is distinct from an inter-domain cleft in both BenM and CatM that can bind muconate (11). It is typical for the Effector binding domains (EBD) of an LTTR to assume the conformation of a periplasmic-binding protein and form a cleft (15, 16, 25), comparable to that in BenM and CatM, to serve as an effector-binding site (11). However, BenM is the only regulator known to have a secondary effector-binding site that enables synergistic activation of transcription in response to two different metabolites (Fig. 2.4.A) (5). To understand the molecular basis of this novel type of regulation, we engineered amino acid replacements to make CatM more similar to BenM.

Two residues in the hydrophobic binding pocket of BenM are known to be critical for benzoate-activated transcription, R160 and Y293 (8, 11). When these amino acids are replaced with those at the comparable positions of CatM, H160 and F293, BenM fails to activate transcription in response to benzoate as a sole effector or in combination with muconate (8). Moreover, benzoate inhibits muconate-activated gene expression by the variant BenM proteins (6, 8). Based on these observations, it seemed that the analogous changes (H160R and F293Y) might generate a benzoate-responsive CatM. As described in this report, our initial efforts were unsuccessful, and such replacements were insufficient for CatM to gain the desired new functionality.

FIGURE 2.4 Ribbon representation of the full-length BenM structure with effectors (benzoate and muconate). (A) Domain organization of a full-length BenM-His subunit. with inducers muconate and benzoate bound in the primary and secondary effector binding sites respectively **(B)** Secondary effector-binding sites of BenM-EBD and CatM-EBD. The structure of CatM-EBD (dark grey) was superimposed onto that of BenM-EBD (light grey). In BenM only, benzoate interacts with residues Y293 and R160. Residues at these positions differ in CatM (F293 and H160) and only water molecules (not benzoate) are found at this region in CatM (not shown).

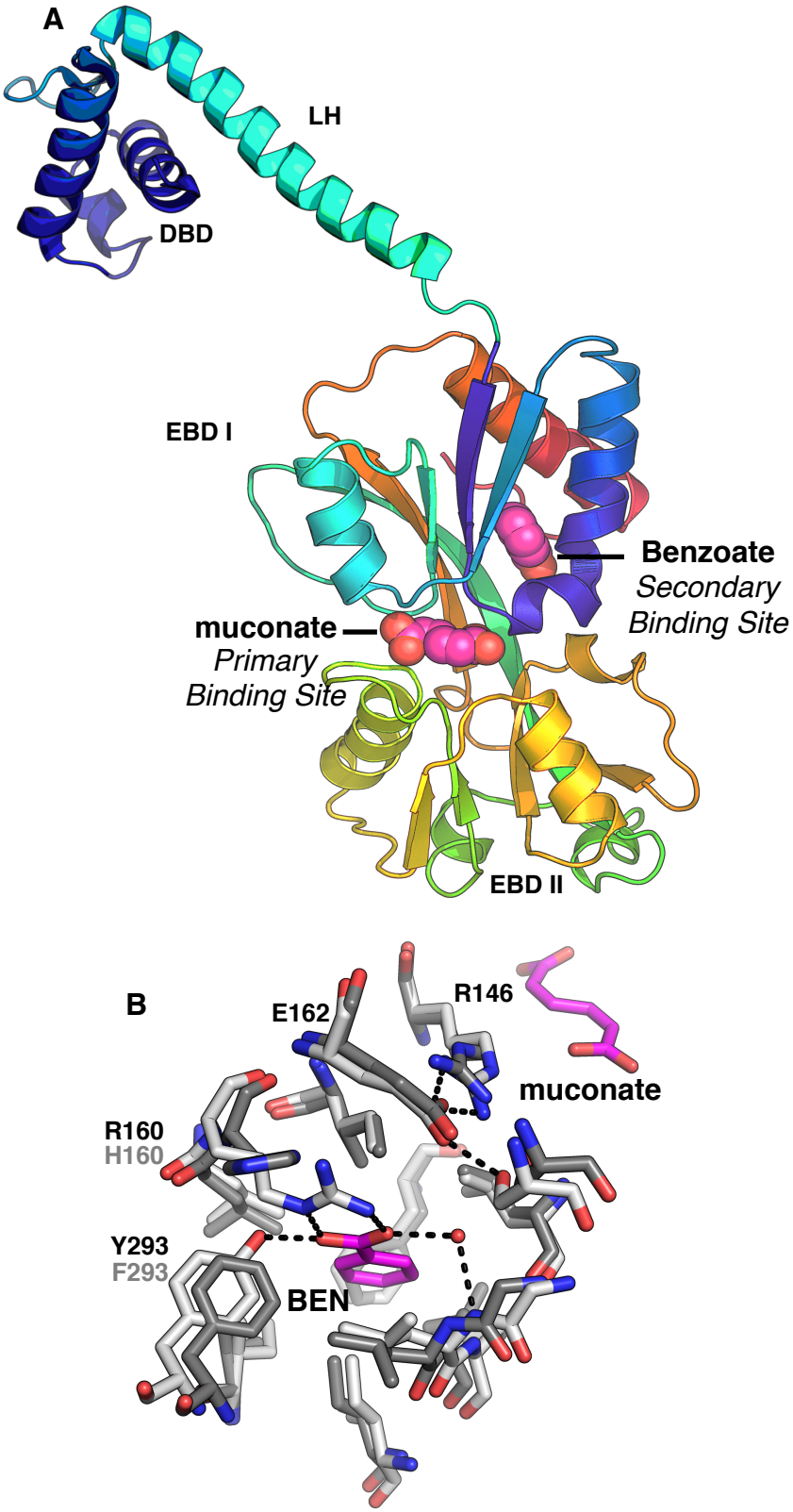
A
LH
DBD
EBD I
Benzoate
Secondary
Binding Site
muconate
Primary
Binding Site
EBD II
B
E162
R146
muconate
R160
H160
Y293
F293
BEN

We built on the initial attempts to modify CatM by combining site-directed mutagenesis with domain swapping, and new spontaneous mutants were also selected. Changes in both the DBDs and the EBDs of BenM and CatM were explored. As discussed below, the isolation and characterization of new mutants expands our understanding of promoter and effector specificity of two similar LTTRs. BenM and CatM serve as representative members of the largest family of homologous transcriptional regulators in bacteria.

Materials And Methods

Bacterial strains and growth conditions. *Escherichia coli* strains were grown on Luria-Bertani broth and *A. baylyi* strains were grown on minimal medium at 37 °C (23, 27). In addition, *A. baylyi* strains were grown in minimal medium with succinate (10 mM), pyruvate (20 mM), benzoate (2 mM), muconate (3 mM), anthranilate (1 mM), as the carbon source. *E. coli* DH5α cells (Invitrogen) and XL-1 blue cells (Agilent Technologies) were used as plasmid hosts. Antibiotics were added as needed at the final concentrations: Ampicillin, 150 μg/ml, kanamycin, 25 μg/ml, spectinomycin, 13 μg/ml and streptomycin, 13 μg/ml. For *A. baylyi* growth curves, succinate-grown colonies were used to inoculate 5 ml cultures for overnight growth with benzoate as the carbon source. Next day, 1 ml of an overnight culture was used to inoculate 100 ml of benzoate medium. Growth was monitored by turbidity and assessed spectrophotometrically (OD_{600}).

BenM-independent Ben$^+$ mutants. Spontaneous mutants that grow on benzoate were isolated from ACN682, a *benM*-disrupted strain with allele *catM5682* (Table 2.1).

Table 2.1. Strains and plasmids used in this study.

Strains or plasmid		
***A. baylyi* Strain**	**Relevant characteristics**[a]	**Source**
ADP1	Wild type (BD413)	(13)
ISA13	*catM*::ΩS*4013*	(20)
ISA36	*benM*::ΩS*4036*	(6)
ACN32	*benA*::*lacZ*-Km^R*5032*	(6)
ACN157	*benA*::*lacZ*-Km^R*5032 benM*::ΩS*4036 benMA5146*	(6)
ACN613	*catM*::*sacB*-Km^R*5613*	This study
ACN637	*benM*::*sacB*-Km^R*5624*	(8)
ACN662	*benM*::ΩS*4036 catM5662* CatM(H160R) ATG →**CC**G (12548)[b]	This study
ACN673	*benA*::*lacZ*-Km^{R}5032 *benM*::ΩS*4036 catM5662* (CatM[H160R])	This study
ACN682	*benM*::ΩS*4036 catM5682* [CatM(F293Y)] AAA → A**T**A (12150)[b]	This study
ACN685	*benM*::ΩS*4036 catM5685* [CatM(H160R,F293Y)]	This study
ACN694	*benA*::*lacZ*-Km^R*5032 benM*::ΩS*4036 catM5685* [CatM(H160R,F293Y)]	This study
ACN717	*benA*::*lacZ*-Km^R*5032 benM*::ΩS*4036 catM5682* [CatM(F293Y)]	This study
ACN827	*benA*::*lacZ*-Km^R*5032 benM*::ΩS*4036 catM5682 benMA5146* [CatM(F293Y)]	This study
ACN832	*benA*::*lacZ*-Km^R*5032 benM*::ΩS*4036 catM5662 benMA5146* [CatM(H160R)]	This study
ACN839	*benA*::*lacZ*-Km^R*5032 benM*::ΩS*4036 catM5685 benMA5146* [CatM(H160R,F293Y)]	This study
ACN843	Δ*benM5389 catM*::*sacB*-Km^R*5613*	(24)
ACN1087	*benM*::ΩS*4036 catM51087* [CatM(ΔD264)] ATCATC → ATC (12236)[b]	This study
ACN1090	Δ*catM51090*	This study
ACN1095	*benM*::ΩS*4036 catM51095* [CatM(I18F)] AAT → AA**A** (12976)[b]	This study
ACN1096	*benM*::ΩS*4036 catM51096* [CatM(R184Q)] TTT → TT**G** (12586)[b]	This study
ACN1108	*benM*::ΩS*4036 benA*::*lacZ*-Km^R*5032 catM51087* [CatM(Δ264)]	This study
ACN1111	*benM*::ΩS*4036 benA*::*lacZ*-Km^R*5032 catM51095* [CatM(I18F)]	This study
ACN1112	*benM*::ΩS*4036 benA*::*lacZ*-Km^R*5032 catM51096*	This study

	[CatM(K148Q)]	
ACN1147	*benM*::ΩS*4036 catM51087* [CatM(ΔD264)] *catB*::*lacZ*-Km^R*5534*	This study
ACN1150	*benM*::ΩS*4036 catM51095* [CatM(I18F)] *catB*::*lacZ*-Km^R*5534*	This study
ACN1151	*benM*::ΩS*4036 catM51096* [CatM(R184Q)] *catB*::*lacZ*-Km^R*5534*	This study
ACN1193	*benM*::ΩS*4036 catM51188* [CatM(K38N)] TTT → **A**TT (12914)[b]	This study
ACN1194	*benM*::ΩS*4036 benA*::*lacZ*-Km^R*5032 catM51188* [CatM(K38N)]	This study
ACN1198	*benM*::ΩS*4036 catM51188* [CatM(K38N)] *catB*::*lacZ*-Km^R*5534*	This study
ACN1225	*benM*::ΩS*4036 catM51225* [CatM(G232S)] GGC → GC**T** (12334)[b]	This study
ACN1228	*benM*::ΩS*4036 benA*::*lacZ*-Km^R*5032 catM51225* [CatM(G232S)]	This study
ACN1232	*benA*::*lacZ*-Km^R*5032 catM*::ΩS*4013*	This study
ACN1234	Δ*benM5389 catM51234* [$_{\text{BenM-DBD}}$]CatM	This study
ACN1236	*benM*::ΩS*4036 catM51225* [CatM(G232S)] *catB*::*lacZ*-Km^R*5534*	This study
ACN1238	*benM*::*sacB*-Km^R*5624* Δ*catM51090*	This study
ACN1239	Δ*benM5389 benA*::*lacZ*-Km^R*5032 catM51234* [$_{\text{BenM-DBD}}$]CatM	This study
ACN1249	Δ*benM5389 catM51249* [CatM(I18F,K38N)]	This study
ACN1251	Δ*benM5389 benA*::*lacZ*-Km^R*5032 catM51249* [CatM(I18F,K38N)]	This study
ACN1293	Δ*benM5389*	This study
ACN1294	*benM51294* [$_{\text{CatM-DBD}}$]BenM Δ*catM51090*	This study
ACN1301	Δ*benM5389 catM51301* [$_{\text{BenM-DBD}}$CatM (H160R, F293Y)]	This study
ACN1302	Δ*benM5389 benA*::*lacZ*-Km^R*5032 catM51301* [$_{\text{BenM-DBD}}$]CatM (H160R, F293Y)	This study
ACN1303	*benM51294* [$_{\text{CatM-DBD}}$]BenM *benA*::*lacZ*-Km^R*5032* Δ*catM51090*	This study
ACN1304	*benM51294* [$_{\text{CatM-DBD}}$]BenM Δ*catM51090 catB*::*lacZ*-Km^R*5534*	This study
ACN1307	Δ*benM5389 benA*::*lacZ*-Km^R*5032*	This study
ACN1308	Δ*benM5389 catB*::*lacZ*-Km^R*5534*	This study
ACN1345	Δ*benM5389 catM51344* [CatM(I18F,K38N,H160R,F293Y]	This study
ACN1347	Δ*benM5389 catM51344 benA*::*lacZ*-Km^R*5032*	This study
ACN1355	*benM51355* [BenM(Q29A)] CTG → **AGC** (2282)[b] Δ*catM51090*	This study
ACN1356	Δ*benM5389 catM51356* [CatM(Q29A)] CTG → CGC (12942)[b]	This study
ACN1357	*benM51355* [BenM(Q29A)] *benA*::*lacZ*-Km^R*5032* Δ*catM51090*	This study
ACN1359	Δ*benM5389 catM51301* [$_{\text{BenM-DBD}}$]CatM(H160R, F293Y) *catB*::*lacZ*-Km^R*5534*	This study
ACN1360	Δ*benM5389 catM51356* [CatM(Q29A)], *catB*::*lacZ*-Km^{R}5534	This Study

ACN1366	Δ*benM5389, benA*::ΩS*51366*, *catB*::*lacZ*-Km^R*5534*	This study
ACN1367	*benM51294* [$_{CatM-DBD}$]BenM *benA*::ΩS*51366* Δ*catM51090* *catB*::*lacZ*-Km^R*5534*	This study
ACN1369	Δ*benM5389 benA*::ΩS*51366 catM51301* [$_{BenM-DBD}$]CatM (H160R, F293Y) *catB*::*lacZ*-Km^R*5534*	This study
ACN1370	Δ*benM5389, benA*::ΩS*51366 catM51234* [$_{BenM-DBD}$]CatM *catB*::*lacZ*-Km^{R}5534	This study
ACN1375	*benA*::ΩS*51366* Δ*catM51090 catB*::*lacZ*-Km^R*5534*	This study
ACN1381	Δ*benM5389 catM5662* [CatM(H160R,F293Y)]	This study
ACN1382	Δ*benM5389 benA*::*lacZ*-Km^R*5032 catM5662* [CatM(H160R,F293Y)]	This study
ACN1383	Δ*benM5389 catM5662* [CatM(H160R,F293Y)] *catB*::*lacZ*-Km^R*5534*	This study
ACN1389	Δ*benM5389 benA*::ΩS*51366 catM5662* [CatM(H160R,F293Y)] *catB*::*lacZ*-Km^R*5534*	This study
ACN1391	Δ*benM5389, catM51344* [CatM(I18F,K38N,H160R,F293)] *catB*::*lacZ*-Km^R*5534*	This study
ACN1394	Δ*benM5389 benA*::ΩS*51366 catM51344* [CatM(I18F,K38N,H160R,F293)] *catB*::*lacZ*-Km^R*5534*	This study
ACN1406	Δ*benM5389 catM51406* [$_{BenM-LH-DBD}$]CatM	This study
ACN1407	*benM51407* [$_{CatM-LH-DBD}$]BenM Δ*catM51090*	This study
ACN1412	*benM51407* [$_{CatM-LH-DBD}$]BenM *benA*::*lacZ*-Km^R*5032* Δ*catM51090*	This study
ACN1414	Δ*benM5389 benA*::*lacZ*-Km^R*5032 catM51406* [$_{BenM-LH-DBD}$]CatM	This study
ACN1415	Δ*benM5389 catM51406* [$_{BenM-LH-DBD}$]CatM *catB*::*lacZ*-Km^R*5534*	This study
ACN1424	Δ*benM5389 benA*::ΩS*51366 catM51406* [$_{BenM-LH-DBD}$]CatM *catB*::*lacZ*-Km^R*5534*	This study
ACN1429	Δ*benM5389 catM51249* [CatM(I18F,K38N)] *catB*::*lacZ*-Km^R*5534*	This study
ACN1443	Δ*benM5389 benA*::ΩS*51366 catM51249* [CatM(I18F,K38N)] *catB*::*lacZ*-Km^R*5534*	
ACN1466	*benM*::*sacB*-Km^R*51466* Δ*benA51431* Δ*catM51090*	This study
ACN1468	*benM51407* [$_{CatM-LH-DBD}$] BenM Δ*benA51431* Δ*catM51090*	This study
ACN1471	*benM51407* [$_{CatM-LH-DBD}$]BenM Δ*benA51431* Δ*catM51090* *catB*::*lacZ*-Km^R*5534*	This study
ACN1472	*benM5641* [BenM(R160H,Y293F)] Δ*benA51431,* Δ*catM51090*	This study
ACN1473	*benM51294* [$_{CatM-DBD}$]BenM Δ*benA51431* Δ*catM51090*	This study

ACN1474	Δ*benA51431* Δ*catM51090*	This study
ACN1475	*benM5641* [BenM(R160H,Y293F)]Δ*benA51431* Δ*catM51090* *catB*::*lacZ*-Km^R*5534*	This study
ACN1476	*benM51294* [$_{\text{CatM-DBD}}$]BenM Δ*benA51431* Δ*catM51090* *catB*::*lacZ*-Km^R*5534*	This study
ACN1477	Δ*benM5389 catM51406* [$_{\text{BenM-LH-DBD}}$]CatM (H160R,F293Y)	This study
ACN1478	Δ*benA51431* Δ*catM51090 catB*::*lacZ*-Km^R*5534*	This study
ACN1479	*benM51479* [$_{\text{CatM-LH-DBD}}$]BenM (R160H,Y293F) Δ*catM51090*	This study
ACN1480	*benM51479* [$_{\text{CatM-LH-DBD}}$]BenM (R160H,Y293F) Δ*benA51431* Δ*catM51090*	This study
ACN1482	Δ*benM5389 catM51406* [$_{\text{BenM-LH-DBD}}$]CatM (H160R,F293Y) *catB*::*lacZ*-Km^R*5534*	This study
ACN1485	*benM51479* [$_{\text{CatM-LH-DBD}}$]BenM (R160H,Y293F) *benA*::*lacZ*-Km^R*5032* Δ*catM51090*	This study
ACN1486	*benM51479* [$_{\text{CatM-LH-DBD}}$]BenM (R160H,Y293F) Δ*benA51431* Δ*catM51090 catB*::*lacZ*-Km^R*5534*	This study
ACN1488	*benM51488* [$_{\text{CatM-DBD}}$]BenM (R160H,Y293F) Δ*catM51090*	This study
ACN1489	*benM51488* [$_{\text{CatM-DBD}}$]BenM (R160H,Y293F) Δ*benA51431* Δ*catM51090*	This study
ACN1491	Δ*benM5389 benA*::*lacZ*-Km^R*5032 catM51406* [$_{\text{BenM-LH-DBD}}$]CatM (H160R,F293Y)	This study
ACN1493	*benM51488* [$_{\text{CatM-DBD}}$]BenM (R160H,Y293F) *benA*::*lacZ*-Km^R*5032* Δ*catM51090*	This study
ACN1495	Δ*benM5389 benA*::ΩS*51366 catM51406* [$_{\text{BenM-LH-DBD}}$]CatM (H160R,F293Y) *catB*::*lacZ*-Km^R*5534*	This study
ACN1501	*benM51488* [$_{\text{CatM-DBD}}$]BenM (R160H,Y293F) Δ*benA51431* Δ*catM51090 catB*::*lacZ*-Km^R*5534*	This study

Plasmid	**Relevant characteristics**	**Source**
pUC18	Ap^R; cloning vector	(30)
pUC19	Ap^R; cloning vector	(30)
pET-21b	Ap^R; T7 expression vector	Novagen
pIB1	Ap^R; partial *cat* region (11605-17916)[b]	(17)
pIB3	Ap^R; partial *catM* (9819-12892)[b]	(17)
pIGG13	Ap^R; partial *ben* region with an internal *KpnI* deletion (1638-4764)[b]	This study
pBAC7	Ap^R; *benKM* (563-2964)[b] region in pUC19	(8)
pBAC54	Ap^R Km^R; *lacZ*-Km^R cassette in *NsiI* site (3761)[b] in *benA* (2316-5663)[b] in	(6)

	pUC19	
pBAC184	Ap^R; partial *cat* region with internal *ClaI* deletion (10649-15901)[b]	(24)
pBAC430	Ap^R; *catM* (12116-13027)[b] in pET-21b	(5)
pBAC433	Ap^R; *benM* (1453-2368)[b] in pET-21b	(5)
pBAC675	Ap^R Km^R; *catB* (13205-14225)[b] *lacZ*-Km^R *catIJF* (15660-17347)[b] in pUC19	(10)
pBAC708	Ap^R Km^R; *catM* region (11950-12892)[b] in pUC19. Contains *sacB*-Km^R cassette	(24)
pBAC709	Ap^R Km^R; *benKM* region (563-2316)[b] in pUC19. Contains *sacB*-Km^R cassette in *SalI* site (1930)[b] in *benM*	This study
pBAC732	Ap^R; *catM5704* (9823-12892)[b] in pUC19	This study
pBAC885	Ap^R; *orf2* fragment (11200-12115)[b] with *HincII* site in pUC18 for Δ*catM* deletion	This study
pBAC886	Ap^R; portion of *catM* and *catB* (13015-14110)[b] with *SmaI* site in pUC18 for Δ*catM* deletion	This study
pBAC887	Ap^R; *orf2* fragment (11200-12115)[b] with *HincII* ligated to portion of *catM* and *catB* (13015-14110)[b] with *SmaI* site in pUC18 for Δ*catM*	This study
pBAC936	Ap^R; *benKM* (563-2368)[b] [BenM(F18I)]	This study
pBAC938	Ap^R; *catM51095* (12381-16031)[b] in pIB1	This study
pBAC939	Ap^R; *catM51096* (12381-16031)[b] in pIB1	This study
pBAC945	Ap^R; *catM* region (11605-13457)[b] in pUC18	This study
pBAC949	Ap^R; *ben* region (1638-4768)[b] in pIGG13 *KpnI* site	This study
pBAC958	Ap^R; *catM51087* (12381-16031)[b] in pIB1	This study
pBAC959	Ap^R; *benKM* (563-2368)[b] [BenM(Q29A)]	This study
pBAC961	Ap^R; *catMB* (11605-13457)[b] [CatM(K38N)]	This study
pBAC962	Ap^R; *catMB* (11605-13457)[b] [CatM(Q29A)]	This study
pBAC975	Ap^R; *benKM* (563-2368)[b] [BenM(N38K)]	This study
pBAC976	Ap^R; *catMB* (11605-13457)[b] [CatM(G232S)]	This study
pBAC1020	Ap^R; *catM51225* (9823-18153)[b] in pUC19	This study
pBAC1025	Ap^R; *catM51234 SacI-PstI* (11200-14110)[b] cloned into pUC18	This study
pBAC1027	Ap^R; *NdeI-XhoI* (12119-13027)[b] fragment from pBAC958 in pET-21b; expression construct for $_{BenM\text{-}DBD}$CatM	This study
pBAC1040	Ap^R; *cat* region (9823-18153)[b] [CatM(I18F,K38N)]	This study
pBAC1041	Ap^R; *benKM* (563-2368)[b] [BenM(F18I,N38K)]	This study
pBAC1042	Ap^R; *NdeI-XhoI* (1453-2368)[b] fragment from pBAC936 in pET-21b; expression construct for BenM(I18F)	This study
pBAC1043	Ap^R; *NdeI-XhoI* (1453-2368)[b] fragment from pBAC1041 in pET-21b; expression construct for BenM(I18F,N38K)	This study

pBAC1044	Ap^R; *NdeI-XhoI* (1453-2368)[b] fragment from pBAC975 in pET-21b; expression construct for BenM(N38K)	This study
pBAC1045	Ap^R; *NdeI-XhoI* (12119-13027)[b] fragment from pBAC1041 in pET-21b; expression construct for CatM(I18F,K38N)	This study
pBAC1046	Ap^R; *NdeI-XhoI* (12119-13027)[b] fragment from pBAC961 in pET-21b; expression construct for CatM(K38N)	This study
pBAC1047	Ap^R; *orf2-catB* (11200-13457)[b] with Δ*catM* deletion (12116-13024)[b] with engineered *XhoI* site (13028)[b] in pUC18	This study
pBAC1048	Ap^R; *benK-benA* (589-3393)[b] with Δ*benM* deletion (1453-2365)[b] with engineered *XhoI* site (2369)[b] in pUC18	This study
pBAC1064	Ap^R Km^R; *sacB*-Km^R cassette cloned into *XhoI* site in pBAC1047	This study
pBAC1065	Ap^R Km^R; *sacB*-Km^R cassette cloned into *XhoI* site in pBAC1048	This study
pBAC1066	Ap^R; Ap^R; *cat* region (9823-18153)[b] [CatM(I18F,K38N,F293Y)]	This study
pBAC1069	Ap^R; *cat* region (11200-14110)[b] with *catM51234* [$_{BenM\text{-}DBD}$CatM (F293Y)]	This study
pBAC1071	Ap^R; *cat* region (9823-18153)[b] [CatM(I18F,K38N,H160R,F293Y)]	This study
pBAC1074	Ap^R; *benM51294 SacI-PstI* (588-3394)[b] cloned into pUC18	This study
pBAC1078	Ap^R; *cat* region (11200-14110)[b] with *catM51234* [$_{BenM\text{-}DBD}$CatM (H160R,F293Y)]	This study
pBAC1086	Ap^R; *NdeI-XhoI* (12119-13027)[b] fragment from pBAC1078 in pET-21b; expression construct for $_{BenM\text{-}DBD}$CatM (H160R,F293Y)	This study
pBAC1085	Ap^R; *NdeI-XhoI* (12119-13027)[b] fragment from pBAC1071 in pET-21b; expression construct for CatM(I18F,K38N,H160R,F293Y)	This study
pBAC1092	Ap^R; *NdeI-XhoI* (1453-2368)[b] fragment from pBAC1074 in pET-21b; expression construct for $_{CatM\text{-}DBD}$BenM	This study
pBAC1108	Ap^R; *catMB* (11605-13457)[b] [CatM(F293Y)]	This study
pBAC1109	Ap^R; *catMB* (11605-13457)[b] [CatM(H160R)]	This study
pBAC1140	Ap^R; *catMB* (11605-13457)[b] [CatM(H160R, F293Y)]	This study
pBAC1157	Ap^R; *benMC* region with Δ*benA* deletion. *XhoI* site generated	This study
pBAC1159	Ap^R; *catM51406 SacI-PstI* (11200-14110)[b] cloned into pUC18	This study
pBAC1160	Ap^R; *benM51407 SacI-PstI* (588-3394)[b] cloned into pUC18	This study
pBAC1161	Ap^R; *benMC* region with Δ*benA::sacB*-Km^R cassette	This study

pBAC1179	Ap^R Km^R; *benKC* region (563-)[b] in pUC19. Contains *sacB*-Km^R cassette in *SalI* site (1930)[b] in *benM* and Δ*benA* deletion	This study
pBAC1189	Ap^R; *catM51477 SacI-PstI* (11200-14110)[b] cloned into pUC18	This study
pBAC1190	Ap^R; *benKM* (563-2964)[b] [BenM(R160H,Y293F)]	This study
pBAC1191	Ap^R; *benM51479 SacI-PstI* (588-3394)[b] cloned into pUC18	This study
pBAC1192	Ap^R; *benKC* region with Δ*benMA* cloned in pUC18	This study
pBAC1193	Ap^R; *benM51488 SacI-PstI* (588-3394)[b] cloned into pUC18	This study

[a]Ap^R, ampicillin resistant; Sm^R, streptomycin resistant; Sp^R, spectinomycin resistant; Km^R, kanamycin resistant; ΩS, omega cassette containing Sm^R Sp^R (Prentki and Krisch, 1994); *sacB*-Km^R, dual selection cassette containing a counterselectable marker and kanamycin resistant cassette (Jones and Williams 2003).
[b]Position in the *ben-cat* sequence in GenBank entry AF009224

These mutants were selected after incubation on benzoate agar plates. Gap-repair methods were used to isolate the *catM* region from these Ben+ mutants (12). To test the ben+ phenotype of the recovered DNA fragments from spontaneous mutants, transformation assays were performed. *benM*-disrupted strains, ACN682, encoding CatM[F293Y] replacement and ISA36, encoding wild-type CatM, were used as the recipients with donor DNA from gap repaired plasmids. Transformants grew on benzoate only when *catM* alleles could be generated to encode CatM variants (10).

Generation of *A. baylyi* strains by allelic exchange. Plasmid-borne alleles were used to replace chromosomal genes. Different methods were used to exploit the high efficiency of natural transformation and recombination in *A. baylyi.* Recipient strains were transformed with linearized plasmids. By homologous recombination, the correspondent chromosomal region is replaced in transformants with donor DNA. Transformants were identified by phenotypic changes. In this study, strains were tested for antibiotic resistance and carbon source utilization. To aid the introduction of alter *benM* or *catM* alleles, a counter-selectable *sacB* marker disrupted chromosomal *benM* and *catM* respectively. To replace the chromosomal *sacB* cassette with modified *benM* or *catM* alleles, linearized appropriate plasmids were used to transform strain ACN843 (*benM*-disrupted strain with *catM*::*sacB),* ACN613 (*catM*::*sacB*), ACN637 (*benM*::*sacB*), ACN1238 (*catM*-disrupted strain with *benM*::*sacB),* ACN1466 (Δ*benA,* Δ*catM* strain with *benM*::*sacB*) or ACN1467 (Δ*benA* strain with *benM*::*sacB*) (Table 2.1). Desired transformants were selected by growth at 30 °C in the presence of 5% sucrose. Under this type of selection, a functional CatM or BenM is not required to growth in this medium.

Chromosomal regions of interest in resultant strains were analyzed by PCR-generated fragment sizes, and Genewiz laboratories confirmed DNA sequences of chromosomal regions.

Plasmid construction. Standard methods were used for DNA purification, digestion, ligation, electrophoresis, and bacterial transformation (23). Plasmids listed in table 2.1. To construct pBAC945, pIB1 was digested with *XbaI* and *FspI* to isolate *catM.* Fragment was gel extracted and ligated to pUC18 digested with *XbaI* and *HincII*. To construct pBAC938, the *catM51095* allele fragment was excised from pBAC937 away from *catM5682* by digestion with *StuI* and *NsiI* and ligated into a similar digested pIB1. Similar strategy was used to construct pBAC939. Starting from pBAC786, single *catM* allele was excised away by digestion with *StuI* and *NsiI* and ligated into pIB1. Plasmid pBAC732 was constructed by digestion with *KpnI* and *EcoRI* and ligation into a similar digested pUC19. To aid homologous recombination in the chromosome, homologous DNA was added to each end of this plasmid. Briefly, pBAC732, was used to transform and restored ben+ growth to ISA36 as described above. Resulting strain, ACN1087, was used for gap repair of pBAC184 digested with *ClaI* to recover the single *catM* allele. Resulting plasmid pBAC958 (*catM51087),* was sent for sequencing analysis. To construct pBAC1161, *sacB*-Kan cassette was excised from pRMJ1 by digestion with *SalI* and ligated to pBAC1157 digested with *XhoI*. Plasmid pBAC1192 (Δ*benMA*) was constructed by digesting pBAC1157 (Δ*benA*) with *XhoI* and *PstI* and ligating the excised fragment to pBAC1048 (Δ*benM*) digested with similar enzymes. To construct pBAC1027, pBAC1045, pBAC1086, and pBAC1092, alleles were amplified by high-fidelity PCR (Roche) that incorporated a 5’

NdeI and a 3' *XhoI.* PCR products were digested with *NdeI* and *XhoI* and cloned to pET21b (Invitrogen). Alleles were confirmed by sequencing analysis.

Construction of $_{\text{BenM-DBD}}$CatM, $_{\text{BenM-DBD-LH}}$CatM, $_{\text{CatM-DBD}}$BenM and $_{\text{CatM-DBD-LH}}$BenM. Overlapping extension PCR generated all hybrid constructs, and high fidelity polymerase (Roche) was used to minimize undesired mutations. ADP1 chromosome was used as template in PCR reactions. A PCR reaction amplified a portion of *benM* or *catM*, which contained their original EBD and LH or EBD alone. The 3' ends of these PCR products have a DNA portion that corresponds to the desired DBD or LH-DBD region added by the reverse oligonucleotide. A second PCR reaction amplified the target DBD or LH-DBD that at its 5' end has a DNA portion that corresponds to the LH or EBD of the other protein. A third PCR reaction was performed to combine PCR1 and PCR2. In this PCR, the oligonucleotides incorporated a 5' *SacI* and a 3' *PstI.* PCR products were gel extracted (Zymo Research) and digested with mentioned restriction enzymes. Digestions were gel extracted and ligated to pUC18 digested with *SacI* and *PstI* respectively. Blue and white colony screen was used to identify clones with desired insert in pUC18. Clones were also screen by restriction digest with *NsiI* (present only in BenM DBD region) and *EcoRI* (present only in CatM DBD region). Resulting plasmids, pBAC1025 ($_{\text{BenM-DBD}}$CatM), pBAC1074 ($_{\text{CatM-DBD}}$BenM), pBAC1159 ($_{\text{BenM-DBD-LH}}$CatM), and pBAC1160 ($_{\text{CatM-DBD-LH}}$BenM) were confirmed by sequence analysis (Genewiz Laboratories).

Site-specific mutagenesis of *catM* and *benM.* Site-directed mutagenesis of plasmid-borne *benM* and *catM* (Turbo *pfu* polymerase, Agilent Technologies) was used to encode

desired amino acids. Plasmids pBAC7, pBAC430, pBAC433, pBAC938, pBAC945, pBAC975, pBAC1040, pBAC1041, pBAC1074, pBAC1078, pBAC1159 and pBAC1160 (Table 2.1) were used as templates in PCR reactions with mutant oligonucleotide primers. Following temperature cycling, the PCR products were treated with *DpnI* for three hours at 37 °C. *DpnI*-treated PCR products were transformed into DH5α cells by heat pulse. Cells were spread onto LB-ampicillin plates and plasmids from resulting colonies were isolated. After confirmation by restriction digests, sequencing was carried out by Genewiz Laboratories to confirm nucleotide substitutions on plasmids.

B-galactosidase assays to measure *lacZ* expression. *benA::lacZ, catB::lacZ,* and *catA::lacZ* transcriptional fusions were inserted into *A. baylyi* strains when indicated by allelic exchange with DNA of pBAC54 digested with *XmnI,* pBAC675 digested with *KpnI,* and pBAC766 digested with *XmnI*. To assay these fusions, strains were grown on minimal medium with pyruvate (20 mM) as the carbon source with no inducer or the following when indicated: 65 μM benzoate, 65 μM muconate, 32.5 μM each. For assays during growth on muconate, cultures were grown overnight on minimal medium with muconate (3 mM). The following morning, 500 μl of each culture was diluted into 5 ml of minimal medium with muconate (3 mM). Growth was measured by optical density (OD_{600}) and assays were done when cultures reached late-exponential phase. Samples (0.5 μl to 5 μl) were lysed with Z buffer, sodium dodecyl sulfate and chloroform. Directions from FlourAce β-galactosidase reporter kit (BioRad) were followed. The hydrolysis of the substrate, 4 methylumbelliferyl-galactopyranoside (MUG) to the product 4-methyllumbelliferone (4MU) was detected with a TD-360 miniflourometer

(Turner Designs). Relative fluorescence unit measurements enable 4MU quantification by comparison with a standard curve.

Purification of BenM and CatM and variant proteins. Previously described plasmids pBAC433 and pBAC430 were used to express the full-length proteins BenM-His and CatM-His, respectively. Plasmids pBAC1027, pBAC1045, pBAC1086, and pBAC1092 which encoded full-length $_{\text{BenM-DBD}}$CatM-His, CatM[I18F,K38N]-His, $_{\text{Ben-DBD}}$CatM[H160R,F293Y]-His, and $_{\text{CatM-DBD}}$BenM-His respectively were used to express these proteins. The protocol for BenM-His purification was followed exactly as described in Ruangprasert *et, al*. 2010. BenM-His was eluted with Q elution buffer [30 mM Tris, 1 M NaCl, 10% glycerol, 250 imidazole and 10 mn BME (pH 9.0)]. Following elution, BenM fractions were pooled and dialyzed extensively (4 times) for 24 hours in BenM-dialysis buffer using snakeskin dialysis tubing (Pierce) to remove imidazole. BenM-dialysis buffer constituted 20 mM Tris-HCl (pH 7.9), 500 mM NaCl, 10% (v/v) glycerol. BenM-His was concentrated to ~ 10 mg ml^{-1}. CatM-His and variant proteins were purified similar as BenM-His, but proteins were eluted with CatM-elution buffer [30 mM Tris, 500 mM NaCl, 30% glycerol (v/v), 500 mM imidazole, and 10 mM BME (pH 7.9)]. Following elution, only CatM fractions were pooled and dialyzed against in CatM solubilization buffer [20 mM Tris-HCl, 250 imidazole (pH 7.9), 500 NaCl, 10% (v/v) glycerol] to increase solubility. CatM-His was concentrated to 2 mg ml^{-1}. Protein concentrations were determined by the method of Bradford with bovine serum albumin as the standard (3). Proteins fractions were frozen with liquid nitrogen and stored at -70 °C until use.

Electrophoretic mobility shift assay. DNA fragments containing the *benA* and *catB* promoters were generated by high fidelity PCR (Roche). The 5' end oligonucleotide of each desired promoter (*benA* and *catB*) was labeled with 6-carboxyfluorescein (6-FAM). Each amplicon was approximately 150-250 bp 6-FAM labeled fragments. After completion of PCR reaction, the samples were gel extracted. The Zymoclean Gel DNA Recovery kit was used to remove the full-length PCR products from the excess primers, DNA polymerase, and unused NTPs. The amount of DNA was determined using the absorbance at 260 nm. For gel shift assays, 1 nM of DNA was incubated with different concentrations of proteins (0, 20 nM, 40 nM, 80 nM, 160 nM, 320 nM, 640 nM and 1.28 μm) for 1 hour at 37 °C with or without muconate, benzoate or both. DNA-protein samples were resolved by electrophoresis in 6% polyacrylamide gels. Before samples were loaded onto polyacrylamide gels, loading dye (methylene blue) was added to the wells of polyacrylamide gel and the gels were pre-runned in 1 X TAE with muconate, benzoate or both when indicated for 40 minutes at 180 volts. Following this step, DNA-protein complexes were loaded onto polyacrylamide gels. Electrophoresis was performed with 1 X TAE and muconate when indicated for 1 hour at 185 volts at 4°C. Gels were immediately analyzed and fluorescent bands were detected using Typhoon PhosphoImager system (Amersham Biosciences) at 526 nm short-pass emission filter. The bound DNA relative to the unbound DNA was quantified by Gel-Pro® analyzer (Media Cybernetics) and these numbers were fitted into a saturation-binding curve to determine K_d (GraphPad PRIMS®).

Results

Engineered variants: altered residues at positions 293 and 160 in CatM. Because R160 and Y293 are required for BenM to respond to benzoate (8), our initial efforts to create a benzoate-binding site in CatM focused on its corresponding amino acids (H160 and F293). The chromosomal copy of *catM* was modified by site-directed mutagenesis and allelic replacement to encode the same amino acids as BenM at these positions. To evaluate the effects of the CatM variants, the mutated alleles were introduced into strains that are unable to produce BenM.

In the absence of BenM, wild-type CatM activates sufficient *cat*-gene expression for growth on muconate, anthranilate, or catechol as the sole carbon source. Consistent with the engineered alleles being able to encode functional regulators, CatM[H160R], CatM[F293Y], and CatM[H160R,F293Y] each allowed its parent strain to grow on these carbon sources (parent strains designated ACN662, ACN682, and ACN685, respectively, Tables 2.1 and 2.2). However, wild-type CatM does not activate high *benABCDE* expression, and therefore *benM* mutants do not grow rapidly on benzoate unless additional mutations increase *ben*-gene expression (6, 7, 10). Like wild-type CatM, CatM[F293Y] did not permit BenM-independent growth on benzoate. In contrast, strains lacking BenM grew on benzoate when the CatM variant had the H160R replacement alone or in combination with an additional F293Y replacement (Table 2.2). We sought to confirm the supposition that the CatM[H160R] and CatM[H160R,F293Y] variants activate higher than normal levels of transcription from the *benA* promoter (P_{benA}).

Table 2.2. Strains with *catM* alleles encoding amino acid replacements and their resultant phenotype

Strain	Amino acid changes		Carbon source		
	By Site-directed Mutagenesis [a]	**Location of changed amino acid in CatM**	**Benzoate growth[c]**	**Anthranilate growth[d]**	**Muconate growth[e]**
ACN662	CatM(H160R)[a]	Effector binding domain	+	+	+
ACN723	CatM(H160R,F293Y)[a]	Effector binding domain	+	+	+
ACN682	CatM(F293Y)[a]	Effector binding domain	No growth	+	+
ACN1249	CatM(I18F,K38N)[a]	DNA binding domain	+	+	+
ACN1345	CatM(I18F,K38N,H160,F293Y)[a]	Effector and DNA binding domain	+	+	+
ACN1301	$_{\text{BenM-DBD}}$ CatM(H160R,F293Y)[a]	Effector binding domain	+	+	+
Strains derived from ACN682	**By Spontaneous Mutation[b]**				
ACN1087	CatM(ΔD264)[b]	Effector binding domain	+	+	+
ACN1096	CatM(K148Q)[b]	Effector binding domain	+	+	+
ACN1225	CatM(G232S)[b]	Effector binding domain	+	+	+
ACN1095	CatM(I18F)[b]	DNA binding domain	+	+	+

[a]*catM* alleles engineered by Site-directed mutagenesis as described in Material and Methods

[b]*catM* alleles isolated as spontaneous mutants from parent strain ACN682 grown on benzoate agar plate. All spontaneous mutants retained the parental F923Yamino acid replacement. Strains shown in this table have the parental mutation removed to assess individual effects on growth and regulation of *ben-cat* genes.

[c, d]and [e] strains able to grow on benzoate, anthranilate and muconate as sole carbon source. (+) represents growth on the provided carbon source.

CatM-mediated *ben*-gene expression. A *benA*::*lacZ* transcriptional fusion was used to replace chromosomal *benA*. The resulting disruption of the *benABCDE* operon prevents benzoate degradation and allows benzoate to act as a non-metabolized effector. β-Galactosidase (LacZ) activity was used to assess transcription from P_{benA} controlled by CatM[F293Y], CatM[H160R], CatM[H160R,F293Y], or wild-type CatM in strains without BenM (ACN717, ACN673, ACN694, and ACN1307, respectively. CatM[F293Y], which did not permit BenM-independent benzoate growth, regulated expression like wild-type CatM (Fig. 2.5.A.B). In strains encoding CatM[H160R] and CatM[H160R,F293Y], muconate-induced LacZ activity was 2 to 3 times higher than for wild-type CatM (Fig. 2.5.B). Although this activity remains significantly below that for BenM (in strain ACN1232), these muconate-induced levels are comparable to those of other CatM variants that grow on benzoate without BenM, as previously discussed (6, 10).

The F293Y and H160R replacements in CatM, which were designed to enable benzoate-dependent transcriptional activation, failed to increase expression in response to benzoate (Fig.2.5.A.B). One possible reason for this failure could involve the promoter specificity of CatM as this regulator does not optimally recognize the operator-promoter region of *benA*. To address this possibility, strains were constructed in which the mutated *catM* alleles could control expression of the *benA*::*lacZ* fusion from a promoter that carries a single T-to-A transversion at position -40 relative to the *benA* transcript start site. This previously characterized mutation (*benMA5146*) increases the ability of CatM to activate *benA* transcription (10).

FIGURE 2.5. Expression of a chromosomal *benA*::*lacZ* fusion in strains encoding BenM, CatM or CatM variants. All strains lack a functional *benM.* Controls include ACN1232, wild-type BenM, and ACN1307, with the Δ*benM* gene deleted. Cultures were grown in LB with addition of effectors where indicated (0.5 mM benzoate, 0.5 mM muconate, or 0.25 mM benzoate and 0.25 mM muconate). β- Galactosidase (LacZ) activity is reported relative to uninduced ACN1232 (2.6 ± 0.51 nmol/min/ml/OD_{600}). Activities are the average of at least four repetitions, and standard deviations were 20% of the average value. (A) Strains grown in LB and LB + benzoate. (B) Strains grown in LB + muconate and LB + benzoate and muconate

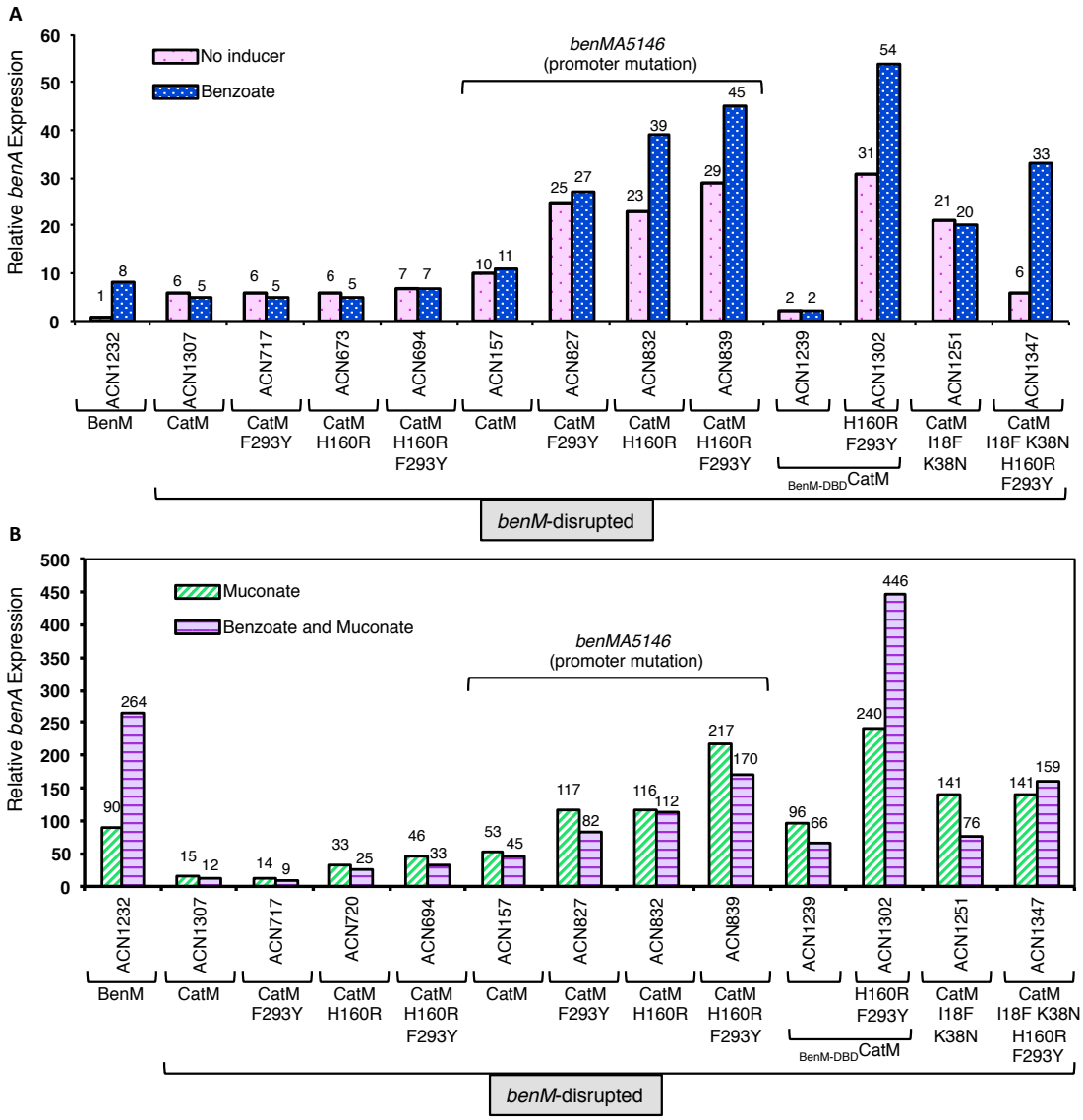
A
Relative benA Expression
No inducer
Benzoate
benMA5146
(promoter mutation)
ACN1232
ACN1307
ACN717
ACN673
ACN694
ACN157
ACN827
ACN832
ACN839
ACN1239
ACN1302
ACN1251
ACN1347
BenM
CatM
CatM F293Y
CatM H160R
CatM H160R F293Y
CatM
CatM F293Y
CatM H160R
CatM H160R F293Y
BenM-DBDCatM
H160R F293Y
CatM I18F K38N
CatM I18F K38N H160R F293Y
benM-disrupted
B
Relative benA Expression
Muconate
Benzoate and Muconate
benMA5146
(promoter mutation)
ACN1232
ACN1307
ACN717
ACN720
ACN694
ACN157
ACN827
ACN832
ACN839
ACN1239
ACN1302
ACN1251
ACN1347
BenM
CatM
CatM F293Y
CatM H160R
CatM H160R F293Y
CatM
CatM F293Y
CatM H160R
CatM H160R F293Y
BenM-DBDCatM
H160R F293Y
CatM I18F K38N
CatM I18F K38N H160R F293Y
benM-disrupted

At this mutated promoter, *ben*-gene expression was higher under all conditions in strains encoding the variants (ACN827, ACN832, and ACN839) relative to wild-type CatM (ACN157; Fig.2.5.A.B). In response to benzoate as sole effector, the H160R replacement caused an increased in expression. For CatM[H160R] (ACN832) or CatM[H160R,F293Y] (ACN839), benzoate led to expression levels 170% or 155%, respectively, of the non-induced levels. Although this increase was the first suggestion that CatM variants might be able to modulate transcription in response to benzoate, the regulatory pattern was dissimilar from that of BenM. The most notable aspect of wild-type regulation is that benzoate works synergistically with muconate to activate maximal levels of gene expression (ACN1232, Fig.2.5.B) (5).

In contrast, for CatM, the addition of benzoate inhibits muconate-mediated activation. For example, benzoate added with muconate typically results in CatM-dependent expression levels approximately 80% of those observed with muconate (Fig.2.5.B) (5, 6). For each engineered variant, the combination of benzoate and muconate resulted in a lower level of expression than with muconate alone. This inhibition resembled the pattern for CatM (ACN1307 and ACN157) and not that for BenM (ACN1232). Therefore, the goal of creating a BenM-like CatM variant was not achieved with these amino acid changes at positions 160 and 293.

Isolation of CatM variants that increase *benA* expression. In additional attempts to identify mutations that enable CatM to respond to benzoate, spontaneous mutants were selected from ACN682 as colonies on solid medium that grew on benzoate as the sole carbon source (ben+ phenotype). Similar approaches previously yielded regulatory

Table 2.3. Effect of *catM* mutations on growth with benzoate as the sole carbon source[a]

Strain	Relevant characteristics	Generation time (min) [b]	Lag time (hr) [c]
ADP1	Wild-type	70 ± 5	4.5 ± 0.5
ISA36	No BenM	No growth	No growth
ACN682	No BenM, CatM[F293Y]	No growth	No growth
ACN1087	No BenM, CatM[ΔD264]	104 ± 5	9 ± 0.5
ACN1225	No BenM, CatM[G232S]	188 ± 2	15 ± 0.6
ACN1096	No BenM, CatM[K148Q]	112 ± 2	12 ± 0.5
ACN1095	No BenM, CatM[I18F]	175 ± 3	18 ± 0.5
ACN1193	No BenM, CatM[K38N]	145 ± 6	11 ± 0.6
ACN1249	No BenM, CatM[I18F,K38N]	85 ± 2	5.5 ± 0.5
ACN1234	No BenM, $[_{\text{BenM-DBD}}]$CatM	82 ± 3	5 ± 0.5
ACN1301	No BenM, $[_{\text{BenM-DBD}}]$CatM(F293Y,H160R)	81 ± 4	5 ± 0.5
ACN1345	No BenM, CatM[I18F,K38N, H160R,F293Y]	83 ± 3	5 ± 0.5
ACN1294	$[_{\text{CatM-DBD}}]$BenM, No CatM	186 ± 6	21 ± 0.5
ACN1488	$[_{\text{CatM-DBD}}]$BenM(Y293F,R160H), No CatM	No growth	No growth
ACN1407	$[_{\text{CatM-DBD-LH}}]$BenM, No CatM	No growth	No growth
ACN1479	$[_{\text{CatM-DBD-LH}}]$BenM(Y293F,R160H), No CatM	No growth	No growth

[a] Strains has comparable growth rates with succinate as the sole carbon source (data not shown)
[b] Averages of at least four determinations
[c] Time between inoculation and start of exponential growth
No growth indicates strains unable to grow over a period of 24 hours

mutants from *benM* mutants with wild-type *catM* (6, 10). The rationale for using ACN682 as the parent strain for selecting ben+ derivatives was based on the possibilitythat the increased *ben*-gene expression resulting from CatM[F293Y] might facilitate the isolation of additional mutations that confer growth on benzoate.

Independent ben+ derivatives of ACN682 were obtained and characterized as described in past studies (6). Briefly, the *catM* region of each mutant was isolated with a method that captures targeted chromosomal DNA on a plasmid following homologous recombination in vivo (18). Plasmid DNA was subsequently linearized and used in a transformation assay to determine whether it restores ben+ growth to a *benM*-disrupted strain via allelic replacement (10). In this fashion, *catM* alleles from four different spontaneous mutants were identified and sequenced and found to contain the parent mutation encoding the F293Y replacement and an additional mutation corresponding to amino acid alteration in either the EBD or DBD region of CatM.

We determined whether the newly identified CatM variants required the F293Y replacement for the ben+ phenotype. Genetic approaches were used to generate strains with *catM* alleles that encode the wild-type residue (F) at position 293 and that carry one of the new mutations elsewhere in the gene (as described in Materials and Methods). By testing the growth phenotypes of the resulting strains, we found that the F293Y replacement was not needed for BenM-independent growth on benzoate for the following CatM variants: CatM [ΔD264], CatM[G232S], CatM[K148Q], and CatM[I18F] (Table 2.2).

BenM-independent growth by CatM EBD variant regulators. Three of the new CatM variants had an alteration in the EBD portion of the regulator. To determine whether these variants responded to benzoate, we generated strains (without *benM*) in which the regulatory ability of each CatM alteration (ΔD264, K148Q, or G232S) could be assessed with a chromosomal *benA*::*lacZ* fusion. As indicated in figure 2.6, Strains ACN1108 (CatM[ΔD264]), ACN1112 (CatM[K148Q]), and ACN1228 (CatM[G232S]) LacZ activity was significantly higher relative to that in ACN1307 when strains were grown on muconate. When benzoate was added to the medium alone or in combination with muconate, no increase in *benA*::*lacZ* activity was detected (data not shown). In the absence of muconate, basal expression at P_{benA} is detected by CatM[G232S]. Since amino acid changes in the EBD may result in increased in basal expression activity, it is plausible that this variant have acquired such characteristic as previously observed in the variant protein CatM[R156H] (10).

Effects of these alleles were tested at the *catBCIJFD* operon where CatM plays a major role and activates high muconate-inducible levels of *catB* expression (Figure 2.7.A). Previous studies have shown that increased muconate-dependent *benA* expression might correlate to decrease in CatB enzyme activity on strains that lack BenM (7). This decrease in CatB activity may permit transient accumulation of muconate, which is needed for CatM-mediated *benA* activation. The *catB*::*lacZ* activity from strains carrying variant proteins that permit high *benA* transcription was lower than wild-type CatM in response to muconate (10) (Figure 2.7.A). A similar activation pattern was detected on all our strains carrying *catM* alleles with amino acid changes in the EBD (Figure 2.7.A).

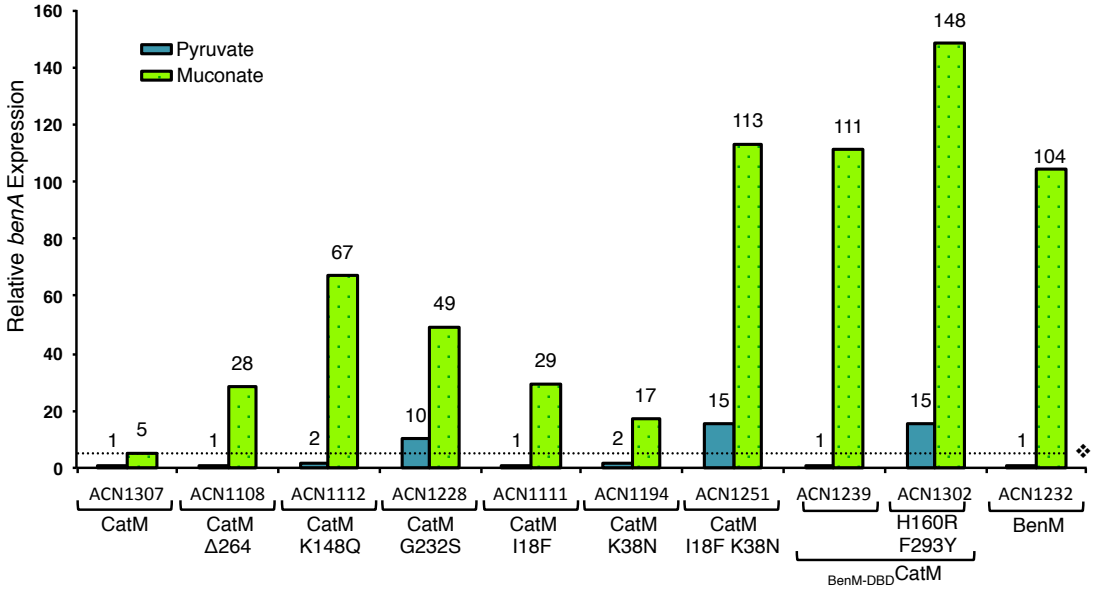

FIGURE 2.6. **Effect of *catM* alleles on expression of a chromosomal *benA*::*lacZ* transcriptional reporter.** Strain encoding their wild type and variant regulator are indicated. All strain lack a functional *benM*. (❖) Dotted bottom line represents the level of wild type CatM-dependent *benA* expression in the presence of muconate (strain ACN1307). Cultures were grown on pyruvate or muconate as indicated. Relative *benA* expression is reported as the ratio of measured LacZ activity to that of uninduced ACN1232 (2.6 ± 0.51 nmol/min/ml/OD_{600}). Data represent the average of at least four independent replicates, and standard deviations were less than 12% of the average value.

Figure 2.7. Effect of *catM* alleles on expression of a chromosomal *catB*::*lacZ* and *catA*::*lacZ* transcriptional reporters. All strains lack a functional BenM. **(A)** Control strain ACN585, wild type CatM. For *catB::lacZ* measurements, strains were grown on pyruvate and muconate was added as indicated. Relative catB activity was determined as the ratio of measure LacZ activity to that of uninduced ACN585 (5.4 ± 0.65 nmol/min/ml/OD_{600}). **(B)** Control strains ACN1498, wild type CatM. Strains were grown on pyruvate or muconate as indicated. Relative *catA* expression is reported as the ratio of measured LacZ activity to that of uninduced ACN1498 (1.1 ± 0.51 nmol/min/ml/OD_{600}). Data represent the average of at least four independent replications, and standard deviations were within 15% of the average value.

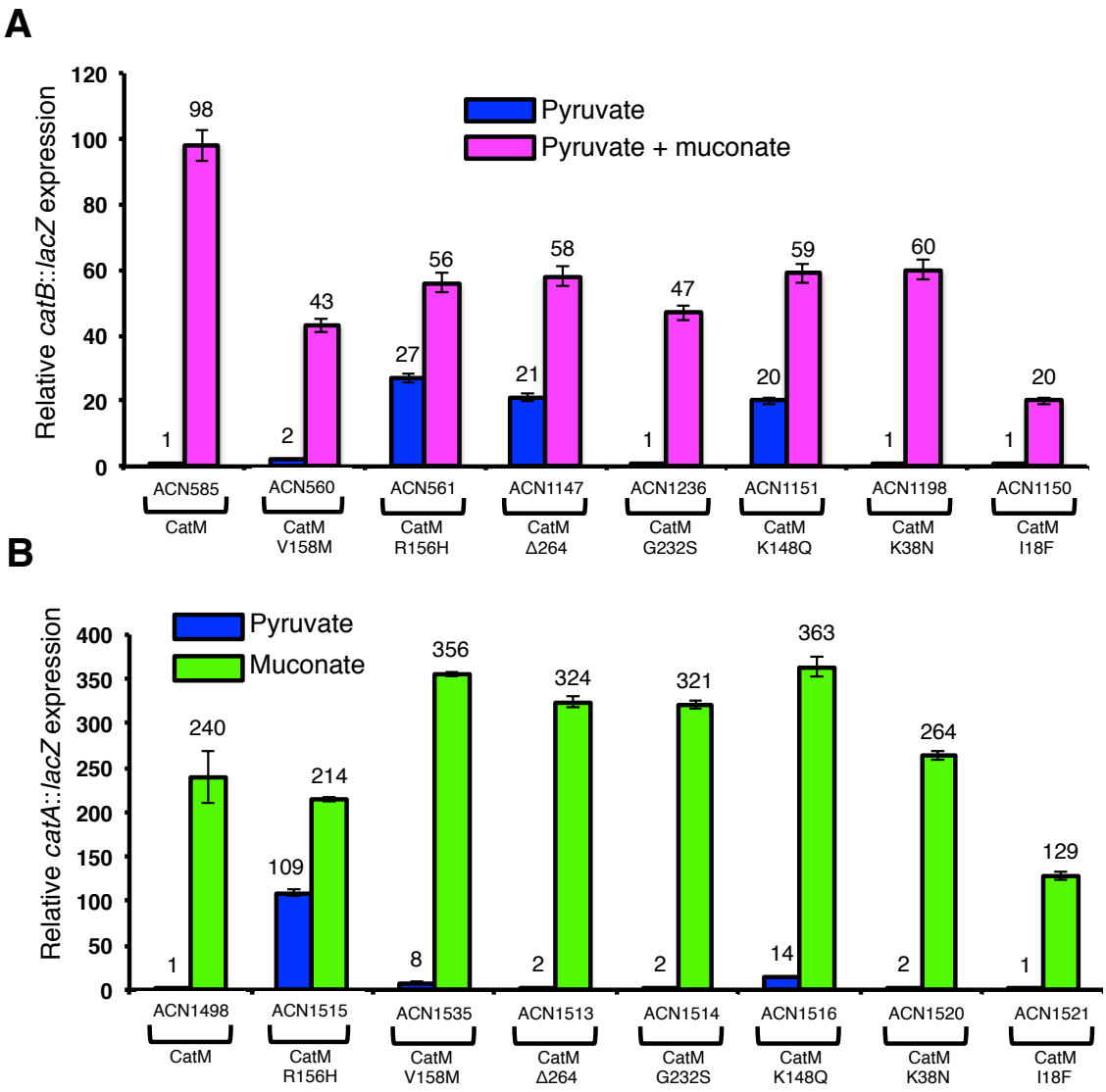
A
Relative catB::lacZ expression
120
100
80
60
40
20
0
Pyruvate
Pyruvate + muconate
98
1
43
2
56
27
58
21
47
1
59
20
60
1
20
1
ACN585
CatM
ACN560
CatM V158M
ACN561
CatM R156H
ACN1147
CatM Δ264
ACN1236
CatM G232S
ACN1151
CatM K148Q
ACN1198
CatM K38N
ACN1150
CatM I18F
B
Relative catA::lacZ expression
400
350
300
250
200
150
100
50
0
Pyruvate
Muconate
240
1
214
109
356
8
324
2
321
2
363
14
264
2
129
1
ACN1498
CatM
ACN1515
CatM R156H
ACN1535
CatM V158M
ACN1513
CatM Δ264
ACN1514
CatM G232S
ACN1516
CatM K148Q
ACN1520
CatM K38N
ACN1521
CatM I18F

Basal *catB* expression from strains ACN1147 (CatM[K148Q] and ACN1151(CatM[ΔD264]) was elevated. This increase in basal expression is also observed in ACN561 (CatM[R156H]. As previously reported, this protein can activate expression in the absence of inducer at the *benA* and *catB* operons. However, the inducer-independent *catB* expression by CatM[K148Q] and CatM[Δ264] is only observed at thisoperon. Therefore, these variants conduct transcriptional activation differently at both *benA* and *catB* to permit benzoate degradation unlike CatM[R156H], which activates high transcription from both operons regardless of effector availability.

It is plausible that activation from the *catA* gene might be affected by these CatM variants to permit rapid catechol to muconate conversion. Thus, permitting the augmentation of this metabolite to allow CatM-mediated *benA* activation. A *catA*::*lacZ* fusion was constructed and inserted in strains carrying *catM* alleles. Muconate-inducible LacZ activity from this fusion was higher than normal CatM-mediated *catA* activation (Figure 2.7.B). This increase in *catA* transcription might correlate to higher CatA enzyme activity, which may result in more CatA enzyme available for muconate generation. Thus, these CatM variants permit benzoate degradation by altering activation at different distant promoter regions, which differs from wild-type CatM-mediated activation.

CatM DNA-binding domain: amino acid replacements that enable BenM-independent benzoate growth. One of the isolated *catM* alleles that restore ben+ growth described above was of interest. Allele *catM51095* encoded an amino acid change at the DBD portion in CatM. Since most of CatM variants that enable BenM-independent growth on benzoate were found to encoded proteins with changes in the EBD portion,

this variant protein provides a different opportunity to examine the role of DBD in transcriptional activation. BenM and CatM are nearly identical in sequence at this region and differ by only nine amino acids (Fig. 2.3). CatM[I18F], substitutes I18 for F18, a residue found in BenM-DBD.

Due to this replacement, it is plausible to speculate that this variant activates *benABCDE* expression similarly to BenM. To test this hypothesis, LacZ activity on this strain was measured (Fig. 2.6). Despite high muconate-dependent activation detected in ACN1111 (CatM[I18F]), this increase was lower than BenM-mediated activation (ACN1232). Similar to other variants that permit benzoate growth in the absence of BenM, muconate and not benzoate is the key effector for increased expression at P_{benA}. It is not clear how this amino acid change in the DBD permits BenM-independent growth on benzoate in this strain. The ben+ phenotype can be attributed to an increase in the variant's response to muconate at P_{benA} (Fig.2.6). These results suggest that CatM can better regulate transcription from P_{benA} if its DBD is more like that of BenM. To expand these studies at CatM-DBD, an additional residue from BenM-DBD was replaced in CatM.

As described in Alanazi *et. al*, 2013, N38 might play a role in indirect readout in BenM-DBD-P_{benA} interactions (2). Thus, the effects of this residue were tested in CatM alone and in combination with F18. Site-directed mutagenesis was used to generate CatM[K38N] and CatM[I18F, K38N]. Plasmid pBAC961, encoding CatM[K38N], and plasmid pBAC1040 (CatM[I18F, K38N]) replaced *catM* gene in the chromosome by allelic exchange generating strains ACN1193 and ACN1249 respectively. Similar to other strains tested here, the *benM* gene is deleted in the chromosome. Protein

functionality was determined by testing growth using anthranilate or muconate as the carbon source. As explained above, a functional CatM is needed to activate *cat* gene expression to permit growth on these carbon sources. Not only these strains were able to utilize these carbon sources, they were able to grow on benzoate as well, albeit at different rates than ACN1095 (CatM[I18F]) (Table 2.3). ACN1249 encoding the double replacement, CatM[I18F, K38N], grew on benzoate faster and with a lag time similar to ADP1 (Table 2.3). Thus, the engineered mutation may encode a variant protein with similar BenM-mediated activation properties that is more adept in optimizing *ben-cat* gene transcriptional regulation.

Muconate-dependent *benA*::*lacZ* expression was evaluated in strains carrying these *catM* alleles, ACN1194, CatM[K38N] and ACN1251, CatM[I18F,K38N] (Fig 2.6). The *benA*::*lacZ* levels in ACN1194 were three-fold higher than ACN1307 but relatively lower than ACN1111 (CatM[I18F]). Muconate-inducible *benA* expression in ACN1251 is comparable to that of ACN1232 (wild type BenM). This elevated muconate-dependent expression at P_{benA} was never observed by other CatM variants, which indicates that changes in CatM-DBD at these two residues may recreate a DBD-*benA* interaction similar to BenM, and this interaction is enhanced by muconate. Interestingly, basal *benA::lacZ* expression was recorded under uninduced conditions in ACN1251. This uninduced-expression indicates distinct promoter specificity in this variant relative to wild-type CatM at P_{benA}. Since BenM or CatM represses *benA* expression under uninduced conditions, it is probable that this repression is loss and this variant CatM protein is not blocking transcription as strongly.

Amino acid replacements in BenM-DBD. Residues F18 and N38 appear to be important for strong transcriptional activation from P_{benA}. To test this conclusion, residues at positions 18 and 38 in BenM were replaced with those of CatM. A strain generated to encode BenM[F18I,N38K], ACN1250, grew on benzoate, albeit very slowly (data not shown). When the ability of this variant to regulate P_{benA} was tested with a *benA*::*lacZ* reporter, expression was significantly decreased under all conditions. Nevertheless, synergistic transcriptional activation in response to benzoate and muconate was observed for this BenM variant (data not shown).

Swapping CatM DBD ([$_{\text{BenM-DBD}}$]CatM) with BenM DBD affects promoter specificity by increasing transcriptional activation of *benA*. Since amino acids at positions 18 and 38 had a dramatic impact on the level of muconate-inducible expression from P_{benA}, we explored the effect of replacing the entire DBD of CatM with that from BenM. Overlapping extension PCR and allelic replacement methods were used create a chromosomal *catM* allele that encodes the desired protein, [$_{\text{BenM-DBD}}$]CatM. The *benM* gene was deleted in the resulting strain, ACN1234, to allow [$_{\text{BenM-DBD}}$]CatM be the sole regulator of the *ben-cat* genes. ACN1234 was able to grow with muconate, anthranilate and benzoate as source of carbon source and energy. To test whether benzoate growth was due to [$_{\text{BenM-DBD}}$]CatM-mediated activation, chromosomal DNA from the *catM* region of ACN1234 was isolated. The DNA corresponding to the *catM51234* allele restored ben+ growth to a ben- strain lacking BenM (ISA36).

Equally to ACN1249, CatM[I18F,K38N], ACN1234 grew on benzoate as sole source of carbon at similar growth rate and lag time than wild-type (Table 2.3). Growth

rates at anthranilate and muconate were similar to wild type as well (data not shown). By carrying the full length BenM-DBD, this variant regulator might be activating high level of P_{benA} expression similar to BenM. To test the effect of the *catM51234* allele ([$_{BenM-DBD}$]CatM) on *ben* gene expression, *benA*::*lacZ* activity was assessed. Strain ACN1239 was constructed and LacZ activity was evaluated under uninduced (pyruvate) and induced (muconate) conditions. Under muconate-induced conditions, *benA*::*lacZ* levels in ACN1239 ([$_{BenM-DBD}$]CatM) were similar to those of ACN1251 (CatM[I18F,K38N]) (Figure 2.6). Similar to other CatM variants described in this study, benzoate-dependent *benA* expression was not recorded on this strain (Figure 2.5.A.B).

F293Y and H160R amino acid replacements combined with BenM-DBD or [I18F,K38N] in CatM: generation of benzoate-responsive CatM variants. Since introducing a benzoate response in CatM had previously failed, a reasonable new approach was to make EBD changes in a variant that activates high-level transcription from P_{benA} in response to muconate, [$_{BenM-DBD}$]CatM. Therefore, we sought to generate a benzoate response in this variant by changing amino acids at positions 160 and 293 with those of BenM as described previously. Plasmid pBAC1078 ([$_{BenM-DBD}$]CatM[H160R,F293Y]) was transformed into ACN843, strain with the *benM* deletion, by allelic replacement to generate ACN1301. Since, [$_{BenM-DBD}$]CatM enables growth on benzoate as sole carbon source, benzoate growth by [$_{BenM-DBD}$]CatM[H160R,F293Y] was expected and similar growth rates were observed by ACN1234 ([$_{BenM-DBD}$]CatM) and ACN1301 ([$_{BenM-DBD}$]CatM[H160R,F293Y]) (Table 2.3).

Transformation assays determined that allele *catM51301* (encoding [$_{BenM-DBD}$]CatM[H160R,F293Y]) was responsible for benzoate growth. The effect of this allele on *benA*::*lacZ* was studied. Strain ACN1302 ([$_{BenM-DBD}$]CatM[H160R,F293Y]) had higher muconate-dependent *benA* expression than all strains tested including ACN1232 (wild type BenM). The amino acid changes in the EBD also resulted in high levels of basal *benA* transcription when grown on pyruvate, typically a non-inducing carbon source. When benzoate response was tested alone and with muconate, benzoate-inducible *benA* activation was increased by almost two-fold compared to uninduced expression (Figure 2.5.A). Similar to wild type BenM, [$_{BenM-DBD}$]CatM[H160R,F293Y] synergistically activated transcription in response to muconate and benzoate. As shown by CatM and CatM variants that lack a benzoate response, this effector reduces muconate-inducible *benA* expression (Figure 2.5.B), which is not observed by [$_{BenM-DBD}$]CatM[H160R,F293Y]. Therefore, this variant has acquired the desired benzoate response and intriguingly, this response requires the BenM-DBD.

While the BenM-DBD portion of this regulator introduces nine amino acid changes (Fig.2.3), two of these changes, I18F and K38N, are sufficient to increase muconate responsiveness (Fig. 2.6). To see if these changes were sufficient for benzoate regulation when combined with the EBD changes, we engineered an allele that encodes CatM[I18F,K38N,H160R,F293Y]. Strain ACN1345 (CatM[I18F,K38N, H160R,F293Y]) was able to grow rapidly on benzoate (Table 2.3). This variant regulator also activated high-level muconate-dependent *benA* transcription (Figure 2.6) and benzoate-dependent transcription (Figure 2.5.A). Maximal *benA* expression by this variant was observed when benzoate and muconate were provided, which is also detected by $_{BenM-DBD}$

CatM(H160R,F293Y), albeit at lower levels. Based on these results, acquisition of benzoate responsiveness by CatM needs the BenM-DBD or at least these two amino acids replacements (I18F, K38N) along with the residues that directly interact with benzoate (Arg160 and Tyr293).

DBD changes affect binding affinity to the *benA* promoter. Protein-DNA interactions between CatM variants and P_{benA} were compared to those of the wild-type CatM. DNase I footprinting experiments have shown that BenM and CatM can bind to the *benA* promoter, but protein-DNA binding affinities were not previously determined. Electrophoretic mobility gel shift assays (EMSA) were performed to determine binding affinities. A fluorescently labeled DNA region containing P_{benA} was incubated with different protein concentrations as described in materials and methods. Both BenM and CatM bind to P_{benA}, albeit with different K_d coefficients (Table 2.4).

Since BenM plays a major role at this region, a higher binding affinity to P_{benA} than CatM is to be expected. Interestingly, binding affinities are not severely affected upon effector binding, which has been described previously for some LTTRs. In regulators such as OccR, the addition of octopine fails to increase binding affinities to its cognate promoter (1). Only upon benzoate addition, BenM K_d to P_{benA} decreases by two fold. Despite maximal *benA* expression observed when both effectors are bound to BenM, it does not correlate with increase in binding affinities in fact the K_d to P_{benA} slightly increases.

Table 2.4. Binding affinities of BenM, CatM and CatM variants to *benA* promoter region under different effector conditions

protein	No effector K_d (nM)[a]	Benzoate[b] K_d (nM)[a]	Muconate[c] K_d (nM)[a]	Muconate + Benzoate[d] K_d (nM)[a]
Wild-type BenM	33 ± 2	16 ± 2	42 ± 3	48 ± 2
Wild-type CatM	70± 4	70 ± 4	68 ± 2	72 ± 3
$_{\text{BenM-DBD}}$CatM	1 ± 1	5 ± 2	3 ± 1	5 ± 1
$_{\text{BenM-DBD}}$CatM[F293Y,H160R]	1 ± 1	5 ± 1	2 ± 1	4 ± 1
CatM[I18F,K38N]	45 ± 3	33 ± 3	33 ± 3	35 ± 3
$_{\text{CatM-DBD}}$BenM	168 ± 5	768	22 ± 3	6 ± 2

[a] Kd, equilibrium dissociation constant.
[b, c] and [d] from 1.6 mM total concentration of inducer per reaction and 800 uM of each inducer when were added together to each reaction.

Binding affinities of CatM-DBD variant proteins to P_{benA} are expected to be higher than wild type CatM. Similar to BenM, CatM[I18F,K38N] has similar K_d values and binding affinities remained relative unchanged upon effector binding. Thus, F18 and K38 increased CatM binding affinity to P_{benA}. However, binding affinities from CatM variants with full-length BenM-DBD ([$_{BenM\text{-}DBD}$]CatM and [$_{BenM\text{-}DBD}$]CatM[H160R,F293Y]) are about 10 fold higher than wild type BenM (Table 2.4). Despite changes in the EBD region, the binding affinities of [$_{BenM\text{-}DBD}$]CatM[H160R,F293Y] to P_{benA} remained similar to those of [$_{BenM\text{-}DBD}$]CatM. Thus Arg160 and Tyr293 do not affect binding affinity at this promoter. Despite sharing the same DBD, it is of interest the higher than normal binding affinities exhibit by [$_{BenM\text{-}DBD}$]CatM and [$_{BenM\text{-}DBD}$]CatM[H160R,F293Y] but not from BenM. It is possible that in CatM, this DBD makes a greater impact in the overall CatM tetramer that is enhanced upon binding to the P_{benA}.

DNase I Footprint analysis was used to confirm binding of CatM[I18F,K38N], [$_{BenM\text{-}DBD}$]CatM and [$_{BenM\text{-}DBD}$]CatM[H160R,F293Y] to P_{benA} intergenic region (See Fig.2.S.1). CatM-DBD variants, [$_{BenM\text{-}DBD}$]CatM, CatM[I18F, K38N] and [$_{BenM\text{-}DBD}$]CatM[H160R,F293Y] showed similar protection patterns to DNase I cleavage than wild-type BenM with and without muconate. Nevertheless, protection of site1 and site 2 is more pronounced by BenM when muconate and benzoate are added. This similar pattern is observed only by [$_{BenM\text{-}DBD}$]CatM and [$_{BenM\text{-}DBD}$]CatM[H160R,F293Y] upon muconate binding and not with CatM[K38N,I18F] and wild-type CatM (See Fig. S3.2). There are no significant changes in DNA protection by [$_{BenM\text{-}DBD}$]CatM[H160R,F293Y] when benzoate and muconate were added together (data not shown).

The effect of BenM-DBD on transcriptional regulation of P_{catB}. Synergistic activation has been observed only at the *benABCDE* operon and it is carried out by BenM. When this synergistic response was tested at the *catBCIJFD* operon, benzoate inhibited muconate-dependent activation by BenM similar to what is observed with CatM, which lacks a benzoate response (Figure 2.8). Since BenM plays a minor role at this operon, it is likely that BenM interactions with this promoter region (P_{catB}) are not ideal comparable with P_{benA}. As described above, CatM variants that activate higher than normal *benA* transcription can result in decreased *catB* gene expression. All these variants lack a benzoate response. Therefore, we sought to test *catB* regulation by the benzoate responsive variants [$_{\text{BenM-DBD}}$]CatM[F293Y, H160R] and CatM[I18F,K38N, H160R, F293Y]). A *catB*::*lacZ* (Fig. 2.1) fusion was introduced in the chromosome to yield strains ACN1359 and ACN1391 respectively. Muconate- dependent activation was observed in all strains and these levels were similar to wild-type CatM (ACN1308) (data not shown). Unlike BenM and CatM, benzoate slightly increases muconate-inducible *catB* activation while benzoate-inducible *catB* activation was minimal on strains ACN1359 and ACN1391 (data not shown).

Since initial benzoate degradation (*ben* operon) is still active in all these strains, the role of benzoate as an effector cannot be accurately measured in this background. Therefore, an omega (ΩS) cassette was inserted in the *benA* gene in all strains to prevent benzoate degradation. *catB* activation patterns by CatM and BenM remained similar under all conditions tested with CatM activating higher levels of *catB* transcription than BenM (Figure 2.8). Muconate-dependent *catB* activation by the benzoate responsive CatM

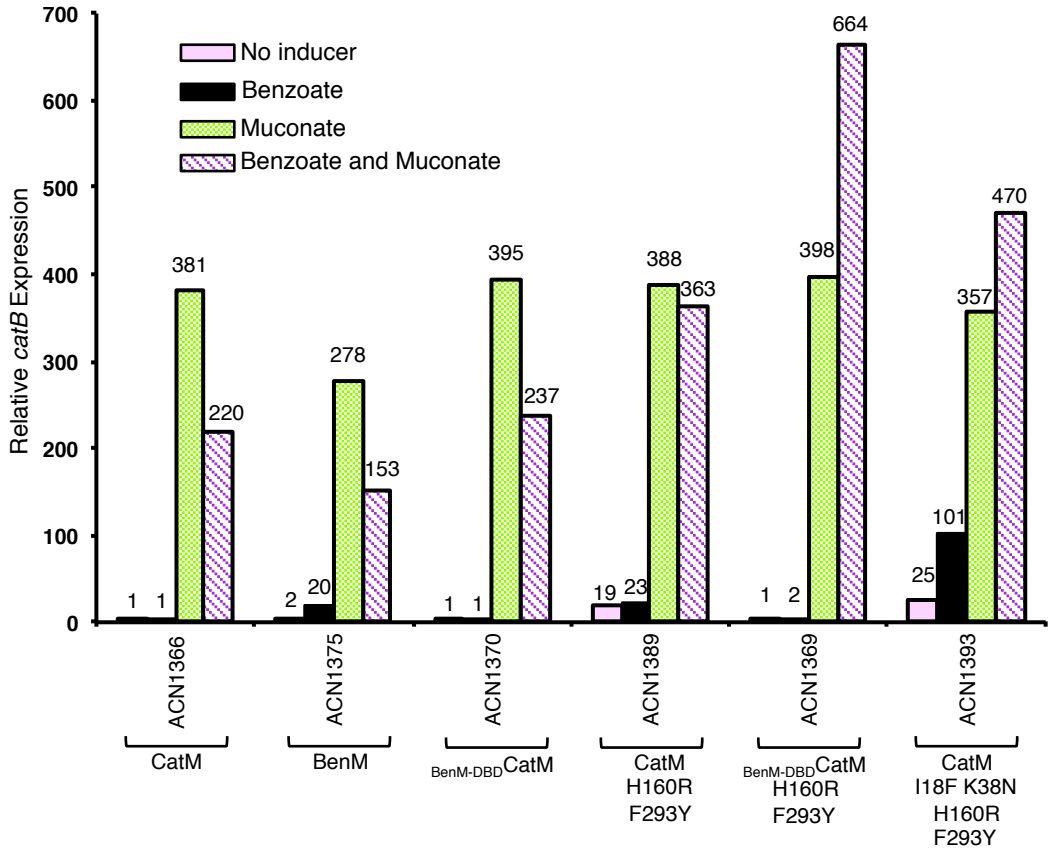

Figure 2.8. Expression of a chromosomal *catB*::*lacZ* fusion in strains encoding CatM, BenM and engineered CatM variants. Cultures were grow on pyruvate (20 mM) with addition of the indicated effector (65 μM benzoate, 65 μM muconate and 32.5 μM benzoate and muconate). A ΩS cassette is inserted in *benA* to prevent benzoate degradation. Relative *catB* expression is reported as the ratio of measured LacZ activity to that of uninduced ACN1366 (0.7 ± 0.3 nmol/min/ml/OD_{600}). Data represent the average of at least four independent replicates, and standard deviations were within 10% of the average value.

Table 2.5. Binding affinities of BenM, CatM and CatM variants to *catB* promoter region under different inducer conditions

protein	No effector K_d (nM)[a]	Benzoate[b] K_d (nM)[a]	Muconate[c] K_d (nM)[a]	Muconate + Benzoate[d] K_d (nM)[a]
Wild-type BenM	26 ± 2	25 ± 2	15 ± 2	20 ± 2
Wild-type CatM	5 ± 1	9 ± 1	9 ± 1	9 ± 1
$_{\text{BenM-DBD}}$CatM	1 ± 0.5	6 ± 1	6 ± 0.5	7 ± 1
$_{\text{BenM-DBD}}$CatM[F293Y, H160R]	5 ± 1	6 ± 1	7 ± 1	5 ± 1
CatM[I18F, K38N]	26 ± 2	13 ± 2	8 ± 1	11 ± 2
$_{\text{CatM-DBD}}$BenM	129 ± 6	54 ± 3	37 ± 3	35 ± 3.5

[a] Kd, equilibrium dissociation constant.
[b, c] and [d] from 1.6 mM total concentration of inducer per reaction and 800 uM of each inducer when were added together to each reaction.

variants (ACN1369 and ACN1393) was similar to those of CatM. However, maximal *catB* expression was observed only when benzoate and muconate were added (Figure 2.8). This synergistic activation was observed clearly in ACN1369 ([$_{\text{BenM-DBD}}$]CatM[F293Y, H160R]) despite low benzoate-inducible *catB* levels. ACN1393 (CatM[I18F,K38N, H160R, F293Y]) has higher than normal benzoate-inducible *catB* activation levels, but in combination with muconate, *catB* activation is less pronounced than ACN1369.

It is unclear which changes (EBD or DBD) are responsible for the synergistic *catB* activation observed by ACN1369 ([$_{\text{BenM-DBD}}$]CatM[F293Y, H160R]). Therefore, the effects on *catB* expression by allele *catM5685* (CatM[H160R, F293Y]) were tested. This variant retains its CatM-DBD, which should govern promoter specificity appropriately at P_{catB}. Interestingly, neither benzoate-dependent *catB* expression nor synergistic activation were observed in strain ACN1389 (CatM[H160R, F293Y]) (Figure 2.8). The latter activation can only be observed in the CatM variant with the full BenM-DBD and the two EBD amino acid replacements. Based on these results, the synergistic activation at the *catB* operon requires the BenM-DBD. Thus changes in the EBD and DBD in CatM have yielded variant proteins able to activate high levels of transcription at *benA* and *catB*.

To determine whether binding affinities at P_{catB} have been altered in [$_{\text{BenM-DBD}}$]CatM[F293Y, H160R], EMSA experiments were performed. As expected, CatM binds to this promoter region with high affinity. Effector binding does not affect K_d values. Despite carrying the BenM-DBD, binding affinities from [$_{\text{BenM-DBD}}$]CatM[F293Y, H160R] are similar to those of wild type CatM (Table 2.5). Similar to binding affinities at the *benA* promoter, values between [$_{\text{BenM-DBD}}$]CatM and [$_{\text{BenM-DBD}}$]CatM[F293Y, H160R]

are similar at P_{catB}, which indicates that changes in the EBD does not affect binding affinities. BenM can also bind to this region and its regulatory importance is reflected in higher K_d values than CatM. Despite having the same DBD as [$_{BenM\text{-}DBD}$]CatM[F293Y, H160R], BenM fails to yield similar binding affinities.

Discussion

Different amino acids in DBD alter gene expression at distant operons. Previous isolated mutants with CatM variants were found to have BenM-independent *ben* expression. Most of these variant proteins revealed the importance of single residues in the EBD portion, which resulted in transcriptional alteration in the *ben-cat* genes to permit CatM-mediated regulation in the absence of BenM (10). However, here a variant CatM protein was identified with an amino acid replacement at the DBD (CatM[I18F]) able to carry out a similar BenM-independent transcriptional activation led to a profounder evaluation of this domain to determine its role in transcriptional activation. Extensive mutagenesis studies at promoter regions from CatR, OccR, AtzR and others have permitted identification of important nucleotide elements needed for adequate LTTR transcriptional activation. Nevertheless, due to the lack of LTTR-DNA crystal structures far less is known about the role of the DBD (19, 26, 29). Solubility factors and protein aggregation problems have prevented generation of DBD structures bound to their cognate promoters. Thus, we could only rely on DBD-DNA models built from full-length LTTR structures. With the newly solved structure of BenM-DBD bound to its cognate DNA *(benA)*, we can begin to identify interactions that cannot otherwise be

possible (2). Taking advantage of this structure, the role of amino acid residues from the DBD described here can be assessed in further detail.

In the case of CatM[I18F], a hydrophobic amino acid, Ile, is replaced with another hydrophobic residue with a greater molecular weight, phenylalanine. It is possible that in CatM the hydrophobicity provide by Phe18 stabilizes surrounding amino acids as occurs in BenM-DBD. Crystallography studies of BenM-DBD bound to *benA* site 1, reveals that N amide side chain of Phe18 acts as a hydrogen bond donor. In addition, this amino acid also makes van der Waals contacts with the DNA phosphate backbone and deoxyribose (2). Interestingly, the phenyl ring of Phe18 is located in close proximity and nearly clashes with residues from the α3 helix, a helix involved in DNA recognition. When replaced with isoleucine, this proximity is loss in the DBD, but the other interactions remained. Interestingly, BenM variant (BenM[F18I]) cannot activate high levels of transcription from P_{benA} as wild-type BenM but can still grow on benzoate, albeit at much lower growth rates (data not shown). Therefore, Phe18 is required in BenM for adequate transcriptional activation from P_{benA}. This residue alone aids CatM-mediated activation probably by recreating needed interactions within the DBD that results in elevated transcriptional activation from promoter. Nevertheless, at the P_{catB}, the opposite effect is observed by CatM[I18F] (data not shown). Based on these results, we can conclude that Phe18 is a key residue involved in BenM's promoter specificity for the *benA* promoter.

Residue Asn38 (polar) in BenM or Lys38 (basic) in CatM is located at the DNA recognition helix (α3 helix), a region that directly interacts with the major groove in DNA. Based on the structure of BenM-DBD bound to *benA* site 1, Arg34, a conserved amino acid between BenM and CatM, orients Asn38 to interact with DNA causing a local

sharpen bend in the DNA duplex in some DBD-DNA structural subunits. When asparagine is changed by lysine at this location, the positive charged residue directly interacts with DNA via hydrogen bonding with an adenine base. With this change, no apparent orientation exert by Arg34 is observed. The BenM variant (BenM[N38K]) also activates lower than normal *benA* transcription and grows much slower on benzoate than wild type (data not shown). It is probable that the direct interaction of Lys38 with DNA is unfavorable at this promoter, but required at the *catB* promoter. CatM[K38N] fails to activate high *catB* transcription similar to CatM (data not shown). Swapping two amino acids unique to BenM-DBD in CatM-DBD is clearly favoring CatM-mediated *ben* gene expression by altering the promoter specificity of the regulator.

In LTTRs, DNA recognition and promoter specificity relay upon direct and indirect readouts between the DBD and DNA (2). The direct readout refers to specific DBD-DNA interactions among conserved protein side chains and nucleotide bases. An example of a direct readout includes Gln29, a well-conserved amino acid among LTTRs. A substitution of this residue in Nac, reduced the binding affinity of the regulator to its cognate promoter (*hut*) and Nac functionality is lost in this variant . In BenM, Gln29 directly interacts with the first adenine based (**A**TAC) in the *benA* promoter site 1 through hydrogen bonding. When this amino acid was substituted with alanine, the resulted variant BenM[Q29A] was unable to activate *benA* transcription and the strain cannot longer grow on benzoate (data not shown). The same changed in CatM (CatM[Q29A]), resulted in complete loss of *catB* activation and lack of growth on muconate (data not shown). Thus, direct readout interactions are essential for DNA

recognition in LTTRs and modification of these residues causes severe damage in DNA recognition and transcriptional activation.

On the other hand, indirect readout refers to the effects of the distinct local nucleotides that cause sequence-dependent deformations of the phosphate backbone that control protein recognition. These nucleotides refer to the bases outside the conserved recognition sequence ATAC and the interaction with these bases can contribute to promoter specificity. Based on the BenM-DBD-*benA* structure, Phe18 and Asn38 in BenM and Ile18 and Lys38 in CatM are involved in this indirect readout, and thus, these residues are important for promoter specificity for *benA* and *catB* promoter respectively. Based on the results described above, the swapping of these residues between BenM and CatM affects their promoter specificity, which results in alteration in transcriptional activation at *benA* and *catB*.

In the case of [$_{\text{BenM-DBD}}$]CatM and [$_{\text{BenM-DBD}}$]CatM[F293Y, H160R], all direct and indirect readouts between BenM-DBD-*benA* should be conserved in these proteins. Interestingly, muconate-dependent *catB* transcriptional activation remains unaffected, and the binding affinities to the *benA* and *catB* promoters are extremely increased in these proteins. This increase in DNA affinity could result from broader promoter specificity by these two variants, which results in these variants binding with equal binding affinities to both promoters and probably to other A-T rich sequences. However, these variant regulators failed to bind a non-specific promoter region (*leuC*), which is under the regulation of another LTTR, LeuR, and to other A-T rich regions tested (data not shown). Therefore, the promoter specificity for *benA* and *catB* is not loss and is rather expanded in both CatM variant proteins, which results in an ideal and unique

transcriptional regulator for the *ben-cat* genes. Interestingly, the BenM-Linker Helix (LH) is not required for the benzoate responsiveness of [$_{BenM\text{-}DBD}$]CatM[F293Y, H160R], which indicates that the LH in CatM is adequate to transmit this response between EBD-DBD. The inclusion of BenM-LH in this variant decreases transcriptional activation from P_{benA} and P_{catB} (data not shown). It is plausible to assume that the interactions between the N-terminal CatM-LH residues and residues from the wing of BenM-DBD in [$_{BenM\text{-}DBD}$]CatM[F293Y, H160R] permit this regulator to expand its promoter specificity and increase the binding affinity for P_{benA} and P_{catB}.

DBD-swapping studies in BenM resulted in a variant with reduced binding affinity than wild type BenM (Table 2.4 and 2.5). BenM variant ([$_{CatM\text{-}DBD}$]BenM) binding affinity is severely affected at both promoters. This binding affinity increased dramatically to both promoters only upon effector binding. At the *benA* promoter, muconate and benzoate reduces the K_d to single digits, which reflects *in vivo* LacZ results where maximal *benA* expression by this variant happens in response to both inducers (Table 2.4 and Figure 2.9.A). At P_{catB}, binding affinity decreased only upon muconate-binding, which also correlates to *in vivo catB::lacZ* results (Table 2.5 and Figure 2.9.B). Although the full-length CatM-DBD of this variant should permit activation at the *catBCIJFD* operon similar to CatM, only when the benzoate response is abolished from this variant, [$_{CatM\text{-}DBD}$]BenM[R160H, Y293F] can activate higher than normal muconate-inducible *catB* expression (Figure 2.9.B). The latter amino acid changes resulted in a strain unable to growth on benzoate, but with growth rates on muconate similar to wild type (data not shown). This inability to grow on benzoate is reflected in the incapability of this variant to activate *benA* transcription (Figure 2.9.A). Unlike [$_{BenM\text{-}}$

$_{DBD}$]CatM[F293Y, H160R], [$_{CatM-DBD}$]BenM[R160H, Y293F] activates transcription similar to CatM at P_{benA} and P_{catB}. When including the CatM-LH along with the CatM-DBD in the BenM variant ([$_{CatM-DBD-LH}$]BenM[R160H, Y293F]), *catB* transcription was slightly lower, but remained higher than wild-type BenM.

EBD effector responses also contribute to promoter specificity. The benzoate response acquired by [$_{BenM-DBD}$]CatM[F293Y, H160R] permits this protein to activate transcription similarly at *benABCDE* and *catBCIJFD* operons, which differs significantly from BenM and CatM. The replacement of Arg160 and Tyr293 alone in CatM does not generate a benzoate response, and it is likely that in CatM[H160R,F293Y], benzoate is competing with muconate for the primary binding site. This competition is attributed to decrease in muconate-inducible activation when benzoate is added in CatM (Figure 2.5.B).

To acquire a benzoate response, CatM-DBD must be modified to achieve specific BenM-DBD-*benA* interactions. These modifications are necessary for CatM to activate higher than normal muconate-dependent *benA* transcription similar to BenM. Only in this background, Arg160 and Tyr293 can recreate the benzoate response in CatM. It is probable that in [$_{BenM-DBD}$]CatM[F293Y, H160R], benzoate binds to the engineered secondary binding site, and the competition with muconate for the primary binding site decreases. As described in Ezezika *et al*. 2007, benzoate bound to this site enhances the muconate response in the primary site via a charge relay mechanism, which draws the surrounding helices more strongly toward muconate. These changes may provoke

Figure 2.9. Effects of *benM* alleles on *benA*::*lacZ* and *catB*::*lacZ* expression on strains grown on pyruvate (20 mM). (A) CatM is deleted on all strains. Inducers were added as indicated. Relative *benA* expression is determined as indicated previously. Standard deviations were within < 10% of the average value of four independent replications. **(B)** *benA* is deleted in all these strains. Relative *catB* expression is determined as indicated previously. Data represented the average of at least four independent replications, and standard deviations were within < 15% of the average value.

A

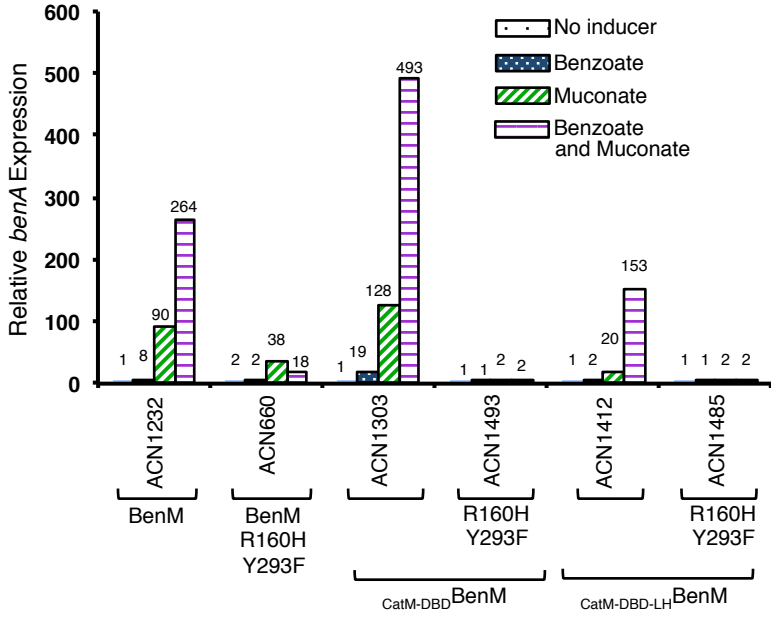
Relative benA Expression
600
500
400
300
200
100
0
No inducer
Benzoate
Muconate
Benzoate and Muconate
1 8 90 264
2 2 38 18
1 19 128 493
1 1 2 2
1 2 20 153
1 1 2 2
ACN1232
ACN660
ACN1303
ACN1493
ACN1412
ACN1485
BenM
BenM R160H Y293F
R160H Y293F
R160H Y293F
CatM-DBDBenM
CatM-DBD-LHBenM

B

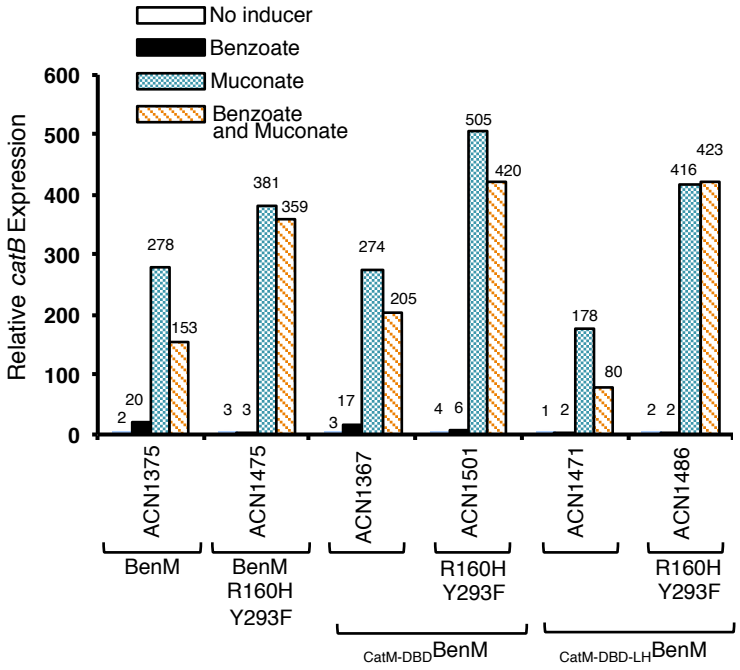
Relative catB Expression
600
500
400
300
200
100
0
No inducer
Benzoate
Muconate
Benzoate and Muconate
2 20 278 153
3 3 381 359
3 17 274 205
4 6 505 420
1 2 178 80
2 2 416 423
ACN1375
ACN1475
ACN1367
ACN1501
ACN1471
ACN1486
BenM
BenM R160H Y293F
R160H Y293F
R160H Y293F
CatM-DBDBenM
CatM-DBD-LHBenM

alterations needed for synergistic transcriptional activation (11). In CatM-EBD, all residues involved in the charge relay mechanism are conserved with the exception of Arg160 and Tyr293. Based on the results described here, [$_{\text{BenM-DBD}}$]CatM[F293Y, H160R] achieves such mechanism upon benzoate and muconate binding to their respective sites in the EBD, but only when specific DBD-*benA* interactions are accomplished.

Thus, it is plausible to assume that in BenM the benzoate-dependent response along with BenM-DBD contributes to the promoter specificity to *benA*. Similar changes in CatM expand promoter specificity to include *benA* and *catB*. It is remarkable that His160 and Phe293 in BenM alone on in combination with CatM-DBD enhance the muconate-dependent *catB* expression. As described in Craven *et al.* 2009 and observed here, BenM[R160H, Y293F] cannot activate high *benA* transcription similar to BenM. Therefore, the secondary binding site or the benzoate response in BenM prevents this regulator to activate high levels of muconate-inducible *catB* transcription similar to CatM. Based on these results, we can assume that the unique response to benzoate in BenM influences its promoter specificity.

Single mutations in EBD contribute to CatM-depended regulation. In the present study, several CatM variants able to act as the sole regulator of the *ben-cat* genes were characterized. From the four variants isolated as spontaneous mutants, three were found to have mutations encoding single amino acid changes at positions 148, 232, and the loss of aspartate at position 264 in the EDB portion of CatM. Despite far less conservation at this domain, these residues, Lys148, Gly232 and Asp264 are conserved in both BenM and CatM.

Lys148 and Asp264 are located in close proximity to a region involved in protein oligomerization, the α10-α10 tetramer interface. As described in Raungprasert *et al.,* 2010, this tetramer interface is present in several LTTRs that have an oligomeric organization similar to CatM, BenM and CbnR. This interface is described to help join two dimeric units into a tetramer (22). Structural analysis of BenM[R156H]-EDB, an inducer-independent variant, was proposed to activate transcription by altering interactions with amino acids that lay within the α10-α10 tetramer interface such as Lys148 and Asp264 (8). It was suggested that His156 may weaken the interaction with Asp264 located at the adjacent EBD subunit. This change alters interactions with Lys148, which impacts the relationship between subunits (8). Lys148, a hydrophobic amino acid, was identified to contribute hydrogen bond interactions between EDB subunits at this interface and forms salt bridges with Glu213 and Asp264 (22). When replaced for glutamine, interaction with Asp264 is loss and a salt bridge is formed with Arg156, thus disrupting bonding in the α10-α10 tetramer interface. Unlike CatM[R156H], CatM[K148Q] cannot activate inducer-independent transcription at *benA*. Interestingly, this muconate-independent activation is observed only at *catB*. It is probable that the interaction between Glu148 and Arg156 causes subtle changes throughout the CatM tetramer that permits higher than normal *benA* transcription.

In the case of Asp264, this amino acid was identified to form salt bridges with amino acids involved in α10-α10 tetramer interface as described in detail in Craven *et al.,* 2009. This amino acid is located in a loop close to the β9 region and forms an ionic interaction with Arg156 and Lys148. Similar to CatM[K148Q], inducer-independent activation by CatM[Δ264] is only observed at *catB*. Thus, the absence of these

interactions may have a subtle impact in this region. It is admissible to say that these alterations at the tetramer interface can be easily amplified and propagated to other parts of the protein and have a more global effect in regulation.

Interestingly, Gly232 is located at another common LTTR interface, the α6/β2-α11dimer interface of the EBDs. Based on structural data from full-length LTTRs, this interface is consistently found in all LTTRs. Previously isolated variants BenM[R225H] and BenM[E226K] were described to activate transcription in the absence of inducers. These amino acid replacements were proposed to cause ionic interactions, which resulted in conformational changes in the dimer interface. Gly232 interacts with, Gln228, Ala235 and Ala 236 in α11. When replaced by serine, the hydroxyl group provide by this hydrophilic residue provides an interaction with Leu101 from the adjacent subunit while other interactions remained. It is interesting to note that EBD variants isolated from spontaneous mutants described here or variants previously published have amino acid replacements located in specific regions involved in protein interlocking. It is probable that a single point mutation in these regions can cause significant changes in transcriptional activation, and thus more facile to reproduce than multiple mutations. As described previously, small changes in conserved regions can propagate to the whole protomer. These changes in interactions may favor a CatM tetramer to be able to activate high levels of *ben* gene expression.

Conclusion

In LTTRs, the EBD is proposed to be involved in signal transduction. In this case, effector binding by small molecules or by chemical modification causes an allosteric

change in this domain. This change is transmitted to other portions of the regulator and can sometimes affect the interaction and affinity of the DBD with DNA (15, 21, 28). However, it is not surprising to suggest that this allosteric effect can go in the opposite direction. Thus, binding by the DBD to the promoter region may result in changes in the EBD. In this case, the CatM-DBD variants described above while bound to the *benA* promoter may be transmitting a signal to other domains in the regulator. This allosteric signal changes as muconate becomes more available and the transcription from the *ben-cat* supraoperonic is activated. Structural investigations including studies on full-length BenM-*benA* promoter DNA and CatM-*benA* promoter DNA are necessary to understand these allosteric changes throughout the tetrameric complexes while activating or repressing transcription.

Acknowledgements

We are grateful to acknowledge Timothy Hoover for helpful suggestions and assistance with DNase I footprinting experiments. We thank Jennifer Morgan, Chelsea Kline and James Valle for isolation of some of the spontaneous mutants and plasmid construction used in this study. We also thank Katherine Elliott for helpful assistance and suggestions on many experiments. Ajchareeya Ruangpraset helped with assistance in protein purification and suggestions with electrophoretic mobility shift assays.

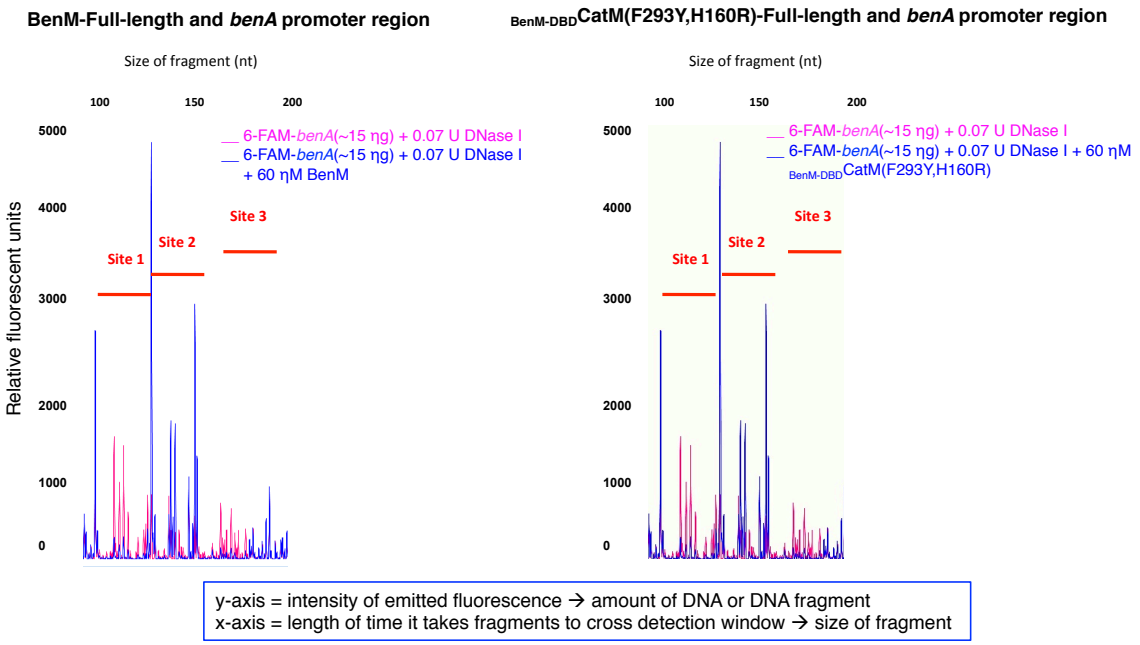

Figure 2.S.1 . DNase I footprint analysis at the *benA* promoter region. The electropherograms showing protection pattern of the *benA* promoter region after digestion with DNase I following incubation in the presence (blue) and absence (magenta) of BenM or $_{\text{BenM-DBD}}$CatM(F293Y,H160R). Predicted DNA binding sites for BenM and $_{\text{BenM-DBD}}$CatM(F293Y,H160R) are indicated. CatM[I18F,K38N] showed similar protection patterns (Data not shown). Fluorescent intensity of dye-labeled DNA fragments (y-axis) plotted against the sequence length of the DNA fragment.

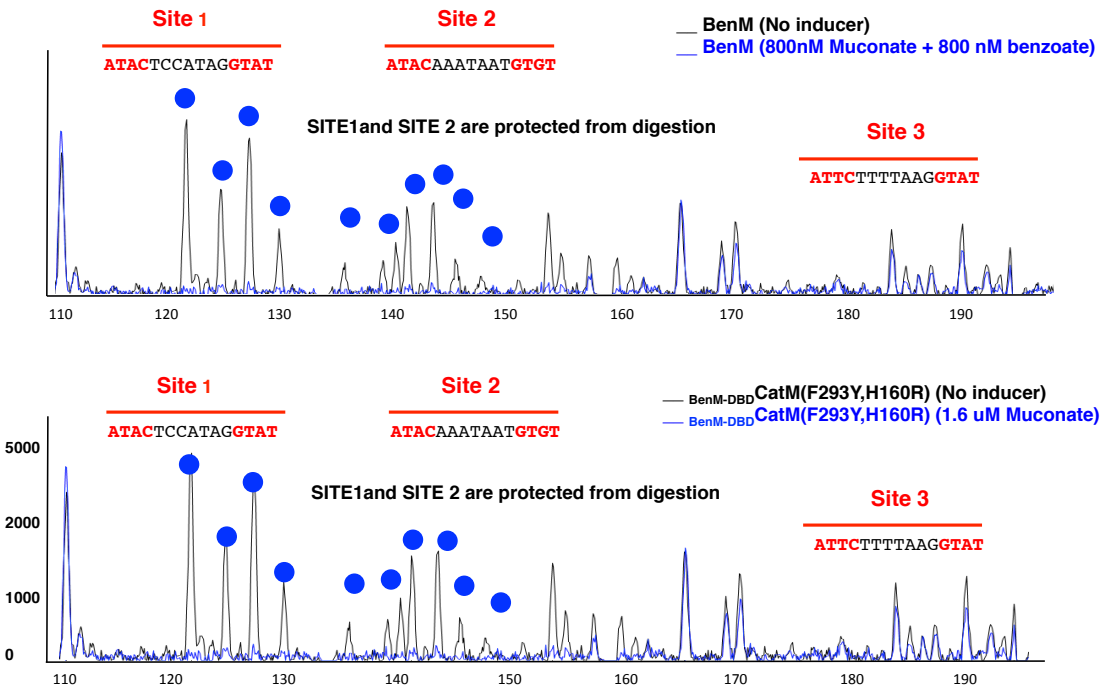

Figure 2.S.2. DNase I footprint analysis at the *benA* promoter. The electropherograms showing protection pattern of the *benA* promoter region after digestion with DNase I following incubation with of BenM or $_{\text{BenM-DBD}}$CatM(F293Y,H160R) in the presence (black) or absence (blue) of effectors. Predicted DNA binding sites for BenM and $_{\text{BenM-DBD}}$CatM(F293Y,H160R) are indicated. Fluorescent intensity of dye-labeled DNA fragments (y-axis) plotted against the sequence length of the DNA fragment.

References

1. **Akakura R, Winans SC.** 2002a. Mutations in the *occQ* operator that decrease OccR-induced DNA bending do not cause constitutive promoter activity. J. Biol. Chem. **277:**15773-15780.
2. **Alanazi AM, Neidle EL, Momany C.** 2013. The DNA-binding domain of BenM reveals the structural basis for the recognition of a T-N11-A sequence motif by LysR-type transcriptional regulators. Acta. Crystallogr. D. **69:**1995-2007.
3. **Bradford MM.** 1976. A rapid and sensitive method for the quantitation of microgram quantities of protein utilizing the principle of protein-dye binding. Anal. Biochem. **72:**248-254.
4. **Bundy BM.** Transcriptional Regulation o the *benABCDE* operon of *Acinetobacter* sp. ADP1: BenM-mediated synergistic induction in response to benzoate and *cis,cis*-muconate. Phd. Thesis. University of Georgia, Athens, GA.
5. **Bundy BM, Collier LS, Hoover TR, Neidle EL.** 2002. Synergistic transcriptional activation by one regulatory protein in response to two metabolites. Proc. Natl. Acad. Sci. U. S. A. **99:**7693-7698.
6. **Collier LS, Gaines GL, 3rd, Neidle EL.** 1998. Regulation of benzoate degradation in *Acinetobacter* sp. strain ADP1 by BenM, a LysR-type transcriptional activator. J. Bacteriol. **180:**2493-2501.
7. **Cosper NJ, Collier LS, Clark TJ, Scott RA, Neidle EL.** 2000. Mutations in *catB*, the gene encoding muconate cycloisomerase, activate transcription of the distal *ben* genes and contribute to a complex regulatory circuit in *Acinetobacter* sp. strain ADP1. J. Bacteriol. **182:**7044-7052.

8. **Craven SH, Ezezika OC, Haddad S, Hall RA, Momany C, Neidle EL.** 2009. Inducer responses of BenM, a LysR-type transcriptional regulator from *Acinetobacter baylyi* ADP1. Mol. Microbiol. **72:**881-894.

9. **Craven SH, Ezezika OC, Momany C, Neidle EL.** 2008. LysR Homologs in *Acinetobacter* : Insights into a Diverse Family of Transcriptional Regulators. In *Acinetobacter Molecular Biology*. Gerischer, U. (ed.). Norfolk: Caiester Academic Press, pp. 163-202.

10. **Ezezika OC, Collier-Hyams LS, Dale HA, Burk AC, Neidle EL.** 2006. CatM regulation of the *benABCDE* operon: functional divergence of two LysR-type paralogs in *Acinetobacter baylyi* ADP1. Appl. Environ. Microbiol. **72:**1749-1758.

11. **Ezezika OC, Haddad S, Clark TJ, Neidle EL, Momany C.** 2007. Distinct effector-binding sites enable synergistic transcriptional activation by BenM, a LysR-type regulator. J. Mol. Biol. **367:**616-629.

12. **Gregg-Jolly LA, Ornston LN.** 1990. Recovery of DNA from the *Acinetobacter calcoaceticus* chromosome by gap repair. J. Bacteriol. **172:**6169-6172.

13. **Juni E, Janik A.** 1969. Transformation of *Acinetobacter calcoaceticus* (Bacterium anitratum). J. Bacteriol. **98:**281-288.

14. **Lochowska A, Iwanicka-Nowicka R, Plochocka D, Hryniewicz MM.** 2001. Functional dissection of the LysR-type CysB transcriptional regulator. Regions important for DNA binding, inducer response, oligomerization, and positive control. J. Biol. Chem. **276:**2098-2107.

15. **Maddocks SE, Oyston PC.** 2008. Structure and function of the LysR-type transcriptional regulator (LTTR) family proteins. Microbiology. **154:**3609-3623.

16. **Muraoka S, Okumura R, Ogawa N, Nonaka T, Miyashita K, Senda T.** 2003. Crystal structure of a full-length LysR-type transcriptional regulator, CbnR: unusual combination of two subunit forms and molecular bases for causing and changing DNA bend. J. Mol. Biol. **328:**555-566.

17. **Neidle EL, Ornston LN.** 1986. Cloning and expression of *Acinetobacter calcoaceticus* catechol 1,2-dioxygenase structural gene *catA* in *Escherichia coli*. J. Bacteriol. **168:**815-820.

18. **Palmen R, Hellingwerf KJ.** 1997. Uptake and processing of DNA by *Acinetobacter calcoaceticus*. Gene. **192:**179-190.

19. **Porrua O, Lopez-Sanchez A, Platero AI, Santero E, Shingler V, Govantes F.** 2013. An A-tract at the AtzR binding site assists DNA binding, inducer-dependent repositioning and transcriptional activation of the P*atzDEF* promoter. Mol. Microbiol. **90:**72-87.

20. **Romero-Arroyo CE, Schell MA, Gaines GL, 3rd, Neidle EL.** 1995. *catM* encodes a LysR-type transcriptional activator regulating catechol degradation in *Acinetobacter calcoaceticus*. J. Bacteriol. **177:**5891-5898.

21. **Rosario CJ, Frisch RL, Bender RA.** 2010a. The LysR-type protein NAC forms complexes with both long and short DNA binding sites in the absence of co-effectors. J. Bacteriol. **192:**4827-4833.

22. **Ruangprasert A, Craven SH, Neidle EL, Momany C.** 2010. Full-length structures of BenM and two variants reveal different oligomerization schemes for LysR-type transcriptional regulators. J. Mol. Biol. **404:**568-586.

23. **Sambrook J, Fritsch F, Maniatis T.** 1989. *Molecular cloning: a laboratory manual, 2nd ed.* Cold Spring Harbor Laboratory Press, Cold Spring Harbor, N.Y.

24. **Seaton SC, Elliott KT, Cuff LE, Laniohan NS, Patel PR, Neidle EL.** 2012. Genome-wide selection for increased copy number in *Acinetobacter baylyi* ADP1: locus and context-dependent variation in gene amplification. Mol. Microbiol. **83:**520-535.

25. **Smirnova IA, Dian C, Leonard GA, McSweeney S, Birse D, Brzezinski P.** 2004. Development of a bacterial biosensor for nitrotoluenes: the crystal structure of the transcriptional regulator DntR. J. Mol. Biol. **340:**405-418.

26. **Tover A, Zernant J, Chugani SA, Chakrabarty AM, Kivisaar M.** 2000. Critical nucleotides in the interaction of CatR with the *pheBA* promoter: conservation of the CatR-mediated regulation mechanisms between the *pheBA* and *catBCA* operons. Microbiology. **146:**173-183.

27. **Vaneechoutte M, Young DM, Ornston LN, De Baere T, Nemec A, Van Der Reijden T, Carr E, Tjernberg I, Dijkshoorn L.** 2006. Naturally transformable *Acinetobacter* sp. strain ADP1 belongs to the newly described species *Acinetobacter baylyi*. Appl. Environ. Microbiol. **72:**932-936.

28. **Verschueren KH, Tyrrell R, Murshudov GN, Dodson EJ, Wilkinson AJ.** 1999. Solution of the structure of the cofactor-binding fragment of CysB: a struggle against non-isomorphism. Act. Crystallogr. **55:**369-378.

29. **Wang L, Winans SC.** 1995. The sixty nucleotide OccR operator contains a subsite essential and sufficient for OccR binding and a second subsite required for ligand-responsive DNA bending. J. Mol. Biol. **253:**691-702.

30. **Yanisch-Perron C, Vieira J, Messing J.** 1985. Improved M13 phage cloning vectors and host strains: nucleotide sequences of the M13mp18 and pUC19 vectors. Gene. **33:**103-119.

CHAPTER 3

LINKER HELIX PROVIDES MORE THAN OLIGOMERIZATION PROPERTIES TO CATM, A LYSR-TYPE TRANSCRIPTIONAL REGULATOR IN *ACINETOBACTER BAYLYI* STRAIN ADP1*

---

* Melissa P. Tumen-Velasquez, Ellen Neidle, Cory Momany. To be submitted to the *Journal of Bacteriology*

Abstract

The LysR-type transcriptional regulator (LLTR) CatM of *Acinetobacter baylyi* strain ADP1 activates catechol degradation *cat* genes (*catA* and *catBCIJFD* operon) in response to *cis, cis*-muconate (hereafter called muconate), a metabolite from the catechol branch of the β-ketoadipate pathway. CatM also activates expression from the *benPK* operon, involved in benzoate uptake and slightly activates genes form the *benABCDE* operon, involved in benzoate conversion to catechol. The latter operon is controlled by the LTTR BenM, whose disruption impaired benzoate utilization as source of carbon and energy in *A. baylyi*. However, spontaneous mutants arise readily in strains without BenM. As reported here, in these strains, three CatM variants increase *ben*-gene expression via elevated transcriptional regulation in response to muconate. These CatM variants with single amino acid changes enable CatM to substitute for the loss of BenM during growth on benzoate. Interestingly, the amino acid replacements were located in the linker helix (LH) region that connects the effector binding domain (EBD) and DNA binding domain (DBD). Although the LH has been described to aid oligomerization and diffuse information between the two domains, a clear function in transcriptional activation has yet to be elucidated. Characterization of these three CatM variants reveals a role for this region in transcriptional regulation.

Introduction

The soil bacterium, *Acinetobacter baylyi* ADP1 is a versatile organism able to metabolize a range of carbon sources including aromatic compounds (3). In ADP1, benzoate degradation is control by two LysR-type transcriptional regulators, BenM and CatM. These regulators control expression of the *ben-cat* supraoperonic cluster whose gene products degrade benzoate to tricarboxylic cycle intermediates succinyl and acetyl coenzyme A (Figure 3.1) (7, 15, 23). Despite sharing high amino acid sequence similarity (59%) and overlapping functionality, BenM and CatM co-regulate target promoter regions in different manners (7, 23). At the *ben* operon, BenM activates gene expression synergistically in response to benzoate and muconate, while CatM fails to activate high levels of expression (6). Thus, CatM-mediated *ben* gene expression is not sufficient for a strain to utilize benzoate as source of energy and carbon in the absence of BenM. Both regulators respond to muconate, but only BenM responds to benzoate. Previous isolated CatM variants with altered effector-dependent regulation served as powerful tools for understanding CatM-mediated regulation at the *ben* operon (11, 31). The foundation of the present study stems from these findings and involves enhancing the role of the linker helix region in CatM-mediated regulation by isolating and characterizing CatM variants with amino acid replacements in this location.

LTTRs are the largest family of prokaryotic transcriptional regulators (19, 27). Properties of these DNA-binding regulators range from metabolism to pathogenesis (19). Mutational analysis and sequence comparisons indicate that LTTRs are composed of two main domains: a highly conserved N-terminal DNA binding domain (DBD) with a winged helix-turn-helix motif (wHTH) and a far less conserved C-terminal

Figure 3.1. Benzoate degradation in ADP1. Degradation is governed by the levels of inducers that interact with BenM and CatM. Genes for benzoate degradation (*ben* and *cat* genes) are clustered in the ADP1 chromosome. ◇ Indicates promoters (numbered 1.3,4) whose expression is controlled by BenM and CatM. Bold text indicates the relative importance of each regulator at these four promoters. At region 1 and 3 both regulators play equal roles in regulation. At regions 2 and 4,BenM or CatM, is the major regulator respectively. At regulatory region number two (◆) BenM controls transcription of its own expression as well as the divergent *benABCDE* operon. CatM can bind to this region but is not sufficient to activate the appropriate levels of gene expression for growth on benzoate as sole source of carbon. Genes for anthranilate degradation (*antABC*) are not under the regulation of BenM and CatM (Bundy *et al.,*1998) (5)

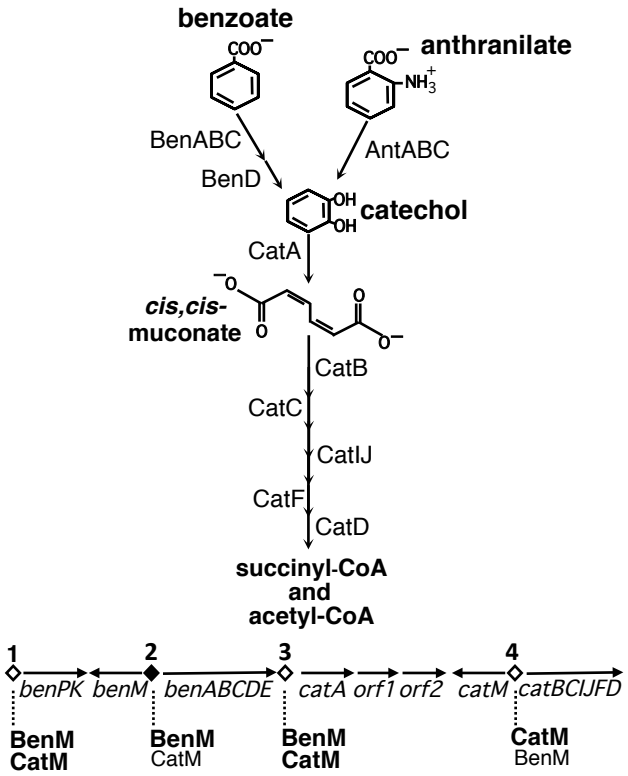
benzoate
anthranilate
BenABC
AntABC
BenD
catechol
CatA
cis,cis-
muconate
CatB
CatC
CatIJ
CatF
CatD
succinyl-CoA
and
acetyl-CoA
1
2
3
4
benPK
benM
benABCDE
catA
orf1
orf2
catM
catBCIJFD
BenM
CatM
BenM
CatM
BenM
CatM
CatM
BenM

effector-binding domain (EBD). A long linker helix (LH) of about 20 amino acids connects these two domains (Figure 3.2) (19, 27). Based on structural data from full-length LTTRs, namely, BenM, CbnR, DntR, TsaR, CysB, CrgA, ArgP, and AphB (20, 21, 25, 29, 30, 34), the LH is described to aid in oligomerization to the tetrameric complex. With CbnR, TsaR and BenM, there is a hinge region located at the C-terminal end of the linker helix, with a proposed role in positioning the EBD and DBD at different angles to one another, thus determining the expanded and compact conformations of the protomer asymmetric units described in TsaR, CbnR and BenM (Figure 3.2)(20, 21, 25). In addition, the LH forms the linker helix interface (LH-LH interface) where two subunits with different conformations are dimerized through their helices by an antiparallel arrangement, and thus plays a critical role in dimer formation and stabilization (20, 21).

According to mutational studies at the LH in LTTRs (particularly NAC, NodD, and OccR), a series of variant proteins have different changes in the protein functionality, including effector-independent activity and altered binding affinity to cognate promoters (2, 16, 24). These studies support the idea that the LH region may be actively involved in LLTR-mediated regulation. Based on these findings, we sought to understand the LH-dependent regulatory function by isolating and characterizing spontaneous mutants with altered CatM-mediated regulation.

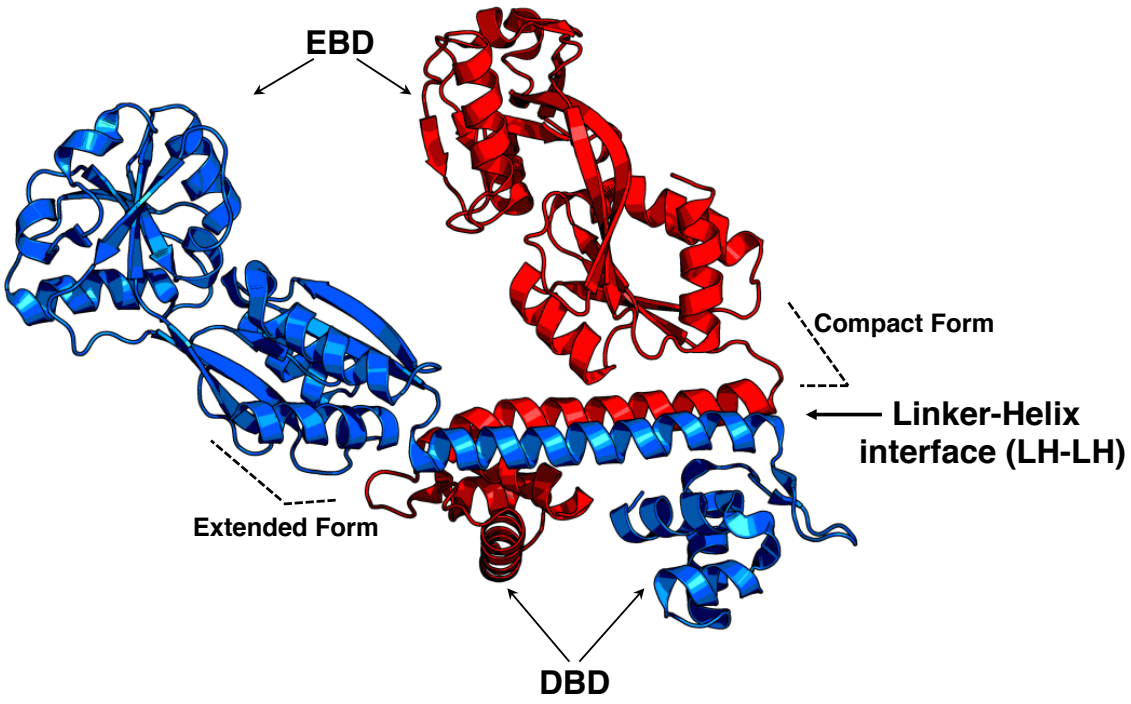

Figure 3.2 Ribbon representation of two CbnR subunits. Similar to CbnR, BenM subunits fold into two conformations (extended and compact as indicated). A hinge region (shown in the figure as a dashed line) is located at the C-terminal end of the linker helix and EBD. This region is proposed to position the EBD and DBD relative to each other with different angles. In CbnR, the angle between LH-EBD is 130° in the extended form, and 50° in the compact form. These asymmetric subunits dimerized through their LHs in an antiparallel arrangement forming the linker-helix interface (LH-LH interface) (Figure adapted from Muraoka *et al*., 2003) (21).

Materials And Methods

Bacterial strains and growth conditions. *Acinetobacter baylyi* strains were grown on minimal medium and *Escherichia coli* strains were grown on Luria-Bertani broth at 37°C (26, 32). In addition, *A. baylyi* strains were grown in minimal medium with succinate (10 mM), pyruvate (20 mM), benzoate (2 mM), muconate (2 mM), or anthranilate (1.5 mM) as the carbon source. *E. coli* DH5α cells (Invitrogen) and *E. coli* XL1-Blue (Agilent Technologies) were used as plasmid hosts. Antibiotics were added as needed at the final concentrations: ampicillin, 150 μg/ml, kanamycin, 25 μg/ml, spectinomycin, 13 μg/ml and streptomycin, 13 μg/ml. When appropriate, the following supplements were added: 0.24 μg/ml, X-gal (5-bromo-4-chloro-3-indolyl-β-D-galactopyranoside) and 80 μM, isopropyl-β-D-thiogalactopyranoside (IPTG). For *A. baylyi* growth curves, succinate-grown colonies were used to inoculate 5 ml cultures for overnight growth with benzoate as a carbon source. The following day, 1 ml of an overnight culture was used to inoculate 100 ml of benzoate medium. Growth was monitored by turbidity and measured spectrophotometrically (OD_{600}). A similar procedure was used for anthranilate and muconate growth curves.

Spontaneous mutants (Ben^+) from strains without BenM. Spontaneous mutants were isolated from ACN682, a *benM*-disrupted (ben-) strain unable to grow on benzoate (Table 3.1). These Ben+ mutants were selected after incubation on benzoate agar plates. Gap-repair methods were used to isolate the *catM* region from these Ben^+ mutants (14). To test the ben+ phenotype of the recovered DNA fragments from spontaneous mutants,

Table 3.1. Strains and plasmids used in this study.

Strains Or plasmid		
***A. baylyi* Strain**	**Relevant characteristics[a]**	**Source**
ADP1	Wild type (BD413)	(17)
ISA36	*benM*::ΩS*4036*	(7)
ACN32	*benA*::*lacZ*-Km^R*5032*	(7)
ACN585	*benM*::ΩS*4036 catB*::*lacZ*-Km^R*5534*	(11)
ACN613	*catM*::*sacB*-Km^R*5613*	(31)
ACN637	*benM*::*sacB*-Km^R*5624*	(9)
ACN682	*benM*::ΩS*4036 catM5682* [CatM(F293Y)] AAA → A**T**A (12150)[b]	(31)
ACN707	*benM*::ΩS*4036 catM5707* [CatM(F293Y,R84Q)] CCG → C**T**G (12777)[b]	This study
ACN736	*benM*::ΩS*4036 catM5736* [CatM(F293Y,A78V)] CGC → C**A**C (12795)[b]	This study
ACN738	*benM*::ΩS*4036 catM5738* [CatM(F293Y,A86T)] TGC → TG**T** (12772)[b]	This study
ACN821	*benM*::ΩS*4036 benMA5146 catM*::*sacB*-Km^R*5613*	This study
ACN1090	Δ*catM51090*	(31)
ACN1088	*benM*::ΩS*4036 catM51088* [CatM(R84Q)]	This study
ACN1089	*benM*::ΩS*4036 catM51089* [CatM(A78V)]	This study
ACN1104	*benM*::ΩS*4036 catM51104* [CatM(A86T)]	This study
ACN1109	*benM*::ΩS*4036 benA*::*lacZ*-Km^R*5032 catM51088* [CatM(R84Q)]	This study
ACN1110	*benM*::ΩS*4036 benA*::*lacZ*-Km^R*5032 catM51089* [CatM(A78V)]	This study
ACN1113	*benM*::ΩS*4036 benA*::*lacZ*-Km^R*5032 catM51104* [CatM(A86T)]	This study
ACN1148	*benM*::ΩS*4036 catM51088* [CatM(R84Q)] *catB*::*lacZ*-Km^R*5534*	This study
ACN1149	*benM*::ΩS*4036 catM51089* [CatM(A78V)] *catB*::*lacZ*-Km^R*5534*	This study

ACN1152	*benM*::ΩS*4036 catM51104* [CatM(A86T)] *catB*::*lacZ*-Km^R*5534*	This study
ACN1232	*benA*::*lacZ*-Km^R*5032 catM*::ΩS*4013*	(31)
ACN1307	Δ*benM5389 benA::lacZ*-Km^R*5032*	(31)
ACN1432	Δ*benA51432*	This study
ACN1467	*benM*::*sacB*-Km^R*51467* Δ*benA51432*	This study
ACN1492	Δ*benMA51487*	This study
ACN1498	Δ*benMA51487 catA*::*lacZ51081*	This study
ACN1499	Δ*benMA51487 catM*::*sacB*-Km^R*5613*	This study
ACN1506	Δ*benMA51487 catM51104* [CatM(A86T)]	This study
ACN1507	Δ*benMA51487 catM51088* [CatM(R84Q)]	This study
ACN1508	Δ*benMA51487 catM51089* [CatM(A78V)]	This study
ACN1517	Δ*benMA51487 catM51104* [CatM(A86T)] *catA*::*lacZ51498*	This study
ACN1518	Δ*benMA51487 catM51088* [CatM(R84Q)] *catA*::*lacZ51498*	This study
ACN1519	Δ*benMA51487 catM51089* [CatM(A78V)] *catA*::*lacZ51498*	This study

Plasmid	**Relevant characteristics**	**Source**
pUC18	Ap^R; cloning vector	(33)
pET-21b	Ap^R; T7 expression vector	Novagen
pIB1	Ap^R; partial *cat* region (11605-17916)[b]	(22)
pBAC54	Ap^R Km^R; *lacZ*-Km^R cassette in *NsiI* site (3761)[b] in *benA* (2316-5663)[b] in pUC19	(7)
pBAC184	Ap^R; partial *cat* region with internal *ClaI* deletion (10649-15901)[b]	(28)
pBAC430	Ap^R; *catM* (12116-13027)[b] in pET-21b	(6)
pBAC433	Ap^R; *benM* (1453-2368)[b] in pET-21b	(6)
pBAC675	Ap^R Km^R; *catB* (13205-14225)[b] *lacZ*-Km^R *catIJF* (15660-17347)[b] in pUC19	(11)
pBAC708	Ap^R Km^R; *catM* region (11950-12892)[b] in pUC19. Contains *sacB*-Km^R cassette	(28)

pBAC766	Ap^R Km^R; *cat* region (7902-9190)[b] in pUC19. Contains *lacZ*-Km^R cassette	This study
pBAC773	Ap^R; *catM5707* (9823-18153)[b] in pUC19	This study
pBAC789	Ap^R; *catM5736* (9823-18153)[b] in pUC19	This study
pBAC931	Ap^R; *catM51088 StuI-EcoRI* (12381-12893)[b] fragment from pBAC773 cloned into pIB3	This study
pBAC932	Ap^R; *catM51089 StuI-EcoRI* (12381-12893)[b] fragment from pBAC789 cloned into pIB3	This study
pBAC944	Ap^R; *catM5738* (9823-18153)[b] in pUC19	
pBAC946	Ap^R; *catM51089* (12381-18153)[b] in pUC19	This study
pBAC947	Ap^R; *catM51088* (12381-18153)[b] in pUC19	This study
pBAC948	Ap^R; *catM51104* (12381-16031)[b] in pIB1	This study
pBAC990	Ap^R; *NdeI-XhoI* (12119-13027)[b] fragment from pBAC946 in pET-21b; expression construct for CatM(A78V)	This study
pBAC991	Ap^R; *NdeI-XhoI* (12119-13027)[b] fragment from pBAC947 in pET-21b; expression construct for CatM(R84Q)	This study
pBAC1021	Ap^R; *NdeI-XhoI* (12119-13027)[b] fragment from pBAC958 in pET-21b; expression construct for CatM(A86T)	This study
pBAC1048	Ap^R; *benK-benA* (589-3393)[b] with Δ*benM* deletion (1453-2365)[b] with engineered *XhoI* site (2369)[b] in pUC18	This study
pBAC1073	Ap^R; *ben* region (1453-5268)[b] with Δ*benA* deletion (2662-4043)[b]	This study
pBAC1108	Ap^R; *catMB* (11605-13457)[b] [CatM(F293Y)]	This study
pBAC1140	Ap^R; *catMB* (11605-13457)[b] [CatM(F293Y, H160R)]	This study
pBAC1157	Ap^R; *ben* region (1453-5268)[b] with Δ*benA* deletion (2662-4043)[b] with engineered *XhoI* site (4051)[b] in pBAC1073	This study
pBAC1161	Ap^R Km^R;; *ben* region (1453-5268)[b], Δ*benA* deletion with *sacB*-Km^R cassette cloned into *XhoI* site in pBAC1157	This study
pBAC1179	Ap^R Km^R;; *benMC* region (1453-5268), Δ*benA* deletion (2662-4043)[b],	

	and *sacB*-Km^R cassette cloned into *salI* site in *benM* (1930)[b]	
pBAC1192	Ap^R; *benK-benC* (589-5268)[b] with Δ*benMA* deletion (1457-4043)[b]	This study

[a]Ap^R, ampicillin resistant; Sm^R, streptomycin resistant; Sp^R, spectinomycin resistant; Km^R, kanamycin resistant; ΩS, omega cassette containing Sm^R Sp^R (Prentki and Krisch, 1994); *sacB*-Km^R, dual selection cassette containing a counterselectable marker and kanamycin resistant cassette (Jones and Williams 2003).
[b]Position in the *ben-cat* sequence in GenBank entry AF009224

transformation assays were performed. *benM*-disrupted strains, ACN682, encoding CatM[F293Y] variant and ISA36, encoding wild-type CatM, were used as the recipients with donor DNA from plasmids. Transformants grew on benzoate only when *catM* alleles could be generated to encode CatM variants. After restoration of ben+ phenotype by the donor DNA from plasmids, sequencing analysis was performed (Genewiz Laboratories) and *catM* alleles were identified. Thus, plasmid-borne alleles: pBAC773 (CatM[F293Y,R84Q]); pBAC789 (CatM[F293Y, A78V]); and pBAC944 (CatM[F293Y,A86T]) were identified.

Generation of *A. baylyi* strains by allelic replacement. Plasmid-borne alleles were used to replace chromosomal genes. Different methods were used to exploit the high efficiency of natural transformation and recombination in *A. baylyi.* Recipient strains were transformed with linearized plasmids. By homologous recombination, the corresponding chromosomal region is replaced in transformants with donor DNA. Transformants were identified by phenotypic changes. In this study, strains were tested for antibiotic resistance and carbon source utilization. To facilitate the introduction of *catM* alleles, a counter-selectable *sacB* marker disrupted chromosomal *catM.* To replace the chromosomal *sacB* cassette with modified *catM* alleles, appropriate linearized plasmids were used to transform strain ACN843 (*benM*-disrupted strain with *catM*::*sacB),* ACN613 (*catM*::*sacB*). Desired transformants were selected by grow at 30 °C in the presence of 5% sucrose. Under this type of selection, a functional CatM is not required to growth in this medium. Chromosomal regions of interest in resultant strains

were analyzed by PCR-generated fragment sizes, and Genewiz laboratories confirmed DNA sequences of chromosomal regions.

Plasmid construction. Standard methods were used for DNA purification, digestion, ligation, electrophoresis, and bacterial transformation. Plasmids are listed in table 3.1. To construct pBAC948, the *catM51104* allele fragment was excised from pBAC944 away from *catM5682* by digestion with *StuI* and *NsiI* and ligated into a similarly digested pIB1. Plasmids pBAC931 and pBAC932 were constructed by digestion of pBAC773 and pBAC789 respectively with *StuI* and *EcoRI* and by ligation into a similar digested pIB3. Digestion with these enzymes allows separation from *catM5682* (encoding CatM[F293Y]). To aid homologous recombination in the chromosome, homologous DNA was added to each end of pBAC931 and pBAC932 plasmids. Briefly, pBAC931 and pBAC932 were used to transform ISA36 and restored ben+ growth as described above. Resulting strains, ACN1088 and ACN1089 were used for gap repair of pBAC184 digested with *ClaI* to recover single *catM* alleles. Resulting plasmids, pBAC947 (*catM51088)*, and pBAC946 (*catM51089*) were sent for sequencing analysis. To construct pBAC990, pBAC991, and pBAC1021, alleles were amplified by high-fidelity PCR (Roche) that incorporated a 5' *NdeI* and a 3' *XhoI.* Strains ACN1088, ACN1089 and ACN1104 were used as templates in PCR reactions. PCR products were digested with *NdeI* and *XhoI* and cloned to pET21b (Invitrogen). Alleles were confirmed by sequencing analysis. Plasmids with complete deletions of *benM* and *benA* were constructed by overlapping extension PCR as described previously (31).

B-galactosidase assays to measure *lacZ* expression. *benA*::*lacZ, catB*::*lacZ* and *catA*::*lacZ* transcriptional fusions were inserted into *A. baylyi* strains when indicated by allelic exchange with DNA of pBAC54 digested with *XmnI,* pBAC675 digested with *KpnI* and pBAC776 digested with *XmnI*. To assay these fusions, strains were grown on minimal medium with pyruvate (20 mM) as the carbon source with no effector or the following when indicated: 65 μM benzoate, 65 μM muconate, 32.5 μM each. For assays during growth on muconate, cultures were grown overnight on minimal medium with muconate (3 mM). The following morning, 500 μl of each culture was diluted into 5 ml of minimal medium with muconate (3 mM). Growth was measured by optical density (OD_{600}) and assays were done when cultures reached late-exponential phase. Samples (0.5 μl to 5 μl) were lysed with Z buffer, sodium dodecyl sulfate and chloroform. Directions from FlourAce β-galactosidase reporter kit (BioRad) were followed. The hydrolysis of the substrate, 4 methylumbelliferyl-galactopyranoside (MUG) to the product 4-methyllumbelliferone (4MU) was detected with a TD-360 miniflourometer (Turner Designs).

Purification of CatM variants Plasmids pBAC990, pBAC991 and pBAC1021 were used to express the full-length proteins CatM[A78V]-His, CatM[R84Q]-His, and CatM[A86T]-His, respectively. The protocol for CatM-His purification was followed exactly as described in chapter 2. Briefly, CatM-His variant proteins were purified similar as CatM-His. Proteins were eluted with CatM-elution buffer [30 mM Tris, 500 mM NaCl, 30% glycerol (v/v), 500 mM imidazole, and 10 mM BME (pH 7.9)]. Following elution, only CatM fractions were pooled and dialyzed against CatM solubilization buffer [20

mM Tris-HCl, 250 imidazole (pH 7.9), 500 NaCl, 10% (v/v) glycerol] to increase solubility. CatM-His was concentrated to 2-5 mg ml^{-1}. Protein concentrations were determined by the method of Bradford (1976) with bovine serum albumin as the standard (4). Proteins fractions were frozen with liquid nitrogen and stored at -70 °C until use.

Electrophoretic mobility shift assay (EMSA) and bending assays. Similar procedure was followed exactly as described in chapter 2 for EMSAs. Briefly for bending assays, ADP1 was as template to generate three DNA fragments labeled with 6-FAM at the 5'-end nucleotide. Each fragment (220 bp) contained the binding sites at a different location from close to the ends and in the middle. The bend angles were estimated using the empirical formula, ($\mu_m/\mu_e = \cos(\alpha/2)$), where μ_m represents the mobility of the protein-DNA complex with a bend at the center of the probe, μ_e is the mobility of the protein-DNA complex with a bend at the end of the probe and $\alpha$is the angle by which the DNA departs from linearity (18).

RNA purification. Strains ISA36, ACN1088, ACN1089 and ACN1104 were used for RNA purification. Uninduced cells were grown in minimal medium with succinate (10 mM) and induced cells were grown on muconate (3 mM). Growth was measured by optical density (OD_{600}). Cells were harvested at early exponential phase (OD_{600} 0.2-0.3). 5 ml of cells were pelleted down and immediately frozen with -70 °C ethanol to prevent RNA degradation. Total RNA was extracted by the TRI Reagent (Molecular Research Center) method. RNA samples were treated with RQ1 DNase I (Promega) until lack of DNA contamination was confirmed by PCR. The quality and quantity of the extracted

RNA were determined spectrophotometricaly using the absorbance at 260 nm (Beckman DU® 640).

cDNA synthesis from total RNA. For samples to be used for real-time PCR, the SuperScript III First-Strand Synthesis for RT-PCR was used (Invitrogen) and random hexamers as primers. Approximately, 1 μg of total RNA was used for cDNA synthesis. Products were analyzed on 2% agarose gel and stored at -20 °C. cDNA generation was tested by RT-PCR with *rpoA* primers (internal transcript control).

Quantitative reverse transcriptase PCR (qRT-PCR). cDNA generated with random hexamers from ISA36, ACN1088, ACN1089, and ACN1104 was used for these experiments. Primer-probes for *rpoA*, *catA* and *catB* were used and designed with PrimerExpress software (Applied Biosystems): qRT-catA-UP: TGCGCACATTCACTATTTTGTTT, qRT-catA-DW: TCGCCAGCCACATTAATTTG, qcatB-for: TTCGTCCGCACAAGCTTTC, qcatB-rev: TCTTCCGTGATGATTTTGATCAA, rpoAfor: GGTTGAAGTTGAAATAGAAGGCG, rpoArev: CATAGCCACGACCTTGAGATAC. The *rpoA* probes were used as internal controls to evaluate the amount of *catA* and *catB* transcripts. Quantitative RT-PCR was performed in StepOnePlus Real-Time PCR systems (Applied Biosystems). Each reaction was carried out in a total volume of 20 μl on an 96-well optical reaction plate (Applied Biosystems) containing 10 μl of SYBR Green (Applied Biosystems), 1 μl of cDNA and two gene-specific primers at a final concentration of 0.2 mM each. To quantify targets, *rpoA*, *catB* and *catA* standard curves were prepared and ADP1 genomic DNA was used

as template for qPCR (12.5 ng to 0.02 ng). A non-template control was used for each primer set. Melting curve analysis verified that each reaction contained a single PCR product. *catA* and *catB* expression levels were normalized to transcripts of the internal control *rpoA*. Relative levels were normalized to uninduced (*catA* or *catB*) wild type (ISA36) transcript levels.

Results

Isolation of ben+ spontaneous mutants with point mutations at the *catM* gene. Taking advantage of the frequency of benzoate spontaneous mutants (10^{-5}) from a *benM*-disrupted strain (ACN682), three mutants were isolated and screened for BenM-independent regulation (31). Chromosomal DNA from the *catM* region was recovered and tested for restoration of ben+ phenotype to ACN682. Similarly to previously described mutants in chapter 2, these *catM* alleles were isolated from ACN682, thus, ben+ isolated mutants isolated from this strain are expected to retain the *catM* parent mutation encoding an amino acid replacement, CatM[F293Y] (31). Sequence analysis reveled distinct *catM* alleles encoding amino acid replacements located in different domains of the protein (chapter 2) including the LH region (Table 3.1 and fig. 3.3) in addition to the parent mutation. Along with mutants described in chapter 2, three alleles with double point mutations in *catM* were identified, CatM[F293Y, A86T], CatM[F293Y, R84Q] and CatM[F293Y, A78V].

LH CatM variants restore ben+ phenotype. To determine whether these double amino acid replacements were working together in CatM to restore ben+ phenotype, plasmids

Table 3.2 Effect of *catM* mutations on growth with benzoate as the sole carbon source.

Strain	Relevant characteristics	Generation time (min) [a]	Lag time (hr) [b]
ADP1	Wild-type	70 ± 5	4.5 ± 0.5
ACN1088	No BenM, CatM[R84Q]	99 ± 5	7 ± 0.5
ACN1089	No BenM, CatM[A78V]	128 ± 4	11 ± 1
ACN1104	No BenM, CatM[A86T]	123 ± 2	13 ± 1
ACN682	No BenM, CatM[F293Y]	No growth	No growth
ISA36	No BenM	No growth	No growth

[a] Averages of three determinations
[b] Time between inoculation and start of exponential growth

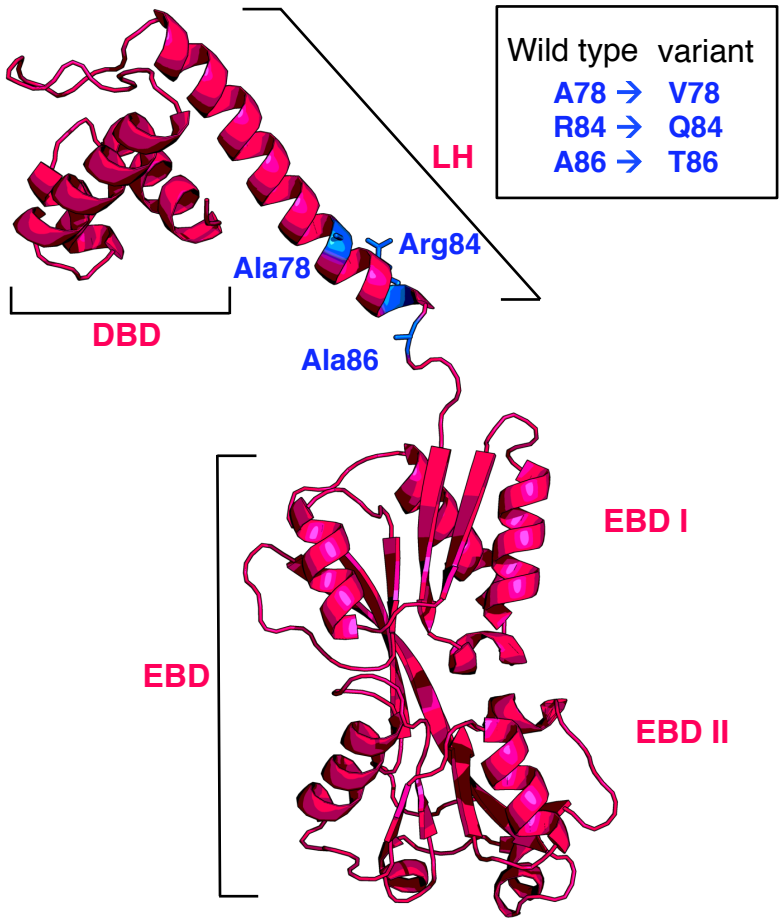

Figure 3.3. Structural model of a CatM subunit. Structure based on crystal structures of BenM (3K1N) (Raungprasert *et, al.* 2010) (25) and CbnR (1IZ1) (Muraoka *et, al.* 2003) (21). Structures shown in backbone ribbon denote α-helices and β-strands. Wild type residues are shown in stick figure. LH variants with changed residues, V78, R84 and T86 are indicated in black box. The modeled CatM is shown with the various domains labeled: DBD, DNA binding domain, LH, linker helix, and EBD, Effector binding domain with subdomains labeled I and II respectivately.

were constructed by methods described above to separate the new *catM* point mutations from *catM5682* (encoding CatM[F293Y]). Three plasmids: pBAC946, pBAC947 and pBAC948 were used as donors to transform ISA36, a *benM*-disrupted strain (Table 3.1). All plasmids were able to restore the ben+ phenotype to this strain, which reveals that these mutants are not working together with CatM[F293Y]. In fact, strains with double and single point mutations grew at a similar rate on benzoate plates. Thus, CatM[F293Y] has no apparent role in ben+ phenotype restoration and may be a silent mutation under these backgrounds. Despite the previously isolation of several ben+ mutants with single point mutations in *catM*, CatM[A86T], CatM[R84Q], and CatM[A78V] are the first variants with amino acid replacements at the LH region to be isolated as ben+ spontaneous mutants in *A. baylyi*. Effects of *catM* point mutations on benzoate growth were tested. ACN1104 (CatM[A86T]), ACN1088 (CatM[R84Q]), and ACN1089 (CatM[A78V]) were grown on benzoate as sole source of carbon and energy. Clearly, these strains were growing slower than wild-type (ADP1) with lag times 2-3 fold longer (Table 3.2). Strains carrying double point mutations in *catM* (Table 3.1) grew at similar rates as ACN1104, ACN1088, and ACN1089, which supports the conclusion that the ability to grow on benzoate depends only on the mutation affecting the LH of the encoded CatM variant (Data not shown). When strains were grown on anthranilate or muconate as sole carbon source, growth rates were close to those of wild-type (data not shown). Therefore slow benzoate growth by these strains indicates that the limited step in growth rate is the conversion of benzoate to catechol (*ben* operon activation) rather than activation from the *cat* genes.

Linker Helix CatM variants exhibit CatM-mediated *benA* activation. As described previously, benzoate growth in the absence of BenM requires high activation from *benABCDE* operon (11, 31). To detect the effects of LH-CatM variants at the *benABCDE* operon, a *lacZ* fusion (*benA*::*lacZ*) was used. B-galactosidase activity was measured in the absence or presence of muconate (Figure 3.4). Basal expression (no inducer) in these variants was 4 to 5-fold higher than basal expression from wild-type CatM (Figure 3.4). Since these strains can still grow on muconate, induced conditions were carried out in a medium containing muconate as sole source of carbon and energy. Under muconate-grown conditions, a significant difference in *benA*::*lacZ* expression was detected between CatM and CatM variants, with CatM[R84Q] activating a 10-fold increase in LacZ activity. The role of benzoate as an effector molecule was tested on these variants. B-galactosidase activity revealed no activation of the *benA*::*lacZ* in response to benzoate (data not shown).

DNA binding activity by CatM LH variants at the *benA* promoter region. DNase I footprinting experiments have shown that CatM can bind to the *benA* promoter as similar positions as BenM (6). In previous work, electrophoretic mobility shift assays demonstrated that CatM binds with lesser affinity to this promoter unlike BenM, a correlation with the *in vivo benA* expression results (31). Since CatM-mediated *benA* activation by CatM variants is significantly higher than wild-type CatM, it raises the question whether binding affinities are altered at this promoter. CatM variants were able to bind to the *benA* promoter with different binding affinities than wild-type CatM.

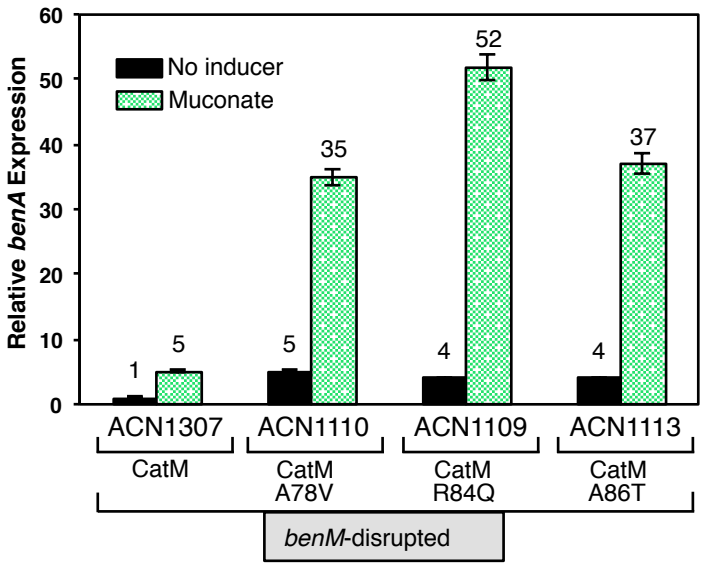

Figure 3.4. Effect of *catM* alleles on expression of a chromosomal *benA*::*lacZ* transcriptional reporter. Strains encoding wild type CatM and variant regulators are indicated. All strains lack a functional *benM* as indicated in the shaded box. Cultures were grown on pyruvate (uninduced conditions) or muconate as indicated. Relative *benA* expression is reported as the ratio of measured LacZ activity to that of uninduced ACN1232, a strain with wild-type BenM as the sole regulator of the *ben* genes (2.6 ± 0.51 nmol/min/ml/OD_{600}). Data represent the average of at least four independent replicates, and standard deviations were within 12% of the average value. Statistical analysis was determined using student t-test ($P<0.05$).

Table 3.3. Binding affinities and bending angles at the *benA* promoter

Protein	No inducer K_d (nM)[a]	bend angle (°)[c] Without Muconate	Muconate[b] K_d (nM)[a]	bend angle (°)[c] With Muconate[b]
Wild-type BenM	33 ± 2	95 ± 4	42 ± 3	84 ± 2
Wild-type CatM	70 ± 4	100 ± 5	68 ± 2	90 ± 3
CatM[A78V]	25 ± 2	102 ± 3	39 ± 2	95 ± 2
CatM[R84Q]	67 ± 3	96 ± 2	41 ± 3	81 ± 2
CatM[A86T]	40 ± 2	95 ± 3	37 ± 2	83 ± 2

[a] Kd, equilibrium dissociation constant.
[b] from 1.6 mM total concentration of effector per reaction.
[c] bending angles calculated as described in materials and methods.
Binding constants and bending angles shown represent the average of at least 3 independent replicates. Standard deviations were maintained within 10%

Although CatM[R84Q] binds with a K_d close to CatM under uninduced conditions, the addition of muconate increases the binding affinity for the *benA* promoter (Table 3.3). Interestingly, this property has not been observed by other CatM variants that normally retained unchanged affinities regardless of addition of muconate (31). Thus, CatM[R84Q] demonstrated a correlation between *in vivo benA* activation and *in vitro benA* promoter binding. All CatM LH have K_d coefficients similar to BenM, which reflects correlation with *in vivo benA* gene expression. As described previously, muconate does not affect the binding affinity properties of BenM and CatM, a property present in other LTTRs as these proteins are able to bind to their recognition binding sequence with similar affinity with or without their cognate effectors (1). Similar to other LTTRs, a difference in complex migration was observed under induced and uninduced conditions, which reveals the conformational change of the protein with a dimer repositioning to site2 or site3. CatM variant-*benA* complexes migrated similarly to BenM-*benA* complexes, thus, these variants appear to be binding with similar tetrameric conformations as BenM.

DNA bending by CatM LH variants. Effector-induced changes in DNA bending have been attributed to be important for transcriptional activation in LTTRs. As described elsewhere, a sharp angle formed by a bend at the middle of a DNA molecule affects the mobility of a fragment more so than the same bend position at the end. This DNA bend is attributed upon LTTR binding while DNA relaxes upon addition of the cognate effector. However, the exact scheme by which DNA bending and effector-mediated conformational changes activate transcription is yet to be elucidated. In order to explore the effects on the DNA by BenM, CatM and CatM variants, bending assays were

performed at the *benA* promoter. In the absence of effectors, CatM and CatM[A78V]-DNA complexes migrated slightly slower than BenM, which correlates to a high angle DNA bend (Table 3.3). For CatM[R84Q] and CatM[A86T]-DNA complexes, protein-mediated bending angles were similar to BenM. Addition of muconate resulted in faster migration of the BenM-DNA complex, which reflects in a partial relaxation of the DNA bending angle by 11° (Table 3.3). Similarly to BenM, CatM and CatM-variant-DNA complexes exhibited a partial decreased in angle bend, thus, muconate caused these proteins to undergo a conformational change that resulted in a lower bend angle. Despite elevated basal expression detected by the *benA*::*lacZ* fusion, it did not link to lower angle DNA bend without muconate. To determine whether the mobility shifts detected were due to changes in DNA bending rather then the number of protein subunits bound to the DNA, assays were repeated with the *benA* promoter located at the end of the probe. In this experiment, all the protein-DNA complexes migrated equally under induced or uninduced conditions (Data not shown). Therefore, changes in DNA bending are due to alteration in protein conformation rather then the number of subunits bound to the promoter.

Regulation of *catB* expression is affected by CatM Variants. CatM variants described in chapter 2, CatM[Δ264], CatM[G232S], CatM[V158M], and CatM[K148Q] able to activate high-*ben* gene expression have the opposite effect at the *catBCIJFD* operon (31). To test this possibility on the CatM linker helix variants, strains carrying out *catB*::*lacZ* fusions were constructed to measure β-galactosidase activity under the presence or absence of muconate. Similar to *benA*::*lacZ* data, basal expression was elevated for the

catB::*lacZ* fusion, which is not observed by wild-type CatM (Figure 3.5A). This basal *catB* expression is higher than what was observed at the *benA* promoter. CatM[A86T] shows close to 40-fold increase in basal expression relative to wild-type CatM, while CatM[R84Q] and CatM[A78V] had uninduced expression levels of 12 and 5-fold increase relative to wild-type CatM. Only CatM[R156H], a variant regulator, had basal expression levels as high as those of CatM[A86T]. Thus, these proteins could be binding to this promoter region in a similar conformation arrangement as to the effector-induced-CatM. Muconate increased β-galactosidase activity by these variants but less than those levels exhibit by CatM. Thus, muconate degradation to tricarboxilic acid intermediates is reduced by these variants probably to maintain equilibrium within muconate as a source of carbon vs. an effector molecule needed for complete benzoate degradation.

To confirm that *lacZ* activity data was a valid measure of *catB* expression, *catB* transcript levels were quantified by means of qRT-PCR. Figure 3.5.B shows high muconate-activated levels of *catB* transcription from a strain with wild-type CatM. However, these levels decrease in strains with variant CatM proteins. Similar to LacZ activity levels, *catB* transcript levels on strains with CatM variants are lower compare to the strain with wild-type CatM. Although basal transcript levels are lower than those in *lacZ* expression experiments, these basal levels are still detected. Low basal transcript levels might relate to succinate repression of genes involved in aromatic degradation pathways, and thus basal expression is repressed and not detected under these conditions (12). These experiments reinforce the rationale that muconate degradation is slowed down to allow needed concentration to complete benzoate degradation.

Figure 3.5. Expression and transcript levels of *catB* by CatM and CatM LH variants. (A) Strains were grown on pyruvate and muconate was added as indicated. All strains lack a functional *benM.* Relative *catB* expression is reported as the ratio of measured LacZ activity to that of uninduced ACN585 (1.2 ± 0.34 nmol/min/ml/OD_{600}). Data represent the average of at least four independent replicates, and standard deviations were within 10% of the average value. (*) Statistical analysis was determined using student t-test ($P<0.05$). **(B)** *catB* transcripts levels in strains encoding CatM variant regulators. Cells grown on succinate (uninduced conditions) and muconate. RNA was immediately isolated when cultures reached early exponential phase (OD_{600} 0.2). Graph represents combined data from three independent biological replicates. Melting curve analysis verified that each reaction contained a single PCR product. *catB* expression levels were normalized to transcripts of the internal control *rpoA.* Standard deviations were within 17% of the average value. (*) Statistical analysis was determined ($P<0.05$).

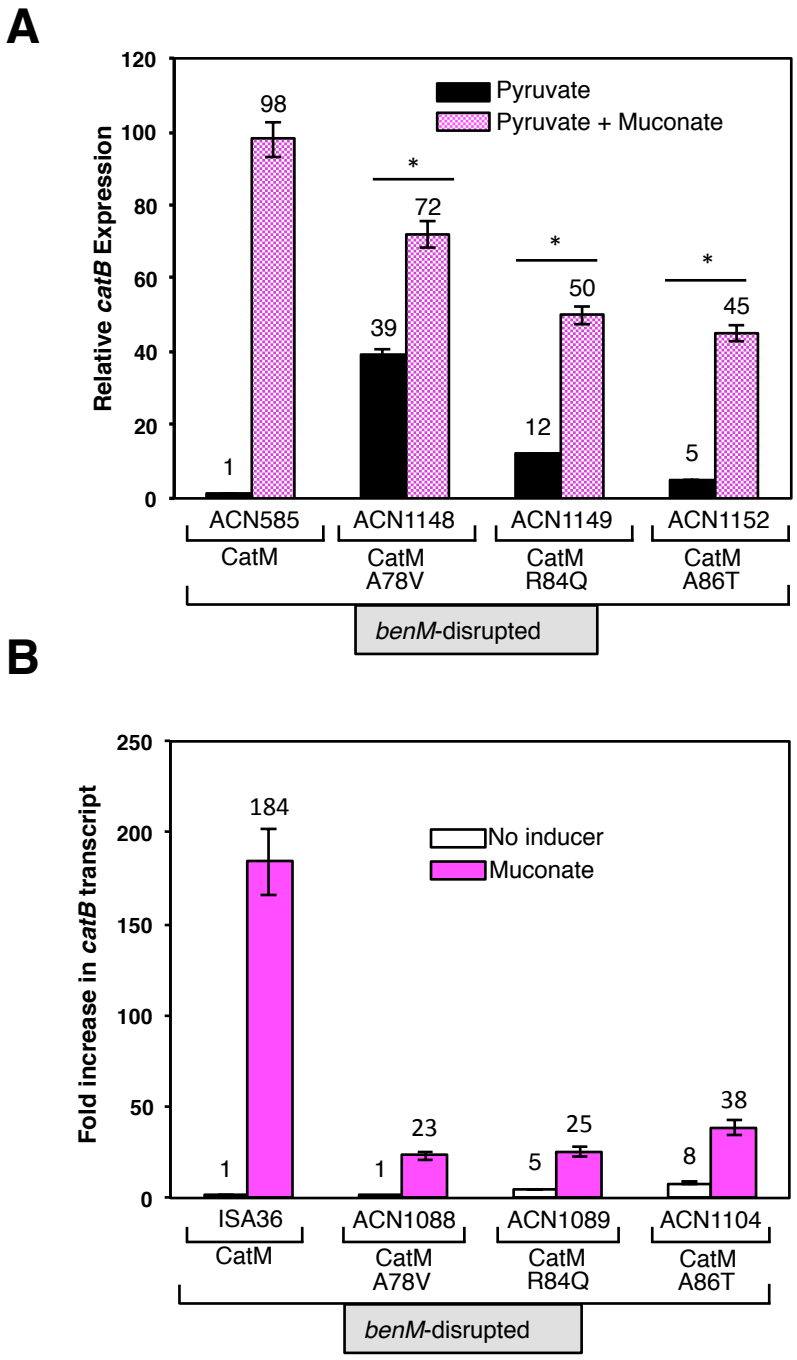
A
Relative catB Expression
120
100
80
60
40
20
0
Pyruvate
Pyruvate + Muconate
98
1
*
72
39
*
50
12
*
45
5
ACN585
ACN1148
ACN1149
ACN1152
CatM
CatM A78V
CatM R84Q
CatM A86T
benM-disrupted
B
Fold increase in catB transcript
250
200
150
100
50
0
No inducer
Muconate
184
1
23
1
25
5
38
8
ISA36
ACN1088
ACN1089
ACN1104
CatM
CatM A78V
CatM R84Q
CatM A86T
benM-disrupted

As determined by previous EMSA experiments, CatM binds strongly to this promoter, and muconate-dependent binding does not increase K_d values (31). Since these variants exhibited significantly elevated effector-independent-*catB* expression, binding affinity and protein-DNA complex migration could be altered. K_d values under uninduced and induced conditions were not different to the values exhibit by CatM at this promoter (Table 3.4). CatM and CatM-variant-DNA complexes migrated with similar mobility with and without muconate, which indicates that CatM-variants bind the *catB* promoter with the same protomeric conformation as CatM. Relocation of the promoter to the end of the fragment showed that complexes still migrated at similar rates. Therefore, protein-DNA mobility depends on protein conformation rather than the number of protein subunits bound to the *catB* promoter.

Effects of CatM variants in muconate generation. Catechol 1-2, dioxygenase, is the enzyme responsible for carrying out ring fission in the *ortho* position of catechol to generate muconate (15). This dioxygenase is encoded by the *catA* gene whose activation is control by BenM and CatM. In the absence of BenM, CatM can readily activate gene expression in response to muconate to carry out degradation of catechol to succinyl and acetyl coenzyme A. To determine whether the LH CatM variants controlled this promoter, a *catA*::*lacZ* fusion was constructed and introduced in these strains to monitor activation at the *catA* promoter. Unlike CatM, CatM-variants displayed basal *catA* expression, a similar activation observed at the other two genes assessed (*benA and catB*) (Fig. 3.6). Nevertheless, levels of

Table 3.4. Binding affinities at the *catB* promoter

Protein	**No inducer** K_d **(nM)**[a]	**Muconate**[b] K_d **(nM)**[a]
Wild type BenM	26 ± 2	15 ± 2
Wild type CatM	5 ± 1	9 ± 1
CatM[A78V]	16 ± 2	8 ± 1
CatM[R84Q]	9 ± 1	7 ± 2
CatM[A86T]	8 ± 1	10 ± 2

[a] Kd, equilibrium dissociation constant.
[b] from 1.6 mM total concentration of inducer per reaction.
Binding constants shown represent the average of at least 3 independent replicates.
Standard deviations were maintained within 10%

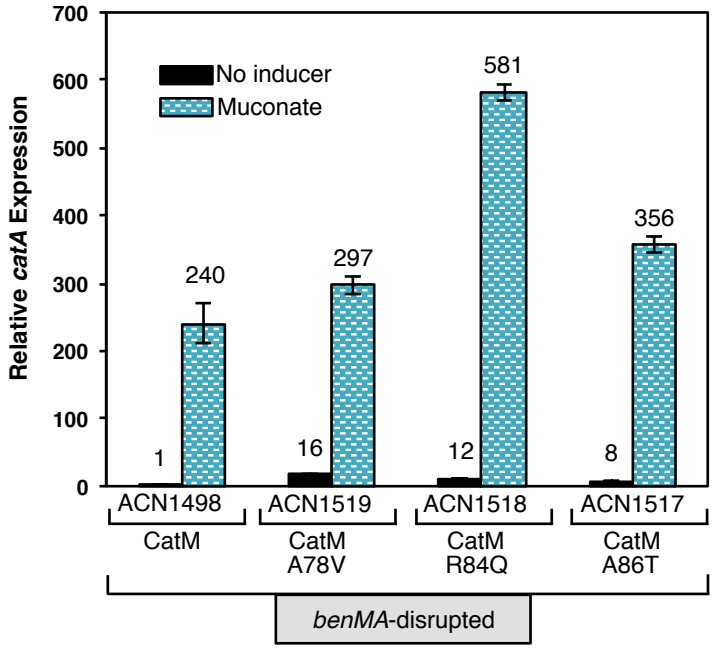

Figure 3.6. *catA*::lacZ activity regulated by CatM variants. Expression of a chromosomal *catA::lacZ* fusion in strains encoding CatM or variant regulators. All strains lack a functional *benM* and *benA.* Relative *catA* expression is reported as the ratio of measured LacZ activity to that of uninduced ACN1498 (3.2 ± 0.65 nmol/min/ml/OD_{600}). Data represent the average of at least four independent replicates, and standard deviations were within 10% of the average value. Statistical analysis was determined ($P<0.05$).

muconate-dependent *catA* expression by CatM variants were far higher than wild-type (Figure 3.6). CatM[R84Q] has the highest β-galactosidase levels (close to 3-fold increase). CatM[A78V] and CatM[A86T] had a muconate-dependent *catA* expression higher than CatM. These results could indicate a rapid availability of catechol 1-2, dioxygenase for muconate generation.

To confirm the LacZ data described above, *catA* transcript levels were directly measured by methods of qRT-PCR from cells grown on succinate and muconate as sources of carbon and energy. The *catA* transcript levels from cells grown on succinate were low on strains with CatM variants unlike the β-galactosidase experiments where *catA* expression was elevated in the absence of effector (Figure 3.7). As mentioned above, this may be because of succinate-dependent repression activity at this locus. However, under muconate-grown conditions, *catA* transcript levels increase in all strains tested, which correlate with data from the *catA::lacZ* fusion experiments. Although transcript levels are different from gene expression levels, both levels are higher than wild type CatM. Therefore, these results confirm that *catA* regulation by these CatM variants is altered, which yields to an increase in catechol 1,2-dioxygenase levels that could correlate to increase in muconate generation.

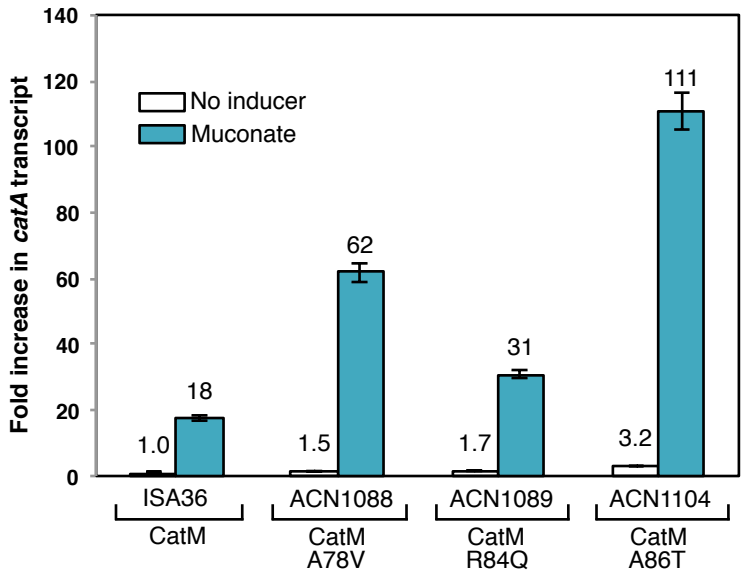

Figure 3.7. Quantitative RT-PCR of *catA*. *catA* transcripts levels in strains encoding CatM variants. Cells grown on pyruvate (uninduced conditions) and muconate. RNA was immediately isolated when cultures reached early exponential phase (OD_{600} 0.2). Graph represents combined data from three independent biological replicates. Melting curve analysis verified that each reaction contained a single PCR product. *catA* expression levels were normalized to transcripts of the internal control *rpoA*. Standard deviations were within 17% of the average value. Statistical analysis was determined ($P<0.05$).

Discussion

CatM-mediated regulation of benzoate degradation by LH variants. In this investigation, three CatM variants with amino acid replacements at the LH region were isolated and characterized. Unlike wild-type CatM, these variants are able to activate genes involved in benzoate degradation in the absence of BenM. The CatM-mediated benzoate degradation exhibited by these variants is muconate-dependent, but activation without effectors is also detected in all genes assessed (*benA, catA,* and *catB*). Basal *benA* expression has been observed only when both regulators, BenM and CatM were disrupted or deleted, but either regulator under uninduced conditions immediately represses this expression (6, 7). Wild-type CatM can activate expression from the *ben* genes in response to muconate albeit at low levels and this activation is insufficient to support growth on benzoate (6). To carry out the CatM-mediated regulation in benzoate degradation by the LH variants, gene expression from *benA, catA* and *catB* is altered and differs form CatM-mediated activation by wild type CatM. In addition, muconate concentration is tightly regulated and altered by controlling genes encoding catechol 1,2-dioxygenase (CatA) and muconate cycloisomerase (CatB), enzymes involved in muconate generation and degradation.

During growth on benzoate, muconate controls its generation and degradation by effector-mediated CatM activation of *catA* and *catBCIJFD.* This fine-tuned regulation on the *cat* genes prevents accumulation of this metabolite, which at high concentrations is toxic (8, 13). Nevertheless, under CatM-dependent regulation of the CatM variants discussed here, muconate is the key effector and its generation is needed for maximum activation of the *ben* operon. Thus, muconate accumulation in these strains must be

tightly coupled with its degradation, but at rates far lower than those observed by wild-type CatM. This slower degradation was observed by decreases in *catB* expression by these CatM variants. The importance of muconate is highlighted by the basal gene expression detected by the lacZ fusions of *catA* and *catB*. This high basal expression, which is not detected by wild-type CatM at these genes, may correlate to the crucial presence of enzymes needed for muconate generation, and degradation to avoid unnecessary accumulation and toxicity.

Based on the results on this study, benzoate degradation in the absence of BenM can be achieved by these CatM variants by modulating gene expression throughout the *ben-cat* supraoperonic cluster. During benzoate growth, initial benzoate conversion to catechol is carried out by the products of the *ben* genes (Figure 3.8). This initial CatM-mediated *ben* gene activation does not require muconate since this metabolite has not been generated at this point, and these variants lack a benzoate-mediated response. Therefore, muconate-independent CatM-mediated *benA* activation is crucial to initiate benzoate degradation, and generate low levels of catechol. Catechol 1, 2-dioxynease, encoded by initial *catA* expression, can then convert these low levels of catechol to muconate. Similar to *benA* activation, this initial CatM-mediated *catA* expression does not require muconate. To prevent accumulation of toxic muconate, muconate cycloisomerase (CatB) degrades muconate to tricarboxilic acid intermediates. The elevated basal *catB* expression by these CatM variant indicates the importance of CatB to regulate muconate intracellular levels under these initial conditions. Increase in muconate levels can then be used for maximal activation of the *ben* operon to continue benzoate

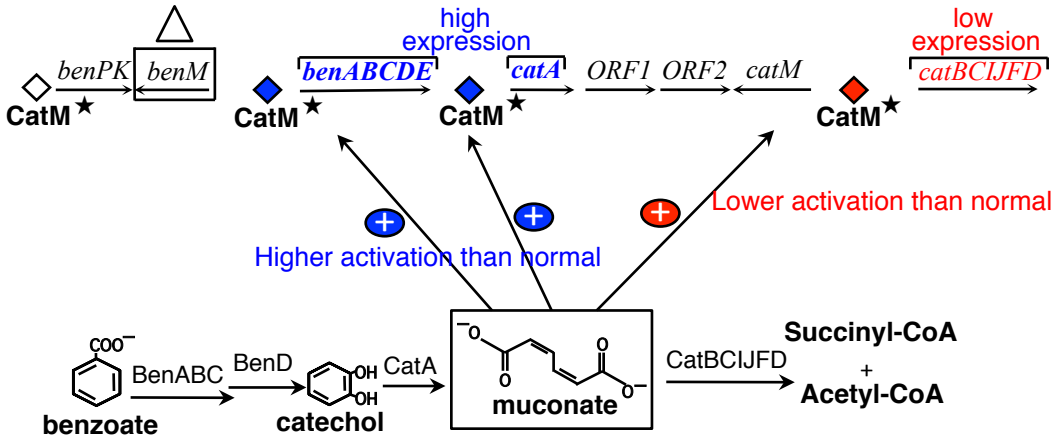

Figure 3.8. Model of CatM-mediated benzoate degradation by CatM LH variants. CatM variants can activate low levels of expression from *benA, catA* and *catB* in the absence of muconate. This basal activation from these genes allows initial benzoate degradation, which results in muconate generation and accumulation. The presence of muconate enhances CatM-mediated transcriptional activation at *benA* and *catA* to maximal levels. However, *catB* expression is decreased to levels lower than normal to maintain muconate levels until benzoate substrate is consumed.

degradation. Similarly, muconate-dependent CatM activation of *catA* increases, which generates more muconate. CatM-mediated activation of the *catBCIJFD* operon is decreased in the presence of muconate to ensure sufficient muconate levels remain available to complete benzoate degradation. Despite this tight CatM-mediated regulation of the *ben-cat* genes, strains carrying these *catM* mutants grow slowly on benzoate. Thus, these mutants are still far less adept in balancing expression from these genes, and the muconate optimization levels may reflect the longer lag times (Table 3.2). Thus, the activation with no effectors exhibited by these CatM variants is necessary to initiate rapid transcription to begin benzoate catabolism, which is enhanced by the muconate response.

LH sequences are less conserved than DNA-binding domains between LTTRs. CatM and BenM are less conserved at this region and shared only 54% in amino acid sequence similarity (Figure 3.9). R84 and A86 are among the few conserved amino acids between both regulators at this location, while M78 substitutes for A78 in BenM. Sequence alignment with regulators in the subfamily that binds muconate or halogen-substituted muconates as effectors reveals lack of conservation of these amino acids. Only A86 is present in TcbR from *Pseudomonas sp*. strain P51. LH sequences aligned with other LTTRs involved in aromatic degradation, shows far less conservation. CatM-LH only shares 28% and 23%, and 22% amino acid sequence similarity with CatR, CbnR and TsaR respectively. TsaR similar to CatM has an alanine residue at position 78. DntR also has an alanine residue (A83) at this region. Amino acids with hydrophobic properties are located at this position in all sequences aligned, which reinforces the hydrophobicity

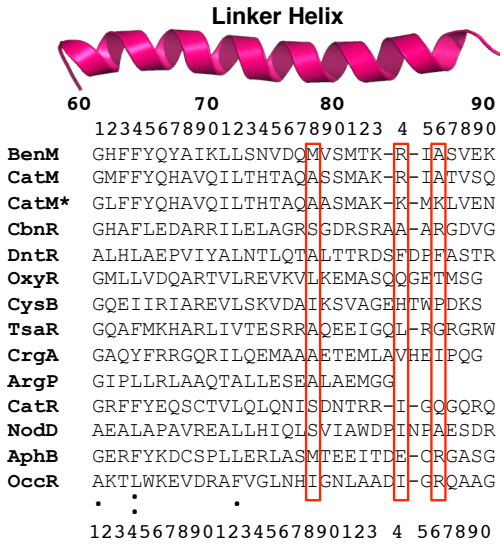

Figure 3.9 Linker-Helix amino acid sequence alignment of BenM and CatM with other LTTRs. The organism and SwissProt sequence identifiers are: BenM (ADP1; O68014), CatM (ADP1; PO7774), CatM* (*A. calcoaceticus* PHEA-2; F0KF40), CbnR (*Ralstonia eutropha*; Q9WXC7), DntR (*Burkholderia* sp. DNT; Q7WT50), OxyR (*E. coli*; P0ACQ4), CysB (*Salmonella typhimurium*; P06614), TsaR (*Comamonas testosterone*; P94678), CrgA (*Neisseria meningitidis*; Q9JPU9), ArgP (*Mycobacterium tuberculosis* H37Rv; P67665), CatR (*P. putida*; P20667), NodD (*Rhizobium leguminosarum*; P04681), AphB (*V. cholera*; Q9KT56), OccR (*A. tumefaciens*; P0A4T4). Sequence alignment performed using the CLUSTALW2 online server (http://www.ebi.ac.uk/Tools/clustalw2/index.html). (:) indicates residues that are similar at that position and share similar properties. (.) indicates residues that are more similar. Red boxes indicates position of linker helix CatM variants compare to other LysR-type regulators.

environment at this domain that is important for linker-linker interactions as discussed below (20, 21). Interestingly, only BenM and CatM have a positively charged residue at position 84, while other LTTRs have hydrophobic residues at the same position. Despite the lack of conservation at this region, LHs are governed by hydrophobic and polar residues that are essential for dimer formation (21).

Linker helix essential for oligomer arrangements. Since a CatM-full length structure is not available, a structural modeling program was used to generate a preliminary model of a CatM subunit based on the BenM and CbnR crystal structures with conserved sequence identity (Figure 3.3) (59% and 28% respectively), and the tetrameric CbnR structure was used to map interactions among LH residues (21, 25). Based on the CbnR tetramer, subunits dimerized through the LH of each asymmetric subunit forming an antiparallel coiled-coil linker. This antiparallel interface is highly conserved in all full-length structures solved by X-ray crystallography (20, 21, 25, 29, 30). This helix-helix interface seems to be essential for oligomerization while other domain interactions vary throughout structures (25). Thus, interactions thought the linker helices in LTTRs may be the major contributor in the tetrameric arrangement. In this LH-LH interface, a hydrophobic patch located on a helix bundle is formed with residues, I71, L74, and A75 and it is located at a central part of the two linkers. At the end of this hydrophobic patch, two hydrogen bonds formed that connects both helices (21). In CatM-LH only I71 is conserved while at positions 74 and 75, histidine and threonine are present. However, it is probable that similar interactions may still occur in LH-LH interface of the CatM tetramer.

Subtle changes in the LH could affect transcriptional activation in CatM. In addition to oligomerization, the LH plays a role in the conformational change between compact and extended forms, thus providing the asymmetry of the monomer subunits, which is essential for tetrameric interactions (25). The hinge located between the LH and the effector-binding domain allows different interactions among residues of both domains in the compact form (20, 21, 25). Based in CbnR tetramer, the angle between the LH-EBD is an acute angle of 50 degrees in the compact form. In this form, three hydrogen bonds are detected between Asp89 (OD)-Arg87(NE), Arg77(NH)-Ser94(OG), and Arg77(NH)-Ser123(OG) (21). In the CatM model only two hydrogen bonds are observed between Ala86(N)-Thr87(OG1) and Glu122(OE1)-Gln77(NE2) in the compact form. In the extended form, the angle between LH-EBD increases 80 degrees that results in lost of interactions among these domains in CbnR. In the CatM model, the interactions among the above residues are loss as well.

To assess the proposed role in transcriptional activation of the amino acid residues described in this study, we mapped the interactions among the CatM LH residues based on the CbnR tetramer. Ala78(O) interacts with Ala82(N) and the amide of Ala78 interacts with His74(O). When Ala78 was replaced with valine, the bond formation remains the same. However, the hydrophobicity of valine is higher than alanine, thus interactions with Ala82 and His74 could be stronger than with alanine. In the case of Arg84, this amino acid may be involve in holding the LH-LH interface by forming hydrogen bonds with residues from the other helix such as Met81. This hydrogen bond seems to be conserved when Gln84 replaces arginine, LH-LH interactions may remain unchanged in this variant. In addition to this hydrogen bond, Arg84 form hydrogen bonds with

surrounding residues such as Thr87. Since Arg84 is located close to the hinge, interactions with other residues may be different within compact and extended forms of the monomeric unit. In fact, Arg84(O)-Thr87(N) bond is loss in the extended form model. This is also observed with Gln84, whose interaction with Thr87 is also loss in this form. However, an additional hydrogen bond is formed between Gln84(OE1) from one helix to Phe63(N) from the other helix in both the compact and extended forms. The higher hydrophobicity of glutamine allows the formation of this additional bond and could result in a tighter coil-coiled linker.

Ala86 is located in the hinge region (Figure 3.3) thus as with Arg84 could have different interactions within compact and extended forms. In addition to interactions with Thr87, Ala86(N)-Lys83(O) bond remains in both monomeric forms. The replacement of Thr86 has no changes in bond formation with Thr87 and Lys83 in the compact form. An additional interaction Thr86(OG1)-Val88(N) was observed in the extended monomeric form. Val88 is located in the hinge region of LH-EBD, thus this interaction may decreased the angle between LH-EBD. Insertion mutations in this region generated changes in effector response in NodD from *Rhizobium leguminosarun* bv. *viciae*, which reveal that changes in the hinge region may affect the overall transcriptional activation (16). In DntR, a single change close to this hinge resulted in a variant unable to activate transcription in the presence of it effector salicylate (10).

Since the linker helix is made up of 18 or 30 amino acids, which results in a formation of a long helical region, it is probable that a subtle change in this portion could propagate rapidly to either EBD or DBD or both domains. This propagation could amplify as it moves up or down in the tetrameric conformation through the antiparallel

LH-LH interface. Since this interface also determines the relative disposition of the respective DBDs, contacts to promoter DNA might be affected by small changes. Therefore the subtle changes from the substituted amino acid residues described here could amplify throughout the helix and may display greater impact to other domains in the CatM tetramer. These alterations in the tetrameric form of CatM may affect transcriptional activation and may permit modulation of distinct operons that it is essential for CatM-mediated regulation.

Acknowledgments

The authors would like to expand their gratitude to Nicole Laniohan for help in strain construction. Cassandra Bartlett performed qRT-PCR for *catA* experiments. Also, we acknowledge K.T. Elliott and Laura Cuff for assistance with qPCR experiments. In addition, we thank Anna Karls for her assistance with bending assay experiments.

References

1. **Akakura R, Winans SC.** 2002b. Constitutive mutations of the OccR regulatory protein affect DNA bending in response to metabolites released from plant tumors. J. Biol. Chem. **277:**5866-5874.
2. **Akakura R, Winans SC.** 2002a. Mutations in the *occQ* operator that decrease OccR-induced DNA bending do not cause constitutive promoter activity. J. Biol. Chem. **277:**15773-15780.
3. **Barbe V, Vallenet D, Fonknechten N, Kreimeyer A, Oztas S, Labarre L, Cruveiller S, Robert C, Duprat S, Wincker P, Ornston LN, Weissenbach J, Marliere P, Cohen GN, Medigue C.** 2004. Unique features revealed by the genome sequence of *Acinetobacter* sp. ADP1, a versatile and naturally transformation competent bacterium. Nucleic. Acids. Res. **32:**5766-5779.
4. **Bradford MM.** 1976. A rapid and sensitive method for the quantitation of microgram quantities of protein utilizing the principle of protein-dye binding. Anal. Biochem. **72:**248-254.
5. **Bundy BM, Campbell AL, Neidle EL.** 1998. Similarities between the *antABC*-encoded anthranilate dioxygenase and the *benABC*-encoded benzoate dioxygenase of *Acinetobacter* sp. strain ADP1. J. Bacteriol. **180:**4466-4474.
6. **Bundy BM, Collier LS, Hoover TR, Neidle EL.** 2002. Synergistic transcriptional activation by one regulatory protein in response to two metabolites. Proc. Natl. Acad. Sci. U. S. A. **99:**7693-7698.

7. **Collier LS, Gaines GL, 3rd, Neidle EL.** 1998. Regulation of benzoate degradation in *Acinetobacter* sp. strain ADP1 by BenM, a LysR-type transcriptional activator. J. Bacteriol. **180:**2493-2501.

8. **Cosper NJ, Collier LS, Clark TJ, Scott RA, Neidle EL.** 2000. Mutations in *catB*, the gene encoding muconate cycloisomerase, activate transcription of the distal *ben* genes and contribute to a complex regulatory circuit in *Acinetobacter* sp. strain ADP1. J. Bacteriol. **182:**7044-7052.

9. **Craven SH, Ezezika OC, Haddad S, Hall RA, Momany C, Neidle EL.** 2009. Inducer responses of BenM, a LysR-type transcriptional regulator from *Acinetobacter baylyi* ADP1. Mol. Microbiol. **72:**881-894.

10. **Devesse L, Smirnova I, Lonneborg R, Kapp U, Brzezinski P, Leonard GA, Dian C.** 2011. Crystal structures of DntR inducer binding domains in complex with salicylate offer insights into the activation of LysR-type transcriptional regulators. Mol. Microbiol. **81:**354-367.

11. **Ezezika OC, Collier-Hyams LS, Dale HA, Burk AC, Neidle EL.** 2006. CatM regulation of the *benABCDE* operon: functional divergence of two LysR-type paralogs in *Acinetobacter baylyi* ADP1. Appl. Environ. Microbiol. **72:**1749-1758.

12. **Fischer R, Bleichrodt FS, Gerischer UC.** 2008. Aromatic degradative pathways in *Acinetobacter baylyi* underlie carbon catabolite repression. Microbiology. **154:**3095-3103.

13. **Gaines GL, 3rd, Smith L, Neidle EL.** 1996. Novel nuclear magnetic resonance spectroscopy methods demonstrate preferential carbon source utilization by *Acinetobacter calcoaceticus*. J. Bacteriol. **178:**6833-6841.

14. **Gregg-Jolly LA, Ornston LN.** 1990. Recovery of DNA from the *Acinetobacter calcoaceticus* chromosome by gap repair. J. Bacteriol. **172:**6169-6172.

15. **Harwood CS, Parales RE.** 1996. The beta-ketoadipate pathway and the biology of self-identity. Annu. Rev. Microbiol. **50:**553-590.

16. **Hou B, Li F, Yang X, Hong G.** 2009a. A small functional intramolecular region of NodD was identified by mutation. Act. Biochim. Biophys. **41:**822-830.

17. **Juni E, Janik A.** 1969. Transformation of *Acinetobacter calcoaceticus* (Bacterium anitratum). J. Bacteriol. **98:**281-288.

18. **Lamblin AF, Fuchs JA.** 1994. Functional analysis of the *Escherichia coli* K-12 *cyn* operon transcriptional regulation. J. Bacteriol. **176:**6613-6622.

19. **Maddocks SE, Oyston PC.** 2008. Structure and function of the LysR-type transcriptional regulator (LTTR) family proteins. Microbiology. **154:**3609-3623.

20. **Monferrer D, Tralau T, Kertesz MA, Dix I, Sola M, Uson I.** Structural studies on the full-length LysR-type regulator TsaR from *Comamonas testosteroni* T-2 reveal a novel open conformation of the tetrameric LTTR fold. Mol. Microbiol. **75:**1199-1214.

21. **Muraoka S, Okumura R, Ogawa N, Nonaka T, Miyashita K, Senda T.** 2003. Crystal structure of a full-length LysR-type transcriptional regulator, CbnR: unusual combination of two subunit forms and molecular bases for causing and changing DNA bend. J. Mol. Biol. **328:**555-566.

22. **Neidle EL, Ornston LN.** 1986. Cloning and expression of *Acinetobacter calcoaceticus* catechol 1,2-dioxygenase structural gene *catA* in *Escherichia coli*. J. Bacteriol. **168:**815-820.

23. **Romero-Arroyo CE, Schell MA, Gaines GL, 3rd, Neidle EL.** 1995. *catM* encodes a LysR-type transcriptional activator regulating catechol degradation in *Acinetobacter calcoaceticus*. J. Bacteriol. **177:**5891-5898.

24. **Rosario CJ, Janes BK, Bender RA.** 2010b. Genetic analysis of the Nitrogen Assimilation Control protein (NAC) from *Klebsiella pneumoniae*. J. Bacteriol. **192:**4834-4846.

25. **Ruangprasert A, Craven SH, Neidle EL, Momany C.** 2010. Full-length structures of BenM and two variants reveal different oligomerization schemes for LysR-type transcriptional regulators. J. Mol. Biol. **404:**568-586.

26. **Sambrook J, Fritsch F, Maniatis T.** 1989. *Molecular cloning: a laboratory manual, 2nd ed.* Cold Spring Harbor Laboratory Press, Cold Spring Harbor, N.Y.

27. **Schell MA.** 1993. Molecular biology of the LysR family of transcriptional regulators. Annu. Rev. Microbiol. **47:**597-626.

28. **Seaton SC, Elliott KT, Cuff LE, Laniohan NS, Patel PR, Neidle EL.** 2012. Genome-wide selection for increased copy number in *Acinetobacter baylyi* ADP1: locus and context-dependent variation in gene amplification. Mol. Microbiol. **83:**520-535.

29. **Smirnova IA, Dian C, Leonard GA, McSweeney S, Birse D, Brzezinski P.** 2004. Development of a bacterial biosensor for nitrotoluenes: the crystal structure of the transcriptional regulator DntR. J. Mol. Biol. **340:**405-418.

30. **Taylor JL, De Silva RS, Kovacikova G, Lin W, Taylor RK, Skorupski K, Kull FJ.** 2012. The crystal structure of AphB, a virulence gene activator from

Vibrio cholerae, reveals residues that influence its response to oxygen and pH. Mol. Microbiol. **83:**457-470.

31. **Tumen-Velasquez MP, Bacon C, Laniohan NS, Neidle EL, Momany C.** 2014a. Engineering CatM, a LysR-type Transcriptional Regulator, to respond synergictically to two different effectors (manuscript in preparation).

32. **Vaneechoutte M, Young DM, Ornston LN, De Baere T, Nemec A, Van Der Reijden T, Carr E, Tjernberg I, Dijkshoorn L.** 2006. Naturally transformable *Acinetobacter* sp. strain ADP1 belongs to the newly described species *Acinetobacter baylyi*. Appl. Environ. Microbiol. **72:**932-936.

33. **Yanisch-Perron C, Vieira J, Messing J.** 1985. Improved M13 phage cloning vectors and host strains: nucleotide sequences of the M13mp18 and pUC19 vectors. Gene. **33:**103-119.

34. **Zhou X, Lou Z, Fu S, Yang A, Shen H, Li Z, Feng Y, Bartlam M, Wang H, Rao Z.** Crystal structure of ArgP from *Mycobacterium tuberculosis* confirms two distinct conformations of full-length LysR transcriptional regulators and reveals its function in DNA binding and transcriptional regulation. J. Mol. Biol. **396:**1012-1024.

CHAPTER 4

BENM AND CATM, TWO LYSR-TYPE TRANSCRIPTIONAL REGULATORS FROM *ACINETOBACTER BAYLYI* STRAIN ADP1, MEDIATE TRANSCRIPTIONAL REGULATION OF *CATA* DIFFERENTLY*

*Melissa Tumen-Velasquez, Walker Whitley and Ellen Neidle. To be submitted to the *Journal of Microbiology*

Abstract

Dual effector synergistic activation has been well-characterized for BenM, a LysR-type transcriptional regulator that controls expression of *benABCDE,* an operon involved in benzoate degradation in *Acinetobacter baylyi* strain ADP1. In BenM, two effector molecules (benzoate and the metabolite *cis, cis*-muconate) bind to distinct sites in the effector-binding domain of the regulator, which results in the synergistic response exhibited by BenM. This synergistic response permits maximal BenM-mediated *benA* transcription. BenM also controls expression of *catA*, a gene located downstream of the *ben* operon whose enzymatic product converts catechol to *cis*-*cis* muconate. As reported here, BenM responds synergistically to benzoate and *cis*-*cis* muconate to activate high levels of *catA* transcription. Therefore, BenM is the only LysR-type regulator identified to synergistically activate two distinct loci. CatM, the other LysR-type regulator involved in benzoate degradation can also activate high *catA* transcription in response to *cis*-*cis* muconate only. Both regulators, BenM and CatM, share 59% amino acid sequence identity, but regulate genes involved in benzoate degradation differently. Here we focus on these two paralogs to understand the significant differences in how they regulate *catA*. These studies contribute to our understanding of complex regulatory circuits that govern aromatic compound catabolism and expand understanding of LysR-type mediated regulation by the largest family of prokaryotic transcriptional regulators.

Introduction

Catechol 1,2-dioxygenase, the enzymatic product of the *catA* gene, is essential for proper benzoate degradation in *Acinetobacter baylyi* strain ADP1. This dioxygenase catalyzes ring fission of its substrate, catechol, to generate *cis, cis*-muconate (hereafter named muconate) via the catechol branch of the β-ketoadipate pathway (28, 29). The latter metabolite serves as an effector molecule for BenM and CatM, two LysR-type transcriptional regulators (10, 35). BenM and CatM control transcriptional activation of genes involved in benzoate metabolism, including *catA* (10). In addition to a muconate-dependent response, BenM also responds to benzoate. CatM lacks such response (6). Both regulators bind similar promoter regions, but they activate transcription differently at each location (Figure 4.1). At *benA*, BenM has a major role and activates gene expression synergistically in response to benzoate and muconate. Unlike BenM, CatM fails to active high levels of *benA* transcription and plays a minor role at this region (10). On the contrary, CatM is the major regulator at the *catBCIJFD* operon, where muconate-dependent activation is observed (35). Previous studies suggested than both regulators equally activate *catA* transcription (10). The study presented here defines more clearly the regulatory roles in *catA* transcriptional activation of BenM and CatM.

Catechol dioxygenases play an important role in aerobic aromatic degradation where a wide range of monocyclic and polycyclic aromatics are converted into relative few intermediates with two adjacent hydroxyl groups (27, 29). In *A. baylyi*, intermediates such as catechol are cleaved at the *ortho* position, in which two atoms of oxygen are incorporated concomitantly by catechol 1, 2-dioxygenase (43). The enzymatic product,

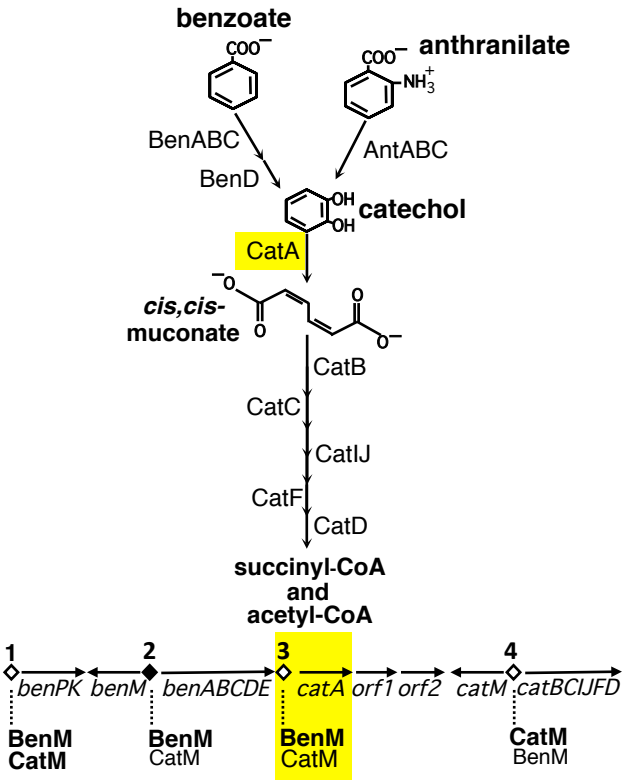

FIGURE 4.1. Benzoate degradation via the β-ketoadipate pathway in *A. baylyi* strain ADP1. Benzoate is converted to catechol by the gene products of the *ben* genes. The subsequent step in benzoate degradation involves ring fission at the *ortho* position of catechol. This step is catalyzed by catechol 1,2-dioxygenase (CatA, depicted in the yellow box). The product of the reaction, *cis,cis*-muconate, is degraded by the enzymatic products of the remaining *cat* genes, which generates succinyl-CoA and acetyl-CoA. The latter products enter central metabolism via the tricarboxylic acid cycle. (◇) Expression of *catA* is controlled by BenM and CatM (yellow box).

muconate, is further metabolized by the subsequent products of the *cat* genes to yield acetyl-coA and succinyl-coA.

In *A. baylyi*, muconate serves as a regulatory metabolite where its presence may be involved in cross-regulation of genes from the protocatechuate branch of the β-ketoadipate pathway (3, 4). Electrophoretic gel shift assays reveal that BenM and CatM bind to an intergenic region upstream *pcaU* and *pcaI* and the interaction was enhanced by the presence of muconate. It is suggested that binding of BenM and CatM to this region may block expression from *pcaK*, a 4-hydroxybenzoate transporter needed for this aromatic and protocatechuate uptake (4). In addition, disruption of *catA* releases repression of genes involved in vanillate and adipate degradation when challenged with benzoate and these carbon sources (2). Thus, regulation of *catA* is paramount to understand this level of cross-regulation between the catechol and protocatechuate branches in ADP1.

LTTRs form the largest family of transcriptional regulators that control a wide variety of cellular functions such as aromatic compound metabolism, amino acid synthesis, oxidative stress, carbon fixation, nitrogen fixation and bacterial virulence (22). Typically, these regulators are composed of 300 amino acids with two defined domains. At the N-terminal (termed the DNA-binding domain (DBD)) LTTRs are most conserved. This domain is connected via a long linker helix to the Effector-binding domain (EBD), a far less conserved domain (22, 37). Full-length LTTR structures determined by X-ray crystallography have shown that these proteins can arrange as tetramers. This tetrameric form is described as a dimer of dimers where proteins assemble as asymmetric subunits (26). This oligomerization permits the LTTRs to bind large regions of DNA where the

tetramer can rearrange upon effector binding. This modulation permits RNA polymerase to properly bind the promoter and initiate transcription (8, 26).

Typically an effector molecule binds to an interdomain cleft region in the EBD, which results in transcriptional activation (14). Structural studies of BenM-EBD and CatM-EBD bound to their cognate effector molecule, muconate, showed that this metabolite binds to this hinge region. Muconate binding is proposed to pull the EBD subdomains together which may result in changes in the protein tetrameric conformation. An additional effector-binding site is located only in the BenM-EBD where benzoate binds. It is proposed that the presence of both effectors bound to their respective binding sites results in the synergistic response exhibited by BenM (14). This type of unusual transcriptional activation by BenM has been reported only at the *benABCDE* operon (6). As described previously, BenM cannot carry out this type of activation at other promoters such as *benPK* and *catB*. In this study, we report that BenM synergistically activates maximal *catA* transcription in the presence of muconate and benzoate. In addition, CatM can also activate high levels of *catA* but in response to muconate only.

Materials And Methods

Bacterial strains and growth conditions. *Acinetobacter baylyi* strains were grown on minimal medium and *Escherichia coli* strains were grown on LB broth or at 37 ° (36, 42). In addition, *A. baylyi* strains were grown in minimal medium with succinate (10 mM), pyruvate (20 mM), benzoate (2 mM), muconate (3 mM), anthranilate (1 mM), catechol (1mM), as the carbon source. *E. coli* DH5α cells (Invitrogen) and XL-1 blue cells (Agilent Technologies) were used as plasmid hosts. Antibiotics were added as needed at

the final concentrations: ampicillin, 150 μg/ml, kanamycin, 25 μg/ml, spectinomycin, 13 μg/ml and streptomycin, 13 μg/ml. For *A. baylyi* growth curves, succinate-grown colonies were used to inoculate 5 ml cultures for overnight growth with anthranilate, muconate oor catechol as the carbon source. Next day, 0.5 ml of an overnight culture was used to inoculate 50 ml of anthranilate, muconate or catechol medium. Growth was monitored turbidometrically with a Klett-Summerson colorimeter or measured spectrophotometrically (OD_{600}).

B-galactosidase assays. A *catA::lacZ* transcriptional fusion was inserted into *A. baylyi* strains when indicated by allelic exchange with DNA of pBAC766 digested with *XmnI*. To assay these fusions, strains were grown on minimal medium with pyruvate (20 mM) as the carbon source with no inducer or the following when indicated: 65 μM benzoate, 65 μM muconate, 32.5 μM each. For assays during growth on muconate, cultures were grown overnight on minimal medium with muconate (3 mM). The following morning, 500 μl of each culture was diluted into 5 ml of minimal medium with muconate (3 mM). Growth was measured by optical density (OD_{600}) and assays were done when cultures reached late-exponential phase. Samples (0.5 μl to 5 μl) were lysed with Z buffer, sodium dodecyl sulfate and chloroform. Directions from FlourAce β-galactosidase reporter kit (BioRad) were followed. The hydrolysis of the substrate, 4 methylumbelliferyl-galactopyranoside (MUG) to the product 4-methyllumbelliferone (4MU) was detected with a TD-360 miniflourometer (Turner Designs). Relative fluorescence unit measurements enable 4MU quantification by comparison with a standard curve.

Table 4.1. Strains and plasmids used in this study.

Strains or plasmid		
***A. baylyi* Strain**	**Relevant characteristics[a]**	**Source**
ADP1	Wild type (BD413)	(18)
ISA13	*catM*::ΩS*4013*	(16)
ISA36	*benM*::ΩS*4036*	(10)
ACN1081	*benM*::ΩS*4036* Δ*benD5472* Δ*pcaIJF51070* Δ*catM51090* *catA*::*lacZ51081*	This study
ACN1082	*catA*::*lacZ51081*	This study
ACN1091	*catM*::ΩS*4013* *catA*::*lacZ51081*	This study
ACN1092	*benM*::ΩS*4036* *catA*::*lacZ51081*	This study
ACN1403	Δ*catM51090* Δ*benA*::*sacB*-Km^R*51403*	This study
ACN1410	Δ*benA*::*sacB*-Km^R*51403*	This study
ACN1432	Δ*benA51432*	(41)
ACN1466	*benM*::*sacB*-Km^R*51466* Δ*benA51432* Δ*catM51090*	(40)
ACN1474	Δ*benA51432* Δ*catM51090*	(40)
ACN1487	Δ*benMA51487* Δ*catM51090*	This study
ACN1492	Δ*benMA51487*	(41)
ACN1496	Δ*benA51432* Δ*catM51090* *catA*::*lacZ51081*	This study
ACN1497	Δ*benMA51487* Δ*catM51090* *catA*::*lacZ51081*	This study
ACN1498	Δ*benMA51487* *catA*::*lacZ51081*	This study
ACN1500	Δ*benA51432* *catA*::*lacZ51081*	This study

Plasmid	**Relevant characteristics**	**Source**
pUC18	Ap^R; cloning vector	(46)
pET-21b	Ap^R; T7 expression vector	Novagen
pIB1	Ap^R; partial *cat* region (11605-17916)[b]	(29)
pBAC430	Ap^R; *catM* (12116-13027)[b] in pET-21b	(6)
pBAC433	Ap^R; *benM* (1453-2368)[b] in pET-21b	(6)
pBAC766	Ap^R Km^R; *cat* region (7902-9190)[b] in pUC19. Contains *lacZ*-Km^R cassette	(41)
pBAC927	Ap^R, Km^R; *cat* region (8107-8560)[b]. Contains *catA* transcriptional start site	This study

pBAC1073	Ap^R; *ben* region (1453-5268)[b] with Δ*benA* deletion (2662-4043)[b]	(41)
pBAC1192	Ap^R; *benK-benC* (589-5268)[b] with Δ*benMA* deletion (1457-4043)[b]	(41)

[a]Ap^R, ampicillin resistant; Sm^R, streptomycin resistant; Sp^R, spectinomycin resistant; Km^R, kanamycin resistant; ΩS, omega cassette containing Sm^R Sp^R (Prentki and Krisch, 1984) (34); *sacB*-Km^R, dual selection cassette containing a counterselectable marker and kanamycin resistant cassette (Jones and Williams 2003) (17).

[b]Position in the *ben-cat* sequence in GenBank entry AF009224

RNA isolation. Strains ADP1, ACN1474, and ACN1492 were used for RNA purification. For RNA used for mapping the *catA* transcriptional start site, ADP1 cells were grown on LB broth with benzoate (3 mM) and muconate (3 mM). For all other RNA isolation preps, ADP1 cells were grown in minimal medium with succinate (10 mM), pyruvate (20 mM), or LB broth. ADP1 cells were grown on muconate (3 mM) or benzoate (2 mM) when indicated. ACN1474 and ACN1492 were grown on pyruvate (20 mM) alone as the carbon source and with inducers when indicated: 500 μM benzoate, 500 μM muconate, 250 μM each. Growth was measured by optical density (OD_{600}). Cells were harvested at early exponential phase (OD_{600} 0.2-0.3), mid-exponential (OD_{600} 0.5-0.6), or late exponential (OD_{600} 0.8-0.9) when indicated. 5 ml of cells were pelleted down and immediately frozen with -70 °C Ethanol to prevent RNA degradation. Total RNA was extracted by the TRI Reagent (Molecular Research Center) method. RNA samples were treated with RQ1 DNase I (Promega) until no DNA contamination was detected by PCR. The quality and quantity of the extracted RNA were determined spectrophotometrically using the absorbance at 260 nm (Beckman DU® 640). Isolated RNA was stored at -70 °C until needed.

cDNA synthesis from total RNA. For samples to be used for real-time PCR, the SuperScrip III First-Strand Synthesis for RT-PCR was used (Invitrogen) and random hexamers as primers. Approximately, 1 μg of total RNA was used for cDNA synthesis. Products were analyzed on 0.8% agarose gel and stored at -20 °C.

5' RACE (Rapid Amplification from cDNA ends). For this experiment, 2 µg of RNA from induced ADP1 and 2.5 ρmoles of GSP-1 catA (Table 4.2) were combined into 15.5 µl total volume reaction. The protocol for 5'RACE System (Invitrogen) was followed. About 20% of the final reaction was used for PCR analysis. Primers GSP-1 catA and 5' RACE Abridged Anchor Primer (Table 4.2) along with *Taq* DNA polymerase were used for 5' RACE product amplification. The reaction was performed with the following PCR settings: 94 °C for 1 minute, 55 °C for 1 minute, 72 °C for 2 minutes for 30 cycles. PCR product was analyzed on 2% agarose gel and gel extracted (Qiagen). Extracted PCR products were cloned using the TOPO® TA cloning Kit (Invitrogen). As described in the manufacturing manual, 5 µl of gel extracted PCR sample, 1 µl of salt solution and 1 µl TOPO® TA vector were combined and gently mixed. The reaction was incubated at room temperature for 10 minutes. The reaction was used to transform chemical competent DH5α *E.coli* cells. Blue and white screen was used to identify clones with an insert. Clones were also screened by restriction digest with *XhoI* and *NcoI.* Resulting plasmids were sequenced to determine the start site of *catA.*

Quantitative reverse transcriptase PCR (qRT-PCR). cDNA generated with random hexamers from uninduced and induced ACN1474 and ACN1492 were used for these experiments. Primer-probes for *rpoA* and *catA* were used and designed with PrimerExpress software (Applied Biosystems): qRT-catA-UP, qRT-catA-DW, rpoAfor, rpoArev (Table 5.2). The *rpoA* probes were used as internal controls to evaluate the amount of *catA* transcripts. Quantitative RT-PCR was performed in StepOnePlus Real-Time PCR systems (Applied Biosystems). Each reaction was carried out in a total

Table 4.2. Primers used in this study

Primer Name	Sequence	Location[c]
catA_Start	5' GCCACCTTCTTGCTCAAGTC 3'	←[a] 8364[c] in *catA*
benE_End	5' CGAGATCCTGCACTGATTAC 3'	→[b] 7541[c] in *benE*
RT_catA	5' CAAGGAGAAAGCCATGGAAG 3'	→[b] 8274[c] in *catA*
GSP2_catA-2	5' TTCGGCATCCATACGCATAT 3'	←[a] 8560[c] in *catA*
GSP1_catA	5' CGCATAACCTACCGATTCAG 3'	←[a] 8649[c] in *catA*
catA-OP-1-UP	5' CGAGATCCTGCACTGATTAC 3'	→[b] 7541[c] in *benE*
catA-OP-1-DW	5' CATTACTATGGTCGAGCAGATATC 3'	←[a] 7897[c] upstream *catA*
catA-OP-2-UP	5' GATATCTGCTCGACCATAGTAATG 3'	→[b] 7874[c] upstream *catA*
catA-OP-2-DW	5' CTTGCACATCCTGAGTATTGA 3'	←[a] 8323[c] in *catA*
catA-OP-FAM[d]	5' /56-FAM/TCACATTATGAGCTAAATTTA 3'	→[b] 7898[c] upstream *catA*
qRT-catA-UP	5' TGCGCACATTCACTATTTTGTTT 3'	→[b] 8952[c] in *catA*
qRT-catA-DW	5' TCGCCAGCCACATTAATTTG 3'	←[a] 9023[c] in *catA*
qRT-rpoA-FOR	5' GCTCGACGCCTTCTATTTCAA 3'	
qRT-rpoA-REV	5' TTTACGTCGCATTCTATTGTCTTCTT 3'	

[a & b] indicate primer directionality (→ upstream) (← downstream)

[c] Position in the ben-cat sequence in GenBank entry AF009224

[d] Labeled oligo with 56-FAM modification added at the 5' end

volume of 20 µl on an 96-well optical reaction plate (Applied Biosystems) containing 10 µl of SYBR Green (Applied Biosystems), 1 µl of cDNA and two gene-specific primers at a final concentration of 0.2 mM each. To quantify targets, *rpoA* and *catA* standard curves were prepared and ADP1 genomic DNA was used as template for qPCR (12.5 ng to 0.02 ng). A non-template control was used for each primer set. Melting curve analysis verified that each reaction contained a single PCR product. *catA* expression levels were normalized to transcripts of the internal control *rpoA*. Relative levels were normalized to uninduced wild type (ADP1) transcript levels.

Results

CatM and BenM bind to a region upstream of *catA*. Previous electrophoretic mobility shift assays (EMSA) demonstrated that CatM was able to bind an intergenic region located upstream of *catA* (35). It is unknown whether BenM can bind this region. Thus, the precise binding region for CatM or BenM as well as the structure of the *catA* promoter was further investigated. There is an intergenic region of 615 base pairs located between *benE* and *catA,* within this region lays the 388 bp fragment to which CatM was shown to bind (35). To determine the precise binding regions for CatM and BenM, this intergenic region was run through the Pattern Locator program to locate possible binding sites with the conserved ATAC-N_7-GTAT sequence motif to which both proteins have been shown to bind (25). Two regions within this sequence were identified as potential binding sites (Figure 4.2). Oligos were designed to bind different sequences of this region to generate probes with distinct sizes for gel shift experiments (Table 4.2). BenM and CatM were able to bind to region 1, which contained the intergenic region between *benE*

and *catA* (Figure 4.2). When this region was divided into two smaller regions, both proteins only bound the region closest to the *catA* coding region (Figure 4.2, region 3).

Mapping *catA* transcriptional start site. Since the DNA region to which CatM and BenM bind was identified, the *catA* promoter was further evaluated by mapping its transcriptional start site. The start site determined by 5' RACE was found 180 bp away from the *catA* start codon (Figure 4.3A). This start site correlated with previous primer extension results (Bundy and Neidle, unpublished results), which reinforces the veracity of the 5' RACE results. Interestingly, the binding site (ATAG-N_7-GCAT) predicted by the Pattern locator program was found 72 bp away from the determined *catA* start site (Figure 4.3A). The location of this site is consistent with the site 1 binding site described for the *benA* and *catB* promoters (Figure 4.3B). Another site (ATAG-N_7-GGAA) identified by the Pattern locator but with less conserved symmetry was found 6 bp downstream of the predicted site, which correlates to the location of site 2 on the *benA* and *catB* promoters (Figure 4.3B). The organization of LysR-binding sites appears to be well conserved with previous determined promoters (Figure 4.3B).

BenM and CatM bind to the *catA* operator-promoter DNA with similar binding affinities. Both regulators were found to bind a region upstream *catA*. Since the *catA* promoter has been determined, the probe used for EMSA experiments was modified and fluorescently labeled to include only region 2. In the absence of inducers, BenM

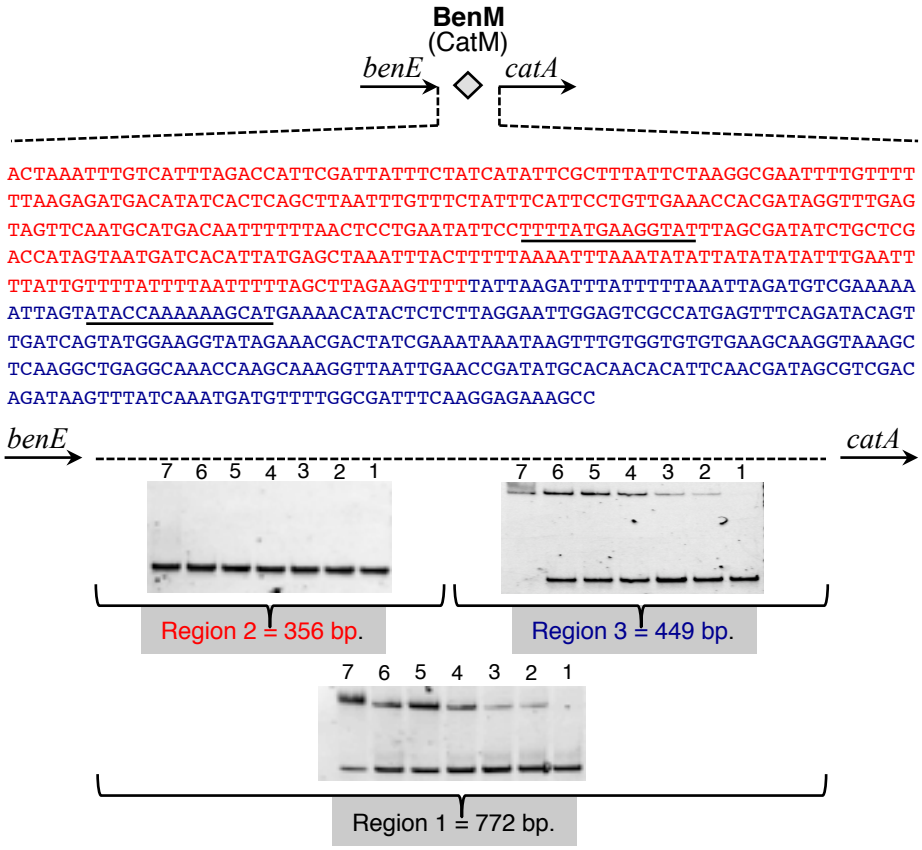

Figure 4.2. Intergenic region between *benE* and *catA*. Region 1 includes the whole intergenic region and additional upstream and downstream DNA. Region 2 (blue), includes the upstream portion of the intergenic region. Region 3 (red), includes downstream of the aforementioned region. BenM protein concentration added as indicated: lane 1 (No protein), lane 2 (20 nM), lane 3 (40 nM), lane 4 (80 nM), lane 5 (160 nM), lane 6 (320 nM), lane 7 (640 nM). Muconate (1.6 μM) was added to all reactions. CatM was added with similar concentrations (data not shown). 4 nM of probe DNA was used in all reactions. Experiments were repeated at least four times.

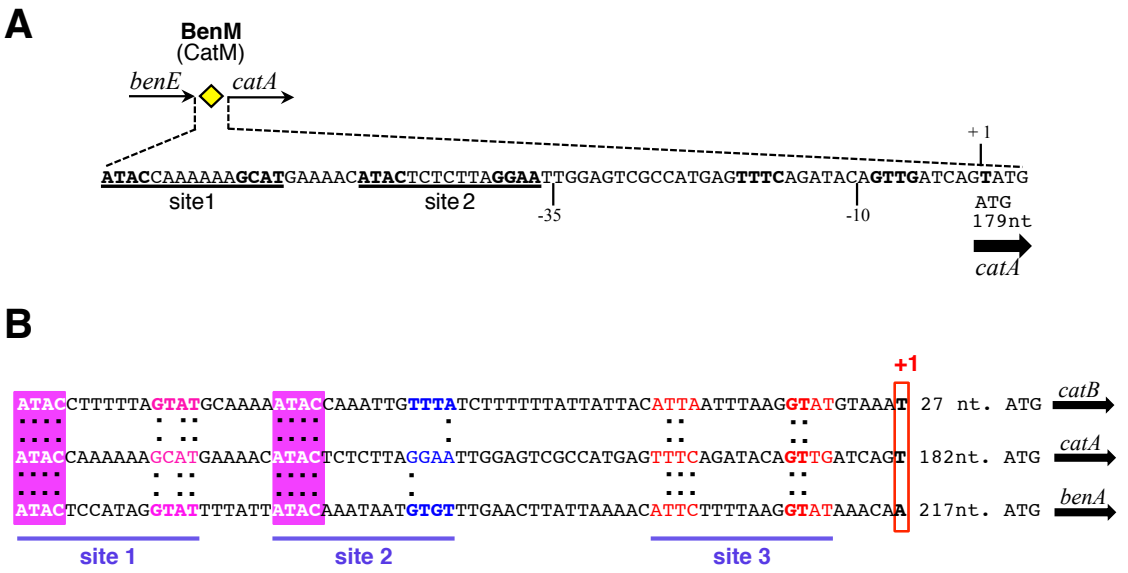

Figure 4.3. Promoter regions of genes controlled by BenM and CatM. (A) *catA* promoter region with indicated (-10) and (-35) elements relative to the +1 transcriptional start site (bold). Predicted binding sites with imperfect dyad symmetry (ATAG-N_7-GTAT) determined by the Pattern Locator (http://www.cmbl.uga.edu/software/patloc.html) are underlined. Less conserve binding site located over the -10 element also indicated in bold. **(B)** Sequence alignment between other promoter regions under the regulation of BenM and CatM (*benA* and *catB*) with *catA*. Pink boxes indicated conserved nucleotides in the first half of site 1 and site 2 among all three promoter regions. (:) Indicates conserved nucleotides in binding sites between all promoter regions. Site 3 is the least conserved binding region in all promoters. Red box indicates position of all +1 transcriptional start sites.

and CatM bind this region with similar binding affinities (Table 4.3). With muconate, CatM binds with higher affinity than BenM. Although binding affinities increase slightly, the lower K_d values were observed only by BenM upon addition of benzoate and muconate to the reaction. As shown in chapter 2, this reduce in binding affinity was not observed at the *benA* promoter where BenM activates this promoter synergistically in response of these two effector molecules. In the case of the *catA* activation, it is unknown whether BenM has this similar type of transcriptional activation at this region.

Assessing *catA* gene expression. CatA enzymatic assays determined that benzoate-dependent CatA induction was observed on strains where BenM was the sole regulator (10). BenM is required for benzoate-mediated expression of *catA* whereas muconate-dependent *catA* activation was attributed to either BenM or CatM. Based on these studies, it is unknown whether the concomitant addition of benzoate and muconate have an effect on *catA* activation. To understand and clarify the regulation of the *catA* gene at the transcriptional level, a *catA*::*lacZ* fusion was constructed. Strains ACN1081, ACN1082, ACN1091 and ACN1092 were constructed and LacZ activity was measured with and without effectors. Each of the aforementioned strains has either or both regulators disrupted to determine the activation role by BenM and/or CatM (Table 4.1). Without BenM or CatM, strain ACN1081 did not have LacZ significant activity under any condition tested. Since BenM and CatM are disrupted or deleted in this background, this result indicates that no other regulatory protein is responsible for *catA* transcriptional activation (Figure 4.4).

Table 4.3. Binding affinities of BenM, CatM to *catA* promoter region under different inducer conditions

protein	No inducer K_d (nM)[a]	Benzoate[b] K_d (nM)[a]	Muconate[c] K_d (nM)[a]	Muconate + Benzoate[d] K_d (nM)[a]
Wild-type BenM	60 ± 3	35 ± 2	48 ± 3	40 ± 3
Wild-type CatM	65 ± 2	69 ± 5	30 ± 3	71 ± 4

[a] Kd, equilibrium dissociation constant.

[b, c] and [d] from 1.6 mM total concentration of inducer per reaction and 800 μM of each inducer when were added together to each reaction.

Binding affinities shown are the average of at least three independent K_d determinations. Standard deviations were maintain within 10% of the average value.

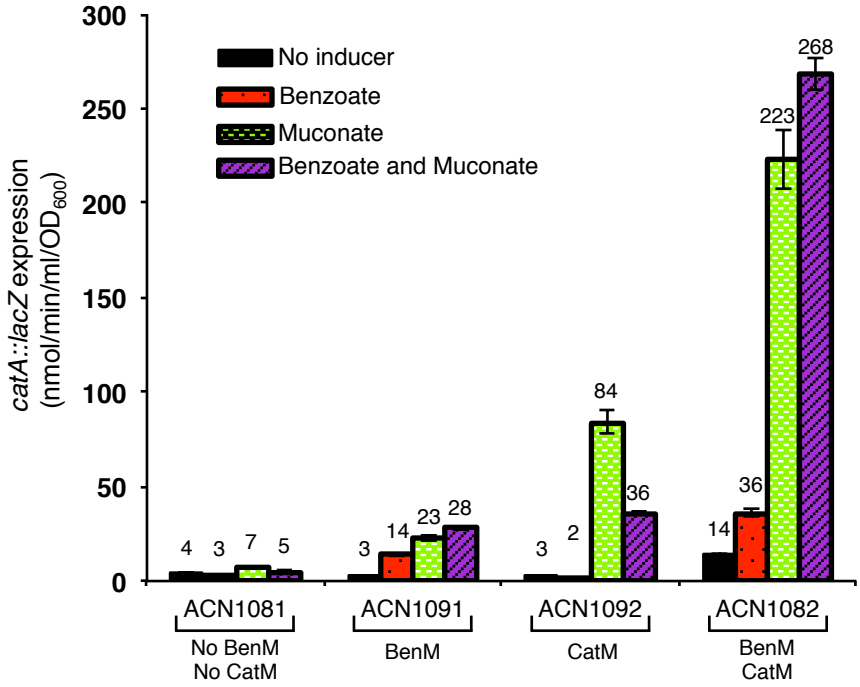

Figure 4.4. Expression of *catA*::*lacZ* fusion. LacZ activity was assayed late in the exponential growth phase (OD_{600} ~0.7-0.8) for the indicated strains. Strains were grown pyruvate with addition of inducers where indicated (1 mM benzoate, 1 mM muconate, or 0.5 mM benzoate and 0.5 mM muconate). Data represent the average of four replicates with standard deviations shown by error bars.

Strain ACN1082 revealed the highest LacZ activity in response to benzoate and muconate. This activation is only slightly elevated when compared to that of muconate-inducible LacZ levels for this strain and cannot be concluded as synergistic. As described elsewhere, synergistic activation is described as maximal expression higher than the sum of individual effector-dependent activation alone. Both regulators are present in this background (ACN1082), which is reflected by the benzoate-inducible LacZ levels that can be attributed to BenM-mediated activation. This benzoate response was also observed for ACN1091, where BenM is the sole regulator. Elevated *catA::lacZ* expression was observed for ACN1092 in response to muconate only where CatM is the sole regulator. Muconate-dependent *catA* activation in ACN1091 (BenM) was three-fold lower than that of ACN1092 (CatM). Since either BenM or CatM can activate *catA* in response to muconate, albeit at different levels, the elevated muconate-dependent *catA* activation observed in ACN1082 could be attributed to CatM rather than BenM. Based on these results, the presence of both regulators yields maximal *catA* transcription with muconate and not benzoate as the main effector.

Since the *ben* genes are still active in all these backgrounds, the effect of benzoate as an effector cannot be measured accurately. The first gene involved in benzoate degradation, *benA* was deleted to generate strains: ACN1432, ACN1474, ACN1487, and ACN1492. These strains contained partial or complete deletions of *benM* and/or *catM* genes (Table 4.1). The *catA*::*lacZ* fusion was introduced in all these strains and LacZ activity was measured again. Strains ACN1496, ACN1498 and ACN1500 with the *benA* deletion have muconate-dependent *catA* expression albeit at different levels (Figure 4.5). ACN1498 (CatM only) and ACN1500 (BenM and CatM only) have the highest

muconate-dependent *catA* expression (Figure 4.5). Muconate-dependent expression from ACN1496 (BenM only) is similar to that of benzoate, which may indicate that maximal *catA* expression in response to muconate is CatM-mediated.

Since genes involved in muconate degradation are still active, expression of *catA*::*lacZ* was measured in strains grown on muconate to mimic wild-type metabolism. The exception was ACN1497 which cannot grow on muconate without BenM and CatM. Under this condition, muconate serves as an effector as well as the source of energy and carbon. Muconate-dependent activation was higher than previously observed on pyruvate grown cultures where muconate was added exogenously (data not shown). In addition, there were no significant differences in LacZ activity within all strains assayed, which may indicate that BenM and CatM activate similarly high levels of *catA* expression in response to muconate.

Benzoate-dependent expression was observed only in strains where BenM is active. Maximal *catA*::*lacZ* activity is observed only when muconate and benzoate are added as effectors in the strain where BenM is the sole regulator (Figure 4.5). Similar to *benA* expression, BenM-mediated *catA* expression is activated synergistically in response to benzoate and muconate. This synergistic response was not observed in ACN1091 where the *ben* genes were still active. Thus, the activation of the *ben* genes degraded benzoate rapidly, which affected the benzoate-dependent activation of *catA* to be observed in these strains.

Measuring *catA* transcripts. To verify the *lacZ* results, *catA* transcript levels were measured by qRT-PCR from strains where either BenM or CatM is the sole regulator

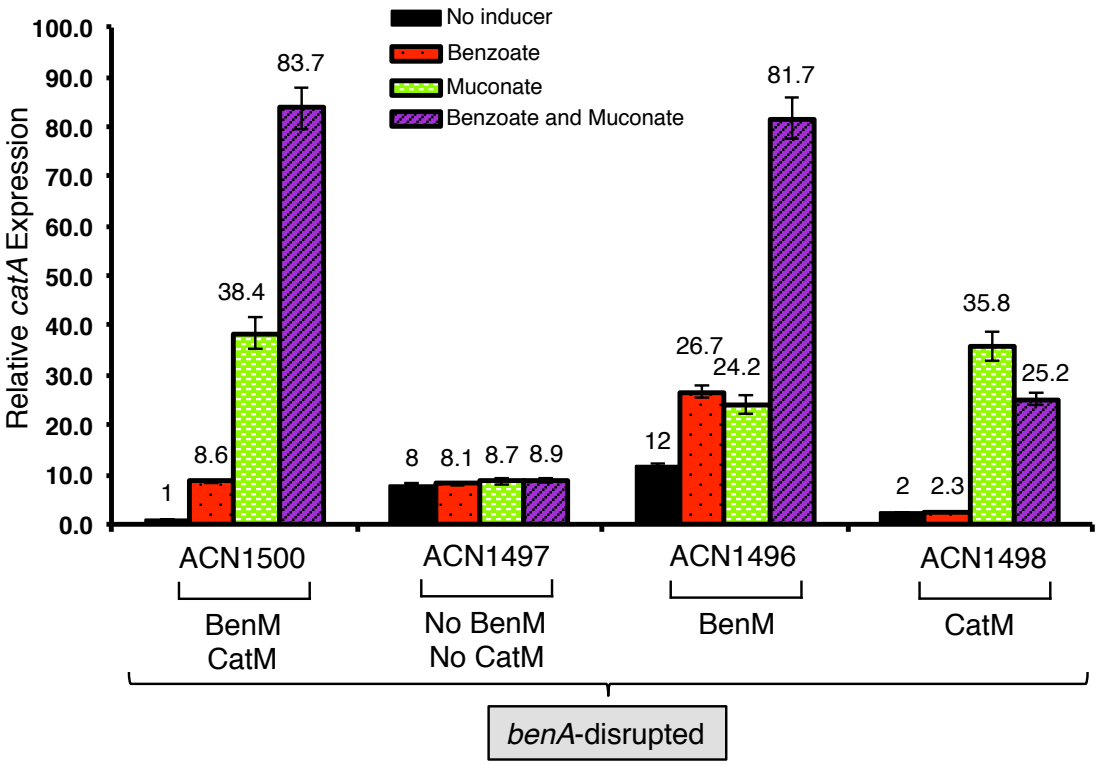

Figure 4.5. Expression of a chromosomal *catA*::*lacZ* fusion in strains encoding BenM or CatM or both regulators. Cultures were grown on pyruvate with addition of the indicated inducers (65 μM benzoate, 65 μM muconate, or 32.5 μM benzoate and 32.5 μM muconate). β-Galatosidase activity is reported relative to ACN1500 grown on pyruvate (0.26 ± 0.05 nmol/min/ml/OD_{600}). Activities are the average of at least four repetitions with standard deviations within 20% of the average value.

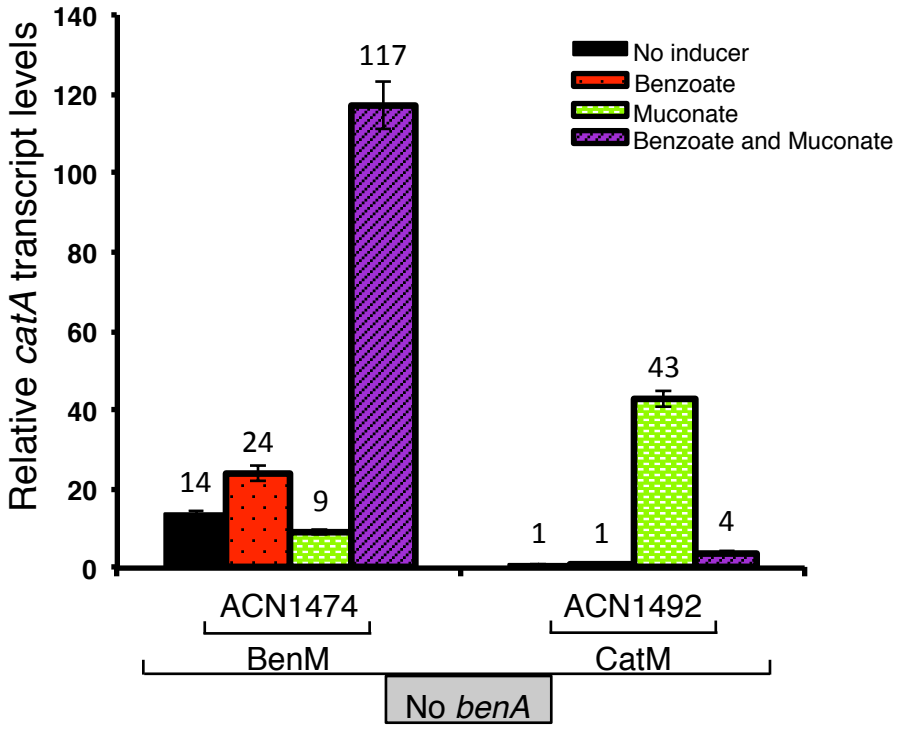

Figure 4.6. Fold increase in *catA* transcript levels measured by qRT-PCR. *catA* transcripts levels in strains with *benA* deleted carrying *catM* and *benM.* Cells were grown on pyruvate with or without effectors. RNA was immediately isolated when cultures reached early exponential phase (OD_{600} 0.2). Graph represents combined data from three independent biological replicates. Melting curve analysis verified that each reaction contained a single PCR product. *catA* expression levels were normalized to transcripts of the internal control *rpoA.* Standard deviations were within 15% of the average value.

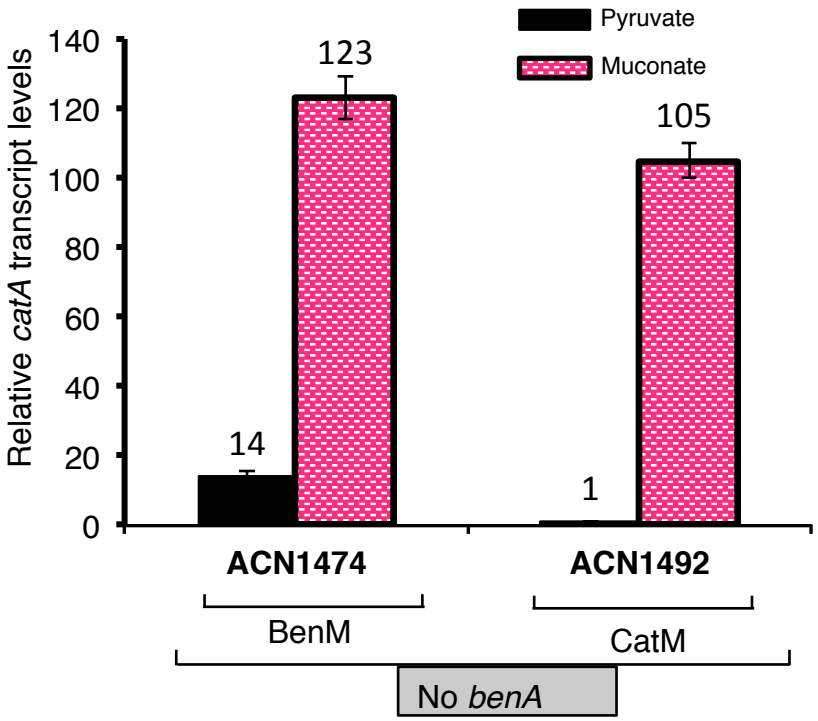

Figure 4.7. Fold increase in *catA* transcript levels measured by qRT-PCR. RNA was isolated from strains grown on 3 mM muconate or 20 mM pyruvate as the source of carbon and energy. Graph represents combined data from two independent biological replicates. Melting curve analysis verified that each reaction contained a single PCR product. *catA* expression levels were normalized to transcripts of the internal control *rpoA*. Standard deviations were within 12% of the average value.

of *catA*. RNA was isolated from strains ACN1474 (BenM only), and ACN1492 (CatM only) grown on pyruvate with an effector where indicted. As shown in figure 4.6, muconate-inducible *catA* transcript levels are highest for ACN1492, which is similar to muconate-dependent *catA*::*lacZ* activity observed for ACN1498 (CatM only). Benzoate-inducible *catA* transcript levels are observed only for ACN1474, which correlates to *catA*::*lacZ* expression observed for ACN1496 (BenM only). Maximal *catA* transcript levels are observed for mRNA isolated from ACN1474 grown on pyruvate with benzoate and muconate as inducers. These results in transcript levels correlate to the synergistic *catA*-activation observed for β-galactosidase assays, where high *catA*::*lacZ* expression is detected in response of benzoate and muconate with BenM as the sole regulator. Therefore, these combine results confirm that similarl to *ben* gene activation, BenM activates high *catA* transcription levels synergistically.

Muconate-dependent *catA* transcripts were also lower than those of benzoate for ACN1474 (BenM only). This low *catA* transcript levels correlates to muconate-dependent LacZ levels determined for ACN1496 (BenM only). It is possible that muconate provided exogenously might not be taken up by the cells due to the toxicity of this metabolite, which might impact LacZ expression and transcript levels. Nevertheless, muconate-inducible LacZ activities were increased when strains were grown on muconate as the sole source of carbon and energy. Thus, RNA was isolated from ACN1474 and ACN1492 grown on muconate only. Similarl to *catA*::*lacZ* levels, muconate-inducible *catA* transcript levels from ACN1474 (BenM only) were relatively higher than that when muconate was provide exogenously with pyruvate (Figure 4.7). Interestingly, *catA* transcript levels were similar between ACN1474 and ACN1492 under

these conditions. It is possible that when muconate is provided exogenously with pyruvate, the *catB*-mediated expression levels by BenM are lower in ACN1474 (BenM only) than ACN1492 (CatM only), which results in slower degradation of muconate. To prevent accumulation of muconate, exogenous muconate might not be taken up by the cells as well as for ACN1492.

Discussion

The *catA* promoter reveals similarities with other promoters regulated by BenM and CatM. Previous studies suggested that either BenM or CatM were responsible for *catA* transcriptional activation where CatM or BenM regulates *catA* expression in response to muconate (10). BenM was identified as the regulator responsible for *catA* expression in response to benzoate only. The study presented here clarifies the regulatory role of BenM at this locus. Electrophoretic mobility shift assays demonstrated binding of BenM to an intergenic region upstream *catA* (Figure 4.2). Similar to previous gel shift results, CatM was also able to bind to this region. The 5' RACE method was used to determine the transcriptional start site for the *catA* gene. Alignment of this region with the promoters controlled by BenM and CatM (*benA* and *catB*) aid in the identification of essential regulatory sequences (Figure 4.3).

With the aid of the Pattern locator program, two potential LysR-type binding sites were identified for this promoter region (25). These consensus-binding sequences found in the *catA* promoter (site 1 and site 2, Figure 4.3A, B) contained the T -N_{11}- A element to which LTTRs bind (22). Similar sequences are found for the *benA* and *catB* promoters as well (Figure 4.3). DNase I footprinting experiments have shown BenM and CatM to

protect these sites from DNase digestion at the *benA* promoter (6). However, protection of these DNA regions depends upon addition of effectors. In the absence of effectors, a BenM or CatM tetramer binds to site 1 and site 3 respectively. With effectors, the tetramer releases protection of site 3 to protect site 2 probably by reposition of the tetramer by sliding to site 2 (6, 13). Methylation experiments along with DNase footprinting indicate that CatM also recognizes an identical sequence in the *catB* promoter (9, 35). Preliminary DNase I footprinting experiments have shown CatM to protect a region (site 1 and site 2) at the *catA* promoter when muconate was introduced in the reaction (data not shown). Therefore, this indicates that these DNA regions may serve as binding sites for CatM at this promoter. Nevertheless, footprinting experiments need to be completed to clarify binding of CatM to the *catA* promoter in the absence of inducers.

It remains unknown whether BenM protects these regions in a similar manner as to the *benA* promoter, and if this protection changes upon addition of effectors. CatR, a LysR-type regulator from *Pseudomonas putida*, controls transcriptional activation of the *cat* and *phe* operons, whose enzymatic products are involved in catechol and phenol degradation (39). The promoter regions from these operons share a high degree of sequence similarity, which resulted in similar footprint patterns by CatR with and without effector (muconate) (24, 39). Based on the similarity between the *benA* and *catA* promoters, it is possible that the BenM tetramer binds the latter promoter region at site 1 and site 3, and that addition of effectors relocates the tetramer to site 1 and site 2. Since maximal BenM-dependent transcriptional activation at *benA* and *catA* happens upon the presence of benzoate and muconate, it is possible that BenM activates these genes through a similar transcriptional activation scheme.

The sequence similarity between promoters regulated by BenM and CatM (Figure 4.3), and the sequence similarity of these transcriptional regulators results in overlapping regulatory functions at these promoters. A similar situation is observed for CatR and ClcR, two LysR-type regulators that share 43% amino acid sequence, where their controlled promoters for *cat* and *clc* operons are highly similar (24, 30). Despite both regulators binding to the same promoter regions, only CatR can activate transcription for the *cat* and *clc* operons while ClcR only activates transcription for the *clc* operon (30). Hence, recognition and binding to similar promoters might not reflect high transcriptional activation or activation at all. A similar situation is observed for the *benABCDE* and *catBCIJFD* operons where BenM and CatM bind and recognize, but transcriptional activation levels vary. Mutational studies revealed that nucleotides in the consensus binding site (ATAG-N_7-GTAT for *clc* and AGAG-N_7-GTAT for *cat*) are essential for regulators (CatR and ClcR) to bind to these regions (30). Mutations at site 1 for the *benA* promoter affect BenM binding (5).Similar studies were observed for OccR where modification of the conserved binding site at the *occQ* promoter, affects OccR-DNA binding (1). Normally LysR-type regulators bind as tetramers with each dimer bound to DNA-binding recognition sites. Thus, the consensus binding site (Figure 4.3B, site 1) serves as the anchor for binding to the other non-consensus binding site (site 2 and site 3). Similar binding has been described for other LysR-type regulators. At AtzR, a dimer was found bind strongly to the consensus binding site while the second dimer adopts two alternative conformations at the other two non-consensus sites (33).

Similar mutational studies suggested that transcriptional activation might involve protein interaction with nucleotides located at the less conserved binding site. Normally,

this non-consensus binding site is located a few nucleotides downstream of the consensus site. At some promoters, this binding site is found to overlap or be close to the -35 element, which suggests interactions with RNA polymerase (22). Mutations introduced at this site for the *occQ* promoter fail to affect OccR binding to this promoter (1). In addition, modifications of this binding site at the *cat* and *clc* promoters affect transcriptional activation by CatR and ClcR respectively, and not binding (31, 39). Conversely, BenM-dependent *benA* activation was reduced when site 2 was altered (Bundy and Neidle unpublished results). Thus, this site is required for transcriptional activation rather than protein binding. Based on the similitudes with the *benA* promoter, the proposed site 2 for *catA* might be involved in transcriptional activation.

Importance of *catA* regulation in *A. baylyi*. As described in this report, BenM and CatM can activate transcription from this gene. This activation varies between both regulators where CatM activates this promoter in response to muconate only, and BenM synergistically activates transcription with benzoate and muconate. The importance of *catA* transcription in *A. baylyi* is emphasized by the need of two regulatory proteins to control expression. This tight control might prevent accumulation of muconate, an important effector that it is toxic at elevated concentrations (16). It has been shown that a strain unable to degrade muconate cannot grow on alternative carbon sources such glucose and succinate when benzoate is provided (16). Thus, the endogenous accumulation of muconate in this strain from benzoate degradation was toxic. Nevertheless, exogenous muconate fails to inhibit growth in the same fashion. As shown in this report, muconate-inducible *catA* expression and *catA* transcript levels were

affected on strains were BenM was the sole regulator when muconate was provided exogenously with pyruvate (Figure 4.5 and 4.6). It is probable that BenM's inability to activate high levels of transcription from the *catBCIJFD* operon, whose gene products degrade muconate, prevent muconate uptake to avoid accumulation at toxic levels. Interestingly, this low muconate-dependent activation levels was not observed when muconate is provided as the sole source of carbon and energy. Under this condition, muconate is forced into the cell and must be uptake in order to be consumed by the bacterium. Therefore, uptake and degradation of muconate is coupled to prevent high intracellular levels.

In addition, muconate serve as a regulatory metabolite by inhibiting degradation of aromatic compounds funneled through protocatechuate branch of the β-ketoadipate pathway. In ADP1, benzoate represses expression of several genes, including *pca, pobA, hca, and vanAB* from the protocatechuate branch (3, 4, 15). This repression was observed when expression levels of aforementioned genes were assessed in the absence of benzoate, and in the presence of 4-hydroxybenzoate and compare to those in the presence of benzoate and 4-hydroxybenzoate (4). Interestingly, on strains where *catA* was disrupted, blocking muconate generation, cross-regulation by benzoate was lost at these operons. Thus, muconate and not benzoate was the effector responsible for repression of these genes (*pca, pobA, hca, and vanAB*) (2). Since muconate is a metabolite generated from aromatics degraded via the catechol branch, CatM and not BenM may play a major role in *catA* activation to generate muconate when growing in alternative substrates besides benzoate.

It is probable that during benzoate growth, BenM activates *benABCDE* and *catA* in response to benzoate to initiate benzoate degradation and generate muconate quickly. The increased in muconate levels serves to repress expression from genes of the protocatechuate branch, which may prevent *A. baylyi* to degrade alternative aromatic compounds through this branch in the presence of benzoate. The presence of both metabolites permits dual effector synergism by BenM at *benABCDE* and *catA*. This rapid response to these effectors prevents accumulation of toxic metabolites such as muconate that can easily be degraded by the remaining *cat* genes whose expression is controlled by CatM. This intricate synergistic response should decrease as benzoate depletes. Muconate levels decrease, which releases repression from genes of the protocatechuate branch and permit degradation of alternative aromatics from this branch. Thus, this permits *A. baylyi* to ensure energy conservation by activating catabolic enzymes only when favored carbon sources such as benzoate are available.

Regulation of the *catA* gene in other *Acinetobacter* species. Several *Acinetobacter* strains isolated from soil environments have been identified to metabolize an array of aromatic compounds including benzoate and catechol in a similar manner to ADP1. However, differences within the genus lie in the number of copies of the *catA* gene present in their respective chromosome. Normally, these *catA* genes are not located adjacent or close to each other, but distinctly separated in the chromosome (23, 47).

In *Acinetobacter radioresistens* S13, two CatA isoenzymatic forms (IsoA and IsoB) are encoded by two different *catA* genes ($catA_A$ and $catA_B$). These genes are located in two separated locations and share only 48% in amino acid sequence identity (7, 32).

Transcript and functional proteomic analysis determined that benzoate alone induces high levels of $catA_B$ transcription, while $catA_A$ is activated under phenol and other aromatic compounds (23). A LTTR consensus-binding site (ATAG-N_7-GTAT) is found 200 nucleotides upstream of $catA_A$. Since muconate is a product of catechol cleavage, it has been proposed that a CatM-like regulator with a muconate response may activate expression from this gene (23). Further studies are needed to determine whether a CatM homolog is present in *A. radioresistens* S13. Less is known about the regulation of $catA_B$, but it is probable that a benzoate-responsive regulator might control its expression during benzoate growth.

Acinetobacter lwoffi K-24 is the first *Acinetobacter* to have three catechol branches with three different *catA* genes. Two *catA* genes ($catA_1$ and $catA_2$) are expressed only under aniline growth conditions while $catA_3$ is expressed only under benzoate degradation (19, 20, 47). Despite characterization of all three catechol 1,2-dioxygenases enzymes, far less is know about the regulation of these genes.

In *Acinetobacter calcoaceticus* PHEA-2, only one *catA* gene has been identified. Similar to ADP1, BenM and CatM homologs are found in this organism, but genes encoding these regulators are separated by almost 1 Mb. in the chromosome (45, 48). The *catA* gene is located in close proximity to other *cat* genes and 1.6 Kb downstream of the divergently transcribed *catM* gene. Based on the location of *catM*, it is probable that CatM controls regulation of these *cat* genes including *catA*. BenM has been identified as the sole regulator of the *ben* genes, and activates transcription in response to benzoate and catechol only. No synergistic *ben* activation by BenM has been reported for PHEA-2 in the presence of benzoate and muconate (48).

Interestingly, multiple copies of *catA* genes in some *Acinetobacter* are the result of duplication events within the chromosome. These *catA* genes share low sequence similarities and encoded CatA enzymes with distinct properties (temperature stability, pH functionality, substrate reactivity, etc.). The rational of multiple copies for expression of catechol 1,2-dioxygenase remains unclear, but it could relate to the demand needed for this enzyme by the bacteria to rapidly metabolize a variety of aromatics through the catechol branch.

Synergistic activation and response to multiple effectors by other LTTRs. Thus far, BenM is the only transcriptional regulator known to have a synergistic response to dual effectors, which results in maximal transcriptional activation from two distinct loci (*benABCDE* and *catA*). Other LTTRs have been identified to respond to different effectors, but less is know about the synergistic-dependent transcriptional activation. Some of these regulators include MvfR, a LysR-type regulator from *Pseudomonas aeruginosa* involved in multiple quorum sensing-regulated virulence factors and signaling compounds. MvfR has been found to respond to 3,4-dihydroxy-2-heptylquinoline (PQS) and its precursor 4-hydroxy-2-heptylquinoline (HHQ) where PQS is dispensable for MvfR-dependent activation (44). In AlsR, from *Bacillus subtilis*, acetate or an acidic pH haven been proposed as effector ligands (11). CbnR, a LTTR from *Ralstonia eutropha* NH9, controls regulation of genes involve in 3-chlorobenzoate degradation in response to muconate, 2-chloro muconate and benzoate derivatives (26). NtdR, a regulator found in strains that are able to degrade nitro-substituted aromatic

compounds, has been identified to exhibit an inducer response to salicylate, 4-nitrobenzoate and benzoate (21).

A simultaneous response upon addition to dual inducers (salicylate and 4-nitrobenzoate) has been identified for DntR, a LysR-type regulator involved in regulation of genes for 2,4-dinitrotoluene and other nitro-substitute aromatics (12, 21, 38). Interestingly, in a truncated DntR crystal structure, salicylate binds to two distinct sites in the effector-binding domain of the regulator (12). Single mutations introduced to the secondary binding site affected the salicylate-inducible response, but the synergistic response to salicylate and 4-nitrobenzoate remained (12). These findings may indicate the presence of a third binding site to which 4-nitrobenzoate binds. Lack of a DntR structure bound to salicylate and 4-nitrobenzoate prevents determination of the synergistic scheme.

Concluding Remarks

In this study, *catA* regulation was explored to understand the regulatory role of two LysR-type paralogs, BenM and CatM. Despite functional and structural similarities, BenM and CatM control transcriptional activation of *catA* differently. CatM activates high *catA* transcription in response to muconate only. Muconate is the more effective inducer but only when CatM is the sole regulator. A BenM-dependent *catA* transcriptional activation is similar to *benA* activation. Under BenM-mediated *catA* expression, benzoate and muconate act synergistically to induce levels of *catA* transcription that is significantly higher than that achieved with equal concentrations of either inducer alone. This unusual *catA* transcriptional activation exhibited by BenM may permit a rapid system for integration of multiple metabolic signals. This rapid response

may prevent intracellular accumulation of toxic intermediates such as catechol and muconate that are generated during benzoate degradation. In addition, rapid generation of muconate might serve as a regulatory metabolite to repress genes of the protocatechuate branch during benzoate metabolism. This hierarchy in carbon preferences ensures minimal energy consumption and maximal conservation, which permits *A. baylyi* to thrive on a constantly changing environment by adapting its response to available sources of carbon.

Acknowledgments

We greatly thank Fenja Foster and Katherine Elliott for suggestions with RNA and 5' RACE experiments. Kim Brown and Nick Galloway helped with protein purification.

References

1. **Akakura R, Winans SC.** 2002a. Mutations in the *occQ* operator that decrease OccR-induced DNA bending do not cause constitutive promoter activity. J. Biol. Chem. **277:**15773-15780.
2. **Bleichrodt FS.** 2011. Analysis of regulatory mechanisms governing aromatic compound degradation in *Acinetobacter baylyi*. PhD. thesis. University of Ulm, Berlin, Germany.
3. **Bleichrodt FS, Fischer R, Gerischer UC.** 2010. The beta-ketoadipate pathway of *Acinetobacter baylyi* undergoes carbon catabolite repression, cross-regulation and vertical regulation, and is affected by Crc. Microbiology. **156:**1313-1322.
4. **Brzostowicz PC, Reams AB, Clark TJ, Neidle EL.** 2003. Transcriptional cross-regulation of the catechol and protocatechuate branches of the beta-ketoadipate pathway contributes to carbon source-dependent expression of the *Acinetobacter sp.* strain ADP1 *pobA* gene. Appl. Environ. Microbiol. **69:**1598-1606.
5. **Bundy BM.** Transcriptional Regulation o the *benABCDE* operon of *Acinetobacter* sp. ADP1: BenM-mediated synergistic induction in response to benzoate and *cis,cis*-muconate. Phd. Thesis. University of Georgia, Athens, GA.
6. **Bundy BM, Collier LS, Hoover TR, Neidle EL.** 2002. Synergistic transcriptional activation by one regulatory protein in response to two metabolites. Proc. Natl. Acad. Sci. U. S. A. **99:**7693-7698.
7. **Caposio P, Pessione E, Giuffrida G, Conti A, Landolfo S, Giunta C, Gribaudo G.** 2002. Cloning and characterization of two catechol 1,2-dioxygenase genes from *Acinetobacter radioresistens* S13. Res. Microbiol. **153:**69-74.

8. **Choi H, Kim S, Mukhopadhyay P, Cho S, Woo J, Storz G, Ryu SE.** 2001. Structural basis of the redox switch in the OxyR transcription factor. Cell. **105:**103-113.

9. **Collier LS.** 2000. Transcriptional regulation of benzoate degradation by BenM and CatM in *Acinetobacter* sp. strain ADP1. Phd. thesis. University of Georgia. Athens, GA.

10. **Collier LS, Gaines GL, 3rd, Neidle EL.** 1998. Regulation of benzoate degradation in *Acinetobacter* sp. strain ADP1 by BenM, a LysR-type transcriptional activator. J. Bacteriol. **180:**2493-2501.

11. **de Oliveira RR, Nicholson WL.** 2013. The LysR-type transcriptional regulator (LTTR) AlsR indirectly regulates expression of the *Bacillus subtilis bdhA* gene encoding 2,3-butanediol dehydrogenase. Appl. Micro. Biotech. **97:**7307-7316.

12. **Devesse L, Smirnova I, Lonneborg R, Kapp U, Brzezinski P, Leonard GA, Dian C.** 2011. Crystal structures of DntR inducer binding domains in complex with salicylate offer insights into the activation of LysR-type transcriptional regulators. Mol. Microbiol. **81:**354-367.

13. **Ezezika OC, Collier-Hyams LS, Dale HA, Burk AC, Neidle EL.** 2006. CatM regulation of the *benABCDE* operon: functional divergence of two LysR-type paralogs in *Acinetobacter baylyi* ADP1. Appl. Environ. Microbiol. **72:**1749-1758.

14. **Ezezika OC, Haddad S, Clark TJ, Neidle EL, Momany C.** 2007. Distinct effector-binding sites enable synergistic transcriptional activation by BenM, a LysR-type regulator. J. Mol. Biol. **367:**616-629.

15. **Fischer R, Bleichrodt FS, Gerischer UC.** 2008. Aromatic degradative pathways in *Acinetobacter baylyi* underlie carbon catabolite repression. Microbiology. **154:**3095-3103.

16. **Gaines GL, 3rd, Smith L, Neidle EL.** 1996. Novel nuclear magnetic resonance spectroscopy methods demonstrate preferential carbon source utilization by *Acinetobacter calcoaceticus*. J. Bacteriol. **178:**6833-6841.

17. **Jones RM, Williams PA.** 2003. Mutational analysis of the critical bases involved in activation of the AreR-regulated sigma54-dependent promoter in *Acinetobacter* sp. strain ADP1. Appl. Environ. Microbiol. **69:**5627-5635.

18. **Juni E, Janik A.** 1969. Transformation of *Acinetobacter calcoaceticus* (Bacterium anitratum). J. Bacteriol. **98:**281-288.

19. **Kim SI, Ha KS.** 1997a. Peptide mapping and amino acid sequencing of two catechol 1,2-dioxygenases (CD I1 and CD I2) from *Acinetobacter lwoffii* K24. Mol. Cells. **7:**635-640.

20. **Kim SI, Leem SH, Choi JS, Chung YH, Kim S, Park YM, Park YK, Lee YN, Ha KS.** 1997b. Cloning and characterization of two catA genes in *Acinetobacter lwoffii* K24. J. Bacteriol. **179:**5226-5231.

21. **Lonneborg R, Brzezinski P.** 2011. Factors that influence the response of the LysR type transcriptional regulators to aromatic compounds. BMC. Biochem. **12:**49.

22. **Maddocks SE, Oyston PC.** 2008. Structure and function of the LysR-type transcriptional regulator (LTTR) family proteins. Microbiology. **154:**3609-3623.

23. **Mazzoli R, Pessione E, Giuffrida MG, Fattori P, Barello C, Giunta C, Lindley ND.** 2007. Degradation of aromatic compounds by *Acinetobacter radioresistens* S13: growth characteristics on single substrates and mixtures. Arch. Microbiol. **188:**55-68.

24. **McFall SM, Chugani SA, Chakrabarty AM.** 1998. Transcriptional activation of the catechol and chlorocatechol operons: variations on a theme. Gene. **223:**257-267.

25. **Mrazek J, Xie S.** 2006. Pattern locator: a new tool for finding local sequence patterns in genomic DNA sequences. Bioinformatics **22:**3099-3100.

26. **Muraoka S, Okumura R, Ogawa N, Nonaka T, Miyashita K, Senda T.** 2003. Crystal structure of a full-length LysR-type transcriptional regulator, CbnR: unusual combination of two subunit forms and molecular bases for causing and changing DNA bend. J. Mol. Biol. **328:**555-566.

27. **Nakai C, Horiike K, Kuramitsu S, Kagamiyama H, Nozaki M.** 1990. Three isozymes of catechol 1,2-dioxygenase (pyrocatechase), alpha alpha, alpha beta, and beta beta, from *Pseudomonas arvilla* C-1. J. Biol. Chem. **265:**660-665.

28. **Neidle EL, Hartnett C, Bonitz S, Ornston LN.** 1988. DNA sequence of the *Acinetobacter calcoaceticus* catechol 1,2-dioxygenase I structural gene *catA:* evidence for evolutionary divergence of intradiol dioxygenases by acquisition of DNA sequence repetitions. J. Bacteriol. **170:**4874-4880.

29. **Neidle EL, Ornston LN.** 1986. Cloning and expression of *Acinetobacter calcoaceticus* catechol 1,2-dioxygenase structural gene *catA* in *Escherichia coli*. J. Bacteriol. **168:**815-820.

30. **Parsek MR, McFall SM, Shinabarger DL, Chakrabarty AM.** 1994. Interaction of two LysR-type regulatory proteins CatR and ClcR with heterologous promoters: functional and evolutionary implications. Proc. Natl. Acad. Sci. U. S. A. **91:**12393-12397.

31. **Parsek MR, Ye RW, Pun P, Chakrabarty AM.** 1994. Critical nucleotides in the interaction of a LysR-type regulator with its target promoter region. catBC promoter activation by CatR. J. Biol. Chem. **269:**11279-11284.

32. **Pessione E, Giuffrida MG, Mazzoli R, Caposio P, Landolfo S, Conti A, Giunta C, Gribaudo G.** 2001. The catechol 1,2 dioxygenase system of *Acinetobacter radioresistens*: isoenzymes, inductors and gene localisation. Biol. Chem. **382:**1253-1261.

33. **Porrua O, Lopez-Sanchez A, Platero AI, Santero E, Shingler V, Govantes F.** 2013. An A-tract at the AtzR binding site assists DNA binding, inducer-dependent repositioning and transcriptional activation of the P*atzDEF* promoter. Mol. Microbiol. **90:**72-87.

34. **Prentki P, Krisch HM.** 1984. In vitro insertional mutagenesis with a selectable DNA fragment. Gene. **29:**303-313.

35. **Romero-Arroyo CE, Schell MA, Gaines GL, 3rd, Neidle EL.** 1995. *catM* encodes a LysR-type transcriptional activator regulating catechol degradation in *Acinetobacter calcoaceticus*. J. Bacteriol. **177:**5891-5898.

36. **Sambrook J, Fritsch F, Maniatis T.** 1989. *Molecular cloning: a laboratory manual, 2nd ed.* Cold Spring Harbor Laboratory Press, Cold Spring Harbor, N.Y.

37. **Schell MA.** 1993. Molecular biology of the LysR family of transcriptional regulators. Annu. Rev. Microbiol. **47:**597-626.

38. **Smirnova IA, Dian C, Leonard GA, McSweeney S, Birse D, Brzezinski P.** 2004. Development of a bacterial biosensor for nitrotoluenes: the crystal structure of the transcriptional regulator DntR. J. Mol. Biol. **340:**405-418.

39. **Tover A, Zernant J, Chugani SA, Chakrabarty AM, Kivisaar M.** 2000. Critical nucleotides in the interaction of CatR with the *pheBA* promoter: conservation of the CatR-mediated regulation mechanisms between the *pheBA* and *catBCA* operons. Microbiology. **146:**173-183.

40. **Tumen-Velasquez MP, Bacon C, Laniohan NS, Neidle EL, Momany C.** 2014a. Engineering CatM, a LysR-type Transcriptional Regulator, to respond synergictically to two different effectors (manuscript in preparation).

41. **Tumen-Velasquez MP, Neidle EL, Momany C.** 2014b. Linker Helix provides more than Flexibility properties to CatM, a LysR-type Transcriptional Regulator in *Acinetobacter baylyi* strain ADP1. (manuscript in preparation).

42. **Vaneechoutte M, Young DM, Ornston LN, De Baere T, Nemec A, Van Der Reijden T, Carr E, Tjernberg I, Dijkshoorn L.** 2006. Naturally transformable *Acinetobacter* sp. strain ADP1 belongs to the newly described species *Acinetobacter baylyi*. Appl. Environ. Microbiol. **72:**932-936.

43. **Walsh TA, Ballou DP, Mayer R, Que L, Jr.** 1983. Rapid reaction studies on the oxygenation reactions of catechol dioxygenase. J. Biol. Chem. **258:**14422-14427.

44. **Xiao G, Deziel E, He J, Lepine F, Lesic B, Castonguay MH, Milot S, Tampakaki AP, Stachel SE, Rahme LG.** 2006. MvfR, a key *Pseudomonas*

aeruginosa pathogenicity LTTR-class regulatory protein, has dual ligands. Mol. Microbiol. **62:**1689-1699.

45. **Xu Y, Chen M, Zhang W, Lin M.** 2003. Genetic organization of genes encoding phenol hydroxylase, benzoate 1,2-dioxygenase alpha subunit and its regulatory proteins in *Acinetobacter calcoaceticus* PHEA-2. Curr. Microbiol. **46:**235-240.

46. **Yanisch-Perron C, Vieira J, Messing J.** 1985. Improved M13 phage cloning vectors and host strains: nucleotide sequences of the M13mp18 and pUC19 vectors. Gene. **33:**103-119.

47. **Yoon YH, Yun SH, Park SH, Seol SY, Leem SH, Kim SI.** 2007. Characterization of a new catechol branch of the beta-ketoadipate pathway induced for benzoate degradation in *Acinetobacter lwoffii* K24. Biochem. Biophys. Res. Commun. **360:**513-519.

48. **Zhan Y, Yu H, Yan Y, Chen M, Lu W, Li S, Peng Z, Zhang W, Ping S, Wang J, Lin M.** 2008. Genes involved in the benzoate catabolic pathway in *Acinetobacter calcoaceticus* PHEA-2. Curr. Microbiol. **57:**609-614.

CHAPTER 5

DISSERTATION SUMMARY

The studies presented in this dissertation have expanded understanding of transcriptional regulation of complex metabolic circuits involved in the degradation of naturally occurring aromatic compounds. To improve bioremediation strategies against harmful xenobiotic compounds, it is paramount to understand the regulatory scheme that governs the transcriptional activation of genes involve in aromatic compound metabolism. In these studies, transcriptional regulation is focused on two well-studied LysR-type transcriptional regulators (LTTR), the largest family of prokaryotic transcriptional regulators.

BenM and CatM are 59% identical and play overlapping roles in the regulation of genes involve in benzoate degradation. This similarity in function and structure was exploited in chapter 2 to understand the transcriptional regulatory differences of BenM and CatM at the *benABCDE* promoter. CatM was shown to activate *ben* genes in a synergistic fashion in response to muconate and benzoate. This synergy was recreated in CatM only when the BenM-DBD was introduced along with amino acid residues that directly interact with the carboxyl group of benzoate in BenM-EBD (Arg160 and Tyr293). This dual effector CatM-mediated activation was also observed at the *catBCIJFD* promoter, and it requires the BenM-DBD. Therefore the studies in this chapter reveal the essential interconnection of regulatory domains within the protein, where a sole domain does not dictate function.

Efforts to generate a benzoate responsive CatM led to the isolation of seven independent CatM variants that activate the *benACBDE* promoter and permit benzoate growth in the absence of BenM. Chapter 3 describes the characterization of variants with amino acid replacements at the linker helix portion of CatM. CatM[A78V], CatM[R84Q], and CatM[A86T] affected regulation differently at distinct promoters (*benA*, *catA* and *catB*). The CatM-mediated regulation by these linker helix variants demonstrated the importance of modulation and balance of transcriptional activation of multiple promoters for successful benzoate degradation. This studies lead to a proposed model for CatM-mediated regulation by these variants where muconate is the essential effector.

In chapter 4, transcriptional regulation of *catA* is assessed in detail. These studies demonstrated that BenM and CatM bind, recognize and activate the *catA* promoter. BenM and/or CatM activate muconate-inducible *catA* transcription. Nevertheless, BenM responds to benzoate and muconate in a synergistic fashion to activate maximal *catA* expression. These studies confirm that this synergistic activation by BenM is not isolated to one promoter region (*benABCDE*), and suggests that this type of unusual activation at the *catA* promoter is required to prevent accumulation of toxic metabolites from the pathway. In addition, this tightly controlled *catA* regulation by BenM and CatM may serve as another level of cross-regulation over the protocatechuate pathway where muconate acts as a regulatory metabolite that affects expression from genes of this branch. Collectively, this dissertation clarifies the regulatory differences and similarities by BenM and CatM, two LysR-type paralogs from *Acinetobacter baylyi* strain ADP1.

APPENDIX A

A NEW LYSR-TYPE TRANSCRIPTIONAL REGULATOR, LEUR, CONTROLS LEUCINE BIOSYNTHESIS IN *ACINETOBACTER BAYLYI* STRAIN ADP1*

---

* Melissa P. Tumen-Velasquez, K. T. Elliott, Cassandra Bartlett, Melesse Nune, Anna C. Karls, Ellen L. Neidle, and Cory Momany. To be submitted to the *Journal of Bacteriology*

Abstract

The LysR-type transcriptional regulator, LeuR controls transcriptional activation of genes involved in leucine biosynthesis in *Acinetobacter baylyi* strain ADP1. In this report, we described that deletion or disruption of this transcriptional regulator results in derepression of the *leuC* gene. Quantitative reverse transcriptase polymerase chain reaction showed that in the absence of this regulator, *leuC* expression increases with or without addition of leucine. However, *leuC* derepression is observed in the wild-type strain only when intracellular levels of leucine are low. Thus, in *A. baylyi* LeuR acts as repressor for the *leuC* gene. In addition, reverse transcriptase experiments reveal that *leuC* is transcribed as part of an operon that includes *leuD* and *leuB* called the *leu* operon. Bioinformatic analysis reveal LeuR and LeuO, a well-studied LysR-type global regulator involved in leucine regulation found in many bacteria, to share 19% of amino acid sequence identity. The regulatory scheme carried out by these proteins in leucine biosynthesis is different. Here, we described the role of LeuR in leucine biosynthetic pathway in ADP1.

Introduction

LysR-type transcriptional regulators (LTTRs) comprise the largest family of homologous regulatory proteins in prokaryotes (17, 19, 24), where several individual genomes encoded more than 100 distinct members. In *Acinetobacter baylyi* strain ADP1, there are 44 predicted LysR-type regulators with proposed roles involved in many cellular functions (1, 21, 28). The genetic malleability make ADP1 an ideal bacterial model for studying LTTRs. Bioinformatic analysis based on sequences of LysR-type regulators and other considered general features predicted an open reading frame (ORF), ACIAD0461, hereafter named *leuR*, to encoded a transcriptional regulator that may have a role in leucine biosynthesis in *A. baylyi*. (7). As described in this study, we demonstrated that LeuR acts as a transcriptional regulator to suppress transcriptional activation of genes involved in leucine biosynthesis.

In *A. baylyi,* leucine biosynthesis branches out from the valine biosynthetic pathway at the end of 2-oxoisovalerate generation, a metabolite from the this pathway. This intermediate serves as a precursor for the further synthesis of leucine by the *leu* genes (Fig. A.1.A). The gene product of *leuA*, 2-isopropylmalate synthase converts 2-oxoisovalerate to (2*S*)-2-isopropylmalate, hereafter referred as IPM. IPM is then converted 4-methyl-2-oxopentanoate by the gene products of *leuCDB.* This last intermediate is converted to L-leucine by the reaction with L-glutamate and the branch-chain amino acid aminotransferase enzyme. This enzyme, encoded by *ilvE* is also needed in the final steps of valine and isoleucine synthesis. Despite studies of leucine biosynthesis in other organisms, transcriptional regulation of genes involved in this biosynthetic pathway remains unclear in ADP1. As described previously, upstream of

Figure A.1. (A) Valine and leucine biosynthetic pathway in *Acinetobacter baylyi* strain ADP1. Enzymes encoded by the *ilv* and *leu* genes for the conversion of 2-pyruvate to L-leucine and L-valine. Proteins in black boxes may be under LeuR regulation. (*) Slightly repressed by LeuR in the presence of leucine. Protein description is included for all genes described in this report. (Red box**) Metabolic intermediate used for further electrophoretic mobility shift assays by LeuR on *leuC* promoter. Pathway adapted from BioCyc website {Caspi, 2010 #613}. **(B)** Chromosomal organization of genes involve in leucine biosynthesis in *A. baylyi* are displayed (solid black arrows). ACIAD0461 (renamed *leuR*) refers to the unique numeric identifier according to the genome sequence annotation described in Barbe *et al.,* 2004 {Barbe, 2004 #316}. *leuR* is located upstream of ACIAD0462 and a *leuC* and transcribed divergently. *leuA* is located about 50 kbp away from *leuC* in ADP1 chromosome.

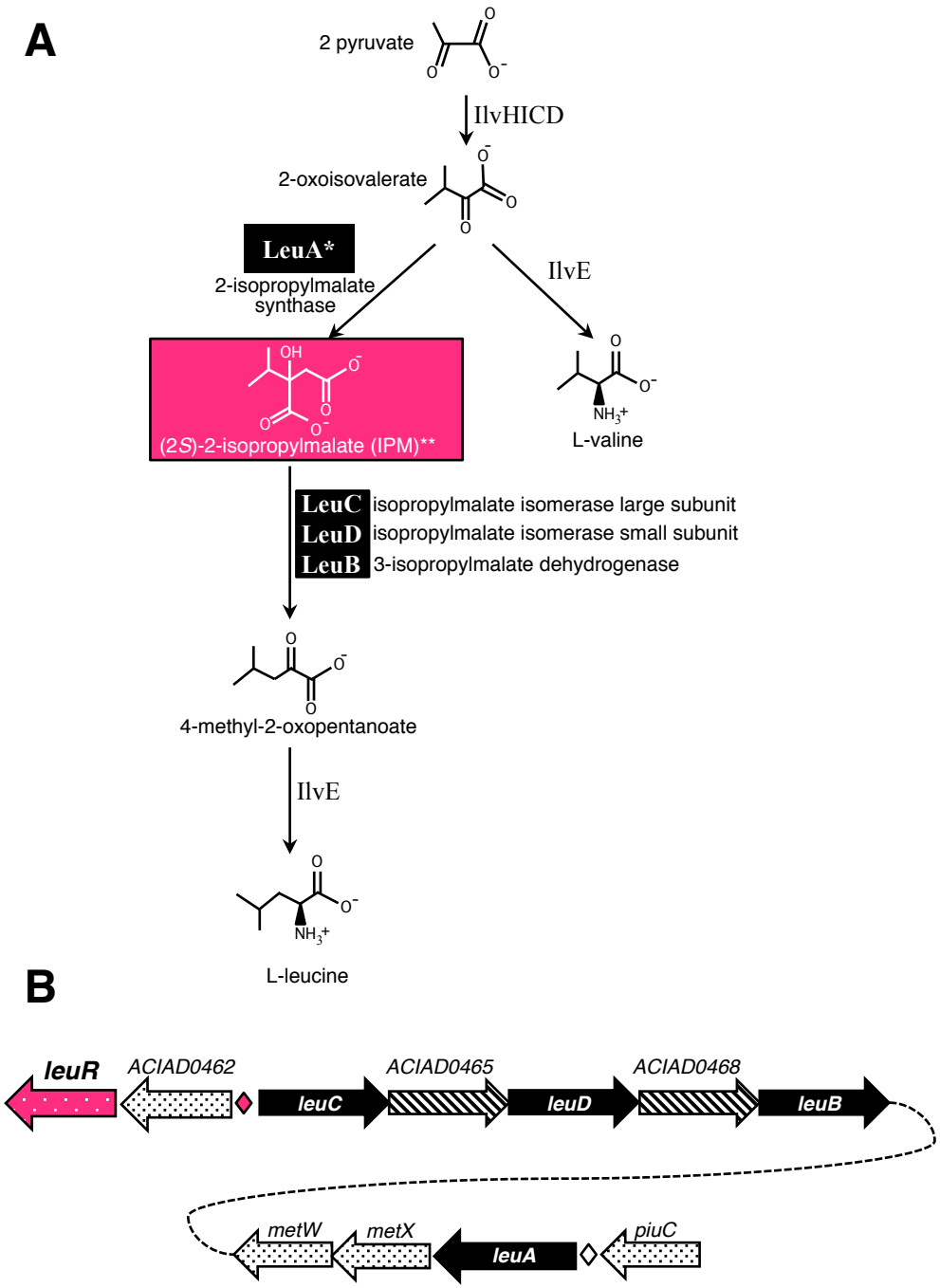
A
2 pyruvate
IlvHICD
2-oxoisovalerate
LeuA*
2-isopropylmalate synthase
IlvE
(2S)-2-isopropylmalate (IPM)**
L-valine
LeuC isopropylmalate isomerase large subunit
LeuD isopropylmalate isomerase small subunit
LeuB 3-isopropylmalate dehydrogenase
4-methyl-2-oxopentanoate
IlvE
L-leucine
B
leuR
ACIAD0462
leuC
ACIAD0465
leuD
ACIAD0468
leuB
metW
metX
leuA
piuC

leuC, lays an open reading frame predicted to encode a LysR-type regulator (Figure A.1.B) (7). This ORF, *leuR,* appears to be transcribed divergently from a cluster of genes involve in leucine generation. Based on the location this ORF, it was a candidate in the regulation of genes involved in leucine biosynthesis. In this report, we sought to assess the functionality of this gene by genetic approaches, including complete chromosomal deletions and determining phenotypes of resulting mutants. These studies help to understand LysR-type transcriptional regulation where LeuR acts as a repressor for leucine biosynthesis in *A. baylyi*.

Materials And Methods

Bacterial strains and growth conditions. *Escherichia coli* strains were grown on LB (23) and *Acinetobacter baylyi* strains were grown on minimal medium at 37 °C (28). In addition, *A. baylyi* strains were grown in minimal medium with succinate (10 mM) as the carbon source. When indicated 0.3 mM isoleucine, leucine and valine was added to the medium. *E. coli* DH5α cells (Invitrogen) and XL1-Blue cells (Agilent Technologies) were used as plasmid host. Antibiotics were added as needed at the final concentrations: ampicillin, 150 μg/ml, kanamycin, 25 μg/ml, spectinomycin, 13 μg/ml and streptomycin, 13 μg/ml.

Plasmid construction: As described next, overlapping extension PCR generated constructs for the deletion of ACIAD0461 (Δ*ACIAD0461* and Δ*ACIAD0461::sacB*-Kan), and high fidelity polymerase (Roche) was used to minimize undesired mutations. The ADP1 chromosome was used as template in PCR reactions. Oligos were designed to flank an in-frame deletion of ACIAD0461 and introduced an *XhoI* site between the start

and stop codons of this fragment to aid the introduction of the *sacB*-Kan^R counterselectable marker (Table A.2). In addition, oligonucleotides incorporated sequences encoding *BamHI* and *PstI* sites at each end respectivately. The resultant PCR product was gel extracted (Zymo Research) and digested with the aforementioned restriction enzymes. Digestions were gel extracted and ligated to pUC19 digested with *BamHI* and *PstI* respectively. Blue and white screening was used to identify clones with inserts in pUC19. The resulting plasmid pBAC1031 was confirmed by restriction digest. To construct pBAC1049, pRMJ1 was digested with *SalI* to isolate *sacB*-Kan marker. The fragment was gel extracted and ligated to pBAC1031 digested with *XhoI.* For the construction of pET-LeuR, expression plasmid for LeuR protein purification, a seamless cloning strategy was used. Briefly, expression vector pET28b(+).SapKO-CH.BspQ1 with two BspQ1 restriction sites oriented between the start codon and the poly-histidine at its 3' end was used (2). Primers ACIAD0461-F and ACIAD0461-R were used to amplify *leuR* from ADP1 chromosomal DNA by PCR (Table A.2). High fidelity polymerase (ROCHE) used for PCR reaction. The reaction was cleaned and eluted in 20 µl (Zymo Research). A digest reaction with BspQ1 was set up as: 1 µl of pET28b(+).SapKO-CH.BspQ1; 2 µl cleaned *leuR* PCR; 1 µl BspQ1; 3 µl 10x Fast-Link ligation buffer (Epicenter) in a total reaction of 23 µl. Reaction was incubated at 50 °C for one hour. Digest reaction was cooled down to room temperature for 30 minutes. Immediately a ligation reaction was set up with the following reagents: 11.5 µl of digest reaction; 1.5 µl 10 mM ATP; 1µl Fast-Link DNA ligase (Epicenter) in a 15 µl total reaction. Mixture was incubated at room temperature for 30 minutes following an incubation at 50 °C for one hour. 1:10 dilution of the ligation reaction was used to transform XL1-Blue cells

Table A.1. Strains and plasmids used in this study.

Strains used in this study		
***A. baylyi* Strain**	**Relevant characteristics[a]**	**Source**
ADP1	Wild type (BD413)	(15)
ACN1259	Δ*leuR*::*sacB*-Km^R*51259*	This study
ACN1279	Δ*leuR 51279*	This study
Plasmids used in this study		
Plasmid	**Relevant characteristics**	**Source**
pUC19	Ap^R; cloning vector	(29)
pET28b(+).SapKO-CH.BspQ1	Km^R; T7 expression vector with BspQ1 site	(2)
pRMJ1	Ap^R, Km^R, *sacB*-Km^R cassette	(14)
pBAC1031	Ap^R, Km^R; complete deletion Δ*leuR*::*sacB*-Km^R (460,444-459,567)[b]	This study
pBAC1049	Ap^R; complete deletion Δ*leuR* (460,444-459,567)[b]	This study
pET-LeuR	Km^R; LeuR-His expression vector	This study

[a]Ap^R, ampicillin resistant; Sm^R, streptomycin resistant; Sp^R, spectinomycin resistant; Km^R, kanamycin resistant; ΩS, omega cassette containing Sm^R Sp^R (Prentki and Krisch, 1994); *sacB*-Km^R, dual selection cassette containing a counterselectable marker and kanamycin resistant cassette (Jones and Williams 2003).
[b]Position in the ADP1 genome sequence according to GenBanK entry CR543861.

by electroporation. Transformation was plated on LB plates with 25 mg/ml Kanamycin. Restriction digests with *StuI* and *EcoRV* were used to evaluate resulting transformants. Plasmid preps with expected restriction size cuts were sent for sequencing analysis (Genewiz). Plasmid was named pET-LeuR.

Generation of *A. baylyi* strains by allelic exchange. Plasmid-borne alleles were introduced in the chromosome by methods that exploit the high efficiency of natural transformation of *A. baylyi.* To aid the introduction of Δ*leuR*, a counter-selectable *sacB* marker with Δ*leuR* allele was first introduced in the chromosome. Plasmid pBAC1049 was digested with *AatII* to transform ADP1. Selection for the inability to grow in the presence of sucrose as carbon source and Kanamycin resistance was tested. Resulting strain, ACN1259 (Δ*leuR*::*sacB*-Kan) was then transformed with pBAC1031 digested with *PstI.* Strain ACN1279 was tested for sucrose growth and kanamycin sensitivity. In the recipient strain, allele Δ*leuR* has replaced the *sacB* counterselectable marker in the chromosome. To test for changes in phenotype in leucine biosynthesis, ACN1279 was also patched onto a minimal media plate containing 0.3 mM of isoleucine, leucine and valine.

RNA purification. Cells were grown in minimal medium with succinate (10 mM) with no inducer or 0.3 mM isoleucine, leucine and valine. Growth was measured by optical density (OD_{600}) and turbidometrically with a Klett-Summerson colorimeter. Cells were harvested at two time points in the exponential phase, early and late (OD_{600} 0.2-0.3 and 0.7-0.9). Cells were pelleted down in 50 ml conical tubes and immediately frozen with -

70 °C Ethanol to prevent RNA degradation. Total RNA was extracted by the TRI Reagent method (Molecular Research Center). RNA samples were treated with RQ1 DNase I (Promega) until no DNA contamination was detected by PCR. The quality and quantity of the extracted RNA were determined spectrophotometrically using the absorbance at 260 nm (Beckman DU 640).

cDNA synthesis from total RNA. For samples to be used for real-time PCR, the SuperScript III First-Strand Synthesis for RT-PCR was used (Invitrogen) and random hexamers as primers. Approximately, 1 μg of total RNA was used for cDNA synthesis. Products were analyzed on 0.8% agarose gel and stored at -20 °C. For samples to be used in other experiments, 2 μg of total RNA isolated from induced ACN1279 was used. To determine the *leu* operon structure, gene-specific primers (GSP) were designed for cDNA synthesis. RNA and primers were combined in a final volume of 17 μl at 75 °C for 5 minutes to allow primer annealing. M-MuLV reverse transcriptase (NEB) was added to the reaction following incubation at 25 °C for 5 minutes, 42 ° C for 60 minutes and 90 °C for 10 minutes. Reactions with M-MuLV omitted were used as controls to detect DNA contamination.

5' RACE (Rapid Amplification from cDNA ends). For this experiment, 2 μg of RNA from induced strain ACN1279 and 2.5 ρmoles of GSP-1 leuC or GSP1-leuA (Table A.2) were combined into 15.5 μl total volume reaction. The protocol for the 5'RACE System (Invitrogen) was followed. About 20% of the final reaction was used for PCR analysis. Primers GSP-3 leuC or GSP2-2 leuA and 5' RACE Abridged Anchor Primer (Table A.2)

along with LongAmp *Taq* DNA polymerase were used for 5' RACE product amplification. The reaction was performed with the following PCR settings: 94 °C for 1 minute, 55 °C for 1 minute, 65 °C for 1 minutes for 30 cycles. PCR products were analyzed on 2% agarose gel and cleaned with DNA clean and concentration kit (Zymo Research). Cleaned PCR products were cloned using the TOPO® TA cloning Kit (Invitrogen). As described in the manufacturing manual, 5 µl of cleaned PCR sample, 1 µl of salt solution and 1 µl TOPO® TA vector were combined and gently mixed. The reaction was incubated at room temperature for 10 minutes. The reaction was used to transform chemically competent DH5α *E.coli* cells. Blue and white screening was used to identify clones with desired insert. Clones were also screened by restriction digest with *XhoI* and *NcoI.* Resulting plasmids were sent for sequencing analysis to determine the start site of *leuC* and *leuA*.

Quantitative reverse transcriptase PCR (qRT-PCR). cDNA generated with random hexamers from ADP1 or ACN1279 was used for these experiments. Primer-probes for *rpoA*, *leuC* and *leuA* were used and designed with PrimerExpress software (Applied Biosystems) (Table A.2). The *rpoA* probes were used as internal control to evaluate the amount of *leuC* and *leuA* transcripts. Quantitative RT-PCR were performed in StepOnePlus™ Real-Time PCR systems (Applied Biosystems). Each reaction was carried out in a total volume of 20 µl on an 96-well optical reaction plate (Applied Biosystems) containing 10 µl of SYBR® Green (Applied Biosystems), 1 µl of cDNA and two gene-specific primers at a final concentration of 0.2 mM each. To quantify targets,

Table A.2. Oligonucleotide Primers used in this study

Primer	Sequence (5'- 3')	Restricition site
ACIAD0461-F	GG**GCTCTTC**GATGAATCTTGCTGCGTTTGAAG	***BspQI***
ACIAD0461-R	CA**GCTCTTC**AGTGAAGTGATTCAGTGAGCGTTG	***BspQI***
0461-SOE1-BamHI	TAGTTA**GGATCC**TGGACTGGGTATCGTATTCTG	***BamHI***
0461-SOE2-XhoI	ATTGATGAAATTGGTGTTGATTTA**CTCGAG**CATAATTTAAATCCAATTTCTCAATGT	***XhoI***
0461-SOE3-XhoI	ACATTGAGAAATTGGATTTAAATTATG**CTCGAG**TAAATCAACACCAATTTCATCAAT	***XhoI***
0461-SOE4-PstI	GATCGA**CTGCAG**AATCATAGTGTTTGTCATCAAGAT	***PstI***
0461-FOR	ACCATCCTCACAGACCTATACC	
0461-REV	AAACCGACCAGCCCAATC	
leuAfor	TGCCAACTCTCCAACTTTCC	
leuArev	TCCCAGATTTCAGTCACAGC	
leuCfor	AGGTCGTGAAAGGTCGTAAAG	
leuCrev	TTGAGGTCGAAGCACAGTG	
GSP1-leuC	CGCCAAACAACCAAAAGC	
GSP2-leuC	GTTATCATCTAGCGTCTGAACC	
GSP3-leuC	GGTGTCGCGATATTGGCATTTAGA	
RT-leuC	CAGTCCAATGGAGCATGACG	
GSP1-leuB	GCCAAGTAAAATCGCATCTG	
GSP2-leuB	CACTTGTAACGGCAGGATAGG	
GSP1-0465	GAATCAACACAGGAACTTTACCAG	
GSP2-0465	CGAGACTTCGTATCTGGTTGATC	
RT-0465	ACATCTCCTACGATGCAGGC	
GSP1-leuD	ACCATATTCATTTAATGCCCAAG	
GSP2-leuD	GGCTTGAACCACAACCAAAGT	
RT-leuD	TTGGATGAAGAGACTGTTGATCA	
GSP1-0468	GTGGTGTTAATCCGCTCAAA	
GSP2-0468	GCATTTGAACTCAGACCAGTTTC	
RT-0468	AGCACAGCAGTATGAGC	
RT-leuC-2	CAAGCAGAGCAAGAAGGTTTG	
GSP1-leuA	CTCAACGCCGACATTTAAAAC	
GSP2-leuA	CGCGTGCCTGTACCAATACT	
GSP3-leuA	CGGTACTCATCCAGATGGGC	

RT-leuA	GCCCATCTGGATGAGTACCG	
ACIAD0461-P1F	TGGGCTGTATTGGATTCTGC	
ACIAD0461-P1R	TGGTCACTTCATGCAATAAATG	
ACIADLeuA-P1F	ATGGGCGCTTTGGTAATTTC	
ACIADLeuA-P1R	GATGAAACTGTACGTAGCTTGC	
rpoAfor	GGTTGAAGTTGAAATAGAAGGCG	
rpoArev	CATAGCCACGACCTTGAGATAC.	

rpoA, *leuC* and *leuA* standard curves were prepared and ADP1 genomic DNA was used as template for qPCR (12.5 ng to 0.02 ng). A non-template control was used per primer set. Melting curve analysis verified that each reaction contained a single PCR product. *leuC* and *leuA* expression levels were normalized to transcripts of the internal control *rpoA*.

Purification of LeuR: Plasmid pET-LeuR was used to express full-length protein LeuR-His with C-terminal hexahistidine tag. The plasmid was transform into *E.coli* BL21-RIPL (DE3). Transformants were grown to stationary phase and subcultured into an autoinduction medium described previously (27). Approximately 4-5 g of cell pellet was obtained per 0.5 L of culture. Pellets were harvested from cultures and suspended in 50 mL binding buffer [20 mM Tris, 0.5 M NaCl, 25 mM Imidazole, 10% glycerol and 10 mM β-mercaptoethanol (BME) (pH 8.0)]. A chilled (4 °C) French pressure system was used to lyse the cells at 15, 000 psi. This step was repeated at least three times to maximize lysing of cells. Cell lysates were centrifuged at 60,000g for 30 minutes at 4°C. Resultant supernatant was applied to a nickel-charged 5-mL HiTrap™ metal-chelating column (GE Healthcare Life Sciences). Purification was performed at room temperature using an ÄKTA (Pharmacia) system. The protein was eluted with a linear buffer gradient at 3 mL/min with the following elution buffer [20 mM Tris, 0.5 M NaCl, 0.5 M Imidazole, 10% glycerol, and 10 mM BME (pH 8.0)]. Purified protein fractions were pooled and extensively dialyze against 20 mM Tris, 1 mM EDTA, 25 mM Imidazole, 10% glycerol, 10 mM BME (pH 8.0). Dialyzed protein was passed through a 5-mL HiTrap™ Q FF anion-exchange column (GE Healthcare Life Sciences) equilibrated with the following buffer [20 mM Tris, 1 mM EDTA, 10 mM BME (pH 8.0)]. Desalted

protein was eluted with Q elution buffer [20 mM Tris, 0.5 M NaCl, 1 mM EDTA, 10 mM BME (pH 8.0)]. Protein fractions were pooled and dialyzed against 20 mM Tris, 1 mM EDTA, 25 mM Imidazole, and 10 mM BME (pH 8.0). Protein was froze with liquied nitrogen and stored at -80 C.

Electrophoretic mobility shift assay. DNA fragments containing the *leuC* and *leuA* promoters were generated by PCR. For the *leuC,* primer set ACIAD0461-P1F (TGGGCTGTATTGGATTCTGC) and ACIAD0461-P1R (TGGTCACTTCATGCAATAAATG) was used to amplify the promoter region, and it generated an amplicon of 633 base pairs. The *leuA* primer set, ACIADLeuA-P1F (ATGGGCGCTTTGGTAATTTC) and ACIADLeuA-P1R (GATGAAACTGTACGTAGCTTGC) generated an amplicon of 659 bp. Different concentrations of LeuR (20 nM – 2 nM) were used in the reactions. The corresponding protein was incubated with DNA (5 nM) at 37 °C for one hour with or without 5 mM isoleucine, 5 mM leucine, 5 mM valine and/or 0.5 mM (2s)-2-isopropylmalic acid (IPM). The binding reaction (10 μl total volume) was carried out in the following binding buffer: 80 mM Tris-acetate (pH 8.0), 100 mM potassium acetate, 25 mM ammonium acetate, 5 mM magnesium acetate, 0.1 mM EDTA, 1 mM dithiothreitol, 1 mM calcium chloride, and 50 μg/ml bovine serum albumin (11). DNA-protein samples were resolved by electrophoresis in 6% polyacrylamide gels. Before samples were loaded onto polyacrylamide gels, loading dye was added to the wells of polyacrylamide gel and the gels were pre-runned in 1 X TAE with inducers when indicated for 40 minutes at 180 volts. Following this step, DNA-protein complexes were loaded onto polyacrylamide

gels. Electrophoresis was performed with 1 X TAE and inducers when indicated for 1 hour at 185 volts. Gels were stained with 2 X SYBR-Green for 30 minutes in the dark.

Results

Deletion of the gene encoding LeuR yielded an unexpected phenotype. As described previously, general features and sequences of LTTRs were considered to predict the functions of the 44 open reading frames likely to encoded LysR-type regulators in *A. baylyi* (7). Based on extensive metabolic pathway database and genome analysis conducted, LeuR was predicted to be a good candidate for regulation of genes involved in leucine biosynthesis. This gene is divergently transcribed and located upstream of a set of genes involve in the leucine pathway (Fig A.1.B). To test this prediction and begin assessing the function of this putative regulator, *leuR* was deleted from the *A. baylyi* chromosome. A deletion of this gene did not generate a leucine auxotroph, and strain ACN1279 was able to grow well on regular minimal medium with similar growth rates as the wild type strain. Since LeuR has been predicted to activate the genes of the leucine pathway, the unexpected phenotype of the *ΔleuR* mutant strain suggests that LeuR may be playing a different role in regulation in this pathway than as a transcriptional activator.

To determine which genes may fall under the LeuR regulon, total RNA was isolated from ADP1 and ACN1279 grown in the presence or absence of leucine. Two genes were chosen as targets for LeuR regulation, *leuC* and *leuA*. *leuC* encodes the isopropylmalate isomerase, an enzyme that carries out the conversion of (2*S*)-2-isopropylomalate to (2*R,*3*S*)-3-isopropylmalate in the leucine biosynthesis pathway (Figure A.1). In addition, *leuC* is the first gene in a cluster of genes encoding enzymes

involved in leucine biosynthesis that is located downstream the *leuR* gene. *leuA* is not located immediately close to *leuR* and *leuC.* However, this gene encodes, 2-isopropylmalate synthase, which converts 2-oxoidovalerate to (2*S*)-2-isopropylomalate, a crucial step needed for valine and leucine synthesis in *A. baylyi*. In addition, the resulting product of this reaction, (2*S*)-2-isopropylomalate, serves as the substrate for the following step carried out by the *leuC* gene product. Semiquantitative RT-PCR revealed that both genes are transcribed in ADP1 and in the *ΔleuR* mutant, ACN1279. Based on the lack of auxotrophy for leucine and the presence of transcripts of *leuC* and *leuA* observed in ACN1279*,* LeuR is not serving as an activator in leucine biosynthesis.

LeuR acts as a repressor in *A. baylyi.* The chosen target genes for LeuR-mediated regulation, *leuC* and *leuA,* were transcribed in both wild type and ACN1279. However, the intensity of RT-PCR products from each strain varied (data not shown). These differences became more evident with RT-PCR results from strains grown in the absence of leucine. The amounts of *leuC* transcripts were similar for the *ΔleuR* mutant strain grown with or without leucine, which may indicate that in this background addition of leucine does not affect transcription of this gene. Nevertheless, *leuC* transcript levels decreased when ADP1 was grown without leucine and are almost undetectable in the presence of leucine. This indicates that the increased intracellular leucine levels directly affect *leuC* transcript quantities. Since LeuR is still present in this background, it is safe to assume that this protein may be acting as a transcriptional repressor for *leuC* expression in the presence of leucine. Thus, LeuR may downregulate the generation of leucine when levels of this amino acid is increased in the cell. RT-PCR results from *leuA*

were not as evident since transcript levels were low in all examined conditions. Thus, it is not clear whether LeuR acts as a repressor at this locus as well.

qRT-PCR confirms that LeuR acts as a repressor of *leuC* in the presence of leucine. RT-PCR experiments showed that LeuR might repress *leuC* expression. Results with *leuA* were less evident than those for *leuC*. To determine whether LeuR represses *leuC* and *leuA* transcriptional activation, quantitative RT-PCR was performed. On RNA isolated from ACN1279, *leuC* transcript levels are increased about 5-fold relative to ADP1 (Figure A.2.A). RNA isolated from ADP1 grown with leucine shows that *leuC* transcript levels are low similar to those of the semi-quantitative RT-PCR results described above. Results for *leuA* are less clear, but transcript levels are 2-fold higher in the absence of LeuR (Fig. A.2.A).

To determine whether elevated levels of leucine may be causing repression by LeuR at *leuC* and *leuA*, RNA was isolated at early exponential phase (OD_{600} 0.2-0.3) from ADP1 grown with and without leucine. At this stage, levels of leucine are expected to be lower in the cell. *leuC* transcript levels are repressed only in the presence of leucine (Figure A.2.B). Despite the presence of LeuR in this background, *leuC* transcript levels are higher when grown on succinate as the sole carbon source. Thus, high intracellular levels of this amino acid may turn off its own biosynthetic pathway via LeuR-mediated repression on *leuC.* For *leuA,* the effect in transcript levels without leucine is not as evident. Based on these results, it is unclear to determine the *leuA*-mediated transcription by LeuR.

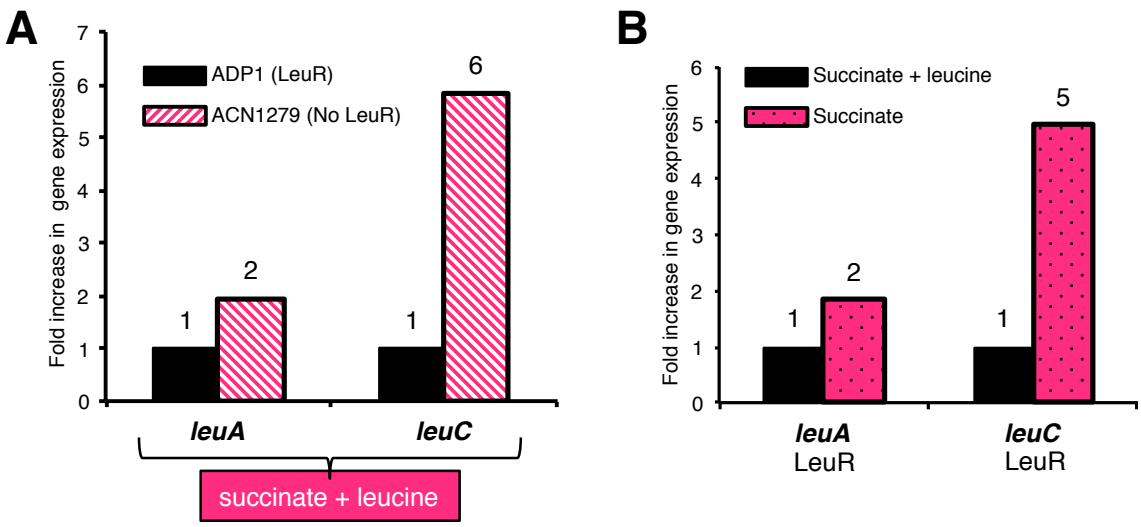

Figure A.2. Quantitative RT-PCR of *leuC* and *leuA*. (A) *leuC* and *leuA* transcript levels from total RNA isolated in the presence (ADP1) or absence of LeuR (ACN1279). Cells were grown on minimal medium with 0.3 mM leucine. RNA was immediately isolated when cultures reached late exponential phase (OD_{600} 0.8). **(B)** *leuC* and *leuA* transcript levels from total RNA isolated in the presence or absence of leucine. LeuR is present under both conditions. RNA was isolated when cultures reached early exponential phase (OD_{600} 0.2). Graph represents combined data from two independent biological replicates. Melting curve analysis verified that each reaction contained a single PCR product. *leuC* and *leuA* expression levels were normalized to transcripts of the internal control *rpoA*. Standard deviations were within 15% of the average value.

Determining the transcriptional start site of *leuC* and LeuR binding properties at the *leuC* promoter. As described above, *leuC* is a clear target for LeuR-mediated regulation. To begin assessing LeuR-mediated regulation at this locus, the intergenic region upstream of *leuC* was evaluated. The transcriptional start site of *leuC* was determined as described previously in materials and methods and it was found to be 38 nucleotides away from *leuC* start codon (Fig A.3.A). With this information, a perfect -10 region was identified along with a weak -35 region. A binding site with the T-N_{11}-A element to which LysR-type regulators are proposed to bind was found by the pattern locator program 55 nucleotides away the *leuC* transcriptional start site (Fig A.3.A) (20). Other binding sites with the T-N_{11}-A element were also observed closer to the transcriptional start site (Fig A.3.A, not underline).

Since a putative LeuR binding site was found for the *leuC* promoter, electrophoretic mobility shift assays (EMSA) were performed to determine the validity of this prediction. The DNA region containing the *leuC* promoter was amplified by PCR. The LeuR protein was purified as described previously. The promoter region was incubated with different concentrations of full-length LeuR (Fig. A.4). In the absence of leucine, a shift was observed as LeuR concentration increased. Thus, LeuR is probably binding to any of the putative T-N_{11}-A binding sites found in this promoter. LeuR binds to the *leuC* promoter region even at low protein concentrations (40 nM), which reflects its relative high binding affinity for this promoter. Surprisingly, addition of leucine to the reaction did not change the binding pattern of LeuR at this promoter (data not shown). Since the presence of leucine repressed *leuC* expression drastically, it unclear

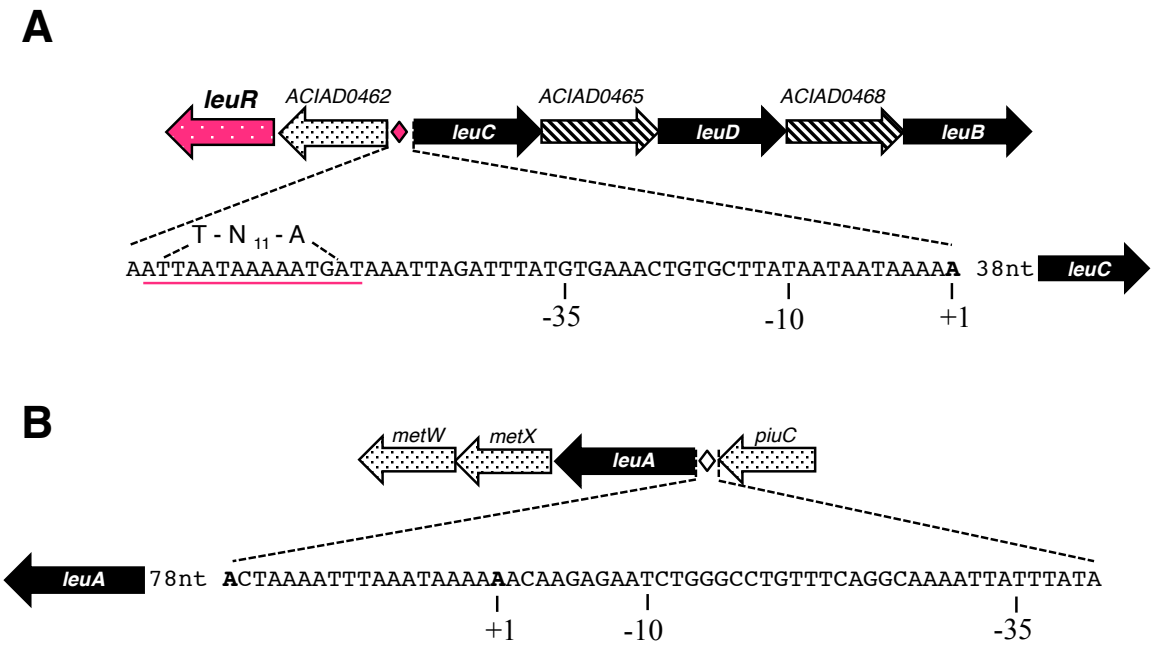

Figure A.3. Transcriptional start sites of *leuC* and *leuA* by 5'RACE. Expansion of intergenic region located upstream the *leuC* and *leuA*. +1 sites are mapped for both genes. -35 and -10 sites are also indicated for *leuC* and *leuA*. Underline sequence indicates a binding site with the T-N $_{11}$-A predicted by the Pattern locator program (Mrazek *et al.,* 2006) in the *leuC* operon.

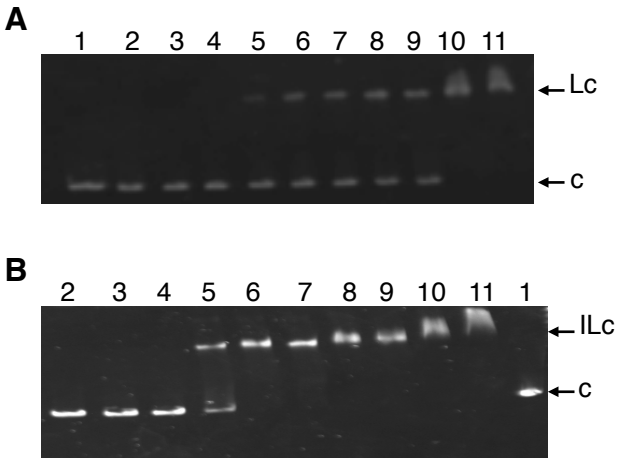

Figure A.4. Electrophoretic mobility shift assays of LeuR with the *leuC* promoter region. DNA probe (5 nM) incubated with different concentrations of LeuR as follows: **1.** DNA only. **2.** 5 nM, **3.** 10 nM, **4.** 20 nM, **5.** 40 nM, **6.** 80 nM, **7.** 160 nM, **8.** 200 nM, **9.** 240 nM, **10.** 320 nM, **11.** 640 nM **(A)** without (2*s*)-2-Isopropylmalate (IPM). **(B)** In the presence of 5 nM IPM. All samples were incubated at 37 °C for one hour. Samples were directly subjected to electrophoresis on a 6% polyacrylamide gel. C, free DNA; Lc, LeuR-*leuC* complexes; Ilc, LeuR-IPM-*leuC* complexes.

why the presence of leucine did not induce a conformational change for the LeuR-*leuC* complexes. These results indicate that leucine may not act as the effector molecule for LeuR-mediated regulation. Thus, it is possible an intermediate molecule from the leucine biosynthetic pathway is acting as an effector molecule instead of leucine.

In the leucine pathway, (2*S*)-2-isopropylomalate (IPM) is the substrate for the *leuC* product and may play a role as a repressor molecule. When IPM was added to the EMSA reactions, the LeuR binding to *leuC* changed drastically (Figure A.4.B). Clearly, the binding affinity of LeuR for the *leuC* promoter increases in the presence of IPM. These findings suggest the accumulation of IPM in the cell may induce conformational changes in LeuR resulting in *leuC* repression.

In the case of *leuA,* transcriptional start site was also mapped (Fig. A.3.B). Nevertheless, no clear LeuR binding sites were observed for this promoter. EMSA experiments revealed that LeuR did not bind the *leuA* promoter region in any case (with or without leucine and IPM).

Characterizing the *leu* operon. Bioinformatics analysis of *leuC* indicates that this gene may be co-transcribed with *leuD*, another gene involve in leucine biosynthesis. Figure. A.1.B shows the organization of these genes in the *A. baylyi* chromosome. *leuB*, a gene that encodes 3-isopropylmalate dehydrogenase, an enzyme that carries out a crucial step in the leucine pathway is located downstream *leuD.* It is a possibility that all these genes, including two genes of unknown function (ACIAD0465 and ACIAD0468) may form an operon. RT-PCR was done to characterize this region, and gene-specific primers

Figure A.5. Operon structure of *leu* genes by RT-PCR analysis. (A) location of designed primers (Table A.2) within *leuC-leuB* genes used to determine whether these genes are present as one transcript. Expected PCR product sizes are indicated and labeled A, B, C, D, E respectively. **(B)** RT-PCR results using primers shown in A. **(C)** RT-PCR results using primers within *rpoA* gene that resulted in a 300 bp product. In both B and C, results from RT-PCR using RNA from ACN1279 (*ΔleuR*) are shown. Control reactions were performed where reverse transcriptase (RT) was not added to the cDNA synthesis reaction (RT-), to rule out the presence of DNA. PCR products resulting from genomic DNA as template were used as a positive control.

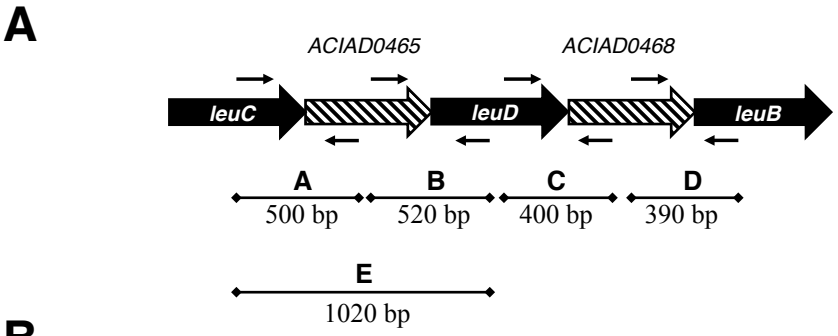
A
ACIAD0465
ACIAD0468
leuC
leuD
leuB
A
B
C
D
500 bp
520 bp
400 bp
390 bp
E
1020 bp

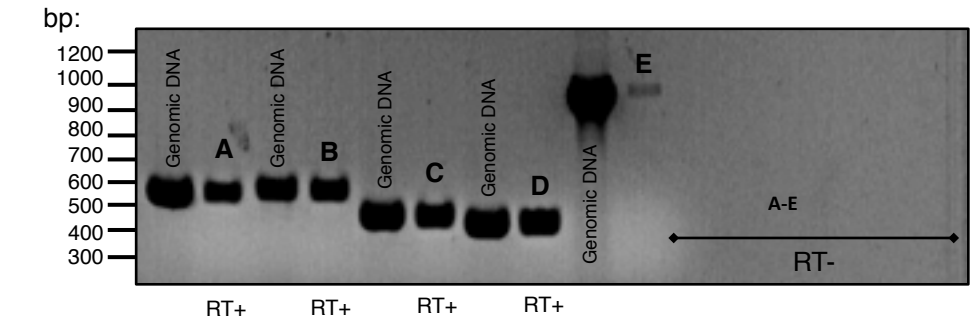
B
bp:
1200
1000
900
800
700
600
500
400
300
Genomic DNA
A
Genomic DNA
B
Genomic DNA
C
Genomic DNA
D
Genomic DNA
E
A-E
RT-
RT+
RT+
RT+
RT+

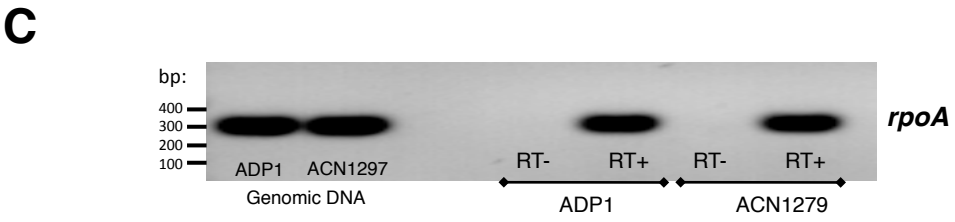
C
bp:
400
300
200
100
ADP1
ACN1297
Genomic DNA
RT-
RT+
RT-
RT+
ADP1
ACN1279
rpoA

(GSP) were designed to anneal to different regions throughout these genes (Figure A.5.A). All targets examined revealed the expected transcript size, which indicates that these genes are transcribed as a single mRNA product (Figure A.5.B). Thus, *leuCDB*, ACIAD0465 and ACIAD0468 form an operon, renamed the *leu* operon. Based on these results, it is plausible to state that LeuR regulates all these genes and represses their expression when intracellular levels of IMA increase.

Discussion

LeuR, a unique LysR-type regulator for leucine biosynthesis. Despite the involvement in leucine biosynthetic regulation, it is important to distinguish that LeuR and LeuO carry out different functions throughout this pathway. As described elsewhere, LeuO, recently identified as a global regulator, carries out distinct functions in several bacteria such as *E. coli, S. enterica* serovar Typhimurium, *Shigella, Yersenia* spp., and *Vibrio cholera* (9, 13, 17). Multiple alignment of LeuO protein sequence of different bacteria (Fig. A.6) assigns this protein to be a transcriptional activator in the Leucine pathway. Interestingly, there are not reports suggesting LeuO as a repressor of genes involve in this biosynthetic path. For instance, LeuO serves as a derepressor of the *leuABCD* operon in *Salmonella enterica* (3). At this locus, the presence of an A-T rich region upstream of the *leu* promoter has a gene-silencing effect that can be relieved by the presence of LeuO, which results on derepression of the *leuABCD* operon (3-5). As described in this report, LeuR acts as a repressor for the *leu* operon probably by blocking RNA polymerase binding when levels of Leucine are high in the cell (figure A.3). It is unclear whether Leucine acts as a repressor molecule in LeuR or if it binds to it at all.

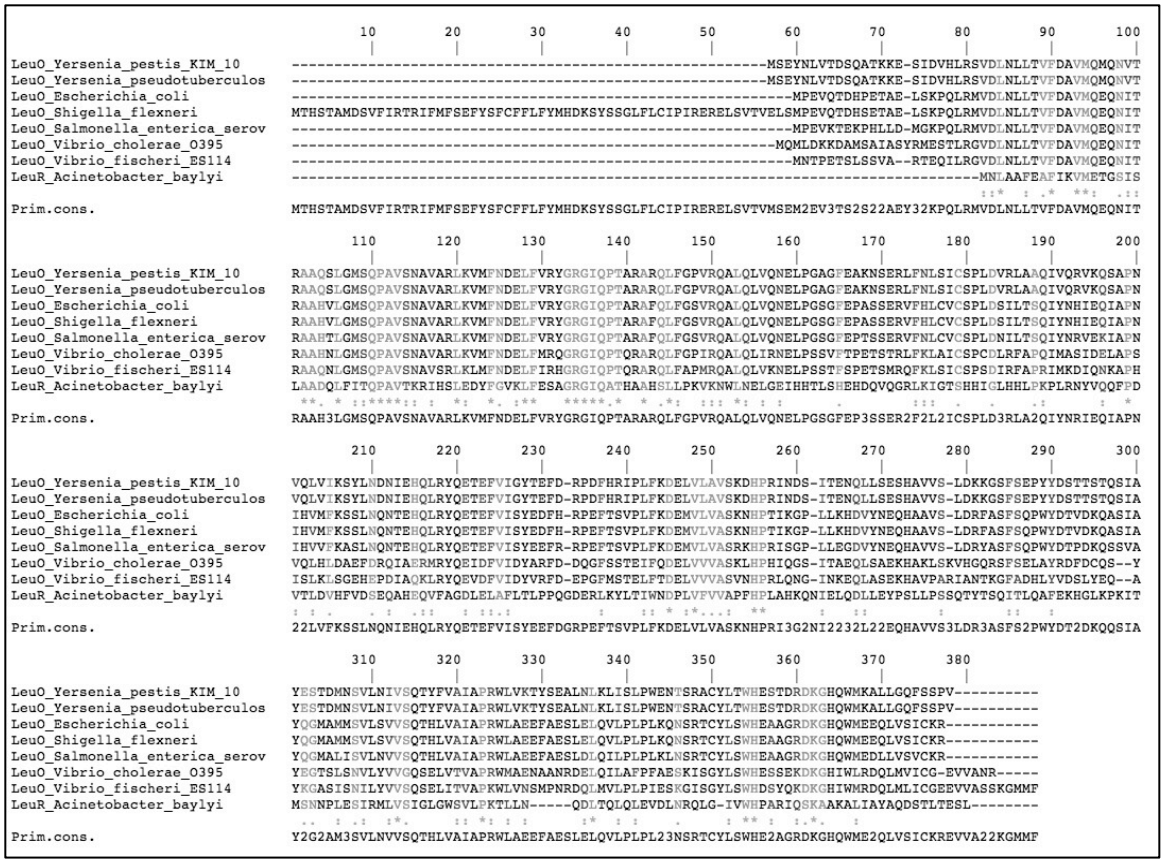

Figure A.6. Multiple protein alignment of *A. baylyi* LeuR with LeuO from other organisms. LeuO sequences: LeuO from *Yersenia pestis* KIM-10 (Q8CZQ2), LeuO from *Yersenia pseudotuberculosis* (Q66EM0), LeuO from *Escherichia coli* K12 (P10151), LeuO from *Shigella flexneri* (I6CC70), LeuO from *Salmonella enterica* serovar Typhymurium (P46924), LeuO from *Vibrio chloreae* O395 (GI4W-2129), LeuO from *Vibrio fischeri* ES114 (Q5E2I6), and LeuR from *Acinetobacter baylyi* strain ADP1 (Q6FEW2). Asterisks indicate identical residues among these sequences. Single and double smaller asterisks indicate similar residues.

However, addition of a metabolite from the leucine pathway, IMA, improves LeuR binding affinity to the *leu* operon significantly. Metabolites acting as binding molecules are very common in LTTRs. In *A. baylyi,* two LTTRs, BenM and CatM control genes involved in benzoate degradation. In this pathway, the intermediate *cis*-cis muconate acts as effector for both of these LysR-type regulators (6, 22). Although the regulatory mechanism employ by LeuR at the *leu* operon remains unclear, the disruption or deletion of this regulator has no a lethal effect on *A. baylyi* cells. Strains ACN1259 and ACN1279 were capable to growth in minimal media in the presence or absence of Leucine. It is possible that in *A. baylyi* LeuR has a more limited role than the global regulator LeuO described in *E.coli* and *Salmonella.*

LeuR functional differences with LeuO. LeuR shared 19% of amino acid sequence identity with LeuO from *E. coli* and *Salmonella enterica*, bacteria from which LeuO has been extensively studied and reported to act as a global regulator. Sequence alignment of LeuR with LeuO from other bacteria shows that LeuR have the highest sequence identity with LeuO from *V. cholera* and *V. fischeri* (~22%). Interestingly, the alignment shows multiple conserved amino acid residues between these sequences. These residues are highly conserved at the N-terminal portion of LeuR, which corresponds to the DNA-binding domain and linker helix of this protein. LTTRs are most conserved at the N-terminal domain (17, 24). Thus, this observed conservation at this domain suggests that LeuR and LeuO may bind DNA in a similar fashion to carry out transcriptional regulation of their target genes.

LeuO has been identified as an antagonist of DNA-binding protein H-NS in both *E.coli* and *Salmonella* (9, 10, 25). H-NS, a global repressor protein that binds A-T rich DNA sequences to repress RNA polymerase activity by blocking its binding to the promoter or by trapping RNA polymerase at the promoter regions (8, 16). Thus, LeuO may carry out its function as an antagonist of H-NS by competing with this protein for DNA binding (25). In *A. baylyi,* BLAST analysis suggests that ACIAD0291 may encode a H-NS-like DNA binding protein and it shares a 38% amino acid identity with H-NS from *E. coli* K-12. However, further studies are needed to determine whether LeuR has a similar antagonistic role with this hypothetic DNA-binding protein as LeuO has for H-NS.

Interestingly, LeuO molecules in the cell vary between exponential and stationary phases in different bacteria (10, 12, 25, 26). The expression of *leuO* gene decreases during exponential phase, but increases significantly at nutrient limited levels. Thus, this suggests that LeuO is not essential during exponential growth, but extremely necessary for cell survival under stressful conditions (18). This abundance of LeuO may correspond to its role as a global regulator. In the case of LeuR, as with other LTTRs, the intracellular concentrations may be lower than LeuO, but may slightly increased during nutrient starvation to control the biosynthesis of Leucine or when intracellular levels of this amino acid are high. Based in this primary report, it seems that LeuR may have a more localized regulatory role than LeuO. However, the complete regulon of LeuR remains unclear. For example, it is unknown whether LeuR regulates other genes such as the *ilv* genes. Thus, further experimental investigation is needed to determine the complete LeuR regulon.

Acknowledgments

We would like to extend our gratitude to the students from the MIBO4600L class (Spring 2012) for their help with plasmids and strains constructions. Curtis Bacon and Nicole Laniohan helped with cDNA synthesis preparations. In addition, we thank Kelsey H. for helping with RNA isolation.

References

1. **Barbe V, Vallenet D, Fonknechten N, Kreimeyer A, Oztas S, Labarre L, Cruveiller S, Robert C, Duprat S, Wincker P, Ornston LN, Weissenbach J, Marliere P, Cohen GN, Medigue C.** 2004. Unique features revealed by the genome sequence of *Acinetobacter* sp. ADP1, a versatile and naturally transformation competent bacterium. Nucleic. Acids. Res. **32:**5766-5779.
2. **Bose N, Greenspan P, Momany C.** 2002. Expression of recombinant human betaine: homocysteine S-methyltransferase for x-ray crystallographic studies and further characterization of interaction with S-adenosylmethionine. Protein. Expr. Purif. **25:**73-80.
3. **Chen CC, Fang M, Majumder A, Wu HY.** 2001. A 72-base pair AT-rich DNA sequence element functions as a bacterial gene silencer. J. Biol. Chem. **276:**9478-9485.
4. **Chen CC, Ghole M, Majumder A, Wang Z, Chandana S, Wu HY.** 2003. LeuO-mediated transcriptional derepression. J. Biol. Chem. **278:**38094-38103.
5. **Chen CC, Wu HY.** 2005. LeuO protein delimits the transcriptionally active and repressive domains on the bacterial chromosome. J. Biol. Chem. **280:**15111-15121.
6. **Collier LS, Gaines GL, 3rd, Neidle EL.** 1998. Regulation of benzoate degradation in *Acinetobacter* sp. strain ADP1 by BenM, a LysR-type transcriptional activator. J. Bacteriol. **180:**2493-2501.

7. **Craven SH.** 2009. Gene expression and dosage distinct mechanisms regulate benzoate degradation in *Acinetobacter baylyi* ADP1. Phd. thesis. University of Georgia. Athens, GA.

8. **Dame RT, Wyman C, Wurm R, Wagner R, Goosen N.** 2002. Structural basis for H-NS-mediated trapping of RNA polymerase in the open initiation complex at the *rrnB* P1. J. Biol. Chem. **277:**2146-2150.

9. **De la Cruz MA, Fernandez-Mora M, Guadarrama C, Flores-Valdez MA, Bustamante VH, Vazquez A, Calva E.** 2007. LeuO antagonizes H-NS and StpA-dependent repression in *Salmonella enterica* ompS1. Mol. Microbiol. **66:**727-743.

10. **Dillon SC, Espinosa E, Hokamp K, Ussery DW, Casadesus J, Dorman CJ.** 2012. LeuO is a global regulator of gene expression in *Salmonella enterica* serovar Typhimurium. Mol. Microbiol. **85:**1072-1089.

11. **Ezezika OC, Collier-Hyams LS, Dale HA, Burk AC, Neidle EL.** 2006. CatM regulation of the *benABCDE* operon: functional divergence of two LysR-type paralogs in *Acinetobacter baylyi* ADP1. Appl. Environ. Microbiol. **72:**1749-1758.

12. **Fang M, Majumder A, Tsai KJ, Wu HY.** 2000. ppGpp-dependent leuO expression in bacteria under stress. Biochem. Biophys. Res. Commun. **276:**64-70.

13. **Hernandez-Lucas I, Gallego-Hernandez AL, Encarnacion S, Fernandez-Mora M, Martinez-Batallar AG, Salgado H, Oropeza R, Calva E.** 2008. The LysR-type transcriptional regulator LeuO controls expression of several genes in *Salmonella enterica* serovar Typhi. J. Bacteriol. **190:**1658-1670.

14. **Jones RM, Williams PA.** 2003. Mutational analysis of the critical bases involved in activation of the AreR-regulated sigma54-dependent promoter in *Acinetobacter* sp. strain ADP1. Appl. Environ. Microbiol. **69:**5627-5635.

15. **Juni E, Janik A.** 1969. Transformation of *Acinetobacter calcoaceticus* (Bacterium anitratum). J. Bacteriol. **98:**281-288.

16. **Lucchini S, Rowley G, Goldberg MD, Hurd D, Harrison M, Hinton JC.** 2006. H-NS mediates the silencing of laterally acquired genes in bacteria. PLoS pathogens **2:**e81.

17. **Maddocks SE, Oyston PC.** 2008. Structure and function of the LysR-type transcriptional regulator (LTTR) family proteins. Microbiology. **154:**3609-3623.

18. **Majumder A, Fang M, Tsai KJ, Ueguchi C, Mizuno T, Wu HY.** 2001. LeuO expression in response to starvation for branched-chain amino acids. J. Biol. Chem. **276:**19046-19051.

19. **Momany C, Neidle EL.** 2012. Defying stereotypes: the elusive search for a universal model of LysR-type regulation. Mol. Microbiol. **83:**453-456.

20. **Mrazek J, Xie S.** 2006. Pattern locator: a new tool for finding local sequence patterns in genomic DNA sequences. Bioinformatics **22:**3099-3100.

21. **Pareja E, Pareja-Tobes P, Manrique M, Pareja-Tobes E, Bonal J, Tobes R.** 2006. ExtraTrain: a database of Extragenic regions and Transcriptional information in prokaryotic organisms. BMC. Microbiol. **6:**29.

22. **Romero-Arroyo CE, Schell MA, Gaines GL, 3rd, Neidle EL.** 1995. *catM* encodes a LysR-type transcriptional activator regulating catechol degradation in *Acinetobacter calcoaceticus*. J. Bacteriol. **177:**5891-5898.

23. **Sambrook J, Fritsch F, Maniatis T.** 1989. *Molecular cloning: a laboratory manual, 2nd ed.* Cold Spring Harbor Laboratory Press, Cold Spring Harbor, N.Y.

24. **Schell MA.** 1993. Molecular biology of the LysR family of transcriptional regulators. Annu. Rev. Microbiol. **47:**597-626.

25. **Shimada T, Bridier A, Briandet R, Ishihama A.** 2011. Novel roles of LeuO in transcription regulation of *E. coli* genome: antagonistic interplay with the universal silencer H-NS. Mol. Microbiol. **82:**378-397.

26. **Shimada T, Yamamoto K, Ishihama A.** 2009. Involvement of the leucine response transcription factor LeuO in regulation of the genes for sulfa drug efflux. J. Bacteriol. **191:**4562-4571.

27. **Studier FW.** 2005. Protein production by auto-induction in high density shaking cultures. Protein. Expr. Purif. **41:**207-234.

28. **Vaneechoutte M, Young DM, Ornston LN, De Baere T, Nemec A, Van Der Reijden T, Carr E, Tjernberg I, Dijkshoorn L.** 2006. Naturally transformable *Acinetobacter* sp. strain ADP1 belongs to the newly described species *Acinetobacter baylyi*. Appl. Environ. Microbiol. **72:**932-936.

29. **Yanisch-Perron C, Vieira J, Messing J.** 1985. Improved M13 phage cloning vectors and host strains: nucleotide sequences of the M13mp18 and pUC19 vectors. Gene. **33:**103-119.